LEVERAGING THE OCCURRENCE OF SPONTANEOUS D_2 RECEPTOR-MEDIATED IPSCS TO UNDERSTAND THE DOPAMINE SYNAPSE

By

Stephanie C. Gantz

A DISSERTATION

Presented to the Neuroscience Graduate Program

Vollum Institute

Oregon Health & Science University

School of Medicine

In Partial Fulfillment

of the Requirements for the Degree of

Doctor of Philosophy

July 2015

School of Medicine

Oregon Health & Science University

CERTIFICATE OF APPROVAL

This is to certify that the Ph.D. dissertation of

Stephanie C. Gantz

has been approved

John T. Williams, Ph.D., Advisor

Craig Jahr, Ph.D., Chair

Tianyi Mao, Ph.D.

Kim A. Neve, Ph.D.

Laurence Trussell, Ph.D.

TABLE OF CONTENTS

LIST OF FIGURES

LIST OF TABLES

LIST OF ABBREVIATIONS

5-CT	5-carboxamidotryptamine
5-HT	5-hydroxytryptamine, serotonin
AADC	L-amino acid decarboxylase
AAV	adeno-associated virus
ACSF	artificial cerebrospinal fluid
ADE	anomalous dopamine efflux
AMPA	a-amino-3-hydroxy-5-methyl-4-isoxazolepropionic acid
AMPH	amphetamine
ANOVA	analysis of variance
BAPTA	1,2-Bis(2-aminophenoxy)ethane-N,N,N',N'-tetraacetic acid
ChR2	channelrhodopsin-2
CPA	cyclopiazonic acid
Cre	Cre recombinase
DA	dopamine
DAT	dopamine transporter
DR	dorsal raphe nucleus
EGTA	ethylene glycol tetraacetic acid
GABA	gamma-aminobutyric acid
GIRK	G protein-coupled inwardly rectifying potassium channel
GPCR	G protein-coupled receptor
GTP	guanosine 5'-triphosphate
IPSC	inhibitory postsynaptic current
eIPSC	produced by electrical stimulation
oIPSC	produced by ChR2 stimulation
sIPSC	produced without stimulation
KO	knock-out
L-DOPA	L-3,4-dihydroxyphenylalanine
MPH	methylphenidate
NMDA	N-methyl-D-aspartic acid
NSD	3-hydroxybenzylhydrazine
PD	Parkinson's disease
PDBu	phorbol 12, 13-dibutyrate
PKA	protein kinase A
PKC	protein kinase C
PBS	phosphate buffered saline
SNc	substantia nigra pars compacta
TH	tyrosine hydroxylase
TpH	tryptophan hydroxylase
TTX	tetrodotoxin
VMAT	vesicular monoamine transporter
VTA	ventral tegmental area
WT	wild type

ACKNOWLEDGEMENTS

I would like to express my humble gratitude to Dr. John T. Williams, my thesis advisor, for his prompt and insightful guidance and continual encouragement. Above all, he gives me inspiration and a lifelong memory of unassuming success and leadership.

I am thankful for my thesis committee members, Drs. Kim Neve, Craig Jahr, Larry Trussell, and Tianyi Mao, for their technical advice, selfless giving of time, and efforts to foster my independence. I also greatly appreciate their critical comments during the writing of this dissertation and any remaining deficiencies or errors are my own.

I am tremendously grateful for my many collaborators, whose names and specific scientific contributions may be found in the prefaces of each chapter. Without their expertise and tireless efforts, these studies would not have been possible.

Many thanks are also due to the past and present members of the Williams laboratory, for their technical instruction, critical scrutiny of my experimental designs, recordings, and writings, as well as their inspiring dialogue, patience, and friendship.

I also wish to acknowledge Dr. Ethan Selfridge for his invigorating optimism and enduring advocacy of my success. I am also incredibly grateful for the unconditional support and encouragement from the Gantz family.

Finally, I would like to recognize the Neuroscience Graduate Program and the financial support that made these studies possible: NIH pre-doctoral training grants (3T32NS007466-12S1 and 5T32DK007680-19), the Oregon Brain Institute Neurobiology of Disease fellowship enabled by the generous donation of Randall and Mary Huebner, the N.L. Tartar Trust fellowship, the OHSU Graduate Research Scholar fellowship, and the NIH grant DA04523 (J.T.W.).

ABSTRACT

Information is transmitted between neurons through a process known as synaptic transmission. We are resolved to study synaptic transmission as an effort to understand the workings of the brain. There has been considerable effort into understanding synaptic transmission mediated by glutamate, GABA, and acetylcholine. Much less emphasis has been on synaptic transmission mediated by monoamine neurotransmitters, dopamine, noradrenaline, and serotonin, despite their critical role in physiology.

The goal of this dissertation is to advance the understanding of dopamine-dependent synaptic transmission. It is established that dopamine neurons in the ventral midbrain release dopamine from the somatodendritic compartment. Once released, dopamine activates G protein-coupled dopamine D_2 receptors on neighboring dopamine neurons. Activated D_2 receptors negatively regulate dopamine release locally and in extensive axon terminal projection areas. Ultimately, somatodendritic dopamine transmission affects dopamine-dependent processes throughout the brain. However, many aspects of the regulation of somatodendritic dopamine transmission are controversial, arising from an incomplete understanding of the somatodendritic dopamine synapse.

Through electrophysiological recordings and immunohistochemical studies in acute mouse brain slices, this work examines the presynaptic and postsynaptic components of the dopamine synapse, as well as their proximity. Work presented in this dissertation describes spontaneous D_2 receptor-mediated inhibitory postsynaptic currents (D_2-IPSCs) produced by action potential-independent exocytosis of dopamine-filled vesicles and the subsequent activation of a D_2 receptor-dependent G protein-coupled inwardly rectifying potassium conductance. The results reveal that dopamine release sites

and D_2 receptors are closely apposed, which allows for temporal and spatial specificity in dopamine signaling despite the slow intrinsic signaling kinetics of G protein-coupled receptors. Moreover, spontaneous dopamine synaptic events alter dopamine neuron excitability, as observed by transient inhibitions in action potential firing that were dependent on vesicular release of dopamine and activation of D_2 receptors.

The occurrence of spontaneous D_2-IPSCs was then leveraged to advance the understanding of the presynaptic and postsynaptic components of the somatodendritic dopamine synapse. The origins of dopamine release was investigated through comparisons of spontaneous and electrically evoked synaptic events. These results revealed an unexpected and robust contribution of serotonin terminal-derived dopamine to D_2 receptor-dependent signaling after *in vivo* or *in vitro* exposure to the dopamine precursor, L-DOPA. Under basal conditions, the results are most consistent with dopamine release occuring strictly from neighboring dopamine neurons. The characteristics and regulation of postsynaptic D_2 receptors were also studied. When virally expressed, either splice variant of the D_2 receptor, D_2S or D_2L, was capable of producing spontaneous D_2-IPSCs. Contrary to the canon, the results suggested that both splice variants may function as somatodendritic autoreceptors in wild type dopamine neurons. Lastly, the study of spontaneous D_2-IPSCs aided in the assessment of somatodendritric dopamine signaling pertrubations in a mouse line that harbors a disease-associated mutation in the dopamine transporter.

In conclusion, the investigation of spontaneous D_2 receptor-mediated IPSCs revealed insights into the structure of the dopamine synapse and the regulation of evoked and spontaneous dopamine transmission, and dopamine neuron excitability. More

broadly, their occurrence demonstrated that many of the defining features of ionotropic receptor- and G protein-coupled receptor-dependent synaptic transmission are similar.

Chapter 1 INTRODUCTION

Neurons communicate through electrical and chemical signaling. In brief, an action potential in the presynaptic neuron leads to the opening of calcium channels and calcium enters the neuron. Calcium entry allows neurotransmitter-filled vesicles to fuse, or exocytose, releasing their contents into the synaptic cleft. Cognate ionotropic ligand-gated ion channels on the postsynaptic neuron bind neurotransmitter, which leads to the opening of an ion channel. Opening of ion channels allows for the movement of charge, generating an electrical response in the postsynaptic neuron.

Ligand-gated ion channels represent one class of receptors. Another class of receptors is the metabotropic G protein-coupled receptors. This superfamily of receptors can recognize an impressive array of ligands, including glutamate, GABA, acetylcholine, and the biogenic amines. These receptors are well-known for modulating ionotropic receptor-mediated synaptic transmission. But they can also mediate synaptic currents. One neurotransmitter system that generates of a lot of interest and, in mammals, acts exclusively through G protein-coupled receptors is the dopamine system.

Dopamine release in the ventral midbrain, the substantia nigra pars compacta (SNc) and ventral tegmental area (VTA), is important in multiple physiological processes ranging from movement to reinforcement learning. Dysfunction in the regulation of the dopamine system is implicated in the etiology of many diseases and disorders. The symptomology of these pathological states reflect the role of dopamine in behavior, namely affecting motor control, attention to salient cues, and reinforcement of behaviors related to reward-acquisition. Putative dopamine dysfunction is so prevalent that pharmaceuticals that target dopamine receptors, reuptake, or alter synthesis and

degradation are widely prescribed. In spite of a wealth of knowledge of dopamine's role in the central nervous system, fundamental questions remain regarding the temporal and spatial specificity and regulation of dopamine-dependent signaling.

Midbrain dopamine neurons release dopamine from their extensive terminal projections and locally from somatodendritic sites. The important aspect of this type of release is that activation of somatodendritric dopamine D_2 autoreceptors can regulate impulse generation, dopamine synthesis, and dopamine release. Ultimately, dopamine release in the midbrain affects dopamine-dependent processes locally and throughout the widespread terminal projection areas. Many aspects of the regulation of somatodendritic dopamine transmission are controversial, arising from an incomplete understanding of the somatodendritic dopamine synapse. Even defining connections between dopamine neurons as *synapses* is met with opposition.

The theory of somatodendritic dopamine release arose from the measurement of high dopamine levels local to dendritic regions in the SNc (Björklund and Lindvall, 1975) despite a paucity of structural evidence for dopamine axon terminals (Juraska *et al.*, 1977). Dopamine could accumulate in the extracellular space following reversal of the dopamine transporter (DAT). However, DAT blockade elevates extracellular dopamine, arguing against DAT-mediated reversal as the exclusive mode of dopamine release (Elverfors and Nissbrandt, 1994; Hoffman and Gerhardt, 1999; Jaffe *et al.*, 1998; Beckstead *et al.*, 2004). In contrast, somatodendritic dopamine release is markedly reduced following inhibition of vesicular monoamine transport with reserpine treatment (Björklund and Lindvall, 1975). In addition, disrupting exocytosis by botulinum toxin-mediated cleavage of SNARE proteins or down-regulation of synaptotagmin expression

strongly reduces somatodendritic dopamine release (Bergquist *et al.*, 2002; Fortin *et al.*, 2006; Mendez *et al.*, 2011). While there may be other ways in which dopamine is extruded from dopamine neurons, there is now little dispute that vesicular somatodendritic release of dopamine occurs.

Structurally, there is some evidence for putative synapses between dopamine somas, dendrites, and spine-like structures. But relative to non-dopaminergic inputs to this area, the density is low (Bayer and Pickel, 1990; Groves and Linder, 1983; Nirenberg *et al.*, 1996a; 1996b; Wassef *et al.*, 1981). Electron micrograph studies of the somatodendritic compartment of dopamine neurons have described a variety of vesicles types and sizes, including small clear synaptic, large dense core, and tubulovesicles or saccules (Bayer and Pickel, 1990; Groves and Linder, 1983; Nirenberg *et al.*, 1996a; 1996b). The vesicular monoamine transporter-2 is localized to these various vesicle structures, indicating they may contain dopamine (Nirenberg *et al.*, 1996a). However, these structures are not often associated with the plasma membrane or are paradoxically found in dendritic spines; structures typically considered "postsynaptic" elements (Nirenberg *et al.*, 1996a).

The lack of solid structural evidence of classical synapses in the midbrain has led to the two main hypotheses regarding somatodendritic D_2 receptor-dependent signaling. First, dopamine neurons form autaptic synapses, where dopamine is released and sensed by the same neuron. Indeed, in single neuron microcultures, dopamine neurons form glutamatergic autapses (Sulzer *et al*., 1998). However, in this culture system, dopamine-mediated inhibition does not occur after depolarizing dopamine neurons (Sulzer *et al*., 1998). The second hypothesis is that dopamine exerts its effects primarily in a paracrine

manner, following release from extrasynaptic sites without a specialized structure. The volume transmission hypothesis is inconsistent with two main electrophysiological and electrochemical observations: 1) the presence of a D_2 receptor-mediated synaptic current, whose activation kinetics is mimicked only by high concentrations of dopamine and 2) the tight control of extracellular dopamine. Studies based on these observations continue to challenge the volume transmission hypothesis as the primary mode of somatodendritic D_2 receptor-dependent dopamine transmission.

D_2 receptors are coupled to heterotrimeric G_i/G_o proteins. Once activated, D_2 receptors via G protein $\alpha_{i/o}$ and $\beta\gamma$ subunits promote calcium mobilization through stimulation of phospholipase C and reduce the production of cyclic AMP through inhibition of adenylyl cyclases. In dopamine neurons, liberated $\beta\gamma$ subunits also lead to the opening of G protein-coupled inwardly rectifying potassium (GIRK) channels (Lacey *et al.*, 1987). Electrical stimulation in the midbrain evokes dopamine release, which in voltage-clamp recording produces an inhibitory postsynaptic current (D_2-IPSC) through D_2 receptor-activation of GIRK channels (Beckstead *et al.*, 2004). The D_2-IPSC is dependent on the biosynthesis of dopamine in dopamine neurons and is abolished by agents that disrupt dopamine loading into vesicles (Beckstead *et al.*, 2004). In addition, the D_2-IPSC is dependent on calcium entry via voltage-gated calcium channels following action potential-dependent depolarization (Beckstead *et al.*, 2004; Ford *et al.*, 2007). These studies are consistent with somatodendritic dopamine release occurring by vesicular exocytosis. In addition, under basal conditions, there is no tonic D_2 receptor-dependent current, which suggests that if dopamine is secreted by another mechanism, it is insufficient to elicit a current.

Further studies indicate that the distance between release sites and postsynaptic D_2 receptors is consistently close in proximity. The time course of paracrine dopamine transmission would be governed by the distance and tortuosity between release sites and postsynaptic D_2 receptors. Consistent with this, dopamine iontophoretically applied at increasing distances from the soma slows the rate of current activation (Beckstead *et al.*, 2004). Even rapid application of low concentrations of dopamine results in currents with a slow rate of activation relative to the D_2-IPSC (Ford *et al.*, 2009). But the kinetics of D_2-IPSCs are identical regardless of stimulus intensity and amplitude (Beckstead *et al.*, 2004, Courtney and Ford, 2014). Moreover, the rising kinetics of D_2-IPSC are mimicked only by a brief application (≤ 100 ms) of high concentrations (>10 μM) of dopamine (Courtney and Ford, 2014; Ford *et al.*, 2009). Therefore, electrically evoked dopamine release must reach postsynaptic receptors at a sufficiently high concentration to result in kinetically identical transmission from cell to cell. While these studies are suggestive of point-to-point contacts between dopamine neurons, much of this work relies on stimulus-induced presynaptic depolarization to evoke dopamine release. Whether this brief and high concentration of dopamine is released intrinsically is unknown.

A common feature at many neurotransmitter release sites is the stochastic fusion of single vesicles. Unstimulated somatodendritic dopamine release has been measured using high-performance liquid chromatography or amperometry from midbrain dopamine neurons in modified brain slices (Jaffe *et al.*, 1998) and cultures (Fortin *et al.*, 2006; Kim *et al.*, 2008; Mendez *et al.*, 2011). Like evoked release, spontaneous somatodendritic dopamine release is due to vesicle exocytosis, as it also requires SNARE proteins and synaptotagmin (Fortin *et al.*, 2006; Mendez *et al.*, 2011). At many synapses, release of

neurotransmitter following exocytosis of a single vesicle is sufficient to elicit a spontaneous electrical response in the postsynaptic neuron. Comparisons between evoked and spontaneous transmission have become a powerful tool to understand the regulation of neurotransmitter release, presynaptic release sites, and postsynaptic receptors. The characterization of spontaneous D_2 receptor-mediated IPSCs would provide the most compelling evidence for point-to-point synaptic transmission between pre- and postsynaptic somatodendritic sites. More broadly, similar to the studies at other synapses, the occurrence of spontaneous D_2 receptor-mediated IPSCs could be leveraged to understand the dopamine synapse.

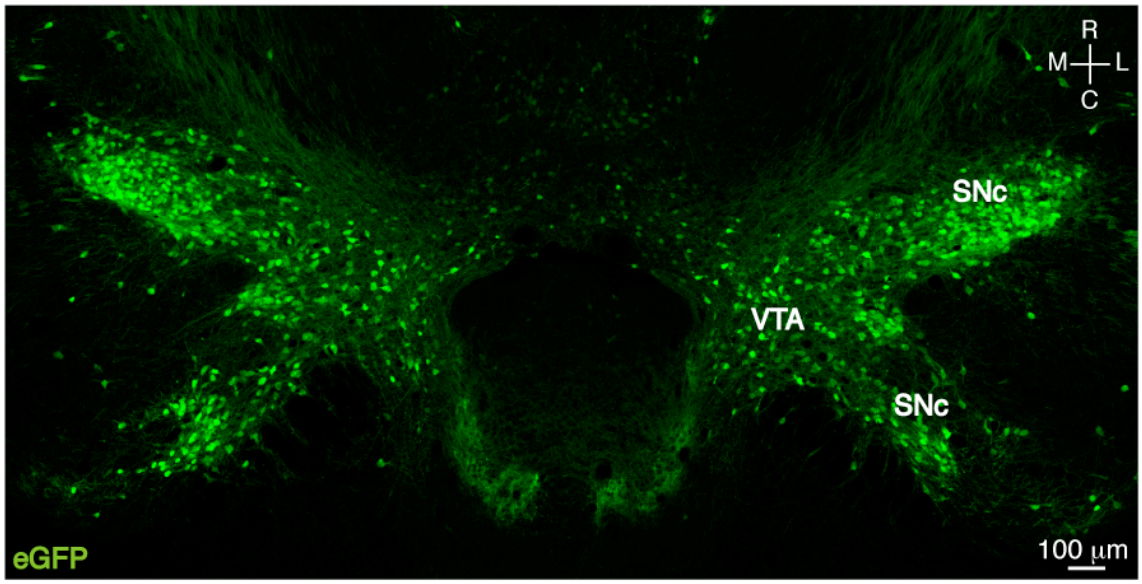

Figure 1.1. Midbrain dopamine neurons expressing eGFP.

Tiled confocal section (10x) of a horizontal mouse midbrain slice, where the expression of eGFP depends on the tyrosine hydroxylase promoter. This image is provided for illustrative purposes of the structure of the ventral midbrain and density of dopamine cell bodies.

THESIS STATEMENT AND COURSE OF DISSERTATION

Since the discovery of spontaneous miniature endplate potentials at the neuromuscular junction over sixty years ago, spontaneous neurotransmitter release has been described at many synapses in the mammalian central nervous system. At these synapses, the recording of spontaneous synaptic events has been utilized to better understand pre- and post-synaptic components of the synapse. The aim of this work is to characterize D_2 receptor-mediated inhibitory postsynaptic currents and demonstrate that their occurrence is leveraged to advance the understanding of the dopamine synapse.

Primarily, work presented in this dissertation was collected through whole-cell patch clamp recordings from midbrain dopamine neurons in acute horizontal mouse brain slices (Figure 1.1). Chapter 3 describes evidence that dopamine when released in the midbrain does not travel far before activating D_2 receptors, indicating that dopamine release sites and D_2 receptors are closely apposed. In Chapter 4, the discovery of spontaneous miniature D_2 receptor-mediated inhibitory postsynaptic synaptic currents (D_2-sIPSCs) in the SNc is described. Pre- and postsynaptic mechanisms regulated the frequency and amplitude of D_2-sIPSCs. Therefore, in Chapters 5 and 6, D_2-sIPSCs are examined to understand pre- and postsynaptic components of the dopamine synapse, respectively. In Chapter 7, D_2-sIPSCs are used to garner information about the dopamine synapse when physiological dopamine transmission is disrupted in a mouse line that harbors a disease-associated mutation in the dopamine transporter. In Chapter 8, the contribution of this work is discussed in the context of somatodendritic dopamine transmission and more generally, signaling by G protein-coupled receptors.

Chapter 2 METHODS AND MATERIALS

ANIMALS

All animals were maintained and sacrificed according to the approved protocols at Oregon Health and Science University and in Chapter 6, by the VA Portland Health Care System (VAPHCS). Wild type male and female mice were used on a C57BL/6J (in studies found in Chapters 4, 5, and 6), DBA/2J (Chapters 3, 4, and 5), hybrid 129S6/SvEvTAc and C57BL/6J (Chapter 7), and BALB/c (Chapter 5) background. All mice used were >26 days old, and mostly were >60 days old. Several lines of genetically modified mice were used. *Drd2*$^{-/-}$ mice were bred at the VAPHCS Veterinary Medical Unit, maintained on a C57BL/6 background, provided by Dr. Kim A. Neve. ePet-Cre$^{+/-}$ mice on a C57BL/6 background were obtained from the Jackson Labs (stock no. 012712). Homozygous DAT Val559 mice on a hybrid 129S6/SvEvTAc and C57BL/6J background were provided by Dr. Randy Blakely (Vanderbilt University, Nashville, TN). Ai9 and Ai32 mice (stock no. 007905 and 012569, respectively), backcrossed onto C57BL/6 background, were kindly provided by Dr. Tianyi Mao. 5-HT$_{1B}$ receptor knockout mice, maintained on a BALB/c background, were kindly provided Dr. Mark Pennesi (Casey Eye Institute, Portland, Oregon).

In vivo treatment

Cocaine-treated mice received one intraperitoneal injection (20 mg/kg) 22-24 h prior to use (Chapters 4 and 6). In Chapter 6, another cohort of mice was treated with equal volume of saline, 22-24 h prior to use. There were no differences found between saline-treated and naïve mice, so data were combined. L-DOPA-treated mice received a once daily subcutaneous injection of L-DOPA methyl ester (100 mg/kg) and benserazide (200

mg/kg) dissolved in saline, or an equal volume of benserazide only (200 mg/kg), for 6 days and were killed 1 h after the last injection (Chapter 5).

TH-hD$_2$S Transgenic Mice

A transgenic mouse expressing the human D_2 dopamine receptor short isoform (hD$_2$S) with a flag epitope on the amino-terminus was generated by nuclear microinjection using standard techniques. The transgene consisted of an 8.5 kb genomic fragment from the rat tyrosine hydroxylase gene (TH) containing 5' regulatory sequences, the basal promoter, and 26 base pairs from the 5' untranslated region in exon 1 followed by a 0.7 kb cassette containing intron 2 and splice donor/acceptor sites from the rabbit beta-globin gene (Arttamangkul *et al.*, 2008). The hD$_2$S construct consisted of a consensus Kozak sequence, a signal peptide from the hemagglutinin influenza followed by the sequence for the FLAG epitope (Vickery and Zastrow, 1999), a full length cDNA for the hD$_2$S containing 1.4 kb of coding sequence and 1.0 kb of 3' untranslated and the bovine growth hormone polyA sequence from pcDNA 3.0 (Invitrogen). After cleavage by the signal peptidase of the signal sequence during translation a hD$_2$S protein with an amino-terminus Flag epitope is expressed in TH-expressing neurons including the dopamine neurons of the midbrain as shown by immunostaining with the M1 anti-Flag antibody (Sigma-Aldrich) using confocal microscopy on sections and two-photon microscopy on on midbrain slice preparations (Figure 6.7). "Transgenic D_2-Short" mice were produced by crossing *Drd2*$^{-/-}$ mice with transgenic TH-hD$_2$S mice.

ELECTROPHYSIOLOGY

Brain slice preparation

Horizontal midbrain or coronal dorsal raphe (220-230 μm) slices were made in ice-cold physiologically equivalent saline solution (modified Krebs buffer, see Recipes) with 10 μM MK-801. Slices were incubated at 30-32 ºC in vials with 95/5% O_2/CO_2 saline with 10 μM MK-801 for at least 30 mins, before recordings. Slices once mounted on a recording chamber attached to an upright microscope (Olympus) were maintained at 33-37 ºC (physiological temperature was used for spontaneous D_2-IPSC experiments) and perfused at a rate of 4.0 ml/min with modified Krebs buffer. Using infrared illumination, the SNc was identified visually, under 5x magnification, by location in relation to the medial terminal nucleus of the accessory optic tract and the midline. The dorsal raphe (DR) was identified by location on the midline, ventral to the cerebral aqueduct. For experiments involving dextran, slices were preincubated for > 30 min at 30-32 ºC in 5-10% dextran-containing (40 kDa) modified Krebs buffer.

Electrophysiological recordings and analysis

Whole-cell patch clamp recordings were obtained with glass electrodes (1.35-2.2 MΩ) and a potassium-based internal solution containing BAPTA (10 mM) or EGTA (0.1 mM), (see Recipes). In Chapter 6, BAPTA internal solution was supplemented with $CaCl_2$ to increase resting free calcium to 300 nM, as determined with use of the EGTAetc program, provided by E.W. McCleskey. The cells were voltage-clamped at -60 mV with an Axopatch 200B amplifier (Molecular Devices). Loose (< 30 MΩ) cell-attached recordings were made with glass electrodes (1.4-2.0 MΩ) and an internal solution containing modified Krebs buffer. Dopamine neurons of the SNc or VTA (Chapter 3) were identified by passive membrane properties, a hyperpolarization-induced I_h current,

the presence of spontaneous pacemaker firing of wide (~2 ms) action potentials at 1-5 Hz, and either the presence of a D_2 receptor-mediated IPSC or the sensitivity to exogenously applied D_2 receptor agonists. 5-HT neurons in the DR were identified by slow, broad, and regular action potential firing upon current injection (Kirby *et al.*, 2003; Li *et al.*, 2001) determined in current clamp mode within 2 min of break-in. Immediately after gaining access to the cell, membrane capacitance, series resistance, and input resistance were measured with the application of 50 pulses (+2 mV for 50 ms) averaged before computation using AxoGraph X (sampled at 50 kHz, filtered at 10 kHz). Transmitter release was evoked by a single (0.5 ms) or train of electrical stimuli (5 x 0.5 ms pulses at 40 Hz for dopamine and 5-HT; 60 Hz for GABA) or in ePet-Cre$^{+/-}$/Ai32$^{+/-}$ slices with a 5-15 ms, 470 nm LED pulse, once every 30-50 s. 4-aminopyridine (100 μM) was used in the SNc to enhance transmitter release from 5-HT terminals (Figure 5.8). D_2-IPSCs, $GABA_B$-IPSCs, and 5-HT_{1A}-IPSCS were pharmacologically isolated by the following receptor blockers in the external bath solution: picrotoxin (100 μM), DNQX (10 μM), hexamethonium (50 μM, for D_2- and $GABA_B$-IPSCs), prazosin (100 nM, for 5-HT_{1A}-IPSCs), and CGP 55845 (200 nM, for D_2-IPSCs) or sulpiride (600 nM, for $GABA_B$-IPSCs). All drugs were applied through bath perfusion, except dopamine, which was applied by iontophoresis. Iontophoretic pipettes (70-110 MΩ) were filled with 1 M dopamine and the tip placed with 10 μm of the soma. A negative backing current (4-11 nA) prevented passive leakage. Dopamine was ejected with the application of positive current (2 -6 s) with an Axoclamp 2A amplifier to elicit a maximal dopamine-induced outward current or by brief (5-25 ms) pulses once every 50 s. In Chapter 5, 5-$HT_{1B/D}$ receptors were activated with the 5-HT_1 receptor agonist 5-Carboxamidotryptamine (5-

CT, 100 nM) or the selective 5-$HT_{1B/D}$ receptor agonist sumatriptan (1 μM). The results using either agonist were not different and the data were combined. For desensitization experiments, cells were dialyzed with internal solution for >10 min prior to drug application (Foehring *et al.*, 2009). Quinpirole and baclofen were applied with >10 min between the agonist applications with the application order alternated between recordings. The amplitude and the decline in the currents were not affected by the order in which the drugs were applied. Slices were exposed to saturating concentrations of each agonist once. For experiments involving dextran, all necessary steps were taken to ensure the flow and temperature of the dextran-containing solution was equivalent to all other solutions. Recordings where the peak amplitude of the current was <50 pA were excluded from desensitization analysis. Synaptic and agonist-induced current peaks were determined by averaging the current ± 20 ms from the greatest upward deflection. For each cell, 3-24 consecutive currents were averaged to determine amplitude, time-to-peak, and duration at 20% of the peak. Data were acquired using AxoGraph X software (sampled at 10 kHz, filtered at 5 kHz) and Chart (AD Instruments).

Detection and measurement of spontaneous D_2-IPSCs

Recordings were post-hoc filtered at 1 kHz, and visually inspected to select spontaneous IPSCs manually. Original recordings were then decimated (averaged 10 points, 1 ms). Single peak spontaneous IPSCs with amplitudes greater than 2.1 times the standard deviation of baseline noise were detected using a semi-automated sliding template detection procedure with AxoGraph X. The template was generated by averaging multiple sIPSCs. Each detected event was visually inspected. Events were discarded if the average baseline noise (> 300 ms) was greater than the peak ± 1.5 s from the peak.

Peak amplitudes were determined by averaging the current ± 20 ms from the greatest upward deflection. The amplitude distribution of the baseline noise was measured by averaging the baseline current ± 20 ms from the greatest upward deflection, 220 ms after a point set to 0 pA, once every 50 s. To compare the kinetics of eIPSCs to sIPSCs, spontaneous events with a single peak were selected. Duration of eIPSCs and sIPSCs was determined by measuring the width at 20% of the peak amplitude (Figure 4.1). For clarity, sIPSC histograms show amplitudes ≤ 30 pA, which accounts for > 97% of all amplitudes measured in each condition. To normalize amplitude counts across conditions, the vertical axes of individual histograms have been scaled, such that the bin with the greatest count equals 1.0.

STEREOTAXIC VIRUS INJECTIONS

In the SNc, D_2 receptors were ubiquitously expressed using an adeno-associated viral (AAV) vector (AAV9 D_2-IRES-GFP; Virovek, Inc.) encoding rat D_2S or D_2L receptors (Neve *et al.*, 2013), or a 1:1 mixture of AAV-D_2S and AAV-D_2L. In the DR, D_2 receptors were ubiquitously expressed using a 1:1 mixture of AAV-D_2S and AAV-D_2L, as described above. Mice were injected when 5-7 weeks old. Mice were immobilized in a stereotaxic alignment system under isoflurane anesthesia or an anesthesia cocktail consisting of 7.1 mg/kg xylazine, 71.4 mg/kg ketamine, and 1.4 mg/kg acepromazine (10 ml/kg). Mice received one midline injection (DR) 500 nL delivered over 5 min or bilateral injections (SNc) 500 nL delivered over 2.5 min. The injection needle was left in place for an additional 5 min before it was slowly withdrawn. The coordinates for injection were (with respect to bregma) for DR: AP -3.9 mm, ML 0.0 mm, DV -2.8 mm; for SNc: AP -3.26 mm, ML 1.2 mm, DV -4.0 mm. Mice recovered for 3 to 5 weeks to

allow for expression. Infected neurons were identified in the slice by visualization of GFP.

IMMUNOHISTOCHEMISTRY AND MICROSCOPY

In Chapter 5, mice were anesthetized with Avertin (i.p.) and transcardially perfused with 5% sucrose in H_2O followed by ice-cold 4% paraformaldehyde in phosphate-buffered solution (PBS, see Recipes). Brains were fixed overnight at 4 °C, then sliced coronally (dorsal raphe) and horizontally (midbrain) in 60 μm sections. Free-floating slices were permeabilized in PBS with 0.3% Triton-X (PBS-T) then blocked in PBS-T with 0.5% fish skin gelatin for 1 h. Slices from ePet-Cre$^{+/-}$ /Ai9$^{+/-}$ mice were incubated 24 h at 24 °C in mouse anti-TH (1:1000 in PBS) primary antibody. Slices were washed then incubated in Alexa Fluor 647-conjugated goat anti-mouse secondary antibody (1:1000 in PBS) for 3 h. Slices were washed then incubated for 48 h at 24 °C in rabbit anti-TpH primary antibody (1:500 in PBS). Following washing, slices were incubated in Alexa Fluor 488-conjugated goat anti-rabbit secondary antibody (1:1000 in PBS) for 3 h. Slices from AAV-D_2-infected wild type mice were incubated in rabbit anti-GFP conjugated to Alexa Fluor 488 (1:1000 in PBS) 24 h at 4 °C.

In Chapter 6, brain slices from TH-hD_2S mice were prepared and allowed to recover, as described for electrophysiology. Slices were incubated in Alexa Fluor 594-conjugated M1 antibody (10 μg/ml, 1:75 in ACSF with 0.00025% pluronic acid) for 40 min at 35 ºC. Live slices were observed with a custom-built two-photon microscope using *ScanImage* Software (Pologruto *et al.*, 2003). Expression of eGFP was visualized using a CCD camera of epi-fluorescence activation. Slices for laser-scanning confocal microscopy were washed 10 min in modified Krebs buffer before fixation in 4%

paraformaldehyde (45 min at 24 ºC) in PBS with $CaCl_2$ (1 mM, PBS+Ca^{2+}). Slices were blocked and permeabilized in PBS+Ca^{2+} with 0.3% Triton-X and 0.5% fish skin gelatin for 80 min. Slices were incubated overnight in rabbit anti-tyrosine hydroxylase antibody (1:1000 in PBS+Ca^{2+} + 0.05% NaN_3). Washed slices were incubated in Alexa Fluor 488-conjugated goat anti-rabbit secondary antibody (1:1000 in PBS+Ca^{2+} + 0.05% NaN_3, 2 h at 24 ºC). All slices were washed then mounted with Fluoromount (Sigma) aqueous mounting medium with #1.5 glass coverslips. Confocal images were collected on a Zeiss LSM 780 microscope with a 20x (0.8 NA) or 40x water-immersion lens (1.2 NA) and processed using Fiji.

DRUGS

CGP 35348, CGP 55845, 5-CT, WAY 100635, and NPEC-caged-serotonin were obtained from Tocris Bioscience. Baclofen and sulpiride were obtained from Research Biochemical Inc. MK-801 and cyclopiazonic acid were obtained from Abcam. Sumatriptan was from Glaxo Wellcome Research and Development. Cocaine hydrochloride and (±)-methylphenidate hydrochloride were obtained from National Institute on Drug Abuse-National Institutes of Health (Bethesda, MD). All other chemicals were obtained from Sigma-Aldrich.

DATA ANALYSIS

Values are given as means ± SEM. Unless otherwise noted, n = number of cells. All distributions with $n > 30$ were tested for normality with Shapiro-Wilk normality test. Nonparametric statistics were used if any data set failed a normality test and was skewed. IPSC amplitude distributions were compared by two-sample Kolmogorov-Smirnov tests. Statistical significance were determined in two group comparisons by paired two-tailed t

tests or two-tailed Mann-Whitney U tests, and in more than two groups comparisons by one-way or one-way repeated measures ANOVAs, Kruskal-Wallis (Nonparametric ANOVA), or Friedman test (Nonparametric repeated measures ANOVA) followed, as appropriate ($p < 0.05$), by Dunnett's, Bonferroni's, uncorrected Fisher's LSD post hoc tests, or Dunn's multiple comparisons test. Correlations were determined by two-tailed Pearson Correlation test. A difference of $p < 0.05$ was considered significant (Prism 4 and AxoGraph X).

Chapter 3 DOPAMINE RELEASE SITES AND RECEPTORS ARE CLOSE

PREFACE

This chapter describes evidence that in the midbrain, dopamine release occurs close to postsynaptic D_2 receptors. Included is a study that examined the regulation of extracellular dopamine by reuptake and diffusion in the midbrain and striatum through electrophysiological and fast-scan cyclic voltammetric recordings in mouse brain slices. Diffusion was limited with the application of a 10% dextran solution and DAT-mediated reuptake was slowed with cocaine.

This study was led by Dr. Christopher P. Ford. My contribution was conducting electrophysiological recordings from dopamine neurons to determine the effect of dextran and cocaine on D_2 receptor-mediated currents, in addition to some voltammetric recordings in the striatum and in free solution, and data analysis.

The results demonstrated that dextran failed to slow electrically evoked D_2 receptor-mediated IPSCs in dopamine neurons in the midbrain. But, dextran significantly slowed the current induced by local iontophoretic application of dopamine. The rise and fall of the dopamine transient detected by fast scan cyclic voltammetry was slowed by dextran in the midbrain and the striatum. Therefore, reuptake and diffusion are both critical in the midbrain and striatum, but the D_2-IPSC is regulated by reuptake. The following results from this study are limited to my contribution, illustrating the effect of dextran on diffusion of dopamine in free solution and dopamine-mediated currents in the midbrain.

In the context of this dissertation, this study demonstrated that dopamine release sites must be closely apposed to D_2 receptors in order to produce D_2-IPSCs.

3.1 CONTROL OF EXTRACELLULAR DOPAMINE AT DENDRITE AND AXON TERMINALS

Christopher P. Ford[1], **Stephanie C. Gantz**[1], Paul E. M. Phillips[2], and John T. Williams[1]

[1]Vollum Institute
Oregon Health and Science University
3181 SW Sam Jackson Park Road
Portland, OR 97239

[2]Department of Psychiatry and Behavioral Sciences
Department of Pharmacology
University of Washington
Seattle, WA, 98195

Acknowledgements: This work was supported by National Institutes of Health Grants DA026417 (C.P.F.), DA04523 (J.T.W.), and DA17155 and DA24140 (P.E.M.P.).

[A portion of this manuscript is presented as published in (Ford *et al.*, 2010), *The Journal of Neuroscience*, May 19, 2010, 30(20):6975-6983]

Results

Ford *et al*. (2010) states:

> Clearance of extracellular dopamine is dependent on the combination of diffusion and reuptake…The diffusion of dopamine in free solution was slowed by the addition of dextran to the extracellular solution (10%, 40 kDa). Dopamine was applied by iontophoresis at different distances away from the [fast-scan cyclic voltammetry] FSCV carbon fiber, and the duration was compared in the absence and presence of the dextran-containing solution. When the tip of the iontophoretic electrode was within ~3 μm of the carbon fiber, dextran increased the duration of the dopamine transient at the carbon fiber to 156 ± 17% of control half-width (n = 6, $p < 0.01$). When dopamine was iontophoresed from a distance of 3 μm, dextran did not alter the latency to onset or the peak concentration of dopamine (n = 6, $p > 0.05$) ([Figure 3.1]*A*), indicating that dextran did not have a significant effect on the electrochemical detection of dopamine. As the iontophoretic electrode was moved farther from the carbon fiber, the amplitude and the time course of the rise and fall of dopamine were reduced in the presence of dextran. When the iontophoretic electrode was ~50 μm from the carbon fiber, the peak concentration of dopamine was decreased to 48 ± 9% of control (n = 6, $p < 0.01$), the time to peak increased to 200 ± 15% of control (n = 6, $p < 0.001$), and the duration increased to 350 ± 42% of control (n = 6, $p < 0.0001$) ([Figure 3.1]*B*). This indicates that dextran slowed the free diffusion of dopamine and altered the kinetics of the extracellular dopamine transient as a function of distance.

Next, dopamine release was evoked in the VTA with a train of electrical stimuli (5 at 40 Hz) and dopamine release was detected electrochemically (FSCV) in the presence and absence of dextran. To prevent D_2 autoreceptor-mediated inhibition, the D_2 receptor antagonist, sulpiride (200 nM), was included in the external solution. In the VTA, dextran significantly slowed the kinetics of the dopamine transient, affecting both the time-to-peak and increasing the half-width. In addition, dextran reduced the peak concentration of dopamine. These results suggest that once released, dopamine diffuses over extended distance before it is detected by the FSCV fiber (data not shown). Impairing dopamine reuptake with the dopamine transporter blocker, cocaine (1 μM), significantly increased the peak concentration of dopamine and slowed the dopamine transient (data not shown). The conclusion is that in the VTA, diffusion and reuptake regulates the presence of dopamine in the extracellular, presumed extrasynaptic space.

Ford *et al.*, (2010) continues:

> …Given that diffusion of extracellular dopamine was slowed by dextran in the VTA, the kinetics of the D_2-IPSC also were expected to slow in the presence of dextran. Surprisingly, however, the kinetics of the D_2-IPSC did not change by the addition of dextran to the extracellular solution ([Figure 3.2]*A*). The amplitude, time to peak, and half-width of D_2-IPSCs were the same in control and dextran solutions (control amplitude: 36 ± 4 pA, $n = 12$; dextran: 33 ± 5 pA, $n = 12$; $p > 0.05$; time to peak control: 320 ± 7 ms, $n = 12$; dextran: 346 ± 11, $n = 12$, $p > 0.05$; half-width control: 89 ± 26 ms, $n = 11$; dextran: 96 ± 34 ms, $n = 12$, $p > 0.05$) ([Figure 3.2]*A*, *B*). As a positive control, in the same slices where dextran

failed to alter the dopamine IPSC, the outward current induced by iontophoretic application of dopamine was dramatically slowed (time to peak control: 625 ± 44 ms, $n = 16$; dextran: 1093 ± 61, $n = 14$, $p < 0.001$; half-width control: 870 ± 47 ms, $n = 15$; dextran: 1325 = 115 ms, $n = 13$, $p < 0.05$) ([Figure 3.2]*A*,*C*). The outward current evoked by iontophoretic application of dopamine has a longer latency and slower kinetics than the IPSC (Beckstead *et al.*, 2004). This is because the location of the iontophoretic tip is further from D_2 receptors than the point of dopamine release mediating the IPSC (Beckstead *et al.*, 2004). As the D_2-IPSC was insensitive to the effects of dextran, these results indicate that synaptically released dopamine does not diffuse over extended distances before binding to D_2 receptors. Thus, postsynaptic D_2 receptors are localized near the site of dopamine release.

Finally, as reported previously (Beckstead *et al.*, 2004; Ford *et al.*, 2006, 2009), cocaine (1 μM) increased the amplitude and time course of the D_2-IPSC as well as the outward current evoked by iontophoretic application of dopamine ([Figure 3.2]*A*, *C*). Thus, transporters tightly regulate the presence of dopamine at postsynaptic receptors during transmission.

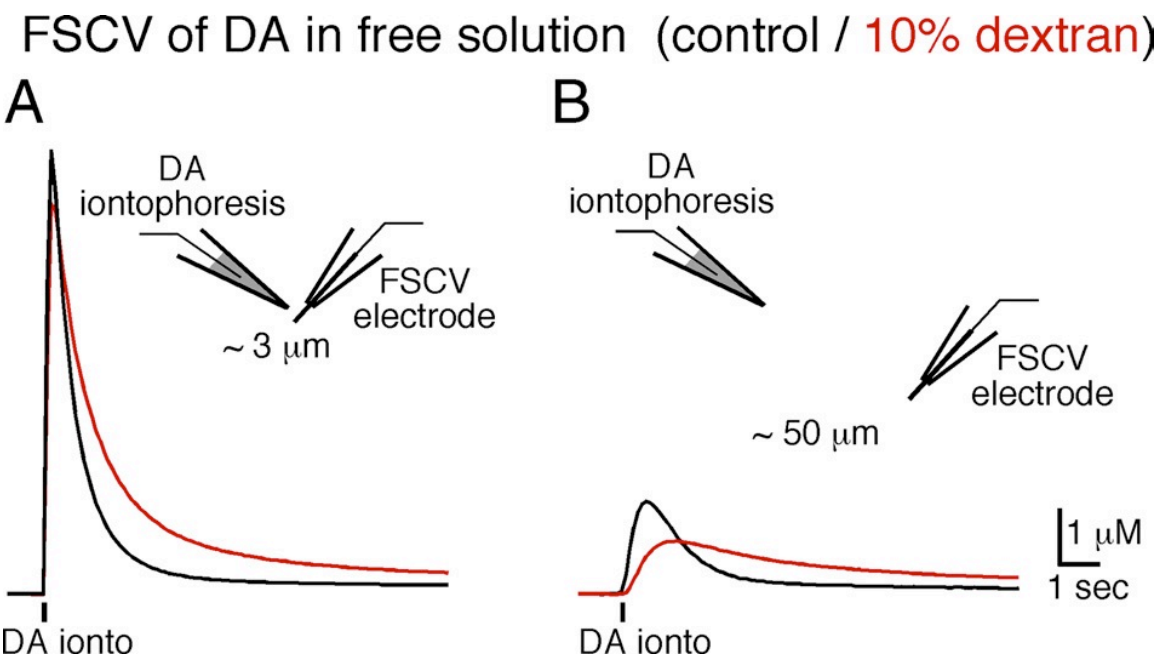

Figure 3.1. Extracellular dextran slows the free diffusion of dopamine.

FSCV measurement of free dopamine in solution. Dopamine was applied by iontophoresis onto a carbon fiber and detected using FSCV with a voltage waveform of -0.4 to 1.3 V at 400 V/s. Dopamine was ejected onto carbon fibers in control solution (black) and in a dextran-containing solution (10% w/v, red). A, B, Representative traces where dopamine was ejected onto the carbon fiber from a distance of ~3 μm (A) or ~50 μm (B). Dextran thus slowed the time to peak and increased the duration of the dopamine transient as a function of distance.

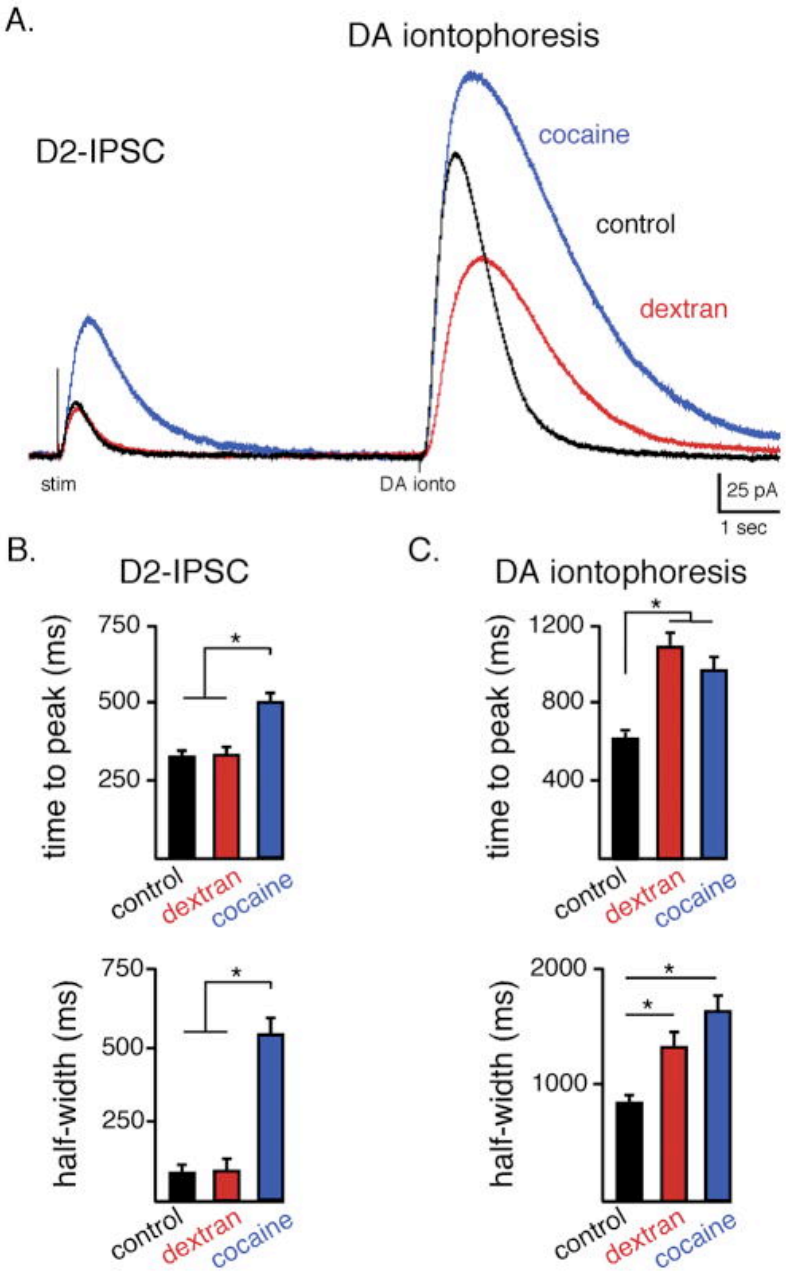

Figure 3.2. Slowing diffusion of dopamine did not alter the D_2-IPSC.

(A) Representative traces illustrating single stimulation evoked D_2-IPSCs and the current evoked by the iontophoretic application of dopamine under control conditions (black), in the presence of dextran (10%) (red), and cocaine (1 μM) (blue). Note the lack of effect of dextran on D_2-IPSCs, yet the increase in amplitude, time to peak and half-width in the presence of cocaine. The current evoked by the iontophoresis of dopamine however is diminished and slowed in the presence of dextran and increased and slowed in the presence of cocaine. (B) Summarized data illustrating the time to peak and half-width of D_2-IPSCs in the above conditions. (C) Summarized data illustrating the time to peak and half-width for the currents evoked by the iontophoretic application of dopamine. * = $p < 0.05$, one-way ANOVA (Tukey test).

Chapter 4 D_2 RECEPTORS MEDIATE SPONTANEOUS IPSCs

PREFACE

This chapter describes spontaneous D_2 receptor-mediated synaptic currents produced by vesicular dopamine release in mouse brain slices.

I conducted this study under the mentorship and assistance of Dr. John T. Williams. I designed and performed the experiments, analyzed and illustrated data, and prepared the manuscript. James R. Bunzow generated the transgenic Flag-D_2 receptor mouse line used in this study. I developed the protocol for Flag-tagged D_2 receptor immunohistochemisty with the help of Dr. Seksiri Arttamangkul.

This study is the first demonstration of spontaneous miniature synaptic currents mediated by a metabotropic G protein-coupled receptor. The results show that in the absence of stimulation, spontaneous miniature D_2 receptor/GIRK-dependent IPSCs occur in dopamine neurons. The kinetics of electrically evoked and spontaneous D_2-IPSCs were similar. The spontaneous D_2-IPSCs (D_2-sIPSCs) were not dependent on calcium entry or intracellular calcium stores. The frequency and amplitude of D_2-sIPSCs were modulated by pre- and post-synaptic mechanisms and were plastic, changing after a single *in vivo* exposure to cocaine. Lastly, D_2-sIPSCs transiently inhibit pacemaker activity of dopamine neurons, suggesting functional importance.

In the context of this dissertation, this chapter constituted the characterization of spontaneous D_2 receptor-mediated IPSCs in dopamine neurons, providing the framework for leveraging their occurrence to understand the dopamine synapse.

4.1 SPONTANEOUS INHIBITORY SYNAPTIC CURRENTS MEDIATED BY A G PROTEIN-COUPLED RECEPTOR

Stephanie C. Gantz[1], James R. Bunzow[1], and John T. Williams[1]

[1]Vollum Institute
Oregon Health and Science University
3181 SW Sam Jackson Park Road
Portland, OR 97239

Acknowledgements: We thank Dr. C.P. Ford for comments on the work and manuscript. Supported by NIH DA04523.

[This manuscript is presented as published in (Gantz *et al.*, 2013), *Neuron*, June 5, 2013, 78:807-812]

Summary

G protein-coupled receptors (GPCRs) affect many physiological processes by modulating both intrinsic membrane conductance and synaptic transmission. This study describes spontaneous miniature inhibitory postsynaptic currents mediated by vesicular dopamine release acting locally on metabotropic D_2 receptors leading to the activation of a G protein-coupled inwardly rectifying potassium conductance. Thus, individual exocytotic events result in spontaneous GPCR-mediated transmission similar to synaptic activation of classical ligand-gated ion channels.

Introduction

The discovery of miniature endplate potentials at the neuromuscular junction critically shaped the understanding of neurotransmitter release and synaptic transmission. Since its discovery, spontaneous neurotransmitter release has been described at many synapses in the mammalian central nervous system, but only where ligand-gated ion channels underlie the postsynaptic response. While a number of G protein-coupled receptors (GPCRs) are known to mediate inhibitory postsynaptic currents (IPSCs) by activating inwardly rectifying K^+ channels (GIRKs), these are thought to result from diffusion of transmitter to extrasynaptic sites (Isaacson *et al.*, 1993; Otis and Mody, 1992). The slow intrinsic kinetics of GPCR signaling and the temporal dispersion of activation resulting from long distance diffusion may obscure GPCR-mediated miniature synaptic events.

Electrical stimulation in the midbrain evokes vesicular dopamine release. The lack of structural evidence for axon terminals in the rat substantia nigra pars compacta

(Bayer and Pickel, 1990; Groves and Linder, 1983) led to the theory that dopamine release, in this region, arises from the somatodendritic compartment. Somatodendritic release has been measured using multiple assays (Fortin *et al.*, 2006; Heeringa and Abercrombie, 1995; Mendez *et al.*, 2011), including whole-cell recording of a D_2 receptor-dependent inhibitory postsynaptic current (IPSC) (Beckstead *et al.*, 2004). Spontaneous, or unstimulated, somatodendritic release of dopamine has been detected by amperometry and high-performance liquid chromatography from midbrain dopamine neurons in brain slices (Jaffe *et al.*, 1998) and cultures (Fortin *et al.*, 2006), but there is no evidence that this spontaneous release activates a GIRK-mediated conductance. This study reports spontaneous miniature IPSCs (sIPSCs) in dopamine neurons from mouse substantia nigra pars compacta (SNc). The results reveal that spontaneous vesicular dopamine release produced sIPSCs by local D_2 receptor activation of GIRK channels that were not dependent on voltage-gated sodium and calcium channels or intracellular calcium stores.

Results and Discussion

Whole-cell voltage-clamp recordings were made from SNc dopamine neurons in horizontal midbrain slices from wild type mice, in the presence of NMDA, AMPA, $GABA_A$, $GABA_B$, and nACh receptor antagonists. Spontaneous IPSCs occurred approximately 1 event/min (Figure 4.1A, Figure 4.3A, 3D), similar to the low frequency of spontaneous amperometric events recorded from SNc neurons (Jaffe *et al.*, 1998). The sIPSCs were abolished by the D_2 receptor antagonist, sulpiride (300 nM, Figure 4.1A). A single electrical stimulus evoked D_2 receptor-mediated IPSCs (eIPSC) (Figure 4.1B and 1C). Blockade of GIRK conductance with Ba^{2+} decreases the current induced by

dopamine in SNc dopamine neurons (Lacey *et al.*, 1987). Ba^{2+} (100 μM) eliminated both evoked and spontaneous IPSCs ($p = 0.009$, $n = 6$, Figure 4.1B). Thus, spontaneous IPSCs are the result of D_2 receptor activation of GIRK channels.

The rise time of the sIPSCs and eIPSCs were identical ($p = 0.76$). However, the duration of sIPSCs, measured at 20% of the peak, was shorter (69%) than the eIPSC ($p < 0.001$, eIPSCs $n = 77$ and sIPSCs $n = 76$, Figure 4.4D). The rise time and duration of sIPSCs were similar to the current evoked using fast application of a high concentration of dopamine (≥ 10 μM) onto membrane patches (Ford *et al.*, 2009). Thus, sIPSCs likely resulted from a sharp rise of a high concentration of dopamine, inconsistent with extended diffusion away from the release site. To compare the amplitude of sIPSCs to eIPSCs, minimal stimulation was employed to evoke eIPSCs with the smallest resolvable amplitude over baseline noise. The eIPSC amplitude distribution from minimal stimulation was normal ($p = 0.4$, mean of 8.8 pA, median of 8.4 pA, Figure 4.1D and 1 E). The amplitude distribution of sIPSCs was right-skewed ($p < 0.001$, mean of 9.2 pA, median of 7.9 pA, Figure 4.1D, 1E, Figure 4.3B) such that the distributions of eIPSC and sIPSC amplitudes were statistically different ($p = 0.007$, $n = 188$ eIPSCs and 1137 sIPSCs). However, the median amplitude of sIPSCs was similar to eIPSCs evoked by minimal stimulation ($p = 0.07$). Although these results are suggestive of a quantal event, the slow kinetics of D_2 IPSCs and low frequency of sIPSCs necessitated the combination of data from multiple cells and therefore limit further quantitative analysis. Taken together, the results suggest that, with the exception of some larger sIPSCs, the current elicited by a single resolvable release event was similar whether the release was spontaneous or evoked.

Next, the mechanism of spontaneous dopamine release was compared to that of electrically evoked release. Disruption of the vesicular monoamine transporter with reserpine (1 μM, > 20 min) eliminated sIPSCs ($p = 0.03$, Figure 4.2A), confirming that spontaneous dopamine release is vesicular. Application of tetrodotoxin (TTX, 600 nM) or Cd^{2+} (100 μM) abolished eIPSCs, but TTX failed to alter the frequency ($p = 0.40$, Figure 4.2B) or amplitude ($p = 0.95$, Figure 4.2C) of sIPSCs, demonstrating sIPSCs were not dependent on action potentials. Likewise, sIPSCs persisted in Cd^{2+}, with no change in frequency ($p = 0.35$, Figure 4.2D), indicating sIPSCs were not dependent on calcium entry via voltage-gated calcium channels. There are conflicting reports of the role of intracellular calcium stores on the release of dopamine in the midbrain (Courtney *et al.*, 2012; Ford *et al.*, 2010; Patel *et al.*, 2009). To determine if spontaneous dopamine release was dependent on intracellular calcium stores, the sarco/endoplasmic reticulum Ca^{2+}-ATPase (SERCA) inhibitor cyclopiazonic acid (CPA) was used to deplete calcium stores. The application of CPA (10 μM, > 3 min) had no effect on the frequency of sIPSCs ($p = 0.41$, Figure 4.2D and 2E), whereas previous experiments found that inositol triphosphate (IP3)-mediated SK currents in dopamine neurons were eliminated (Ford *et al.*, 2010). Perfusion with calcium-free ACSF reduced the frequency, but did not eliminate the sIPSCs ($p = 0.04$, Figure 4.2D and 2F). While the established theory suggests that evoked and spontaneous IPSCs are the result of somatodendritic dopamine release, the site of release remains to be determined. Furthermore, the question of whether a single neuron releases dopamine onto itself has not been resolved. The experimental conditions (voltage-clamp and strong intracellular calcium buffering with BAPTA) make it unlikely that eIPSCs are induced by release from the recorded neuron. However, it remains

possible that sIPSCs may result from dopamine release from the recorded neuron, since spontaneous release is TTX-insensitive and does not require voltage-gated calcium channels.

The amplitude and frequency of spontaneous miniature postsynaptic currents can fluctuate due to presynaptic and postsynaptic mechanisms, including differences in transmitter content (Frerking *et al.*, 1995), probability of release (Fatt and Katz, 1952), transmitter clearance (Liu *et al.*, 1999), and postsynaptic receptor/channel availability (Edwards *et al.*, 1990). Cytosolic and vesicular dopamine levels are increased after treatment with the catecholamine precursor L-DOPA (Pothos *et al.*, 1998), thus enhancing the eIPSC (Beckstead *et al.*, 2004). Incubation in L-DOPA (10 μM, 10 min) increased the frequency and amplitude of sIPSCs ($p < 0.001$, Figure 4.3A and 3B). L-DOPA can be taken up by 5-HT neurons, metabolized to dopamine (Arai *et al.*, 1994), and in parkinsonian rats, released from 5-HT terminals (Carta *et al.*, 2007). The increase in frequency of sIPSCs following treatment with L-DOPA could involve aberrant dopamine release from 5-HT terminals. This possibility was examined with the application of the selective 5-HT1 agonist, 5-CT, since activation of 5-HT1 receptors potently inhibits release from 5-HT terminals (Bobker and Williams, 1989; Carta *et al.*, 2007). Application of 5-CT (1 μM) had no effect on the frequency of the sIPSCs (ACSF: 0.6 ± 0.2 per min, 5-CT: 1.0 ± 0.3 per min, paired two-tailed *t* test, $p = 0.3$, $n = 7$ cells) even after treatment of slices with L-DOPA (Control: 0.8 ± 0.1 per min, L-DOPA: 3.7 ± 0.7 per min, Two-way ANOVA, $p = 0.96$, $n = 7$ cells). Activation of adenylyl cyclase with forskolin increased the amplitude of eIPSCs (Beckstead *et al.*, 2007). Forskolin (1 μM) also increased the frequency ($p < 0.05$, Figure 4.3D) and amplitude of sIPSCs ($p =$

0.005, median of 8.7 pA). The uptake of dopamine by dopamine transporters is the primary mechanism of terminating dopamine signaling in the midbrain (Ford *et al.*, 2010). In the presence of cocaine, a nonspecific monoamine transporter blocker, the clearance of extracellular dopamine is prolonged (Ford *et al.*, 2010), potentiating the eIPSC (Beckstead *et al.*, 2004; Ford *et al.*, 2009; 2010). Cocaine (300 nM), in the presence of forskolin (1 μM), further increased the amplitude ($p < 0.001$, median of 10.0 pA, Figure 4.3C) and frequency ($p < 0.001$, Figure 4.3D) of sIPSCs.

The role of postsynaptic receptor availability on the frequency and amplitude of sIPSCs was examined using experiments with a transgenic mouse strain (TH-hD_2S) that expressed a human D_2 receptor (short isoform) with an amino-terminal FLAG epitope targeted to catecholamine neurons, in addition to endogenous D_2 receptors (See TH-hD_2S Transgenic Mice). Functional coupling of D_2 receptors to GIRK channels in TH-hD_2S mice was evaluated by measuring the maximal D_2 receptor-mediated outward currents evoked by iontophoretic application of dopamine onto dopamine neurons, normalized to capacitance (dopamine current density). The dopamine current density of SNc neurons in wild type mice was 8.9 ± 0.4 pA/pF ($n = 37$), consistent with previously reported values (Gantz *et al.*, 2011), and the dopamine current density in TH-hD_2S mice was elevated (14.6 ± 1.0 pA/pF, $p < 0.01$, $n = 32$). There was no difference in current density evoked by the $GABA_B$ agonist, baclofen, in TH-hD_2S (11.1 ± 0.9 pA/pF, $p = 0.57$, $n = 14$) compared to wild type mice (12.2 ± 0.8 pA/pF, $n = 19$). Thus, the increased expression of D_2 receptors in the TH-hD_2S mice did not interfere with the activation of GIRK by other GPCRs. The frequency and amplitude of sIPSCs from dopamine neurons in TH-hD_2S mice was greater than those from wild type mice ($p < 0.001$, Figure 4.3A and 3E). These

results suggest that the level of D_2 receptor expression is factor in determining the amplitude of the IPSC, although it is not known to what extent the overexpression of D_2 receptors has on other processes such as tyrosine hydroxylase expression, dopamine synthesis, or the expression of dopamine transporters. Taken together, the results indicate that the frequency and amplitude of spontaneous D_2 receptor-mediated IPSCs are altered by both pre- and postsynaptic mechanisms.

Exposure to drugs of abuse causes morphological and functional changes to midbrain dopamine neurons (Heikkinen *et al.*, 2008; Saal *et al.*, 2003; Sarti *et al.*, 2007). Many of these changes occur after a single exposure, including potentiated spontaneous GABA- (Melis *et al.*, 2002) and glutamate- (Ungless *et al.*, 2001) synaptic currents. To determine if dopamine-dependent sIPSCs were similarly plastic, mice were treated with a single dose of cocaine (20 mg/kg, i.p.). One day after treatment, the dopamine current density in SNc neurons from cocaine-treated mice was elevated (12.3 ± 0.7 pA/pF, $p < 0.01$, $n = 26$), and the frequency and amplitude of sIPSCs were increased ($p < 0.01$, Figure 4.3A; $p < 0.001$, Figure 4.3F). There was no change in baclofen current density (11.3 ± 0.8 pA/pF, $p = 0.57$, $n = 15$). Therefore spontaneous dopamine transmission, like GABA- and glutamate-dependent transmission, was increased by a single exposure to cocaine.

In vitro, dopamine neurons fire action potentials in a regular, pacemaker pattern. Electrical stimulation causes a sulpiride-sensitive pause in firing, indicating eIPSCs inhibit spontaneous firing (Beckstead and Williams, 2007; Beckstead *et al.*, 2004; Courtney *et al.*, 2012). Loose cell-attached recordings were made from SNc dopamine neurons from wild type mice to assess if sIPSCs can inhibit firing. A single electrical

stimulus caused a pause (e-pause) in pacemaker firing (Figure 4.4A and 4C). Spontaneous pauses (s-pause) occurred approximately 1 event/min (Figure 4.4A and 4B). Exposure to L-DOPA (10 μM, 10 min) increased the frequency of s-pauses ($p < 0.05$, $n =$ 13 cells, Figure 4.4A and 4B). The s-pauses were abolished by sulpiride (600 nM, $p <$ 0.01, Figure 4.4A), indicating that the s-pauses were the result of D_2 receptor activation. The duration of the pauses was calculated by subtracting the mean inter-spike interval (ISI) from the time between two action potentials (Figure 4.4C). The duration of the s-pause was shorter (71%) than the e-pause ($p < 0.01$, $n = 59$ e-pauses and 50 s-pauses, Figure 4.4D). It is interesting to note that the difference in duration is the same as that when comparing the evoked and spontaneous IPSCs (Figure 4.4D). After L-DOPA, the duration of the s-pause remained shorter than the e-pause (74% of e-pause, $p < 0.001$, $n =$ 130 e-pauses and 255 s-pauses, Figure 4.4E). In a separate set of experiments, reserpine was used to verify that vesicular release of dopamine underlies the s-pauses. Application of reserpine (1 μM, 10 min) dramatically reduced the frequency of s-pauses (L-DOPA: 2.43 ± 0.8 per min; reserpine: 0.15 ± 0.1 per min; paired two-tailed *t* test, $p = 0.03$, $n = 8$ cells). Taken together, these results indicate that sIPSCs and spontaneous pauses result from spontaneous dopamine release. Thus, spontaneous release of dopamine in brain slices influences the firing pattern of dopamine neurons.

The presence of spontaneous miniature GIRK-mediated IPSCs is the strongest evidence to date that signaling mediated by GPCRs can be similar to transmission mediated by ligand-gated ion channels. First, the results of this study demonstrate that despite the slow intrinsic signaling kinetics of GPCR activation, these receptors can signal in a point-to-point manner, where the presynaptic site of release is located very

close to postsynaptic receptors. Second, as in other neurotransmitter systems, the postsynaptic currents elicited by evoked and spontaneous dopamine release are largely indistinguishable. Lastly, spontaneous D_2 receptor-mediated transmission was altered by pre- and postsynaptic mechanisms and was plastic, changing after a single *in vivo* exposure to cocaine. Thus, the factors that regulate synaptic transmission mediated by D_2 receptors and ligand-gated ion channels are similar. It is likely that spontaneous GIRK-dependent IPSCs are common, adding an unrealized role of GPCR-dependent signaling in neuronal regulation.

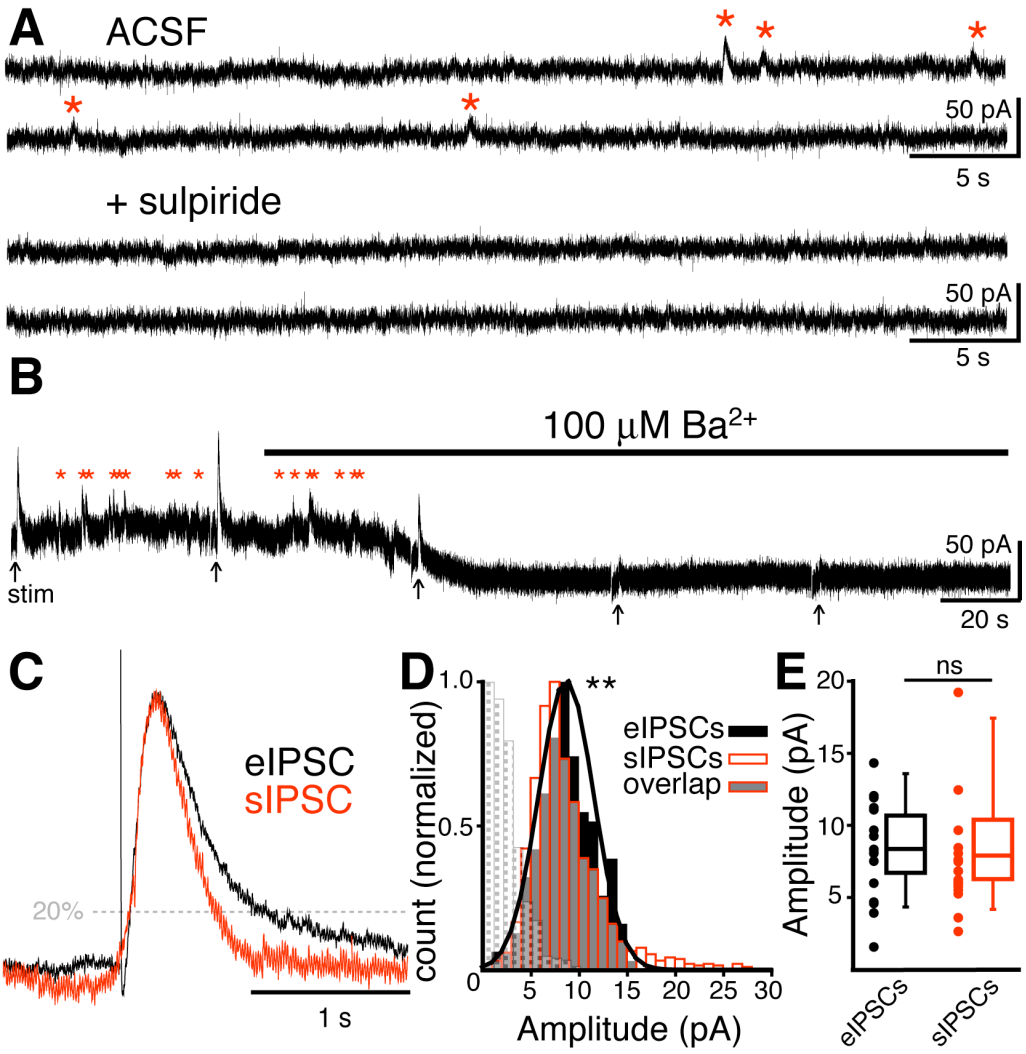

Figure 4.1. D_2 receptor activation of GIRK conductance mediates spontaneous IPSCs.

(A) Representative traces of sIPSCs (red stars) recorded in the absence of stimulation, blocked by the D_2 receptor antagonist, sulpiride (300 nM). (B) Ba2+ blocked eIPSCs (arrows) and sIPSCs (red stars) recorded in forskolin (1 μM) and cocaine (300 nM) (See Figure 4.3D). Stimulation artifacts were blanked for clarity. The inward current produced by $BaCl_2$ (42 ± 8.5 pA, n = 5 cells) was present in sulpiride (45 ± 10.3 pA, $p = 0.84$, n = 7 cells), thus not related to D_2 receptor activation. (C) Average eIPSC and sIPSC scaled to the peak. (D) Histograms of minimal stimulation eIPSC and sIPSC amplitudes in ACSF (1 pA bins, two-sample KS test, n = eIPSCs:188 and sIPSCs:1137) along with baseline noise (checked) and Gaussian fit of eIPSC amplitudes (black line). Vertical axes have been scaled to normalize for n (see Detection and measurement of spontaneous D_2-IPSCs, p.12). (E) Box-and-whisker plots of eIPSC amplitudes from minimal stimulation and sIPSCs, box limits designate 25 and 75 percentiles, central line represents the median, and whisker ends show 5 and 95 percentiles (Two-tailed Mann-Whitney U test). Values from a single experiment are shown by the filled circles. ns indicates not significant and $^{**}p < 0.01$.

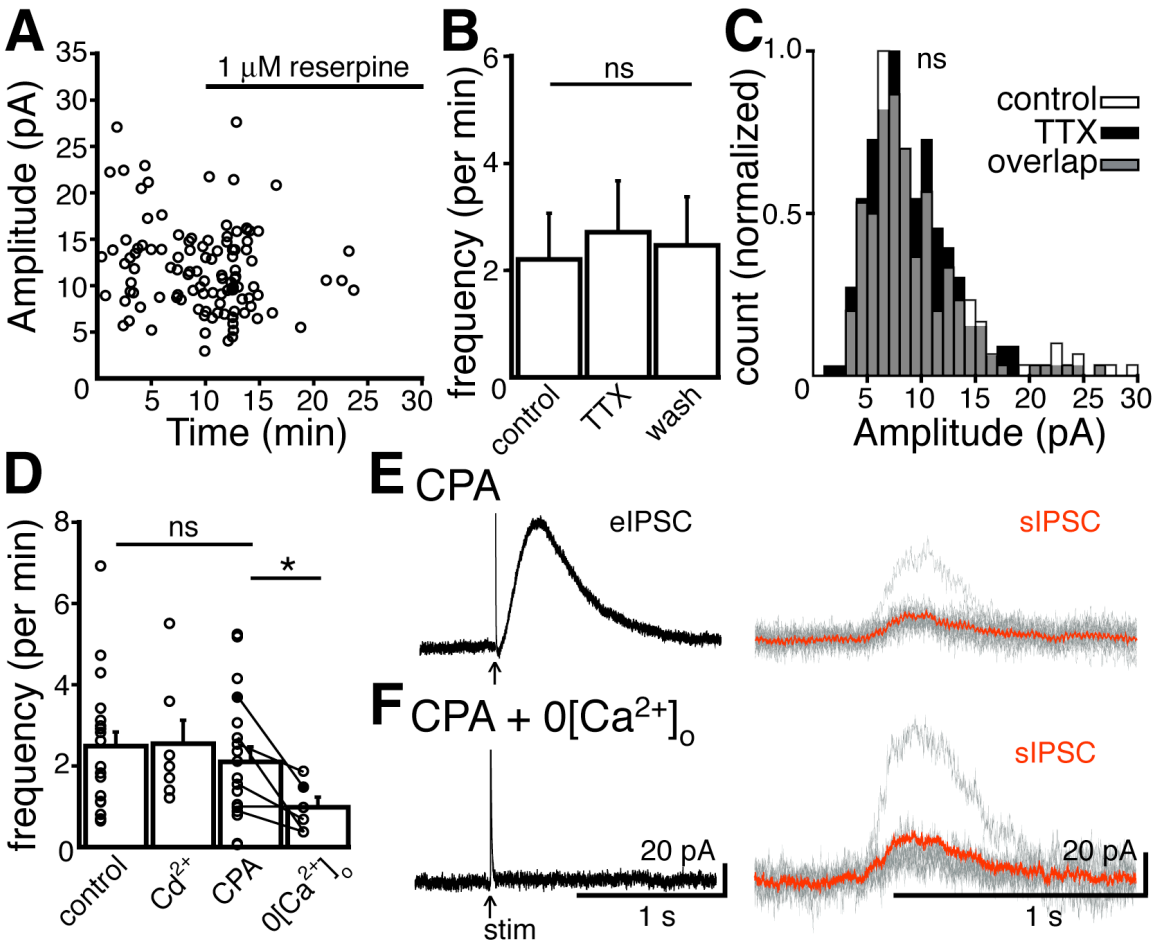

Figure 4.2. Vesicular dopamine release underlying spontaneous IPSCs is resistant to TTX, inhibition of voltage-gated calcium channels, and depletion of intracellular stores of calcium.

(A) Plot of spontaneous IPSC amplitude versus time from a single experiment showing the inhibition by reserpine. (B) Blocking action potentials with TTX (600 nM) did not alter the frequency (Repeated measures ANOVA, n = 5 cells) or (C) amplitude of sIPSCs (1 pA bins, two-sample KS test, n = sIPSCs in control:245 and TTX:193). Vertical axes have been scaled to normalize for n (See Detection and measurement of spontaneous D_2-IPSCs, p.12). (D) Cd^{2+} and CPA did not alter the frequency of sIPSCs. Removing extracellular calcium ($0[Ca^{2+}]_o$) did not eliminate the sIPSCs (paired two-tailed t tests, n = cells in Cd^{2+}:6, CPA:16, and $0[Ca^{2+}]_o$:6. (E) Traces from a single experiment (filled circles in D) showing the average eIPSC and sIPSCs (average is red) recorded in CPA. (F) Removal of extracellular Ca^{2+} abolished the eIPSC but sIPSCs persisted. All recordings were made in the presence of forskolin (1 µM) and cocaine (300 nM) to increase frequency of sIPSCs (see Figure 4.3) Mean ± SEM. ns indicates not significant and $*p < 0.05$.

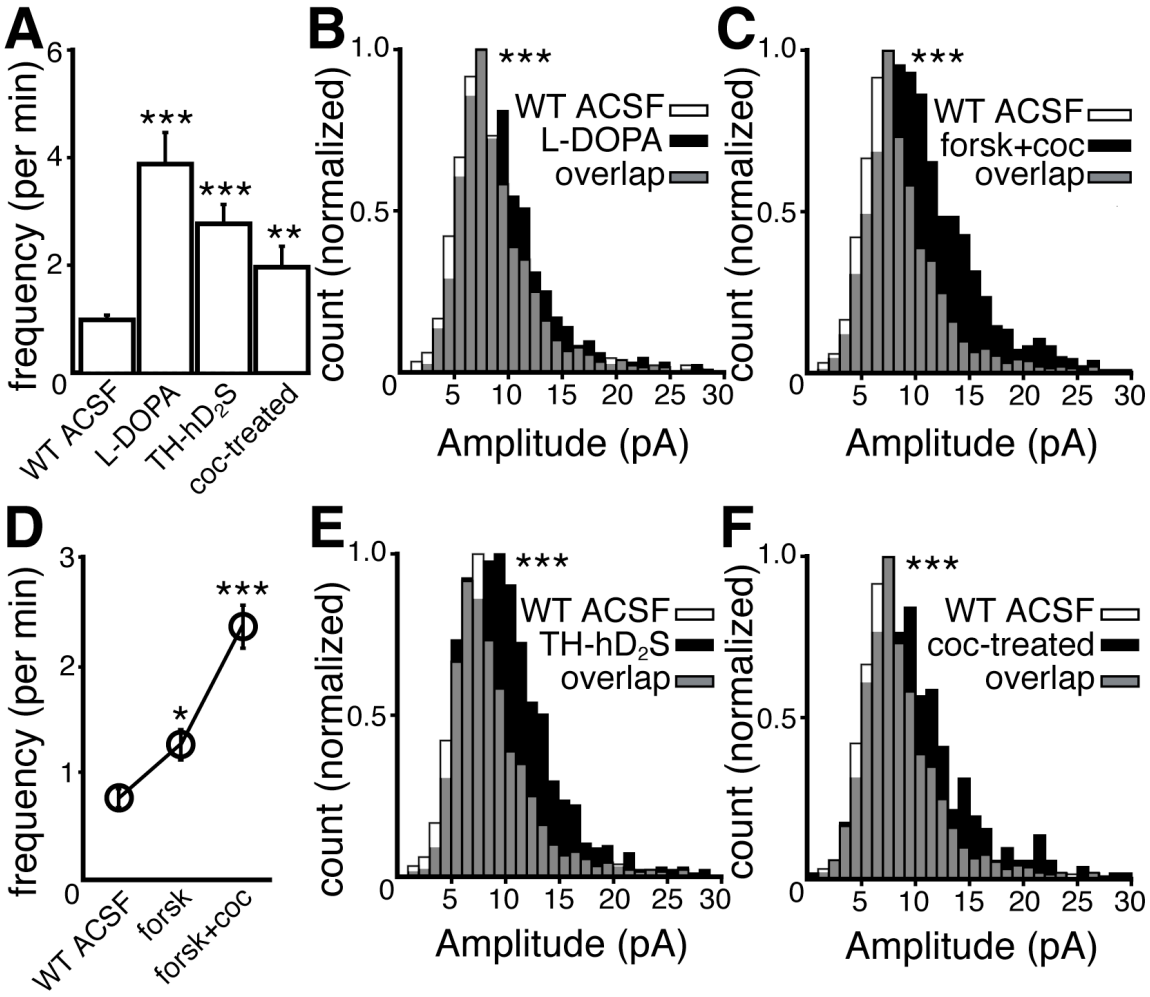

Figure 4.3. The frequency and amplitude of spontaneous IPSCs are modulated by pre- and postsynaptic mechanisms and are plastic.

(A) Frequency of sIPSCs per minute (Kruskal-Wallis test, n = cells in WT ACSF:95, L-DOPA:12, TH-hD_2S: 29, and coc-treated:20) Mean ± SEM. (D) Frequency of sIPSCs per minute was increased by forskolin and the subsequent addition of cocaine (forsk+coc) (Friedman test, n = 53 cells), Mean ± SEM. (B, C, E, F) Amplitude of sIPSCs (1 pA bins, two-sample KS test, n = sIPSCs in WT ACSF:1137, L-DOPA:939, forskolin+cocaine:1605, TH-hD_2S:1223, and coc-treated:400). Vertical axes have been scaled to normalize for n (See Detection and measurement of spontaneous D_2-IPSCs, p.12). *$p < 0.05$, **$p < 0.01$ and ***$p < 0.001$.

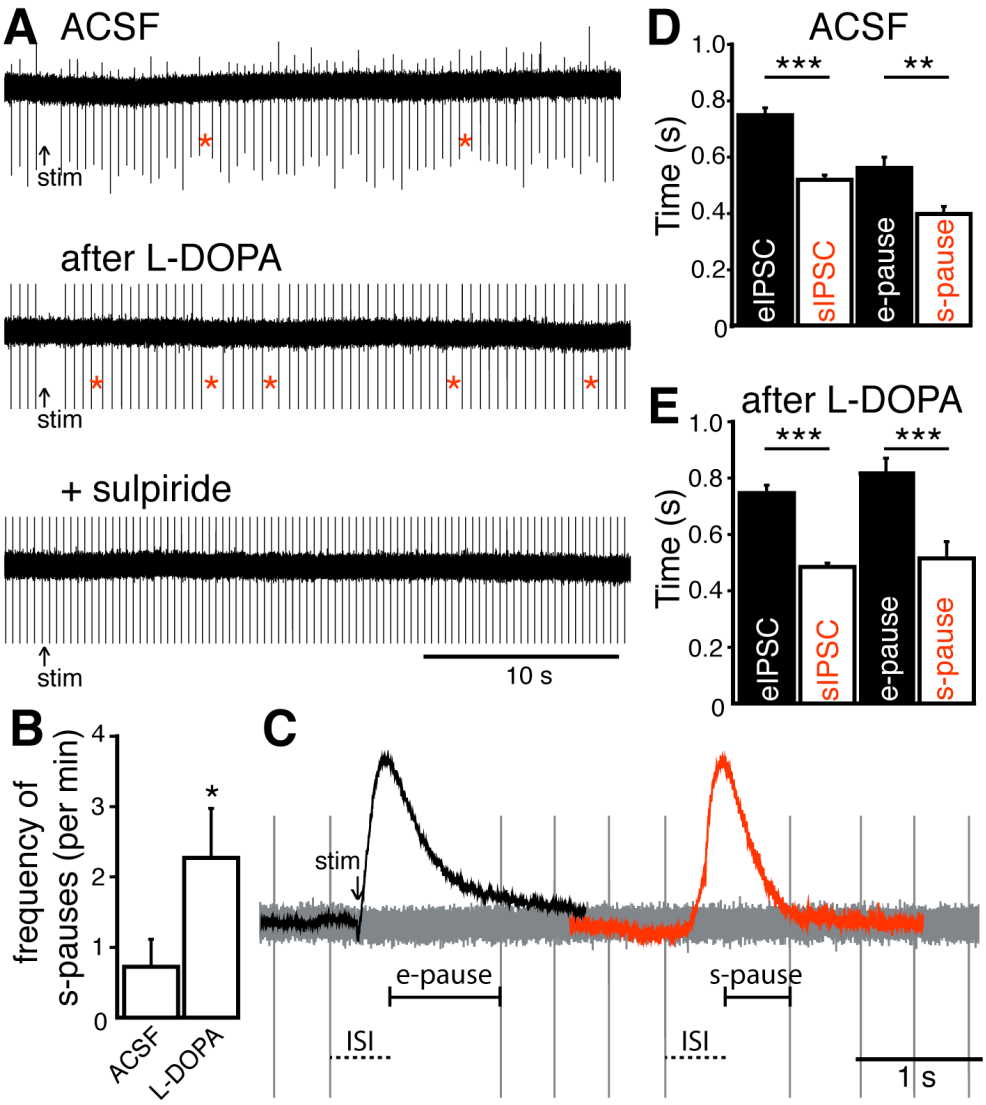

Figure 4.4. Spontaneous IPSCs transiently inhibit pacemaker firing.

(A) Loose cell-attached recordings from an experiment showing the pause in firing after electrical stimulation (arrow, e-pause) and spontaneous pauses (red stars, s-pause), blocked by the D_2 receptor antagonist, sulpiride (600 nM). (B) Frequency of spontaneous pauses per minute increased with exposure to L-DOPA and were abolished by sulpiride (Repeated measures ANOVA, n = 13 cells) (C) Loose cell-attached recording with scaled eIPSC and sIPSC superimposed. eIPSC was positioned by aligning the time of stimulation in cell-attached and whole-cell recording (arrow). sIPSC was positioned based on alignment of eIPSC rise time with respect to ISI. (D and E) Duration of eIPSC, sIPSC (both measured at 20% peak amplitude, see Figure 4.1C), e-pause, and s-pause in ACSF and after exposure to L-DOPA (Kruskal-Wallis tests, ACSF n = eIPSCs:77, sIPSCs:76, e-pauses:59, s-pauses:50; L-DOPA n = eIPSCs:41, sIPSCs:71, e-pauses:130, s-pauses:255). In traces, stimulation artifacts were blanked and action potential currents were truncated for clarity. Mean ± SEM. *$p < 0.05$, ** $p < 0.01$, and ***$p < 0.001$.

4.2 ADDITIONAL EXPERIMENTS

Potentiation of spontaneous D_2-IPSCs after *in vivo* cocaine exposure may involve protein kinase A.

After a single *in vivo* exposure to cocaine, the frequency and amplitude of spontaneous D_2-IPSCs was increased (Figure 4.3). Exposure to drugs of abuse is known to potentiate the amplitude and frequency of GABAergic synaptic currents by increasing the probability of GABA release via protein kinase A- (PKA) dependent pathways (Bonci and Williams, 1997; Melis *et al.*, 2002). Data are presented that demonstrate activation of PKA with forskolin (1 μM) increased the amplitude of the evoked D_2-IPSC and also increased the frequency and amplitude of spontaneous D_2-IPSCs. In slices from cocaine-treated mice, forskolin increased the evoked D_2-IPSC (142.9 ± 11.6% of baseline, n = 9), to a similar extent to that observed in slices from naïve mice (161 ± 15.8% of baseline, p = 0.46, n = 18, unpaired t test). However, in slices from cocaine-treated mice, forskolin (1 μM) did not increase the frequency or amplitude of spontaneous D_2-IPSCs (ACSF: 1.5 ± 0.3 per min; forsk: 1.8 ± 0.3, p = 0.31, n = 11, paired t test; ACSF: median of 9.1 pA, n = 400 sIPSCs; forsk: median of 9.2 pA, n = 106 sIPSCs, Mann Whitney U test). Thus, the potentiation of spontaneous dopamine transmission after *in vivo* cocaine may involve PKA-dependent pathways. Forskolin, albeit at higher concentrations than used in this study, increases the D_2 receptor-dependent current produced by exogenous dopamine (Beckstead *et al.*, 2009). In this study, exposure to cocaine also increased the maximal D_2 receptor-dependent outward current, so it remains to be determined whether spontaneous dopamine transmission was potentiated by pre- or postsynaptic mechanism(s).

Chapter 5 PRESYNAPTIC COMPONENTS

PREFACE

This chapter describes work towards determining presynaptic sites of dopamine release in the SNc. It begins with direct follow-up studies to the result presented in Chapter 4, that L-DOPA increases the frequency of spontaneous D_2-IPSCs. Then, data are presented that assessed whether spontaneous IPSCs are due to dopamine release from the recorded neuron itself. Next, a study is presented that assessed the ability of 5-HT terminals in the midbrain to release dopamine after L-DOPA.

I conducted this study under the mentorship and assistance of Dr. John T. Williams. I designed and performed experiments, analyzed and illustrated data, and wrote the manuscript. Drs. John T. Williams, Erica S. Levitt, and Nerea Llamosas also performed electrophysiological recordings in the dorsal raphe. Dr. Kim A. Neve provided the AAV-D_2 receptor virus. All co-authors assisted in the preparation of the manuscript.

The results demonstrate that the increase in spontaneous IPSC frequency following L-DOPA is not likely simply an artifact of signal detection. Next, it was determined that spontaneous D_2-IPSCs are, at least not exclusively, autaptic. Lastly, the results demonstrate that L-DOPA augments D_2 receptor-mediated synaptic transmission in the midbrain. The augmentation was largely due to dopamine release from serotonin terminals. In the dorsal raphe, serotonin neurons released dopamine from vesicles after L-DOPA leading to a long-lasting depression in 5-HT-mediated synaptic transmission in the dorsal raphe.

In the context of this dissertation, this chapter is a direct follow-up to results described in Chapter 4. After L-DOPA, serotonin terminals contribute to electrically evoked D_2-IPSCs. However, it is unlikely these terminals participate in spontaneous dopamine transmission, which may be due to their position at a slight distance from D_2 receptors.

5.1 USING L-DOPA TO STUDY THE REGULATION OF DOPAMINE RELEASE

It is commonly considered that pre- and post-synaptic mechanisms govern the frequency and amplitude of spontaneous synaptic currents, respectively. However in the central nervous system, the delineation is less clear. In Chapter 4, data are presented that application of the dopamine precursor, L-DOPA, increases the frequency of spontaneous D_2-IPSCs (Figure 4.3), presumably by increasing the biosynthesis of dopamine. L-DOPA also increased the amplitude of spontaneous D_2-IPSCs (Figure 4.3). L-DOPA has no augmenting effect on the D2 receptor-dependent current produced by iontophoretic application of dopamine (data presented in Chapter 6, Results). The results suggest that the L-DOPA-induced increase in D_2-sIPSC frequency and amplitude occurs primarily through a presynaptic mechanism. The established theory is that evoked and spontaneous D_2 receptor-mediated IPSCs are from somatodendritic dopamine release, but the site of release remains unknown. An increase in frequency of spontaneous D_2-IPSCs following L-DOPA, if not artifactual, could reflect recruitment of other dopamine release sites.

Dopamine content in vesicles is labile

In dopamine neuron cultures and PC 12 cells, L-DOPA increases the quantal size of dopamine release evoked by a high-potassium solution, without increasing the number of exocytotic events (Pothos *et al.*, 1996), suggesting that the vesicular content is labile. To determine if changes in spontaneous D_2-IPSC amplitude could reflect changes in vesicular content, the loading of dopamine into vesicles was disrupted by reserpine (> 5 min, recorded in the presence of 1 μM forskolin and 300 nM cocaine). After 5-10 min in reserpine (1 μM), before spontaneous D_2-IPSCs are abolished, there was a decrease in D_2-sIPSC amplitude (control median: 9.9 pA; after 5' in reserpine median: 8.8 pA, Mann-

Whitney test, $p < 0.001$, n = sIPSCs in control:122 and reserpine:91 from 7 cells, Figure 5.1). In combination with the small increase in amplitude after L-DOPA, these data indicate that changes in vesicle content can be measured by modest changes in spontaneous D_2-IPSC amplitude.

L-DOPA increases the frequency of spontaneous D_2-IPSCs

In order to assess whether the increase in frequency could be an artifact of better detection of spontaneous D_2-IPSCs due to the increase in amplitude, the effect of L-DOPA was examined in dopamine neurons from TH-hD_2S mice. TH-hD_2S mice overexpress D_2 receptors and the basal amplitude of spontaneous D_2-IPSCs is greater than wild type (Figure 4.3). In dopamine neurons from TH-hD_2S mice, application of L-DOPA (10 μM, 10 min) significantly increased the frequency of spontaneous D_2-IPSCs (ACSF: 3.6 ± 1.0 per min; L-DOPA:11.1 ± 3.1 per min, paired two-tailed t test, p = 0.01, n = 8 cells). The L-DOPA-induced increase in frequency was similar between dopamine neurons in wild type and TH-hD_2S mice (two-way ANOVA, p = 0.22, Figure 5.2) These results are inconsistent with the L-DOPA-induced increase in frequency being a simple artifact of increasing signal over noise. It is possible that L-DOPA is increasing the quantal size of dopamine release events, such that spontaneous D_2-IPSCs are better resolved over noise. Alternatively, it is possible that L-DOPA recruits new dopamine release sites.

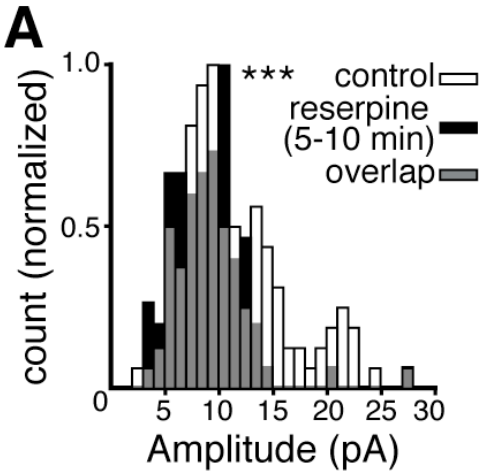

Figure 5.1. The amplitude of spontaneous D_2-IPSCs is decreased rapidly by reserpine.

(A) Amplitude of sIPSCs (1 pA bins, two-sample KS test, *n* = sIPSCs in WT ACSF:122, after 5-10 min in reserpine:91). Vertical axes have been scaled to normalize for *n* (See Detection and measurement of spontaneous D_2-IPSCs, p.12). All recordings were made in the presence of forskolin (1 μM) and cocaine (300 nM) to increase frequency of sIPSCs (see Figure 4.3D).

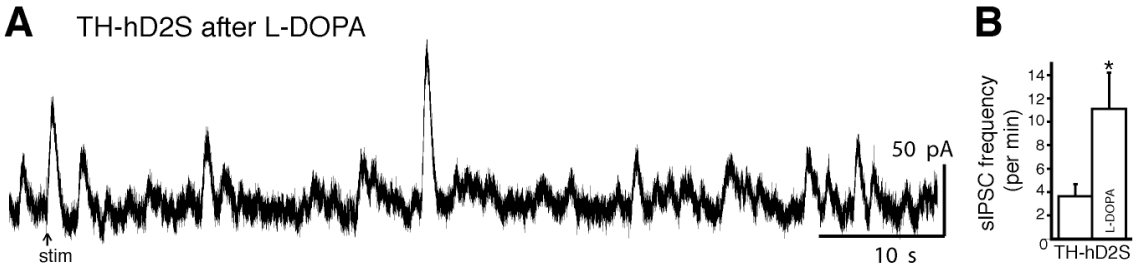

Figure 5.2. L-DOPA increased the frequency of spontaneous D_2-IPSCs in dopamine neurons from TH-hD_2S mice.

(A) Representative trace of D_2-eIPSC (arrow) and D_2-sIPSCs recorded in a TH-hD_2s slice after application of L-DOPA (10 μM, 10 min). (B) L-DOPA increased the frequency of D_2-sIPSCs in slices from TH-hD_2S mice (paired t-test, *n* = 8). Mean ± SEM. **p* < 0.05

Spontaneous D_2-IPSCs are not strictly autaptic

Spontaneous D2-IPSCs are evidence of focal dopamine release nearby to receptors. When performing simultaneous whole-cell voltage clamp recordings from two dopamine neurons, spontaneous D_2-IPSCs were never found to co-occur in the two neurons, suggesting specificity in pre- and postsynaptic partners. Evoked D_2-IPSCs are dependent on action potentials and calcium entry. Evoked D_2-IPSCs are typically recorded in voltage-clamp and with strong intracellular calcium buffering (10 mM BAPTA). Thus, action potential- and voltage-gated calcium channel-dependent dopamine release from the recorded neuron is blocked. Consistent with this, application of the membrane-permeable BAPTA-AM (50 μM, 10 min, recording in 1 μM forskolin and 300 nM cocaine) reduced the amplitude of the evoked IPSC by 62 ± 7% ($p = 0.01$, $n = 5$, paired t test), indicating that dopamine is released from neighboring neurons onto the recorded neuron. However, the possibility that a dopamine neuron also releases dopamine onto itself has not been resolved despite repeated attempts with various recording conditions. Dopamine-dependent hyperpolarizations have not been observed after inducing action potential firing in the recorded dopamine neuron.

Spontaneously released dopamine however was not dependent on action potentials, voltage-gated calcium channels, and persisted in calcium-free external solution. Additionally, spontaneous D_2-IPSCs persisted after application of BAPTA-AM (forsk+coc: 2.6 ± 0.7 per min; +BAPTA-AM: 2.5 ± 1.3, $p = 0.9$, $n = 4$ cells, paired t test). To test whether spontaneous D_2-IPSCs were produced by autapses, recording were made after whole-cell dialysis (> 35 min) of internal solution containing reserpic acid (10 μM) – a less membrane-permeable analog of reserpine in the internal solution. Evoked and

spontaneous IPSCs were observed with the reserpic acid-containing internal solution. In the same neurons, bath application of reserpine (1 µM) abolished evoked and spontaneous D_2-IPSCs. This suggests that the spontaneous release is, at least, not exclusively from the recorded neuron.

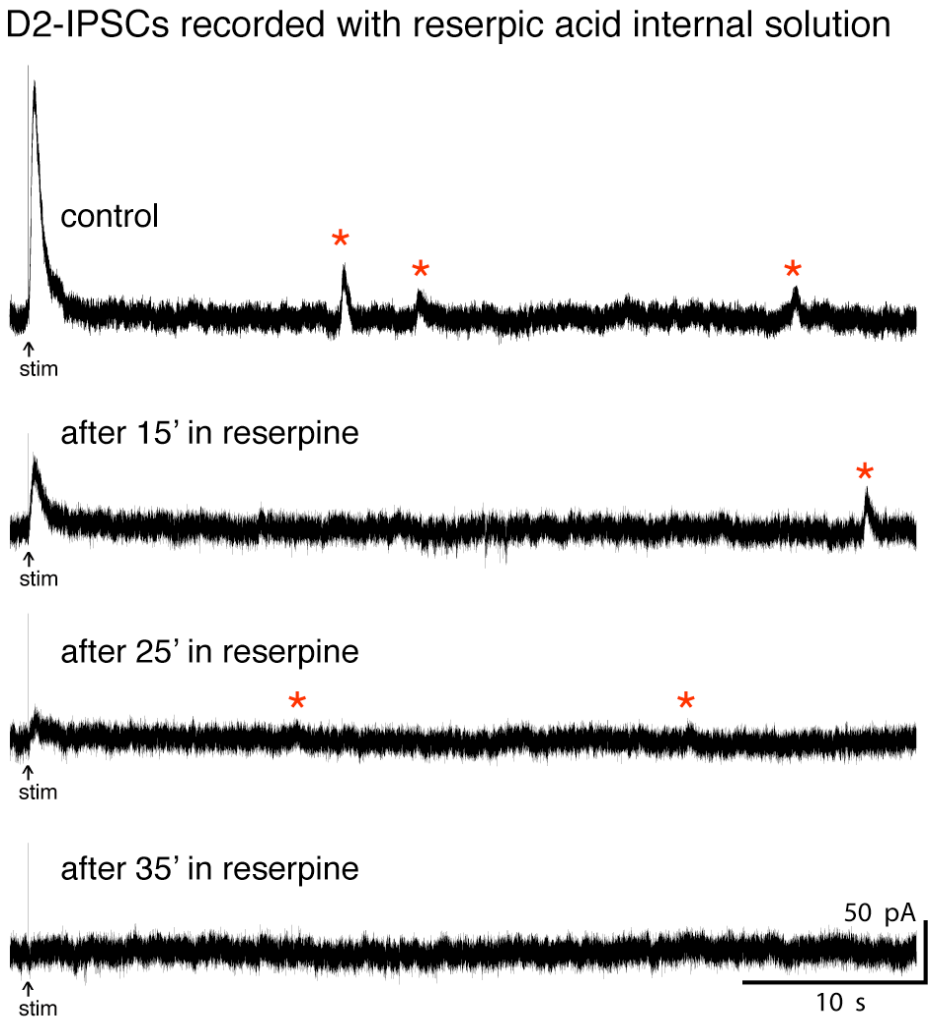

Figure 5.3. Reserpic acid in the internal recording solution does not prevent evoked and spontaneous D_2-IPSCs.

Traces of voltage clamp recordings from a single neuron after whole-cell dialysis (> 35 min) with an internal solution containing reserpic acid (10 µM) – a membrane-impermeable form of reserpine. Evoked (stim) and spontaneous (red stars) D_2-IPSCs were recorded. Bath application of reserpine (1 µM) abolished both the evoked and spontaneous D_2-IPSCs. Recordings were made in the presence of forskolin (1 µM) and cocaine (300 nM) to increase frequency of sIPSCs (see Figure 4.3)

5.2 DEPRESSION OF SEROTONIN SYNAPTIC TRANSMISSION BY THE DOPAMINE PRECURSOR L-DOPA

Stephanie C. Gantz[1], Erica S. Levitt[1], Nerea Llamosas[2], Kim A. Neve[3], and John T. Williams[1]

[1]Vollum Institute
Oregon Health & Science University
3181 SW Sam Jackson Park Road
Portland, OR 97239

[2]Department of Pharmacology, Faculty of Medicine and Dentistry
University of the Basque Country UPV/EHU
Leioa, Spain, 48940

[3] Research Service, VA Portland Health Care System; and
Department of Behavioral Neuroscience
Oregon Health & Science University
Portland, OR, 97239

Acknowledgements: This work was supported by NIH DA04523 and DA034388 (J.T.W.) and by Merit Review Award BX000810 from the US Department of Veterans Affairs Biomedical Laboratory Research and Development (K.A.N.). We thank Drs. Tianyi Mao and Mark Pennesi for supplying Ai9 and Ai32 mice, and 5-HT_{1B} receptor KO mice, respectively, and Maozhen Qin for help with mouse husbandry.

[This manuscript is presented as published in (Gantz *et al.*, 2015a), *Cell Reports,* August 11, 2015, 12(6):944-954]

Summary

Imbalance between the dopamine and serotonin (5-HT) neurotransmitter systems has been implicated in the comorbidity of Parkinson's disease (PD) and psychiatric disorders. L-DOPA, the leading treatment of PD, facilitates the production and release of dopamine. This study assessed the action of L-DOPA on monoamine synaptic transmission in mouse brain slices. Application of L-DOPA augmented the D_2 receptor-mediated inhibitory postsynaptic current (IPSC) in dopamine neurons of the substantia nigra. This augmentation was largely due to dopamine release from 5-HT terminals. Selective optogenetic stimulation of 5-HT terminals evoked dopamine release producing D_2 receptor-mediated IPSCs following treatment with L-DOPA. In the dorsal raphe, L-DOPA produced a long-lasting depression of the $5\text{-}HT_{1A}$ receptor-mediated IPSC in 5-HT neurons. When D_2 receptors were expressed in the dorsal raphe, application of L-DOPA resulted in a D_2 receptor-mediated IPSC. Thus, treatment with L-DOPA caused ectopic dopamine release from 5-HT terminals and a loss of 5-HT-mediated synaptic transmission.

Introduction

The monoamine neurotransmitters, noradrenaline, dopamine, and serotonin, modulate basic physiological functions including sleep, motor control, food intake, sexual arousal, as well as influence mood, temperament, and behavioral reinforcement. Dysfunction of the dopamine system has been associated with substance abuse, schizophrenia, attention-deficit hyperactivity disorder, and Parkinson's disease (PD). Imbalance in the serotonin (5-hydroxytryptamine, 5-HT) system has been linked to the etiology of complex emotional disorders including anxiety, bipolar, impulsivity, and depression. The

prevalence of comorbidity in these disorders implicates significant interaction between the dopamine and 5-HT systems. Understanding interactions between the monoamine systems is necessary to reduce side effects of pharmaceuticals that target these systems.

The focus of this study is the immediate dopamine precursor L-3,4-dihydroxyphenylalanine (L-DOPA), the leading therapy to treat the motor symptoms of PD. Chronic L-DOPA treatment produces undesirable side effects, including the development of dyskinesias and fluctuations in mood that exacerbate psychiatric symptoms such as anxiety, impulsivity, and depression in humans (Cools *et al.*, 2003; Damãsio *et al.*, 1971) and rodent models (Borah and Mohanakumar, 2007; Eskow Jaunarajs *et al.*, 2012). Many studies have implicated an imbalance between dopamine and 5-HT as the cause of these detrimental side effects (Borah and Mohanakumar, 2007; Carta *et al.*, 2007; Eskow Jaunarajs *et al.*, 2012; Hornykiewicz, 1975; Navailles *et al.*, 2011). There is also significant recent interest in using L-DOPA to treat a myriad of health conditions, including Angelman Syndrome, Tourette Syndrome, Restless Legs Syndrome, subacute back pain, and cocaine dependence. Because these conditions are often comorbid with 5-HT-linked psychiatric symptoms, a greater understanding of the action of L-DOPA on the serotonergic system is necessary.

5-HT neurons can convert L-DOPA to dopamine through the L-amino acid decarboxylase (AADC, Arai *et al.*, 1994; Ng *et al.*, 1970). Exposure of 5-HT neurons to L-DOPA results in vesicular packaging of dopamine via the vesicular monoamine transporter (VMAT2) and activity-dependent release of dopamine (Kannari *et al.*, 2000; Tanaka *et al.*, 1999). Since VMAT2 preferentially transports dopamine (Finn and Edwards, 1997), production of dopamine in 5-HT neurons could reduce the content of

vesicular 5-HT. But, the consequence of L-DOPA on 5-HT-dependent synaptic transmission has not been reported. Furthermore, evidence that 5-HT terminal-derived dopamine activates postsynaptic dopamine receptors has not been described. The present study describes a depression in serotonin synaptic transmission after L-DOPA. The results reveal that following treatment with L-DOPA serotonin terminals participate in D_2 receptor-dependent dopamine signaling in the substantia nigra (SNc) and reduce 5-HT_{1A} receptor-dependent signaling in the dorsal raphe (DR).

Results

Acute L-DOPA enhances dopamine transmission in the substantia nigra

In the SNc, vesicular dopamine release elicits D_2 receptor-mediated inhibitory postsynaptic currents (IPSCs) through the activation of G protein-coupled inwardly rectifying potassium (GIRK) channels (Beckstead *et al.*, 2004). Whole-cell voltage clamp recordings were made from SNc dopamine neurons in horizontal midbrain slices from wild type mice. A single electrical stimulus was used to evoke D_2-IPSCs (D_2-eIPSC) once every 50 s in the presence of NMDA, AMPA, $GABA_A$, $GABA_B$, and nACh receptor antagonists. As previously reported, application of L-DOPA (10 μM, 10 min) had three actions (Beckstead *et al.*, 2004; Gantz *et al.*, 2013; Mercuri *et al.*, 1990). First, L-DOPA (10 μM) produced an outward current (62±6 pA, $p<0.001$, paired *t* test, Figure 5.4A, B, and Figure 5.5A), which returned to baseline upon wash out or was reversed by the D_2 receptor antagonist, sulpiride (600 nM). Pretreatment with sulpiride prevented the outward current induced by L-DOPA (5±3 pA, $p=0.22$, $n = 6$). Second, L-DOPA produced a robust augmentation of the D_2-eIPSC amplitude (252±19% of baseline,

$p<0.001$, paired *t* test, Figure 5.4C and D, Figure 5.5B, and Figure 5.6C). Lastly, L-DOPA increased the amplitude ($p<0.001$, Mann-Whitney U test) and frequency of spontaneous D_2-sIPSCs ($p=0.02$, one-way ANOVA, Figure 5.4E and F) that result from vesicular release of dopamine in the absence of stimulation (Gantz *et al.*, 2013). The transient outward current produced by iontophoretically-applied dopamine (I-DA) was not increased by L-DOPA. In fact, there was a small decrease in I-DA that correlated with the amplitude of the outward current induced by L-DOPA (reduction in I-DA: 34±11 pA; outward current: 45±9 pA, $p<0.05$, $n = 9$, Pearson Correlation). The results indicate that acute application of L-DOPA enhanced evoked and spontaneous dopamine transmission in the SNc by a presynaptic mechanism.

The conversion of L-DOPA to dopamine is required

L-DOPA is converted to dopamine by the L-amino acid decarboxylase (AADC). To determine if the conversion to dopamine was required, brain slices were treated with the AADC inhibitor, NSD-1015 (20 μM, >15 min). NSD-1015 blocked the outward current induced by L-DOPA (NSD: 7±3 pA, NSD and L-DOPA: 0±4 pA, $p=0.37$, Figure 5.5A). In addition, NSD-1015 prevented the L-DOPA-induced enhancement in D_2-eIPSC amplitude (NSD: 18±2 pA, NSD and L-DOPA: 16±2 pA, $p=0.07$, paired *t* test, Figure 5.5B), and the L-DOPA-induced increase in spontaneous D_2-sIPSC frequency (ACSF: 0.9 per min, NSD: 1.2 per min, NSD and L-DOPA: 0.8 per min, $p=0.27$, Figure 5.5C). Thus, the metabolism of L-DOPA to dopamine was required to affect dopamine-dependent transmission.

5-HT terminals release dopamine in the substantia nigra after acute or *in vivo* L-DOPA

Dopamine neurons in the SNc receive a prominent projection from 5-HT neurons in the raphe nuclei (Dray *et al.*, 1976; Moukhles *et al.*, 1997). Given that 5-HT neurons can convert L-DOPA to dopamine through the AADC (Arai *et al.*, 1994), the ability of 5-HT terminals in the SNc to participate in dopamine signaling after L-DOPA was assessed. 5-HT terminals, but not dopamine neurons, have 5-$HT_{1B/D}$ receptors that strongly inhibit 5-HT release (Cameron and Williams, 1994; Morikawa *et al.*, 2000). Application of the selective 5-$HT_{1B/D}$ receptor agonist, sumatriptan (1 μM), alone had no effect on the D_2-eIPSC (p=0.77, Figure 5.6A and B), consistent with a previous report that used the 5-HT1 receptor agonist, 5-CT (Ford *et al.*, 2006). However, sumatriptan reduced and reversed the L-DOPA-induced enhancement of the D_2-eIPSC. Sumatriptan, when applied before L-DOPA, significantly reduced the enhancement of the D_2-eIPSC by L-DOPA (136±11% of baseline, p<0.001, Figure 5.6C and D). When applied following L-DOPA, sumatriptan decreased the D_2-eIPSC to 142±13% of its original amplitude, which was not statistically different from the enhancement by L-DOPA following pretreatment of sumatriptan (p=0.79, n = 9, unpaired t test). While sumatriptan markedly reduced the L-DOPA-induced enhancement of the D_2-eIPSC, the L-DOPA-induced increase in the presence of sumatriptan was still significant (p=0.001, paired t test, Figure 5.6A, C, and D). This indicates that L-DOPA also increased dopamine release from dopamine neurons. Furthermore, in the presence of sumatriptan, L-DOPA increased the frequency of spontaneous D_2-sIPSCs (p<0.001, Figure 5.6E), to the same extent and with a similar time course as in control (p=0.997, two-way ANOVA, Figure 5.4F and Figure 5.6E,

(Gantz *et al.*, 2013). Pretreatment with sumatriptan also had no effect on the outward current produced by L-DOPA (82.5±10.5 pA, p=0.53, n = 21, Mann-Whitney U test). These results suggest that 5-HT terminals released dopamine after acute exposure to L-DOPA.

To determine whether this phenomenon persists after chronic L-DOPA treatment, mice were treated with L-DOPA (100 mg/kg, subcutaneous) and a peripheral AADC inhibitor, benserazide (200 mg/kg, subcutaneous), or with benserazide alone once daily for 6 days. Brain slices were prepared 1 h after the final injection. D_2-eIPSCs were evoked with a single stimulus (1 stim) or a train of 5 stimuli (5 stims), to obtain better signal-to-noise ratio (Figure 5.6F). In slices from mice treated with benserazide alone, sumatriptan had no effect on the D_2-eIPSC amplitude (1 stim: 94±5%; 5 stims: 100±5% of baseline, Figure 5.6G). In slices from mice treated with L-DOPA however, sumatriptan significantly decreased the D_2-eIPSC amplitude, whether evoked by 1 stim (67±5% of baseline, $p<0.001$) or 5 stims (72±5% of baseline, $p<0.001$, Figure 5.6F and 3G). Taken together, these results demonstrate that dopamine release in the SNc, after acute or chronic *in vivo* L-DOPA exposure, was attenuated by activation of $5\text{-HT}_{1B/D}$ receptors, suggesting that dopamine was released from 5-HT terminals.

An optogenetic strategy was employed to selectively activate 5-HT terminals in the SNc, using the ePet-Cre transgenic mouse line that expresses Cre recombinase in serotonin neurons (Scott *et al.*, 2005). The selective expression of Cre recombinase in 5-HT neurons in the ePet-Cre line was validated by immunohistochemistry. ePet-$Cre^{+/-}$ mice were crossed with the Ai9 Cre reporter mouse line that produces cytosolic tdTomato in Cre^+ cells. Mice were transcardially perfused and the brains were sectioned

for immunohistochemistry (Figure 5.7A-C and Figure 5.9A). No tdTomato$^+$ cells were detected in ePet-Cre$^{-/-}$ sections. In ePet-Cre$^{+/-}$ sections, cell counts (n = 4330) were made in the DR (Figure 5.7), which contains the majority of 5-HT neurons in the rodent brain (Dahlstroem and Fuxe, 1964). Sections were stained for tyrosine hydroxylase (TH) and tryptophan hydroxylase (TpH), the rate-limiting enzymes in the production of dopamine and 5-HT, respectively. In the DR, 82% of the Cre$^+$ cells were TpH$^+$, whereas 7% of the Cre$^+$ cells were TH$^+$ and not TpH$^+$. Generally, the TH$^+$ cells had smaller somas and were located close to the cerebral aqueduct. The remaining Cre$^+$ cells (11%) did not co-stain with TpH or TH (Figure 5.7B). Lastly, 24% of TpH$^+$ neurons were not Cre$^+$ (Figure 5.7C). In midbrain sections, TpH$^+$/Cre$^+$ fibers were found throughout the SNc, as well as Cre$^+$-only and TpH$^+$-only fibers. Importantly, no SNc dopamine neurons (TH$^+$) were Cre$^+$ (Figure 5.9A).

The ePet-Cre$^{+/-}$ mice were crossed with the Ai32 mouse line to express the light-activated cation channel, channelrhodopsin-2 (ChR2) in Cre$^+$ cells. In slices from these mice, L-DOPA augmented the electrically evoked D_2-eIPSC to the same extent as in slices from wild type mice (244±28%, p=0.81, n = 10, unpaired t test). ChR2-expressing axon terminals were activated with a light pulse (LED, 470 nm, 5-15 ms) every 50 s, in the presence of NMDA, AMPA, $GABA_A$, $GABA_B$, and nACh receptor antagonists, and 4-aminopyridine (100 μM, see Electrophysiological recordings and analysis, p. 10, and Figure 5.8). In 16/18 recordings, the activation of ChR2 had no effect prior to the application of L-DOPA. In the other 2 recordings, activation of ChR2 evoked an IPSC that was blocked by the 5-HT_{1A} receptor antagonist, WAY 100635 (100 nM). This observation is similar to previous work done in slices from guinea pig, demonstrating a

small population of dopamine neurons with 5-HT_{1A} receptor-mediated inhibitory postsynaptic potentials (Cameron *et al.*, 1997). After treatment with L-DOPA (10 μM, 10 min), in every case, activation of ChR2 induced a D2 receptor-mediated oIPSC (10±1 pA, Figure 5.9B and C). The oIPSCs were completely eliminated by the D_2 receptor antagonist, sulpiride (600 nM, 1±0.4 pA, p=0.004, n = 5, paired t test). The time-to-peak and duration of the D_2-oIPSC were longer than the D_2-eIPSC, recorded in the same conditions (time-to-peak: oIPSC: 389±11 ms; eIPSC: 305±14 ms; p<0.001, Figure 5.9D; duration at 20%: oIPSC: 1071±83 ms, eIPSC: 795±37 ms, p=0.007, Mann-Whitney U test). Activation of 5-$HT_{1B/D}$ receptors with sumatriptan or 5-CT (100 nM) inhibited the D_2-oIPSCs (80±3% inhibition, p<0.001, Figure 5.9B and C). Thus after treatment with L-DOPA, selective activation of 5-HT terminals in the SNc evoked dopamine release and produced a D_2 receptor-mediated synaptic current from 5-HT terminal derived dopamine.

Acute L-DOPA reduces serotonin transmission in the dorsal raphe

To determine if L-DOPA-induced synaptic release of dopamine from 5-HT terminals affected vesicular 5-HT release, recordings were made from 5-HT neurons in the DR. In the DR, 5-HT release produces 5-HT_{1A} receptor-mediated IPSCs through the activation of GIRK channels (Williams *et al.*, 1988). Whole-cell recordings were made from 5-HT neurons in coronal DR slices from wild type mice. 5-HT neurons were identified by slow, broad, and regular action potential firing upon current injection. 5-HT_{1A}-eIPSCs were evoked by a single electrical stimulus once every 50 s, in the presence of NMDA, AMPA, $GABA_A$, and α-1 adrenergic receptor antagonists. The 5-HT_{1A}-eIPSC was blocked by the 5-HT_{1A} antagonist, WAY 100635 (100 nM), or inhibited by activation of

5-$HT_{1B/D}$ receptors with sumatriptan (1 μM). Application of L-DOPA (10 μM, 10 min) attenuated the 5-HT_{1A}-eIPSC amplitude (80±6% of baseline, p=0.002, Figure 5.10A), without changing the holding current (-9±4 pA, p=0.06, n = 11, paired t test). Higher concentrations of L-DOPA (30 and 50 μM) caused larger reductions in the 5-HT_{1A}-eIPSC that did not recover upon L-DOPA wash out (30 μM: 33±7% of baseline, p<0.001; 50 μM: 10±2% of baseline, p<0.001, Figure 5.10A-C and F).

In recordings from 5-HT neurons from the ePet-$Cre^{+/-}$/$Ai32^{+/-}$ mice, light stimulation (10 ms, LED, 470 nm) caused a depolarization that elicited one to two action potentials (Figure 5.7D). ChR2 activation evoked a 5-HT_{1A}-oIPSC (Figure 5.8 and Figure 5.10D) that followed the ChR2-induced inward current. 5-HT_{1A}-IPSCs were evoked once every 25 s, alternating between electrical and optical stimulation. Application of L-DOPA (30 μM, 10 min) significantly attenuated the 5-HT_{1A}-oIPSC (14±6% of baseline, p=0.004, paired t test, Figure 5.10D and E), which did not recover after a 20 min wash. The L-DOPA-induced attenuation in amplitude and limited recovery of electrically- or optically-evoked synaptic currents was indistinguishable (p=0.73, two-way ANOVA, Figure 5.10E). These results indicate a selective action of L-DOPA on 5-HT terminals.

In PD patients, the level of L-DOPA in the cerebral spinal fluid (CSF) fluctuates and varies considerably from patient to patient. The concentration in the CSF varies from ~130 nM up to 8 μM and remains elevated for > 1 h following a single dose (Nyholm *et al.*, 2002; Olanow *et al.*, 1991; Stocchi *et al.*, 2005; Tohgi *et al.*, 1995). In the present study, prolonged application of a low concentration of L-DOPA (1 μM, 50-65 min) resulted in a significant reduction of the 5-HT_{1A}-eIPSC (48±8% of baseline, p=0.03,

paired *t* test, Figure 5.11). Thus, a clinically relevant concentration of L-DOPA depressed 5-HT_{1A} receptor-mediated synaptic currents.

L-DOPA reduced serotonin transmission through the production of dopamine

The AADC inhibitor, NSD-1015 (20 μM, >15 min) was used to determine if the conversion of L-DOPA to dopamine was required. In slices exposed to NSD-1015, L-DOPA (30 μM) had no effect on the 5-HT_{1A}-eIPSC (NSD: 90±17 pA, NSD and L-DOPA: 90±17 pA, $p>0.05$, Figure 5.10F). Therefore, the production of dopamine from L-DOPA was required to affect 5-HT-dependent transmission. When NSD-1015 was applied after L-DOPA (30 μM, 10 min), the amplitude of the 5-HT_{1A}-eIPSC remained depressed (recovery following 10-15 min wash: ACSF: 36±7% of baseline, $n = 7$; NSD: 33±3% of baseline, $n = 4$, $p=0.76$, unpaired *t* test). Thus, ongoing dopamine synthesis was not required after L-DOPA wash out.

When 5-HT currents were evoked by photolysis of caged-serotonin (I-5-HT, 5-25 ms, 365 nm), application of L-DOPA (50 μM, 10 min) caused a modest reduction (81±5% of baseline, $p<0.05$, Figure 5.12A and B) and a small outward current (16±3 pA, $p<0.001$, Figure 5.12A and C). This postsynaptic effect of L-DOPA was readily reversed with wash out, or the addition of NSD-1015 (20 μM, I-5-HT: 98±6% of baseline, $p<0.001$; outward current: -9±4 pA, $p<0.001$, Figure 5.12A-C). The results suggest that dopamine produced from L-DOPA exerted a small, transient postsynaptic effect. Therefore, the long-lasting L-DOPA-induced depression of 5-HT-mediated synaptic transmission occurred primarily through a presynaptic dopamine-dependent mechanism.

In the DR, 5-HT activates presynaptic 5-HT_{1B} receptors that inhibit further 5-HT release (Morikawa *et al.*, 2000). To determine if L-DOPA or dopamine activates 5-HT_{1B} receptors, the effect of dopamine on the 5-HT_{1A}-eIPSC was tested in 5-HT_{1B} receptor knockout mice (5-HT_{1B} KO) and their wild type littermates (WT). Sumatriptan (1 μM) caused a marked inhibition of the 5-HT_{1A}-eIPSC in WTs (85±5% inhibition) and only a small inhibition in 5-HT_{1B} KOs (34±5% inhibition, $p<0.001$, Figure 5.12D). In slices from WT mice, dopamine (10 μM, 10 min) inhibited the 5-HT_{1A}-eIPSC (41±5% of baseline, $p<0.001$, Figure 5.12E). The inhibition induced by dopamine reversed after wash out (after 10-15 min wash: 98±14% of baseline, RM one-way ANOVA, Figure 5.12E). The transient action of dopamine was unlike the prolonged depression induced by L-DOPA. In slices from 5-HT_{1B} KO mice, dopamine inhibited the 5-HT_{1A}-eIPSC (60±6% of baseline, $p<0.001$) and recovered after wash out (after 10-15 min wash: 105±7% of baseline, RM one-way ANOVA), though the inhibition was slightly less than in WT slices ($p = 0.02$, unpaired *t* test, Figure 5.12E). The dopamine-induced reduction in the 5-HT_{1A}-eIPSC also persisted in the presence of sumatriptan (1 μM, 58±7% of baseline, $n = 5$) in 5-HT_{1B} KO mice, indicating 5-$HT1_D$ receptors were not involved. In addition, dopamine (10 μM) decreased the 5-HT_{1A}-oIPSC in slices from ePet-$Cre^{+/-}$ /$Ai32^{+/-}$ mice (41±5% of baseline, $p=0.009$, $n = 8$, paired *t* test). L-DOPA (30 μM, 10 min) also produced similar inhibitions of the 5-HT_{1A}-eIPSC in both WT and 5-HT_{1B} KO mice that did not recover upon wash out (WT: 24±3% of baseline; 5-HT_{1B} KO mice: 28±2% of baseline, $p=0.31$, unpaired *t* test, Figure 5.12F). Thus, the L-DOPA-induced depression of the 5-HT_{1A}-IPSC cannot be explained by action on the 5-HT_{1B} autoreceptor.

5-HT neurons release dopamine in the dorsal raphe after acute L-DOPA

The ability of DR 5-HT neurons to package and release dopamine after treatment with L-DOPA was examined through the activation of virally-expressed D2 receptors in the DR. Wild type mice received a midline injection of an adeno-associated virus vector generating D_2 receptor and GFP expression, as previously described (Neve *et al.*, 2013). Infected neurons were identified by visualization of GFP (Figure 5.13A). Electrical stimulation (1 or 5 stims) evoked IPSCs, in the presence of NMDA, AMPA, $GABA_A$, and α-1 adrenergic receptor antagonists. The resulting eIPSCs were inhibited by the 5-HT_{1A} receptor antagonist, WAY 100635 (100 nM, 88±3% inhibition, $p<0.001$, Figure 5.13B and C). In 7/12 recordings, the eIPSC was not completely blocked by WAY 100635 (9±2 pA). It is unclear whether this WAY-resistant D_2 component originates from dopamine release from local dopamine (TH^+) neurons (Figure 5.7A and B) or dopamine terminal projections (Dorocic *et al.*, 2014; Kitahama *et al.*, 2000) or D_2 receptor activation from the release of noradrenaline (Onali *et al.*, 1985; Yoshimura *et al.*, 1985). In the presence of WAY 100635, L-DOPA (10 μM, 10 min) produced a transient outward current (69±11 pA, $p<0.001$, $n = 12$, paired *t* test, Figure 5.13B), and D_2 receptor-mediated eIPSCs that persisted long after the outward current recovered upon wash out (29±6 pA, $p=0.01$, Figure 5.13B and D). 5-CT (100 nM) significantly inhibited the L-DOPA-induced D_2-eIPSCs (65±6% inhibition, $p=0.002$, Figure 5.13E), indicating that most of the dopamine was from 5-HT terminals. The D_2 receptor antagonist, sulpiride (600 nM) completely abolished the D_2-eIPSC (1±0.3 pA, $p<0.001$, Figure 5.13F). Disruption of the vesicular monoamine transporter with reserpine (1 μM,

1 h) abolished the 5-HT_{1A}-eIPSC (4±0.3% of baseline, p=0.005, n = 3, paired t test, see also (Pan *et al.*, 1989). After reserpine, L-DOPA still produced an outward current (61±22 pA, n = 4). However, pretreatment with reserpine completely prevented the L-DOPA-induced D_2-eIPSC (in WAY and reserpine: 2±0.6 pA; in WAY, reserpine, and L-DOPA: 1±0.5 pA, p=0.15, n = 6, paired t test). Thus, viral-mediated expression of D_2 receptors in 5-HT neurons revealed that treatment with L-DOPA resulted in dopamine release by a vesicular mechanism. The time course of dopamine release mirrored that of the depression of the 5-HT_{1A}-IPSC.

Discussion

The ability of 5-HT terminals to convert and release dopamine after L-DOPA was first described forty-five years ago (Ng *et al.*, 1970). Nevertheless, the ability of 5-HT terminal-derived dopamine to activate postsynaptic dopamine receptors or the inhibition of serotonin transmission by displacement with dopamine has not been reported. This study assessed the action of L-DOPA on monoamine synaptic transmission on dopamine neurons in the SNc and 5-HT neurons in the DR. The results reveal that treatment with L-DOPA causes ectopic dopamine release from 5-HT terminals and a simultaneous loss of 5-HT-mediated synaptic transmission.

Ectopic release of dopamine from 5-HT terminals

Numerous studies have demonstrated that 5-HT terminals can convert L-DOPA to dopamine that is then packaged into vesicles and released in an activity-dependent manner (Arai *et al.*, 1994; Kannari *et al.*, 2000; Ng *et al.*, 1970; Tanaka *et al.*, 1999). However, the majority of studies isolated 5-HT terminals by first ablating nigrostriatal

dopamine neurons. By preserving the nigrostriatal dopamine neurons, this study assessed the ability of 5-HT terminals to release dopamine, activate postsynaptic D_2 receptors, and otherwise mimic dopamine-dependent synaptic transmission.

In the SN, dopamine is released from the somatodendritic compartment spontaneously and after electrical stimulation to produce D_2-IPSCs (Beckstead *et al.*, 2004; Gantz *et al.*, 2013). This study found that L-DOPA increased dopamine release from dopamine neurons, augmenting D_2-IPSCs. These dopamine neurons also receive projections from the 5-HT neurons in the raphe nuclei (Dray *et al.*, 1976; Moukhles *et al.*, 1997). The release of dopamine from 5-HT terminals after L-DOPA was demonstrated using pharmacological and optogenetic experiments. The terminals of 5-HT neurons have 5-$HT_{1B/D}$ receptors, which inhibit transmitter release (Cameron and Williams, 1994; Morikawa *et al.*, 2000). Under control conditions, the activation of these receptors did not alter the amplitude of the D_2-eIPSC. However, after acute L-DOPA application, activating 5-$HT_{1B/D}$ receptors decreased the D_2-eIPSC. In addition, following 6 days of *in vivo* L-DOPA treatment, activation of 5-$HT_{1B/D}$ receptors inhibited the D_2-eIPSC. Lastly, following L-DOPA, selective stimulation of ChR2-expressing 5-HT axon terminals found throughout the SNc evoked dopamine release resulting in a D_2 receptor-mediated IPSC. Thus, acute and *in vivo* treatment with L-DOPA produced dopamine release from 5-HT terminals in the SN.

Taken together, this study made three observations related to the ability of 5-HT terminals to mimic dopamine synaptic transmission after treatment with L-DOPA: (1) 5-HT terminals in the SNc are positioned such that the release of dopamine activates D_2 receptors on dopamine neurons; (2) 5-HT terminal-derived dopamine does not likely

contribute to spontaneous D_2 receptor-mediated synaptic transmission; and (3) the release of newly synthesized dopamine from 5-HT terminals is greater and persists for longer than the release from dopamine neurons.

The projections of 5-HT neurons are widespread, including the prefrontal cortex, hippocampus, and nucleus accumbens, and form somatic, dendritic, and axonal contacts in these areas (Milner and Veznedaroglu, 1993; Van Bockstaele *et al.*, 1993). An *in vivo* microdialysis study, using a rodent model of PD, found that dopamine levels were increased in these regions following an intraperitoneal injection of L-DOPA and destruction of 5-HT neurons attenuated the L-DOPA-induced increase in dopamine (Navailles *et al.*, 2010). As found in the present study in the SN, dopamine receptors in each of these projection areas could be activated by dopamine from 5-HT terminals.

Depression of 5-HT-mediated synaptic currents by L-DOPA

Reduced 5-HT levels and altered 5-HT metabolism are often reported in PD patients (reviewed in Eskow Jaunarajs *et al.*, 2011) and rodent models of PD treated with L-DOPA (Borah and Mohanakumar, 2007; Navailles *et al.*, 2011; Ng *et al.*, 1970; Stansley and Yamamoto, 2014). However, the impact of L-DOPA on 5-HT receptor-mediated signaling had yet to be examined.

The present study describes a long-lasting L-DOPA-dependent depression of 5-HT_{1A} receptor-mediated IPSCs in 5-HT neurons in the DR. The decrease in 5-HT transmission resulted from the production and packaging of dopamine into vesicles. This most likely resulted from displacement of vesicular 5-HT, since VMAT2 transports dopamine more efficiently than serotonin (Finn and Edwards, 1997). Inhibition of the

AADC prevented the L-DOPA-induced depression in the 5-HT_{1A}-eIPSC, demonstrating the synthesis of dopamine was required. Finally, with the expression of D_2 receptors in the DR, L-DOPA resulted in D_2 receptor-mediated IPSCs. Inhibition of VMAT2 disrupted the loading of dopamine into vesicles and completely prevented the D_2-eIPSCs. Therefore, the D_2-eIPSCs were due to vesicular release of dopamine from 5-HT terminals. The ectopic release of dopamine from 5-HT terminals is likely dysregulated, since exogenous application of dopamine had little effect on 5-HT_{1B} autoreceptors. However, dopamine caused a transient inhibition of the 5-HT_{1A}-IPSC that was not explained fully by action on the 5-HT_{1A} and 5-$HT_{1B/D}$ receptors, suggesting another mechanism by which dopamine may inhibit release from 5-HT terminals. It is possible that 5-HT terminal-derived dopamine contributes to the depression of the 5-HT_{1A}-IPSC through this dopamine-mediated inhibition. Taken together, this study demonstrates that after L-DOPA, dopamine is released from 5-HT neurons impairing 5-HT-mediated synaptic transmission.

The significance of these results likely extends beyond the depression of the 5-HT_{1A}-eIPSC in the DR. The projections of 5-HT neurons will be affected similarly (Törk, 1990). 5-HT can activate as many as 14 distinct 5-HT receptors, influencing multiple effectors and modulating the release of glutamate, GABA, acetylcholine, in addition to monoamine neurotransmitters (reviewed in Fink and Gothert, 2007). Thus, the reduction in 5-HT release will have widespread actions throughout the central nervous system.

Implications for the experimental and clinical use of L-DOPA

This study demonstrates that after treatment with L-DOPA, 5-HT terminals participate in dopamine signaling at the expense of 5-HT synaptic transmission. These actions were observed with clinically relevant concentrations of L-DOPA and without ablation of dopamine neurons. Therefore, the participation of 5-HT terminals in dopamine release must be considered during experimental and clinical use of L-DOPA.

In advanced PD with substantial dopamine denervation, the release of dopamine from 5-HT terminals in the forebrain is thought to be beneficial, but the ectopic release has been suggested to be more detrimental than therapeutic, particularly to affective symptoms (Borah and Mohanakumar, 2007; Carta *et al.*, 2007; Eskow Jaunarajs *et al.*, 2012; Hornykiewicz, 1975; Navailles *et al.*, 2011). Thus, in the context of PD treatment, this study provides a cellular and synaptic basis for testing pharmaceuticals that recruit 5-HT neurons to synthesize and release dopamine while sparing 5-HT receptor-mediated signaling. In addition to PD, there is substantial recent interest in L-DOPA treatment for other health conditions, including Angelman Syndrome, Tourette Syndrome, and cocaine dependence. These conditions are often comorbid with affective disorders, notably impulsivity (Belin *et al.*, 2008; Ersche *et al.*, 2010; Palumbo and Kurlan, 2007; Pelc *et al.*, 2008), as seen in PD patients treated with L-DOPA (Cools *et al.*, 2003). Impulse control is influenced by 5-HT neurons in the dorsal raphe, where reduced 5-HT levels promote impulsive behavior (Fonesca *et al*., 2015; Miyazaki *et al*., 2014). Thus, a greater understanding of the action of L-DOPA on the serotonin system is necessary when considering its use when certain affective symptoms are also present. Indeed, in PD patients and animal models, combination therapies with L-DOPA, 5-HT_{1A} and 5-HT_{1B} receptor agonists have proven effective in treating dyskinesias and psychiatric symptoms,

such as depression and anxiety (Munoz *et al.*, 2008 and reviewed in Shimizu and Ohno, 2013).

Concluding remarks

Taken together, this study demonstrates L-DOPA is driving ectopic dopamine release from 5-HT neurons. Dopamine derived from 5-HT terminals can activate D_2 receptors in the SNc and mediate inhibitory postsynaptic currents. However in 5-HT neurons, newly synthesized dopamine is transported into vesicles, where it ultimately impairs 5-HT-mediated synaptic transmission in the DR. Thus, L-DOPA generates an imbalance between the dopamine and 5-HT neurotransmitter systems. Given the extensive projections of each system, such an imbalance will have widespread consequences throughout the central nervous system.

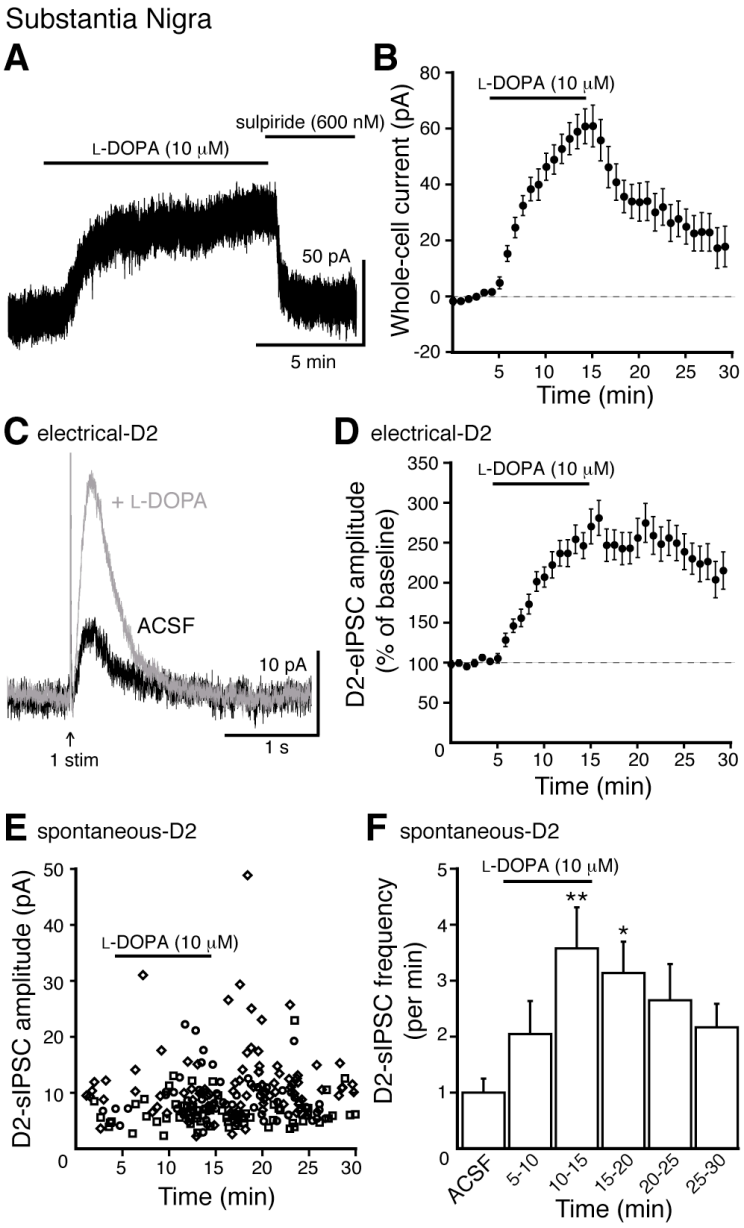

Figure 5.4. Acute L-DOPA in the SNc enhances evoked and spontaneous D_2-IPSCs.

(A) Representative trace of a whole-cell voltage clamp recording of the outward current induced by bath application of L-DOPA (10 μM), which was reversed by the D_2 receptor antagonist sulpiride (600 nM). (B) Outward current to L-DOPA application, mean±SEM (n = 23). (C) Representative traces of D_2-eIPSCs from a single experiment in ACSF and after L-DOPA. (D) D_2-eIPSCs were evoked once every 50 s. L-DOPA increased the D_2-eIPSC amplitude, mean±SEM, baseline: mean amplitude of six D_2-eIPSCs preceding L-DOPA application (n = 22). (E) Plot of spontaneous D_2-sIPSC amplitude versus time from three experiments (circle, square, and diamond) showing the increase in frequency by L-DOPA. (F) The frequency of D_2-sIPSCs (per min, 5 min bins) increased during and after L-DOPA application, mean±SEM (n = 8-17, one-way ANOVA). *$p<0.05$ and **$p<0.01$.

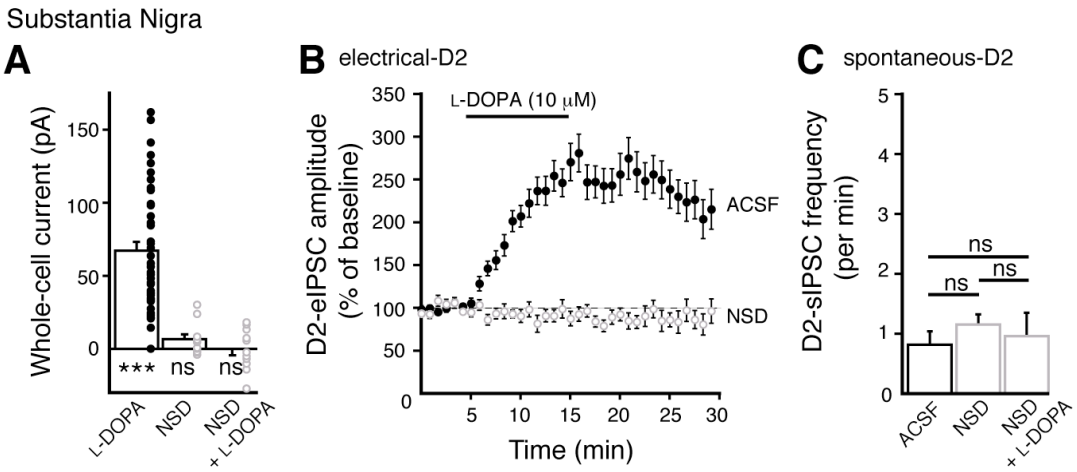

Figure 5.5. In the SNc, the conversion of L-DOPA to dopamine is required.

(A) Peak outward current to L-DOPA (10 μM) application, mean±SEM (black circles, n = 23, paired t test). The AADC inhibitor, NSD-1015 (NSD, 20 μM, 15 min), prevented the outward current induced by L-DOPA (open circles, n = 9, RM one-way ANOVA). (B) D_2-eIPSCs were evoked once every 50 s. NSD prevented the augmentation of D_2-eIPSC by L-DOPA (black circles in ACSF, as shown in Figure 5.4D, open circles in NSD, n = 13), mean±SEM, baseline: mean amplitude of six D_2-eIPSCs preceding L-DOPA application. (C) NSD prevented the L-DOPA-induced increase in spontaneous D_2-sIPSC frequency, mean±SEM (per min, n = 11, RM one-way ANOVA). ns indicates not significant and ***p<0.001.

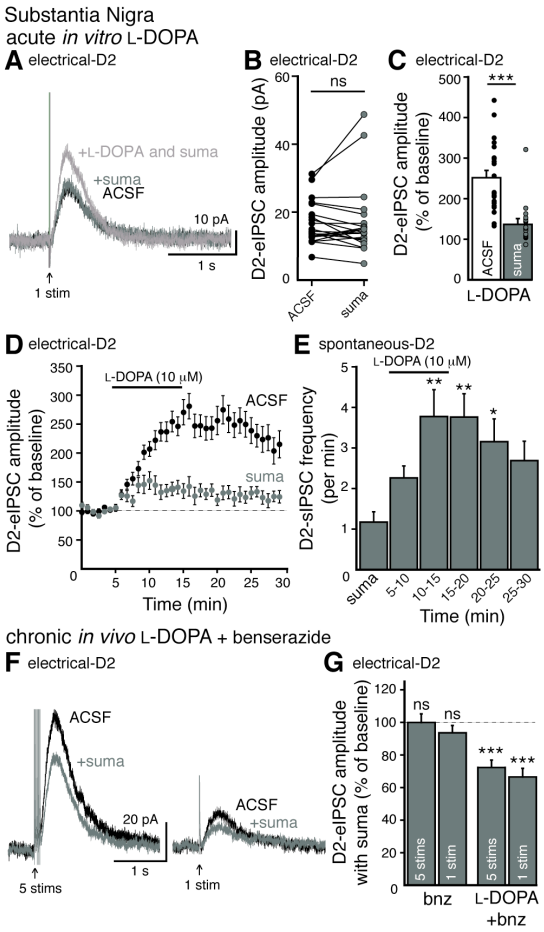

Figure 5.6. Activation of 5-HT autoreceptors attenuates the L-DOPA-induced increase in evoked D_2-IPSCs in the SNc.

(A) Representative traces of D_2-eIPSCs from a single experiment in ACSF, after the addition of the 5-$HT_{1B/D}$ receptor agonist, sumatriptan (1 μM), and after bath application of L-DOPA (10 μM) with sumatriptan. (B) Sumatriptan alone did not change the D_2-eIPSC amplitude (n = 21, paired t test). (C and D) D_2-eIPSCs were evoked once every 50 s. Pretreatment with sumatriptan significantly blunted the L-DOPA-induced increase in the D_2-eIPSC amplitude, compared to the increase in ACSF (ACSF: black circles, sumatriptan: gray circles, n = 20-22, unpaired t test), mean±SEM, baseline: mean amplitude of six D_2-eIPSCs preceding L-DOPA application. (E) In the presence of sumatriptan, L-DOPA increased the frequency of spontaneous D_2-sIPSCs (per min, 5 min bins), mean±SEM (n = 14-17, one-way ANOVA). (F and G) Sumatriptan decreased the D_2-eIPSC amplitude following chronic *in vivo* treatment with L-DOPA and a peripheral AADC inhibitor, benserazide (bnz). (F) Representative traces of D_2-eIPSCs evoked by a single (1 stim) or train (5 stims) of electrical stimuli, in ACSF and after application of sumatriptan. (G) Sumatriptan decreased the D_2-eIPSC amplitude following chronic *in vivo* L-DOPA and bnz treatment, but had no effect after bnz treatment alone, mean±SEM, baseline: mean amplitude of six D_2-eIPSCs preceding sumatriptan application. (n = 9-11, two-way RM ANOVAs). ns indicates not significant, *p<0.05, **p<0.01, and ***p<0.001.

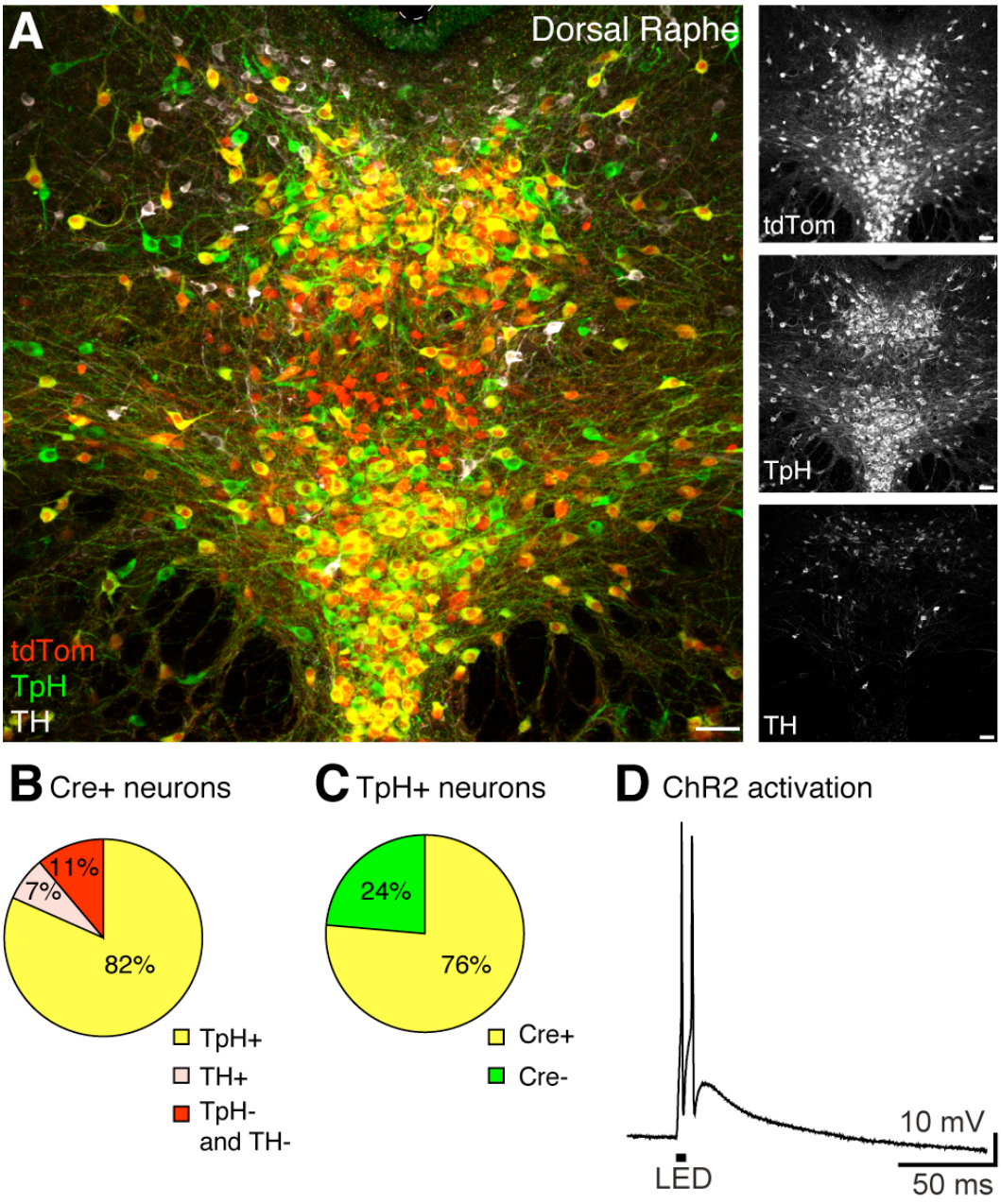

Figure 5.7. In DR slices from ePet-Cre$^{+/-}$ mice, Cre recombinase in 5-HT neurons drives selective expression of ChR2.

(A) Representative maximum intensity projection confocal image of cells in the DR of ePet-Cre$^{+/-}$/Ai9$^{+/-}$ brain slices. Cre^{+} cells express cytosolic tdTomato (tdTom, red). Sections were immunostained for tryptophan hydroxylase (TpH, green) and tyrosine hydroxylase (TH, gray), scale bars: 50 µm. (B) Percent of Cre^{+} cells (n = 3345) that co-stained for TpH, or TH, or neither TpH nor TH. (C) Percent of TpH^{+} neurons (n = 3573) that were Cre^{+}. (D) Representative whole-cell current clamp recording from a 5-HT neuron in a DR slice from ePet-Cre$^{+/-}$/Ai32$^{+/-}$ mice. ChR2 activation (10 ms, 470 nm LED) caused a depolarization and elicited one to two action potentials.

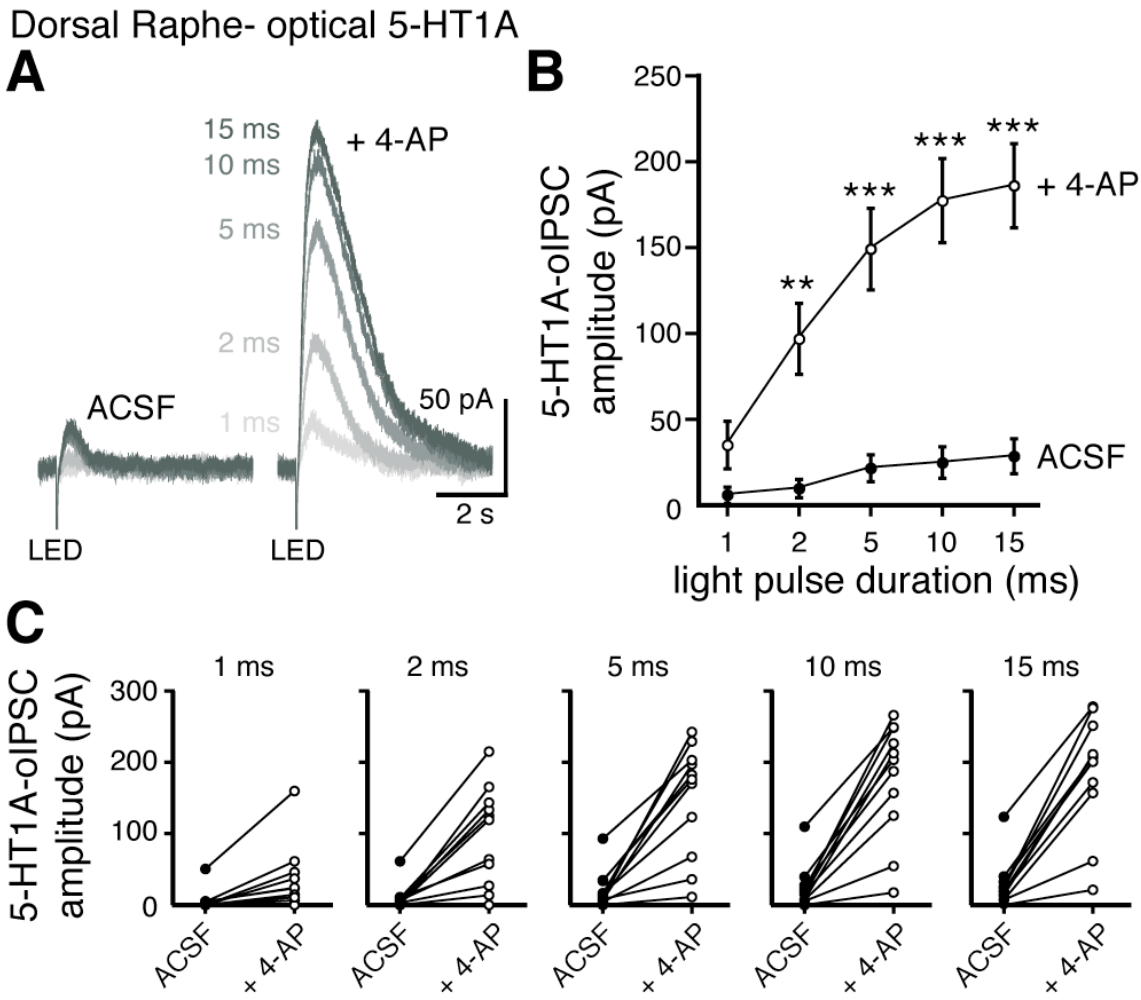

Figure 5.8. In DR slices from ePet-Cre$^{+/-}$ mice, 4-aminopyridine enhances 5-HT$_{1A}$-IPSCs evoked by ChR2 activation.

(A) Representative traces of 5-HT$_{1A}$-IPSCs evoked by ChR2 activation (oIPSC) using increasing durations of light pulses (1-15 ms) before (ACSF) and after the addition of 4-AP (100 μM). (B-C) Increasing the duration of the light pulse and the addition of 4-AP significantly increased the amplitude of the 5-HT$_{1A}$-oIPSC, shown as (B) mean±SEM, (*n* = 11, two-way ANOVA) and (C) paired data.

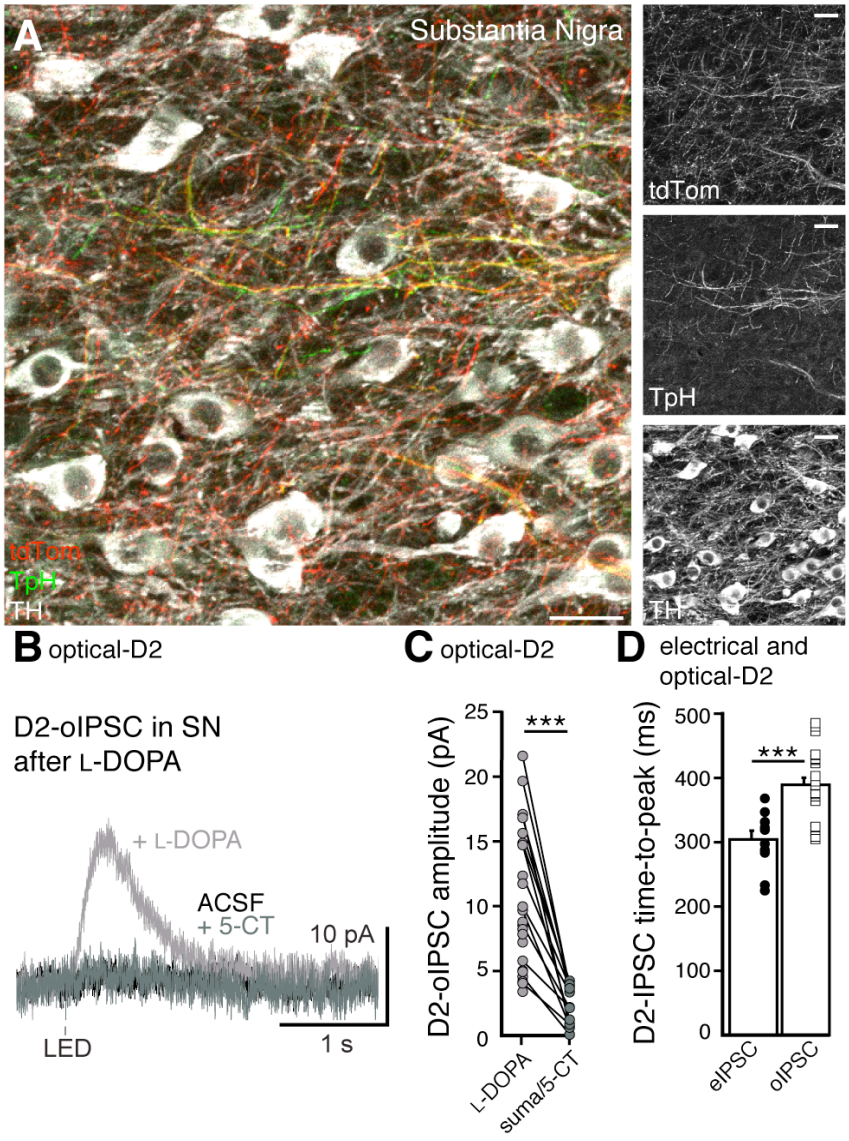

Figure 5.9. Selective activation of 5-HT terminals in the SNc elicits a D_2-IPSC after L-DOPA.

(A) Representative maximum intensity projection confocal image of dopamine neurons in the SNc of ePet-Cre$^{+/-}$/Ai9$^{+/-}$ brain slices. Cre^{+} cells express cytosolic tdTomato (tdTom, red). Sections were immunostained for tyrosine hydroxylase (TH, gray), labeling dopamine neurons, and tryptophan hydroxylase (TpH, green), labeling 5-HT fibers. Cre^{+} fibers colocalized with 5-HT fibers, and no dopamine neurons were Cre^{+}, scale bars: 25 µm. (B and C) ChR2 activation in ePet-Cre$^{+/-}$/Ai32$^{+/-}$ midbrain slices (5-15 ms, 470 nm LED) did not produce a current before application of L-DOPA. With L-DOPA (10 µM), ChR2 activation evoked a D_2-oIPSC (n = 24) that was inhibited by 5-CT, shown in (B) representative traces and (C) the decrease in amplitude with 5-CT (100 nM) or sumatriptan (1 µM) (n = 14, paired t test). (D) The time-to-peak of the D_2-eIPSC (electrically evoked) was significantly faster than that of the D_2-oIPSC (optically evoked), mean±SEM (n = 11-24, unpaired t test). ***p<0.001. See also Figure 5.7 and Figure 5.8.

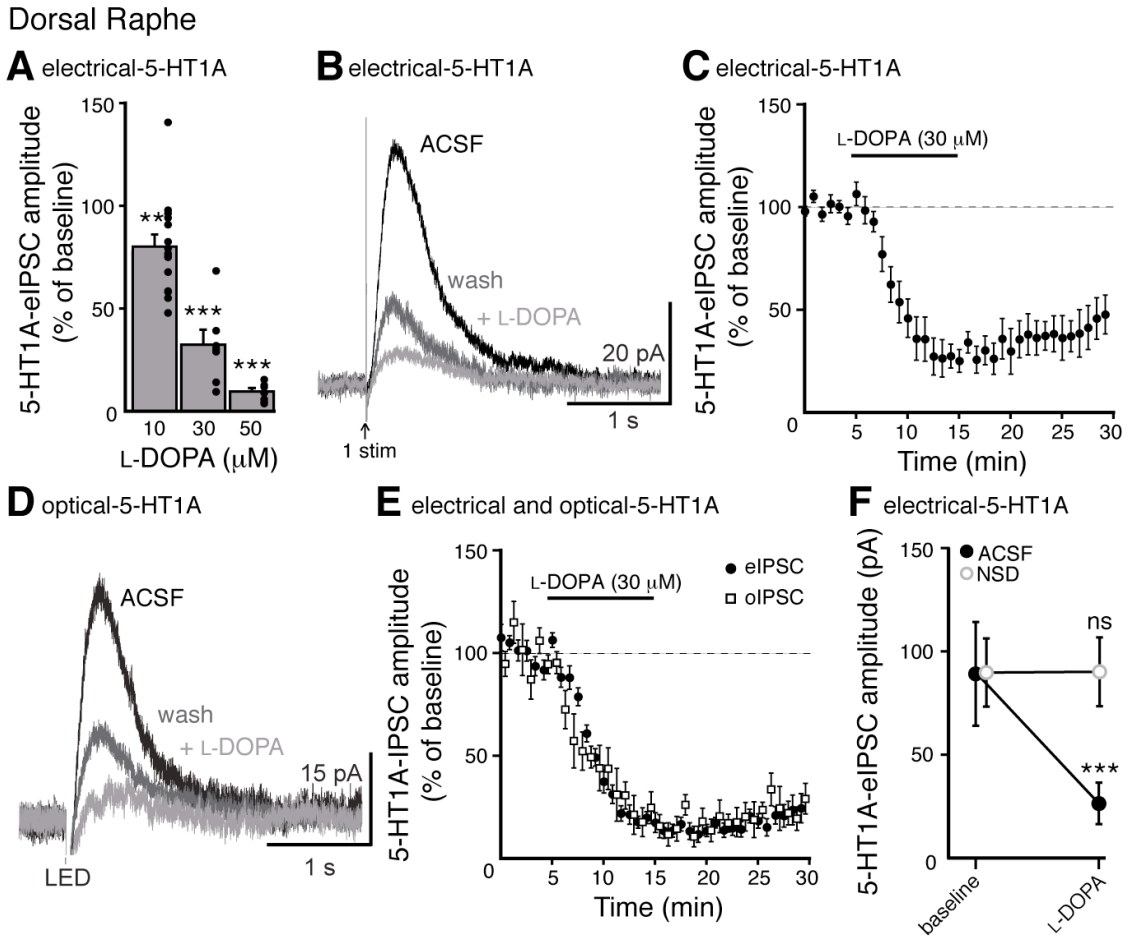

Figure 5.10. Acute L-DOPA reduces 5-HT$_{1A}$-IPSCs in the DR.

(A) Concentration-dependent depression induced by L-DOPA (10 min) in 5-HT$_{1A}$-eIPSCs, mean±SEM, baseline: mean amplitude of six 5-HT$_{1A}$-eIPSCs preceding L-DOPA application, (n = 15,7, and 10 for 10, 30 and 50 μM, respectively, paired t tests). (B) Representative traces of 5-HT$_{1A}$-eIPSCs from a single experiment in ACSF, after bath application of L-DOPA (30 μM), and after a 20 min wash. (C) 5-HT$_{1A}$-eIPSCs were evoked once every 50 s. L-DOPA significantly depressed the 5-HT$_{1A}$-eIPSC with little recovery after wash, mean±SEM, (n = 7). (D and E) In ePet-Cre$^{+/-}$/Ai32$^{+/-}$ DR slices, 5-HT$_{1A}$-IPSCs were evoked once every 25 s, alternating between electrical and optical stimulation. (D) Representative traces of 5-HT$_{1A}$-IPSC, evoked by ChR2 activation (oIPSC). L-DOPA depressed the 5-HT$_{1A}$-oIPSC with little recovery in wash. (E) L-DOPA-induced depression in the 5-HT$_{1A}$-IPSC, whether electrically evoked (eIPSC, black circles) or optically evoked (oIPSC, open squares) was indistinguishable, mean±SEM, (n = 7-8). (F) Application of the AADC inhibitor, NSD-1015 (NSD, 20 μM, 15 min), prevented the depression of the 5-HT$_{1A}$-eIPSC by L-DOPA, mean±SEM (ACSF: black circles, n = 7; NSD: open circles, n = 7, two-way RM ANOVA). Baseline: mean amplitude of six 5-HT$_{1A}$-IPSCs preceding L-DOPA application, ns indicates not significant, **p<0.01, and ***p<0.001. See also Figure 5.7 and Figure 5.9.

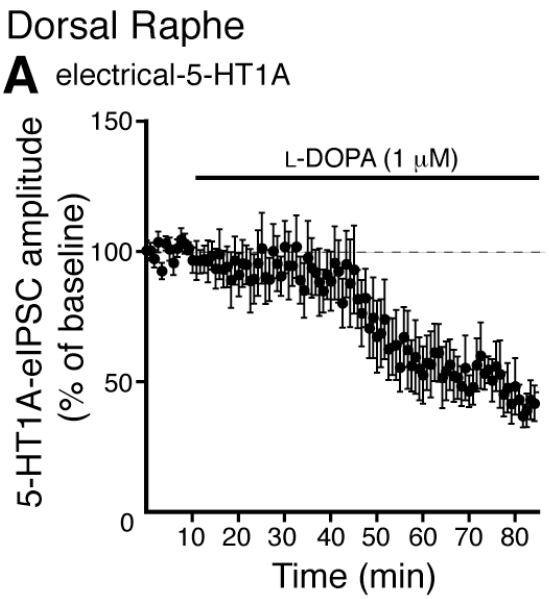

Figure 5.11. Prolonged exposure to a low concentration of L-DOPA reduces 5-HT_{1A}-IPSCs in the DR.

(A) 5-HT_{1A}-eIPSCs were evoked once every 50 s. L-DOPA (1 μM) significantly depressed the 5-HT_{1A}-eIPSC after prolonged exposure, mean±SEM, (n = 4-8). Baseline: mean amplitude of twelve 5-HT_{1A}-eIPSCs preceding L-DOPA application.

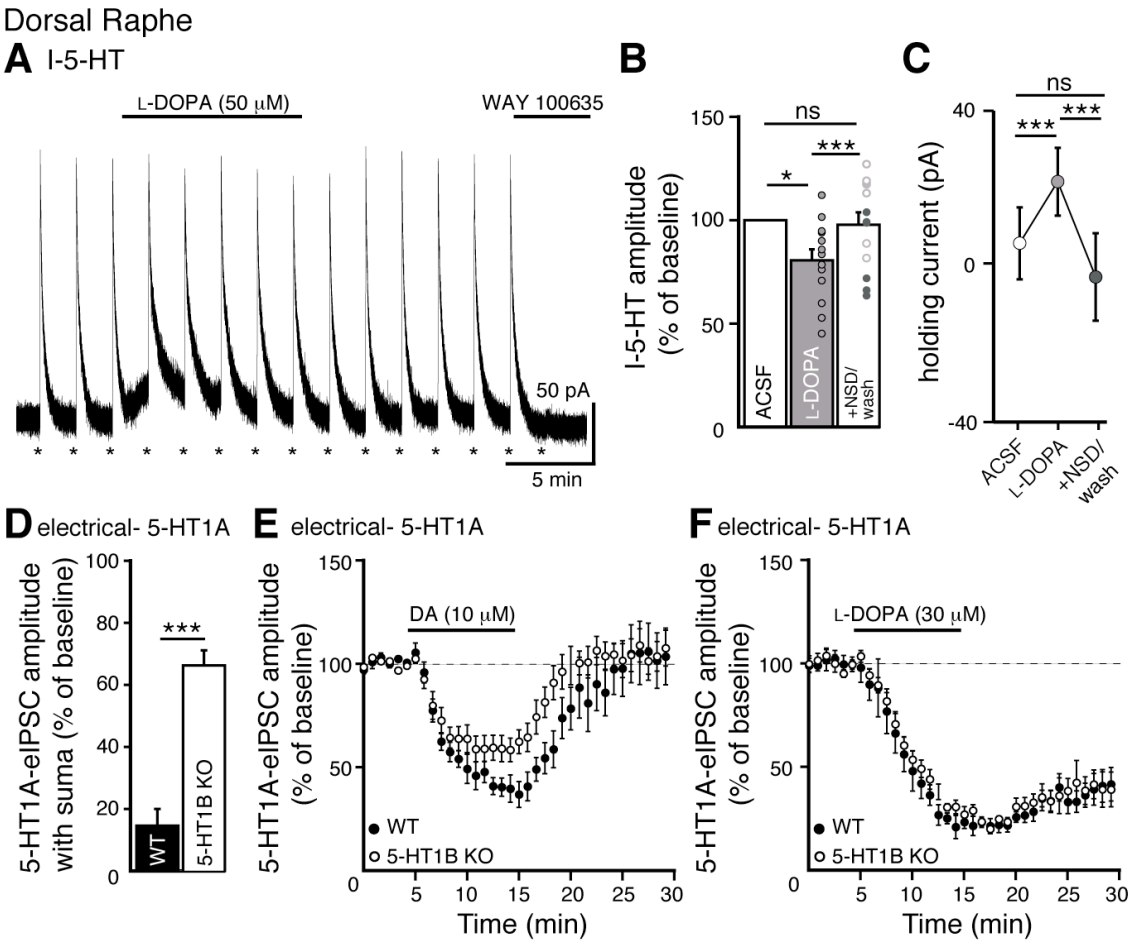

Figure 5.12. Dopamine poorly activates 5-HT$_{1A}$ and 5-HT$_{1B}$ receptors.

(A) Whole-cell voltage clamp recording of the 5-HT$_{1A}$ receptor-mediated currents induced by photolysis of caged-serotonin once every 2 min (I-5-HT, denoted by *) during bath application of L-DOPA (50 μM). I-5-HT was blocked by WAY 100635 (10 μM). (B) L-DOPA reduced I-5-HT and the reduction was reversed with the addition of NSD-1015 (20 μM, open circles) or wash out (filled circles), mean±SEM (n = 13, RM one-way ANOVA). (C) L-DOPA induced an outward current that was reversed with the addition of NSD-1015 or wash out, mean±SEM, (n = 14, RM one-way ANOVA). (D) Inhibition of the 5-HT$_{1A}$-eIPSC by sumatriptan (1 μM) was less in slices from 5-HT$_{1B}$ receptor KO mice (5-HT$_{1B}$ KO) than from their wild type littermates (WT), mean±SEM (n = 7-8, unpaired t test). (E) Dopamine (10 μM) transiently inhibited the 5-HT$_{1A}$-eIPSC in slices from WT (black circles, n = 10) and 5-HT$_{1B}$ KO mice (open circles, n = 8), mean±SEM. (F) L-DOPA (30 μM)-induced depression in the 5-HT$_{1A}$-eIPSC was indistinguishable in slices from 5-HT$_{1B}$ KO (open circles, n = 7) and WT mice (black circles, n = 6), mean±SEM. Baseline: mean amplitude of three I-5-HTs or six 5-HT$_{1A}$-IPSCs preceding L-DOPA application, ns indicates not significant, *p<0.05, and ***p<0.001.

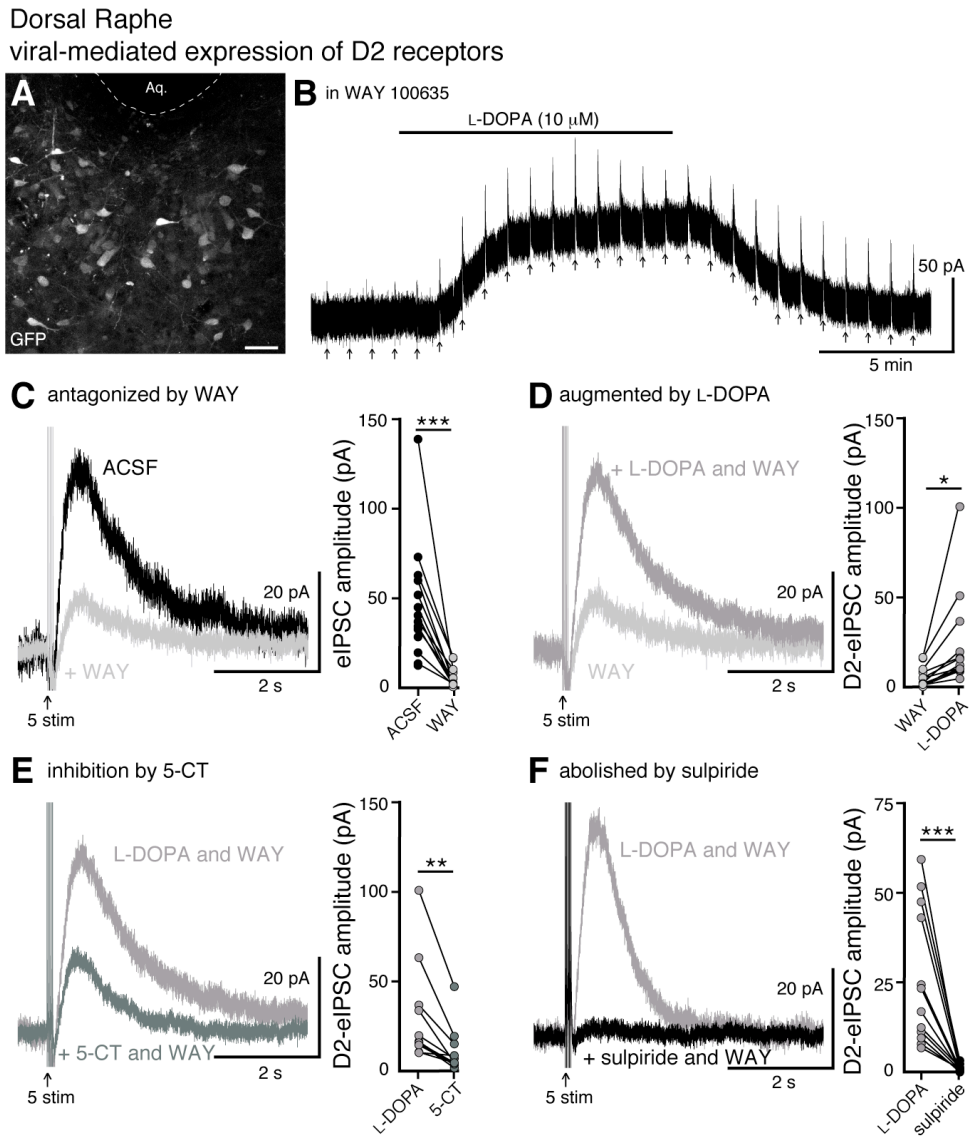

Figure 5.13. Virally expressed D_2 receptors in the DR mediate D_2-IPSCs after L-DOPA.

(A) Representative maximum intensity projection confocal image of GFP^+ neurons in the DR (ventral to the cerebral aqueduct, aq.) infected with AAV-D_2, scale bar: 50 μm. (B-F) Representative traces from a single experiment. (B) Whole-cell voltage clamp recording of the outward current and D_2-eIPSCs induced by bath application of L-DOPA (10 μM), in the presence of WAY 100635 (100 nM). eIPSCs were evoked by electrical stimulation (arrow, 1 or 5 stims) once every 50 s, stimulation artifacts were blanked for clarity. (C) eIPSCs in ACSF and after WAY 100635. 5-HT_{1A}-eIPSCs were inhibited by WAY 100635 (n = 12, paired t test). (D) D_2-eIPSCs in WAY 100635 and after L-DOPA in the continued presence of WAY 100635. L-DOPA augmented the D_2-eIPSC (n = 18, paired t test). (E) L-DOPA-induced D_2-eIPSCs in WAY 100635 and after 5-CT (100 nM). D_2-eIPSCs were inhibited by 5-CT (n = 11, paired t test). (F) L-DOPA-induced D_2-eIPSCs in WAY 100635 and after sulpiride (600 nM). Sulpiride completely eliminated the D_2-eIPSCs (n = 12, paired t test). *p<0.05, **p<0.01, and ***p<0.001.

5.3 ADDITIONAL EXPERIMENTS

Dopamine diffuses after L-DOPA application

In SNc brain slices, application of L-DOPA increased the amplitude of evoked D_2-IPSCs. This augmentation was largely due to the release of dopamine from 5-HT terminals. The D_2-IPSC produced by selective ChR2 activation of 5-HT terminals in the SNc was significantly slower than the D_2-IPSC produced by electrical stimulation. The differences in kinetics may reflect differences intrinsic to the stimulation paradigm. However, L-DOPA also increased the frequency of spontaneous D_2-IPSCs, without likely involvement of 5-HT terminals. Inhibiting transmitter release from 5-HT terminals had no effect on the L-DOPA-induced increase in spontaneous D_2-IPSC frequency (Figure 5.4 and Figure 5.6). These results suggest the possibility that 5-HT terminals are not directly synapsing onto dopamine neurons.

To determine if the diffusion of dopamine was required for L-DOPA to augment evoked and spontaneous dopamine transmission, recordings were made from dopamine neurons in a dextran solution (5-10%), which slows activation of D_2 receptors by dopamine from extrasynaptic, but not synaptic sites (Figure 3.2). Application of L-DOPA (10 μM, 10 min) in dextran solution significantly increased the amplitude of the evoked D_2-IPSC (160 ± 16% of baseline, $p = 0.003$, $n = 17$, Figure 5.14A and B). However, in the presence of dextran, the L-DOPA-induced augmentation was significantly less than measured in control solution ($p < 0.001$, unpaired *t* test, Figure 5.14A and B). After application of L-DOPA, the contribution of dopamine release from 5-HT terminals was assessed by application of the 5-HT_{1B} receptor agonist, sumatriptan (1 μM) . In 8/11 cells, the amplitude of the evoked D_2-IPSC was reduced by sumatriptan. When sumatripan was

applied before L-DOPA in dextran, the L-DOPA-induced augmentation in the evoked D_2-IPSC was not significantly different than without sumatriptan (130 ± 12%, $p = 0.47$, $n = 3$, unpaired t test). Thus, it is possible that some 5-HT terminal-derived dopamine was augmenting the evoked D_2-IPSC, but the contribution is likely small. Unlike evoked release, dextran solution did not alter the L-DOPA-induced increased in spontaneous D_2-IPSC frequency (Figure 5.14C). Taken together, these results suggest that after L-DOPA, dopamine release from 5-HT terminals must travel some distance before activating D_2 receptors. If dopamine is released spontaneously from 5-HT terminals, it is too diffuse or otherwise insufficient to produce spontaneous D_2-IPSCs.

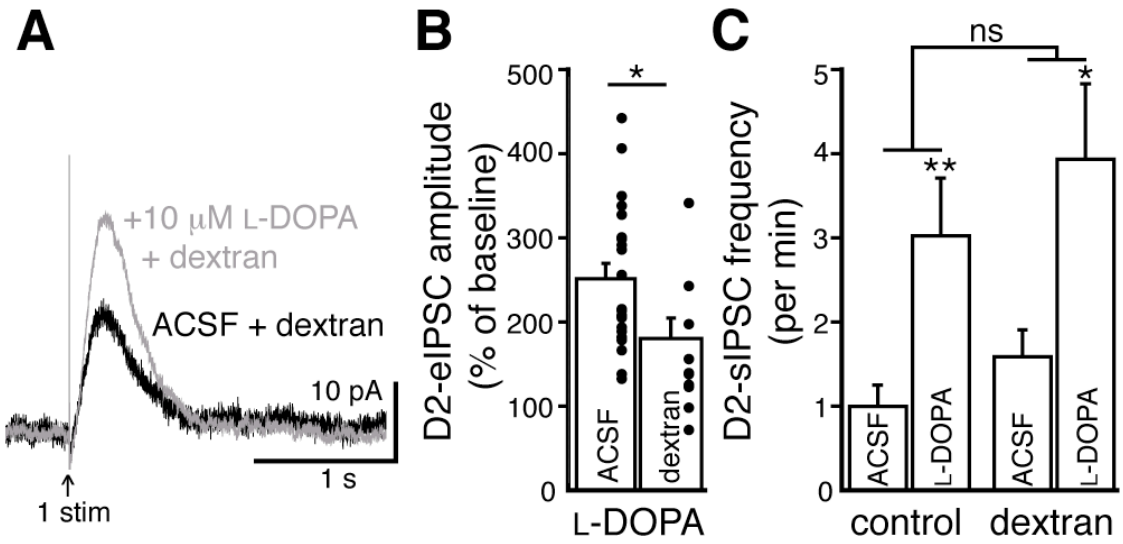

Figure 5.14. Slowing diffusion of dopamine reduces the L-DOPA-induced increase in the evoked D_2-IPSC amplitude, but not in spontaneous D_2-IPSC frequency.

(A) Representative traces of D_2-eIPSCs from a single experiment in dextran-containing ACSF and after addition of L-DOPA. (B) The L-DOPA-induced increase in the D_2-eIPSC amplitude was reduced in dextran, compared to the increase in ACSF (n = 17-22, unpaired t test), mean±SEM, baseline: mean amplitude of six D_2-eIPSCs preceding L-DOPA application. (C) L-DOPA increased the frequency of D_2-sIPSCs (per min) in control and dextran-containing solution, mean±SEM (n = 6-17, two-way ANOVA followed by Bonferroni). ns indicates not significant, *p<0.05 and **p<0.01.

Chapter 6 POSTSYNAPTIC COMPONENTS

PREFACE

This chapter describes work investigating postsynaptic components of the dopamine synapse, including postsynaptic changes after *in vivo* cocaine exposure described in Chapter 4. Included is a study that examined the regulation of acute desensitization and drug-induced plasticity of GIRK-mediated currents activated by the two splice variants of the D_2 receptor, D_2S and D_2L. The study also describes the localization of Flag-D_2 receptors. Lastly, preliminary work towards determining the sites of D_2 receptor-mediated synaptic currents is described.

I conducted the study on the D_2 receptor splice variants under the mentorship and assistance of Drs. John T. Williams and Kim A. Neve. I designed and performed experiments, analyzed and illustrated data, and wrote the manscript. All electrophysiology was done in close collaboration with Dr. Brooks G. Robinson. Dr. John T. Williams also performed electrophysiological recordings and two-photon microscopy. David C. Buck performed stereotaxic virus injections. James R. Bunzow generated the transgenic Flag-D_2 receptor mouse line used in this study. Rachael L. Neve generated the viral constructs. All co-authors assisted in the preparation of the manuscript. The preliminary work towards determining the sites of D_2 receptor-mediated synaptic currents was done in collaboration with Drs. John T. Williams, Craig Jahr, and Brett Carter.

The results demonstrate that both D_2S and D_2L functioned as somatodendritic D_2 receptors but were differentially modified by intracellular pathway for calcium signaling. In addition, the results indicate that the removal of calcium-dependent desensitization after *in vivo* cocaine exposure involved the expression of D_2L receptors. Lastly, Flag-D2 receptors were found clustered on the soma, dendrites, and spine-like structures on dopamine neurons, and focal uncaging of dopamine onto similar structures was sufficient to elicit an outward current.

In the context of this dissertation, this chapter demonstrates that $D2_S$ and $D2_L$ receptors mediate spontaneous D_2-IPSCs and further examines the possibility that the D_2 receptor splice variants are involved in cocaine-induced plasticity at the somatodendritic dopamine synapse.

6.1 DISTINCT REGULATION OF DOPAMINE D_2S AND D_2L AUTORECEPTOR[A] SIGNALING BY CALCIUM

Stephanie C. Gantz[1], Brooks G. Robinson[1], David C. Buck[2], James R. Bunzow[1], Rachael L. Neve[3], John T. Williams[1], and Kim A. Neve[2]

[1]Vollum Institute
Oregon Health & Science University
Portland, OR 97239

[2]Research Service, VA Portland Health Care System
and
Department of Behavioral Neuroscience
Oregon Health & Science University
Portland, OR, 97239

[3]Department of Brain and Cognitive Sciences
MIT
Cambridge, MA, 02139

Acknowledgements: This work was supported by the Merit Review Award BX000810 from the US Department of Veterans Affairs, Veterans Health Administration, Office of Research and Development, Biomedical Laboratory Research and Development (K.A.N.) and by NIH P50 DA018165 (K.A.N.), F32 DA038456 (B.G.R), DA04523 (J.T.W.), and DA034388 (J.T.W.).

[This manuscript is presented as published in (Gantz *et al.*, 2015b) *eLife,* August 26, 2015, 4]

[A] The term *autoreceptor* is used in this portion of the dissertation to distinguish the receptors described here from D_2 heteroceptors expressed on non-dopamine neurons.

Abstract

D_2 autoreceptors regulate dopamine release throughout the brain. Two isoforms of the D_2 receptor, D_2S and D_2L, are expressed in midbrain dopamine neurons. Differential roles of these isoforms as autoreceptors are poorly understood. By virally expressing the isoforms in dopamine neurons of D_2 receptor knockout mice, this study assessed the calcium-dependence and drug-induced plasticity of D_2S and D_2L receptor-dependent GIRK currents. The results reveal that D_2S, but not D_2L receptors, exhibited calcium-dependent desensitization similar to that exhibited by endogenous autoreceptors. Two pathways of calcium signaling that regulated D_2 autoreceptor-dependent GIRK signaling were identified, which distinctly affected desensitization and the magnitude of D_2S and D_2L receptor-dependent GIRK currents. Previous *in vivo* cocaine exposure removed calcium-dependent D_2 autoreceptor desensitization in wild type, but not D_2S-only mice. Thus, expression of D_2S as the exclusive autoreceptor was insufficient for cocaine-induced plasticity, implying a functional role for the co-expression of D_2S and D_2L autoreceptors.

Introduction

Central dopamine transmission coordinates reinforcement learning, including recognition of reward-predictive stimuli and initiation of goal-directed movements. Natural rewards, reward-predictive cues, and drugs of abuse elicit a rapid increase in dopamine release from dopamine axon terminals and somatodendritic sites within the ventral midbrain. Dopamine release is negatively regulated by the activation of dopamine D_2 autoreceptors on somatodendritic and axon terminals (reviewed in Ford, 2014). Loss of D_2 autoreceptor-mediated inhibition results in elevated extracellular dopamine and is associated with perseverative drug-seeking, enhanced motivation for food, and novelty-

induced hyperactivity (Anzalone *et al*., 2012; Bello *et al*., 2011; Holroyd *et al*., 2015; Marinelli and White, 2000; Marinelli *et al*., 2003). Chronic D_2 autoreceptor activation impairs the formation of dopamine- and glutamate-releasing axon terminals (Fasano *et al*., 2010). Thus, D_2 autoreceptors regulate structural and functional plasticity of dopamine neurons and are essential in limiting impulsivity and reward-seeking behaviors.

A prominent feature of somatodendritic D_2 autoreceptors is their activation of G protein-coupled inwardly rectifying potassium (GIRK) channels, resulting in inhibition of action potential firing and subsequent dopamine release. During prolonged activation, desensitization of D_2 autoreceptors reduces the D_2 autoreceptor-dependent GIRK current. A component of desensitization is dependent on intracellular calcium (Beckstead and Williams, 2007). Single or repeated exposure to drugs of abuse modifies D_2 autoreceptor function (Gantz *et al*., 2013; Henry *et al*., 1989; Jones *et al*., 2000; Madhavan *et al*., 2013; Marinelli *et al*., 2003; Wolf *et al*., 1993), including a loss of the calcium-dependent component of D_2 autoreceptor-GIRK desensitization (Perra *et al*., 2011). The mechanism(s) that underlie acute desensitization and drug-induced plasticity of D_2 autoreceptor-mediated inhibition remain incompletely characterized.

There are two splice variants of the D_2 receptor, which differ by a 29-amino acid insert in the third intracellular loop in D_2-Long (D_2L) that is absent in D2-Short (D_2S). Biased expression of D_2S or D_2L receptors alters behavioral responses to drugs of abuse (Bulwa *et al*., 2011; Smith *et al*., 2002) and has been associated with drug addiction in human studies (Moyer *et al*., 2011; Sasabe *et al*., 2007). Functionally distinct roles for D_2S and D_2L receptors have been proposed based on characterization of mice lacking

D_2L (Usiello *et al*., 2000; Wang *et al*., 2000) or D2S (Radl *et al*., 2013). Behavioral and biochemical studies have designated D_2L as the postsynaptic receptor expressed on non-dopaminergic medium spiny neurons in the basal forebrain and D_2S as the autoreceptor (Khan *et al*., 1998; Lindgren *et al*., 2003; Usiello *et al*., 2000). However, both D_2S and D_2L receptors are expressed in dopamine neurons and function as somatodendritic autoreceptors (Dragicevic *et al*., 2014; Jang *et al*., 2011; Jomphe *et al*., 2006; Khan *et al*., 1998; Neve *et al*., 2013). Biochemical studies indicate that D_2S receptors internalize and desensitize more readily than D_2L receptors (Ito *et al*., 1999; Itokawa *et al*., 1996; Liu *et al*., 1992; Morris *et al*., 2007; Thibault *et al*., 2011), but acute desensitization and drug-induced plasticity of D_2S and D_2L receptor-dependent GIRK currents have not been characterized. Using virus-mediated expression of the D2 receptor splice variants in D_2 receptor knockout mice, this study reveals that D_2S but not D_2L receptor-dependent GIRK signaling exhibited calcium-dependent desensitization. Manipulations of pathways involved in D_2 autoreceptor desensitization had distinct actions on D_2S and D_2L receptor-dependent GIRK currents. Lastly, a single *in vivo* cocaine exposure removed the calcium-dependent component of D_2 autoreceptor-GIRK desensitization in wild type mice, but not D_2S-only mice; thus, the expression of D_2S as the exclusive autoreceptor was insufficient for drug-induced plasticity. Taken together, the results of this study imply a physiological role for the co-expression of D_2S and D_2L autoreceptors.

Results

Both D_2S and D_2L can function as autoreceptors

To examine the ability of D_2S and D_2L receptors to activate a GIRK conductance, single isoforms were expressed in midbrain dopamine neurons. *Drd2*$^{-/-}$ mice received bilateral

injections of an adeno-associated viral (AAV) vector generating either rat D_2S or D_2L receptor and GFP expression, as previously described (Neve *et al*., 2013). Infected neurons in brain slices containing the substantia nigra *pars compacta* (SNc) were identified by GFP visualization. Whole-cell patch clamp recordings were made from SNc dopamine neurons using an internal solution containing the calcium chelator, BAPTA (10 mM), as used previously (Neve *et al*., 2013). Application of a saturating concentration of the D_2 receptor agonist, quinpirole (30 μM), produced an outward current that was reversed by application of the D_2 receptor antagonist, sulpiride (600 nM, Figure 6.1A-B). There was no difference in the peak amplitude of quinpirole-induced currents mediated by D_2S and D_2L receptors (Figure 6.1B). In the continued presence of agonist, D_2 autoreceptors desensitize resulting in a decline in the agonist-induced outward current (Beckstead *et al*., 2009; Perra *et al*., 2011). The decline in the quinpirole-induced current mediated by D_2S and D_2L receptors was indistinguishable (Figure 6.1A and C).

In the SNc, dopamine release from neighboring dopamine neurons elicits D_2 receptor-mediated inhibitory postsynaptic currents (IPSCs) through the activation of GIRK channels (Beckstead *et al*., 2004; Gantz *et al*., 2013). D_2S and D_2L receptors mediate kinetically-identical IPSCs following electrically stimulated dopamine release (Neve *et al*., 2013). Stimulus-independent dopamine release also occurs, resulting in spontaneous D2 receptor-mediated IPSCs (Gantz *et al*., 2013). In slices from mice infected with either D_2S or D_2L, spontaneous IPSCs were abolished by application of sulpiride (600 nM, Figure 6.1D-E). The durations of D2S, D2L, and wild type D2 receptor-mediated spontaneous IPSCs were identical (Figure 6.1F, [from Gantz *et al*., 2013, WT: 515±17 ms, n=76 sIPSCs]). Amplitude and frequency of spontaneous IPSCs

are affected by the level of D_2 receptor expression and dopamine synthesis (Gantz *et al*., 2013 and 2015a). Since these parameters may be influenced by variegated viral infection, the amplitude and frequency of D_2S- and D_2L-sIPSCs were not compared. Taken together, the results confirm previous work indicating that D_2S and D_2L can serve as autoreceptors at somatodendritic dopamine synapses (Neve *et al*., 2013).

Calcium entry promotes desensitization of D_2 autoreceptors in wild type dopamine neurons

Desensitization in the GIRK current induced by D_2 receptor agonists is affected by intracellular calcium buffering. Weak calcium buffering with intracellular EGTA (0.025 – 0.4 mM) results in greater decline in the GIRK current induced by D_2 receptor agonists, without affecting the decline in the GIRK current induced by $GABA_B$ receptor agonists (Beckstead and Williams, 2007; Perra *et al*., 2011). These results were confirmed in wild type mice using internal solutions containing either EGTA (0.1 mM, EGTA internal) or BAPTA (10 mM, BAPTA internal). Application of quinpirole (10 μM) or the $GABA_B$ agonist, baclofen (30 μM), resulted in outward currents that declined in the continued presence of agonist (Figure 6.2A, 6.2E). The peak amplitudes of the quinpirole- and baclofen-induced currents were larger when using BAPTA internal than EGTA internal (Figure 6.2A-B, 6.2E-F). The quinpirole-induced current desensitized more quickly with EGTA internal compared with experiments using BAPTA internal (Figure 6.2A, 6.2C-D). This calcium-dependent desensitization was specific to the D_2 receptor since the decline in baclofen-induced current was not dependent on the internal solution (Figure 6.2E, 6.2G-H). Thus, as reported previously (Beckstead and Williams, 2007; Perra *et al*.,

2011), D_2 autoreceptors exhibited a calcium-dependent desensitization that resulted in a larger decline in the D_2 autoreceptor-dependent current when intracellular calcium was buffered with a low concentration of EGTA.

EGTA and BAPTA have a similar affinity for calcium but differ in the kinetics of binding. This property is frequently used to characterize the distance between a calcium source and a calcium sensor. Buffering with EGTA allows calcium to diffuse farther (microdomain) than BAPTA, which limits calcium spread (nanodomain) from a calcium source. However, the concentrations of EGTA and BAPTA used in this study may also result in different levels of resting free calcium (Adler *et al*., 1991). To determine whether the difference in D2 autoreceptor desensitization observed with the two internals was explained by resting free calcium concentration, the level of free calcium in the BAPTA internal was increased to 300 nM by addition of $CaCl_2$ (7.37 mM) (BAPTA+Ca^{2+}, see Materials and Methods). The peak amplitude and the decline in the quinpirole-induced current recorded with BAPTA+Ca^{2+} internal were not different from measurements recorded with BAPTA alone (Figure 6.3A-B). Interestingly, BAPTA+Ca^{2+} internal decreased the peak amplitude of the baclofen-induced current significantly relative to the amplitude recorded with BAPTA internal (Figure 3C), and was not different from the current measured with EGTA internal (Figure 3C). The decline in the baclofen-induced current was unaffected by BAPTA+Ca^{2+} (Figure 3D).

To verify that the resting free calcium was increased using BAPTA+Ca^{2+} internal, the positive modulator of the small conductance calcium-activated potassium channel (SK), NS309 (10 μM) was applied. Although NS309 did not produce a current using either BAPTA or EGTA internals, it caused an outward current with BAPTA+Ca^{2+}

internal (Figure 6.4A-B). The NS309-induced current was reversed by the SK channel blocker apamin (200 nM). Thus, the BAPTA+Ca^{2+} internal increased resting free calcium.

Taken together, the results indicate that the resting free calcium had differential actions on D2 and $GABA_B$ receptor-dependent GIRK currents. The magnitude of the $GABA_B$ receptor-dependent current was sensitive to resting free calcium, but the decline in current was independent of resting free calcium. The decline in D_2 autoreceptor-dependent current was dominated by the spatial regulation of intracellular calcium, not resting free calcium.

Desensitization in D_2S- but not D_2L-GIRK currents is calcium-dependent

Recordings were made from dopamine neurons that expressed D_2S or D_2L receptors using an internal solution containing EGTA (0.1 mM). Application of quinpirole (30 μM) produced an outward current that declined and was reversed by sulpiride (600 nM). In D_2S neurons, the decline using EGTA internal was faster than the decline using BAPTA internal (Figure 6.5A, 6.5D, Figure 6.6A). In contrast, in D_2L neurons, the decline with EGTA and BAPTA internal was not different (Figure 6.5A, 6.5D, Figure 6.6B). The insensitivity of the decline in D_2L neurons to calcium buffering resulted in significantly more desensitization of D_2S than D_2L with EGTA internal (Figure 6.5B). The peak amplitude of the quinpirole-induced currents in D_2S and D_2L neurons was not different (Figure 6.5C), indicating the difference between D_2S and D_2L is unlikely to be due to differences in the level of expression of D_2 receptors. Application of the $GABA_B$ agonist, baclofen (30 μM), produced an outward current that was reversed by the $GABA_B$

antagonist, CGP-55845 (200 nM). The peak amplitude of the baclofen-induced current was not different among D_2S (EGTA: 259±28 pA; BAPTA: 531±94 pA), D_2L (EGTA: 277±29 pA; BAPTA: 520±43 pA), D_2-KO (AAV-GFP-only, EGTA: 279±54 pA; BAPTA: 664±80 pA), and wild type dopamine neurons ($p>0.05$). There was also no change in the decline in the baclofen-induced current in D_2S- or D_2L-expressing neurons (Figure 6.5E).

To minimize potential confounds of ectopic D_2 receptor expression in non-dopamine neurons in the midbrain, the calcium-sensitivity of D_2S receptor-GIRK desensitization was validated using a transgenic D_2-Short mouse line, generated by a cross between TH-hD_2S (Gantz *et al*., 2013) and D_2 receptor knockout mice. In this line, the expression of Flag-tagged human D_2S receptors depends on the tyrosine hydroxylase promoter (Figure 6.7). In slices from these mice, quinpirole (10 μM) produced larger outward currents using BAPTA internal compared to EGTA internal (Figure 6.5F). The currents were significantly larger than those recorded in wild type dopamine neurons (Figure 6.2B, 6.5F), indicating overexpression of D_2 receptors. Despite the overexpression, the magnitude of the decline in the quinpirole-induced current was similar to wild type (Figure 6.2C-D, 6.5H). Also consistent with wild type, the decline in the quinpirole-induced current using EGTA internal was significantly faster than the decline using BAPTA internal (Figure 6.5G-H). Taken together, these results indicate that D_2S but not D_2L receptor-GIRK signaling exhibited calcium-dependent desensitization.

Calcium signaling regulates D_2 autoreceptor-activated GIRK conductance

Intracellular calcium stores

Endoplasmic calcium stores contribute to calcium-dependent desensitization of D_2 autoreceptor-GIRK signaling (Perra *et al*., 2011). Cyclopiazonic acid (CPA) disrupts the sarco/endoplasmic reticulum calcium-ATPase leading to rapid depletion of intracellular calcium stores (Ford *et al*., 2010). Brain slices were exposed to CPA (10 μM) >20 min prior to making recordings. As shown previously in wild type dopamine neurons, CPA reduced the decline in the quinpirole-induced current using EGTA internal and had no effect when using BAPTA internal (Figure 6.8A). CPA did not change the decline in the baclofen-induced current recorded with either internal (Figure 6.8B). In D_2S neurons, CPA also reduced the decline in the quinpirole-induced current, but the decline in the quinpirole-induced current in D_2L neurons was not changed (Figure 6.8C). These results indicate that calcium release from intracellular stores contributed to D_2S but not D_2L receptor-GIRK desensitization.

In wild type neurons with EGTA internal, CPA had no significant effect on the magnitude of the maximal current produced by bath application of quinpirole (control: 172±19 pA, *n*=15; CPA: 194±22 pA, *n*=13, p=0.46, unpaired *t* test). In a previous study, sub-saturating D_2 receptor-dependent currents repeatedly produced by pressure ejection of dopamine are augmented by bath application of CPA for 10-20 min (Perra *et al*., 2011). Therefore, the effect of CPA was examined on submaximal dopamine currents produced by iontophoretic application of dopamine once every 50 s (I-DA). In wild type neurons using an EGTA internal, CPA (10 μM) significantly augmented I-DA (Figure 6.8D). While CPA rapidly depletes intracellular calcium stores, the CPA-induced augmentation of I-DA did not plateau until >15 min (Figure 6.9). CPA also significantly

augmented I-DA in D_2S and D_2L neurons (Figure 6.8E and Figure 6.9). However, the magnitude of the increase was significantly greater for D_2L receptor-dependent currents than D_2S (Figure 5E). Thus, depletion of calcium from intracellular stores differentially increased D_2S and D_2L receptor-dependent GIRK signaling.

L-type calcium channels

In SNc dopamine neurons, calcium entry via somatodendritic low-voltage-activated L-type calcium channels occurs during tonic 'pacemaker' action potential firing, creating oscillations of elevated cytosolic calcium in the somatodendritic compartment (Chan *et al*., 2007; Hage and Khaliq, 2015; Puopolo *et al*., 2007). L-type calcium channels may be involved in D_2 autoreceptor desensitization, (Dragicevic *et al*., 2014; Goldberg *et al*., 2005; Guzman *et al*., 2010), but no studies have directly measured D2 autoreceptor-dependent GIRK signaling. To determine if L-type calcium channels regulate D_2 autoreceptor-dependent GIRK signaling, brain slices were exposed to the L-type calcium channel blocker, isradipine (300 nM), >20 min prior to making recordings. In wild type dopamine neurons, isradipine did not significantly change the decline in the quinpirole-induced current using either EGTA or BAPTA internal (Figure 6.10A). Isradipine also had no effect on the decline in baclofen-induced current (Figure 6.10B). However, isradipine reduced the decline in the quinpirole-induced current in D_2S neurons, without affecting the decline in D_2L neurons (Figure 6.10C). Taken together, the results suggest that calcium influx via L-type calcium channels was not involved in desensitization of D_2 autoreceptor-dependent GIRK currents in wild type dopamine neurons, but promoted desensitization of D_2S receptors.

In wild type neurons with EGTA internal, isradipine had no significant effect on the magnitude of the maximal current produced by bath application of quinpirole (control: 172±19 pA, *n*=15; israd: 178±28 pA, *n*=11, p=0.86, unpaired *t* test). Therefore, the effect of isradipine on I-DA was examined. In wild type dopamine neurons using an EGTA internal, isradipine (300 nM) significantly augmented I-DA (Figure 6.10D) after >10 min (Figure 6.11). In D_2S and D_2L neurons, I-DA was also augmented by isradipine (Figure 6.10E and Figure 6.11). As was found with CPA, the magnitude of the increase was greater for D_2L receptor-dependent currents than D_2S (Figure 6.10E). Thus, inhibition of calcium entry via L-type calcium channels differentially increased D_2S and D_2L receptor-dependent GIRK signaling.

A single *in vivo* cocaine exposure decreases calcium-dependent D_2 autoreceptor desensitization

Drugs of abuse change the D_2 autoreceptor activation of GIRK conductance (Arora *et al*., 2011; Beckstead and Williams, 2007; Dragicevic *et al*., 2014; Gantz *et al*., 2013; Sharpe *et al*., 2014). One of these changes is a loss of the calcium-dependent component of D_2 autoreceptor desensitization after repeated ethanol exposure (Perra *et al*., 2011). Wild type mice were given a single injection of cocaine (20 mg/kg, i.p.) or an equal volume of saline, and brain slices were made 24 h later. With EGTA internal, the quinpirole-induced current declined significantly less in slices from cocaine-treated mice compared to control mice (saline-treated and naïve, Figure 6.12A). In fact, the decline was no longer statistically different from that found with BAPTA internal (Figure 6.12A). There was no difference in the decline in the quinpirole-induced current in slices taken from

control or cocaine-treated mice with BAPTA internal (Figure 6.12A). There was no change in the decline in the baclofen-induced current, using either internal (Figure 6.12F). Thus, in wild type mice, a single *in vivo* cocaine exposure resulted in the loss of calcium-dependent D_2 autoreceptor desensitization without affecting $GABA_B$ receptor desensitization.

A loss of calcium-dependent D_2 autoreceptor desensitization after cocaine exposure in wild type neurons could be due to a change in calcium signaling or a functional increase in the contribution of D_2L receptors. To test whether D_2L receptors are involved, *Drd2*$^{-/-}$ mice that had received midbrain injections of AAV-D_2S or AAV-D_2L were given a single injection of cocaine (20 mg/kg, i.p.) and brain slices were made 24 h later. In D_2L neurons, cocaine exposure did not alter the decline in quinpirole-induced current (Figure 6.12B). Likewise, cocaine exposure did not alter the calcium-dependent decline in the quinpirole-induced current in D_2S neurons. Similar to naïve AAV-D_2S mice, the decline of the quinpirole-induced current was greater using EGTA internal than with BAPTA internal (Figure 6.12C). Thus, unlike what was found in slices from wild type mice, cocaine exposure did not reduce the calcium-dependent decline in the quinpirole-induced current. This result was not dependent on overexpression as it was also observed in D_2S neurons in which quinpirole produced outward currents of similar magnitude to wild type neurons (data not shown). This result was also recapitulated in the transgenic D2-Short mice (Figure 6.12D), where expression of D_2S receptors in the midbrain is restricted to dopamine neurons. Since wild type, but not D_2S-only dopamine neurons exhibited a reduction in calcium-dependent desensitization after cocaine

exposure, these results suggest that constitutive or viral-mediated expression of D_2S as the exclusive autoreceptor was insufficient for cocaine-induced plasticity.

To determine if the expression of D_2L was sufficient to enable loss of calcium-dependent D_2 receptor desensitization of D_2S, *Drd2*$^{-/-}$ mice received bilateral injections of a 1:1 mixture of AAV-D_2S and AAV-D_2L. In dopamine neurons from mice infected with both splice variants, the amplitude of the quinpirole-induced currents was similar to those measured in neurons expressing D_2S- or D_2L-only (EGTA: 333±48 pA, n=9; BAPTA: 442±86 pA, n=6, see Figures 6.1B and 6.5C for comparison). This suggests a similar level of D_2 receptor overexpression as in neurons that express single variants. Surprisingly, the decline in the quinpirole-induced current was similar between EGTA and BAPTA internals (Figure 6.12E). Therefore, the viral expression of both D_2S and D_2L receptors did not mimic D_2 receptor-dependent GIRK signaling in naïve wild type mice. Moreover, the decline in the quinpirole-induced current did not change after *in vivo* cocaine exposure (Figure 6.12E), suggesting that the viral expression of both D_2S and D_2L receptors precluded cocaine-induced plasticity in D_2 receptor-dependent GIRK signaling. To ensure that this result was not due to preferential expression of D_2L receptors following injection of the D_2S/D_2L virus mixture, dopamine neurons in transgenic D_2-Short mice were infected with AAV-D_2L. The expression of D_2S was confirmed by labeling dopamine neurons with an Alexa Fluor 594-conjugated M1 antibody and imaging on a two-photon microscope (e.g. Figure 6.7B). Recordings were made from neurons with Flag-D_2S staining that were also GFP$^+$ (AAV-D_2L). With EGTA internal, the decline in the quinpirole-induced current in transgenic D_2-Short neurons also expressing D_2L was equivalent to the decline measured in neurons receiving

the D_2S/D_2L virus mixture, and significantly less than the decline in the quinpirole-induced current in transgenic D_2-Short-only neurons (Figure 6.12D). As observed in wild type, there was no change in the decline in the baclofen-induced current after cocaine exposure in any of the groups ($p>0.05$ for all comparisons, data not shown). Taken together, the results indicate that regardless of the presence of D_2S, the viral expression of D_2L eliminated calcium-dependent D_2 receptor desensitization and precluded cocaine-induced plasticity.

Discussion

Alternative splicing generates two isoforms of the dopamine D_2 receptor, D_2S and D_2L. D_2S has been considered the autoreceptor, but both are expressed and functional in midbrain dopamine neurons. Evidence of distinct functional roles for the splice variants as autoreceptors has not been described. This study assessed the calcium-dependence and drug-induced plasticity of the desensitization of GIRK currents mediated by D_2S and D_2L receptors expressed in SNc dopamine neurons. The results reveal that the D_2S receptor, but not the D_2L receptor, exhibited calcium-dependent desensitization. Manipulating pathways for calcium signaling removed the calcium-dependent component of D_2S receptor desensitization, demonstrating these receptors were amenable to plasticity. Cocaine exposure eliminated calcium-dependent D_2 autoreceptor desensitization in dopamine neurons from wild type mice without altering desensitization of neurons expressing only D_2S or D_2L. Furthermore, viral expression of D_2L eliminated calcium-dependent desensitization, resembling the D_2 autoreceptor desensitization observed in dopamine neurons from wild type mice after *in vivo* cocaine exposure.

Calcium-dependent regulation of D_2 autoreceptor-dependent GIRK conductance

Calcium entry promotes desensitization of D_2 autoreceptors in wild type dopamine neurons. Buffering intracellular calcium with BAPTA reduces the decline in D_2 autoreceptor-, but not $GABA_B$ receptor-mediated GIRK currents (Beckstead and Williams, 2007; Perra *et al*., 2011). In this study, the calcium-dependent component of D_2 autoreceptor desensitization was observed in wild type and D_2S-only expressing dopamine neurons. However, in neurons where D_2L receptors were virally expressed, there was no calcium-dependent desensitization. This was observed whether D_2L receptors were expressed alone, or in conjunction with transgenic or virally expressed D_2S receptors.

This study describes two calcium sources that regulate D_2 autoreceptor-dependent GIRK currents: intracellular calcium stores and L-type calcium channels. These intracellular pathways did not regulate desensitization of $GABA_B$ receptor-dependent GIRK currents. Consistent with a previous report (Perra *et al*., 2011), depleting intracellular calcium stores removed calcium-dependent D_2 autoreceptor desensitization in wild type neurons. Depleting intracellular calcium stores also reduced the magnitude of D_2S receptor desensitization to a saturating concentration of agonist, without affecting D_2L receptor desensitization. Preventing calcium entry from L-type calcium channels also reduced D_2S receptor desensitization, without affecting wild type or D_2L receptor desensitization. The results demonstrate that the calcium-dependent component of D_2S receptor desensitization was readily modifiable.

Desensitization of D_2 autoreceptors in wild type dopamine neurons was controlled by elevated concentrations of calcium in intracellular microdomains and could not be

enhanced by raising the resting free calcium concentration. The lack of a calcium-dependent component in D_2L receptor desensitization could be due to localization outside of the calcium microdomains, despite showing similar distribution in the somatodendritic compartment as D_2S receptors (Jomphe *et al*., 2006), or to another property of this isoform. Depleting intracellular calcium stores or blocking L-type calcium channels produced robust augmentation in D_2L receptor-dependent GIRK currents produced by iontophoretically applied dopamine that was greater than the augmentation of D_2S receptor-dependent GIRK currents. The lack of effect of manipulating calcium signaling on D_2L receptor desensitization in the presence of a saturating concentration of quinpirole suggests that the enhanced response of D_2L to iontophoretically applied dopamine does not reflect removal of tonic desensitization. Nonetheless, the same intracellular pathways interacting with D_2S receptors also modified D_2L receptor-dependent GIRK currents. It is therefore likely that D_2S and D_2L receptors are in similar calcium microdomains and the lack of apparent calcium-dependent desensitization upon saturating agonist exposure is a property specific to the D_2L isoform.

Plasticity of the calcium-dependent D_2 autoreceptor desensitization

Drugs of abuse cause functional changes to dopamine neuron physiology, including regulation of D_2 and $GABA_B$ receptor activation of GIRK conductance (Arora *et al*., 2011; Beckstead *et al*., 2009; Dragicevic *et al*., 2014; Padgett *et al*., 2012; Perra *et al*., 2011; Sharpe *et al*., 2014). Several recent studies reported drug-induced changes in D_2 autoreceptor mediated-GIRK signaling that are contingent on the method of recording (whole-cell versus perforated-patch, Dragicevic *et al*., 2014) or the calcium buffering

capabilities of the whole-cell internal solution (Perra *et al*., 2011; Sharpe *et al*., 2014) implicating dependence on intracellular calcium. In this study, 24 h after a single *in vivo* cocaine exposure, the calcium-dependent component of D_2 autoreceptor desensitization was eliminated, similar to the change observed after repeated ethanol exposure (Perra *et al*., 2011). Thus, this study confirms the Perra *et al*. (2011) finding and further demonstrates that the plasticity in D_2 autoreceptor function did not require repeated drug exposure. Whether this plasticity was due to a change in calcium-dependent pathways or the D_2 autoreceptors themselves was previously unresolved. The findings of this study support the latter.

Cocaine exposure may change the calcium-dependent pathways examined in this study. Twenty-four h after a single cocaine exposure, metabotropic glutamate receptor 1 signaling is attenuated (Kramer and Williams, 2015). The activation of metabotropic glutamate receptors decreases D_2 autoreceptor-dependent GIRK currents (Perra *et al*., 2011) and may desensitize D_2 autoreceptors through calcium release from intracellular stores. A change in the contribution of calcium influx via L-type calcium channels to D_2 autoreceptor desensitization may also result from cocaine exposure (Dragicevic *et al*., 2014). In this study, depleting intracellular calcium stores or blocking L-type calcium channels readily removed calcium-dependent D_2S receptor desensitization. Given these results, it was surprising that cocaine exposure did not alter calcium-dependent D_2S receptor desensitization. This result was recapitulated in dopamine neurons from transgenic D_2-Short mice indicating it was not an artifact of virus-mediated expression. Thus, these results suggest that the expression of D_2S as the exclusive autoreceptor is insufficient for cocaine-induced plasticity observed in wild type dopamine neurons.

In wild type dopamine neurons, it may be that the expression of D_2L receptors is involved in cocaine-induced plasticity. Biased expression of D_2S and D_2L receptors has been associated with drug abuse. The loss of D_2L receptors and concomitant overexpression of D_2S receptors in D_2L-deficient mice is associated with altered drug-taking (Bulwa *et al*., 2011) and conditioned place preference (Smith *et al*., 2002). In addition, single nucleotide polymorphisms that result in overexpression of D_2S receptors are observed in humans with a history of drug abuse (Moyer *et al*., 2011; Sasabe *et al*., 2007). In this study, the viral expression of D_2L receptors, alone or with D_2S receptors, resulted in a loss of calcium-dependent D_2 receptor desensitization. Moreover, it precluded any further cocaine-induced reduction in calcium-dependent D_2 receptor desensitization. These results suggest that the overexpression of D_2L receptors resembles cocaine-induced plasticity. Transient elevation in extracellular dopamine up-regulates D_2L mRNA (Giordano *et al*., 2006; Oomizu *et al*., 2003; Wernicke *et al*., 2010; Zhang *et al*., 1994; but see Dragicevic *et al*., 2014; Filtz *et al*., 1993). In addition, D_2L receptors are retained in intracellular compartments more so than D_2S receptors and exposure to D_2 agonists results in the preferential translocation of existing and nascent D_2L receptors to the membrane (Filtz *et al*., 1993; Ng *et al*., 1997; Starr *et al*., 1995; Zhang *et al*., 1994; Fishburn *et al*., 1995; Prou *et al*., 2001). Thus, it may be that exposure to cocaine in wild type mice increases functional D_2L receptors, resulting in the loss of calcium-dependent D_2 autoreceptor desensitization. Virally expressed D_2L receptors may not be subject to the same regulation as endogenously expressed D_2L receptors, in such a way that virus-mediated overexpression of D_2L mimics and eliminates any requirement for up-regulation of D_2L function.

Both D_2S and D_2L function as autoreceptors

The D_2S isoform has been thought to be the D_2 autoreceptor due to preservation of autoreceptor-mediated behaviors in D_2L-deficient mice and more abundant D_2S immunolabeling in the SNc (Khan *et al*., 1998; Usiello *et al*., 2000). However, immunolabeled D_2L receptors are found in SNc dopamine neurons (Khan *et al*., 1998) and rodent studies describe dopamine neurons expressing both D_2S and D_2L mRNA, D_2L-only, or D_2S-only (Dragicevic *et al*., 2014; Jang *et al*., 2011). Both variants are capable of inhibiting action potential firing (Dragicevic *et al*., 2014; Jang *et al*., 2011; Jomphe *et al*., 2006). In this study, D_2S and D_2L receptors, when expressed in dopamine neurons, activated a GIRK conductance and were capable of producing IPSCs occurring from spontaneous fusion of dopamine-filled vesicles. Thus, D_2S and D_2L can serve as autoreceptors at somatodendritic dopamine synapses, as previously demonstrated (Neve *et al*., 2013).

Although many of the basic properties of D_2S and D_2L receptor-dependent currents were similar, there were some differences that suggest both D_2S and D_2L are autoreceptors in wild type dopamine neurons. The calcium-dependent component of D_2 autoreceptor desensitization in wild type neurons was similar to D_2S-only neurons. However, results from manipulating calcium signaling in wild type neurons were more consistent with a mix of D_2S and D_2L receptor expression. Intracellular pathways for calcium signaling that regulated D_2S receptor-GIRK desensitization modified the magnitude of D_2L receptor-dependent GIRK currents. In wild type dopamine neurons, manipulating these pathways resulted in a decrease in acute desensitization and larger

GIRK currents, suggesting that D_2S and D_2L receptor regulation may operate in parallel in wild type neurons. In addition, cocaine-induced plasticity occurred in wild type, but not D_2S-only neurons, indicating a loss of some process in neurons which express D_2S as the exclusive autoreceptor that is not permissive to cocaine-induced plasticity. However, the viral-mediated co-expression of D_2S with D_2L receptors also did not resemble wild type, and instead was similar to D_2L-only. Although it is not known to what extent developmental compensation, virus-mediated expression, and variegated D_2 receptor expression in *Drd2*$^{-/-}$ mice affected D_2 receptor translation or trafficking (i.e. affecting the ratio of functional D_2S and D_2L receptors), or other regulatory elements of D_2 receptor signaling, this result suggests that in wild type dopamine neurons, the functional expression of D_2L may be limited. Changes in calcium signaling or exposure to cocaine may bring about an increased contribution of D_2L, although this has yet to be directly demonstrated. Taken together, this study suggests that D_2S may serve as the predominant autoreceptor under basal conditions, but the functional contribution of D_2L autoreceptors may be revealed after drug exposure.

Concluding remarks

This study advances the understanding of D_2 autoreceptor regulation. Two pathways for calcium signaling that regulated D_2 autoreceptor-dependent GIRK signaling were identified, which distinctly affected D_2S and D_2L receptors. In addition, distinct action of *in vivo* cocaine exposure in wild type, D_2S, and D_2L receptor-GIRK signaling was demonstrated. Since not all dopamine neurons express both D_2S and D_2L receptors, this study suggests that D_2 autoreceptors in a subset of dopamine neurons are regulated

differently by calcium and resistant to cocaine-induced plasticity. Given the heterogeneity of dopamine neurons and their projections (reviewed in Roeper, 2013), a greater understanding of this subset may reveal insights into plasticity in their projection areas.

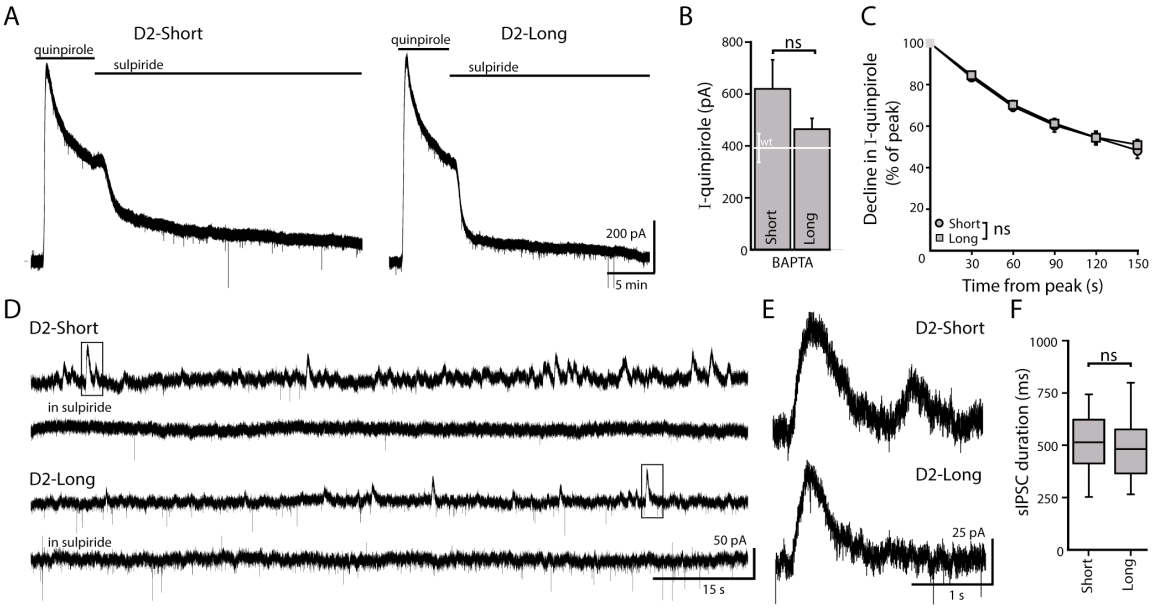

Figure 6.1. When virally expressed in midbrain dopamine neurons, D_2S and D_2L function as autoreceptors.

(A) Representative traces of whole-cell voltage clamp recordings, using a BAPTA-containing internal solution, of the outward current in D_2S and D_2L neurons induced by bath application of quinpirole (30 μM), which was reversed by sulpiride (600 nM). (B) The amplitude of quinpirole-induced currents in D_2S and D_2L neurons using BAPTA internal did not differ (n = 12-14, unpaired t test). (C) There was no difference between D_2S and D_2L in the decline of the D_2 receptor-dependent current in the continued presence of quinpirole using BAPTA internal (two-way ANOVA). (D-E) Representative traces of spontaneous D_2-sIPSCs mediated by D_2S and D_2L receptors, blocked by sulpiride. Inset boxes are shown enlarged in (E). The frequency and amplitude of D2S- and D2L-sIPSCs were not analyzed since these parameters may be influenced by the expression of D2 receptors in presynaptic dopamine neurons, which cannot be confirmed. (F) The duration of D_2S-sIPSCs and D_2L-sIPSCs did not differ (n = 84-100 sIPSCs, Mann-Whitney U test). ns indicates not significant.

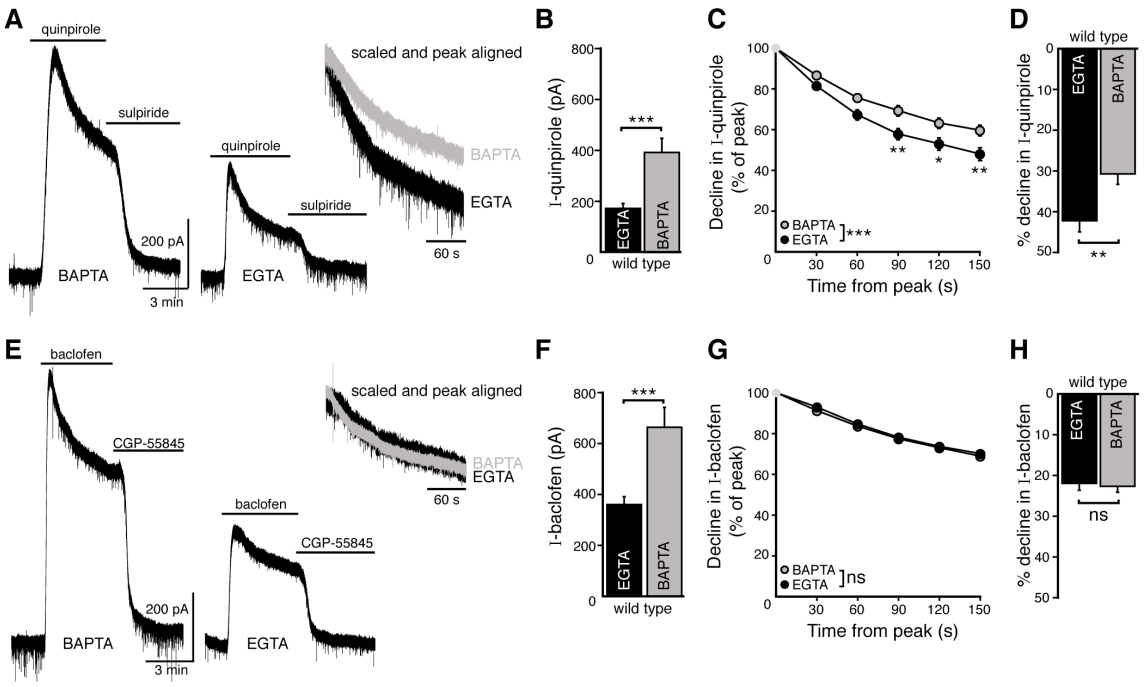

Figure 6.2. Weak intracellular calcium buffering reveals calcium-dependent desensitization of D_2 autoreceptor-dependent GIRK currents in wild type dopamine neurons.

(A) Representative traces of whole-cell voltage clamp recordings of the outward current induced by bath application of quinpirole (10 μM) that was reversed by sulpiride (600 nM), using a BAPTA or EGTA-containing internal solution. (B) The amplitude of the quinpirole-induced current was larger using BAPTA than EGTA internal (n = 15 each, unpaired t test). (C-D) The decline in quinpirole-induced current was faster using EGTA internal compared to BAPTA (C: two-way ANOVA followed by Bonferroni, D: unpaired t test) (E) Representative traces of whole-cell voltage clamp recordings of the outward current induced by bath application of baclofen (30 μM) which was reversed by CGP-55845 (200 nM), using BAPTA or EGTA internal. (F) The amplitude of the baclofen-induced current was larger using BAPTA than EGTA internal (n = 14-16, unpaired t test). (G-H) There was no difference in the decline in baclofen-induced current recorded with EGTA and BAPTA internals (G: two-way ANOVA, D: unpaired t test). ns indicates not significant, *p<0.05, **p<0.01. ***p<0.001.

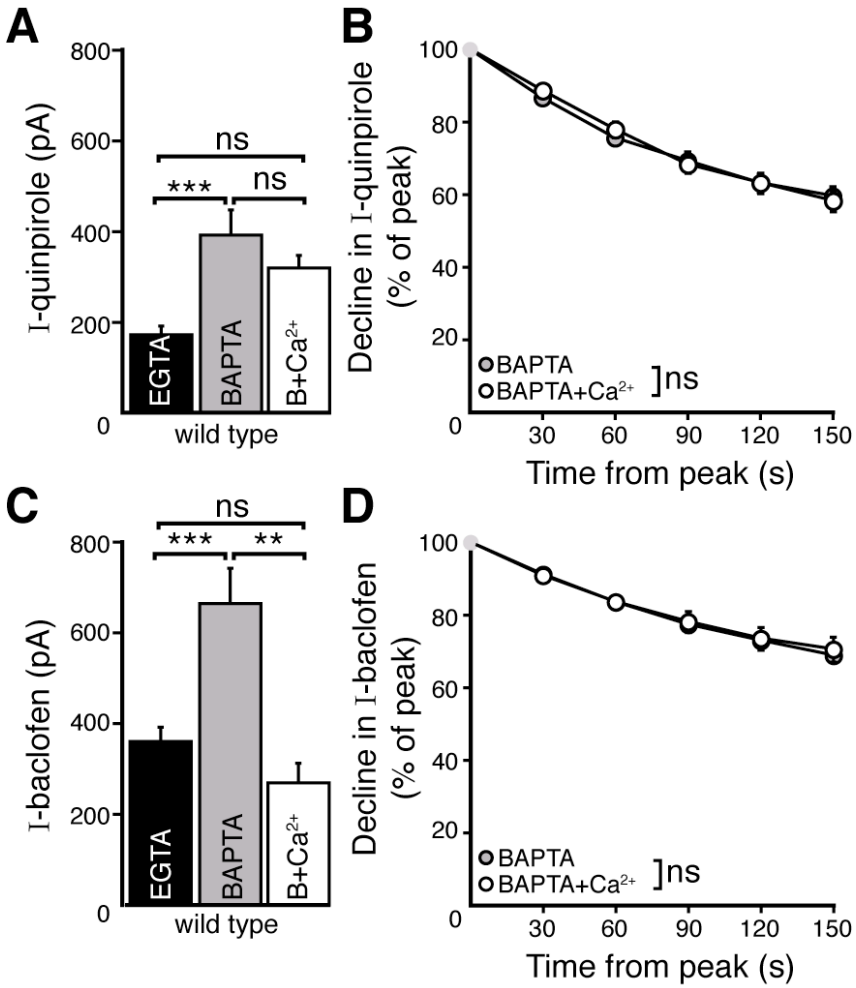

Figure 6.3. Increasing resting free internal calcium does not enhance the desensitization of D_2 autoreceptor-GIRK currents.

(A) The amplitude of the quinpirole-induced current using BAPTA+Ca^{2+} internal solution was not different from the amplitudes using BAPTA or EGTA internal solutions (n = 7-15, ANOVA followed by Bonferroni). (B) Increasing resting free calcium with BAPTA+Ca^{2+} had no effect on the decline in quinpirole-induced current (two-way ANOVA). (C) Increasing resting free calcium with BAPTA+Ca^{2+} internal decreased the amplitude of the baclofen-induced current, making it no greater than the amplitude recorded using EGTA internal (ANOVA followed by Bonferroni). (D) Increasing resting free calcium with BAPTA+Ca^{2+} had no effect on the decline in baclofen-induced current (two-way ANOVA). Additional experiments that demonstrate BAPTA+Ca^{2+} internal increased resting free calcium can be found in Figure 6.4. ns indicates not significant, **p<0.01, ***p<0.001.

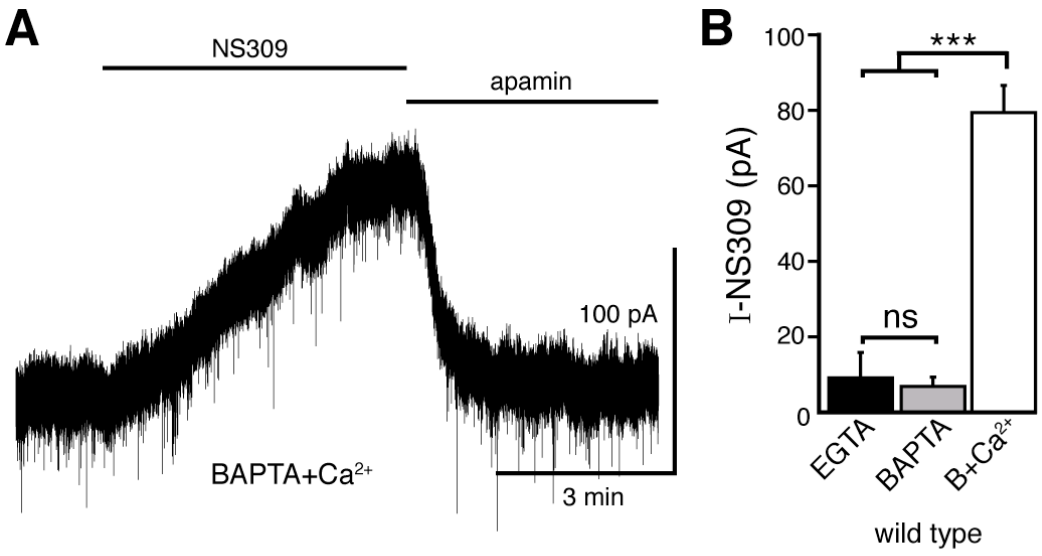

Figure 6.4. The positive modulator of the SK channel, NS309, produces an outward current when using the BAPTA+Ca^{2+} internal solution.

(A) Representative trace of whole-cell voltage clamp recordings of the outward current induced by bath application of NS309 (10 μM), which was reversed by apamin (200 nM), using a BAPTA+Ca^{2+} internal. (B) NS309 produced a current using a BAPTA+Ca^{2+}, but not BAPTA or EGTA internal (*n* = 5-6, ANOVA followed by Bonferroni). ns indicates not significant, ***p<0.001.

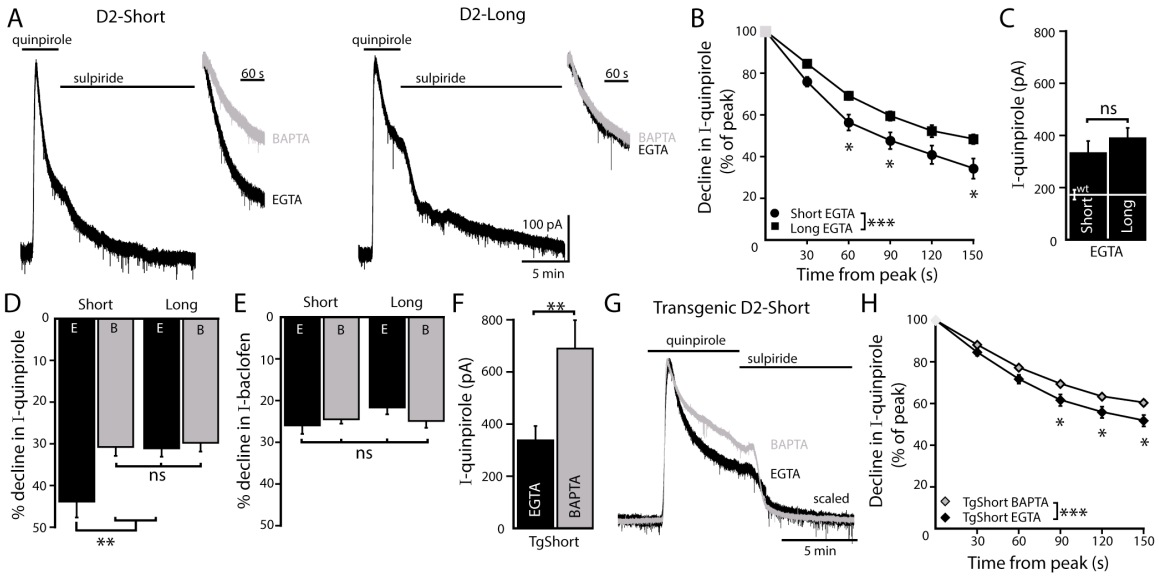

Figure 6.5. D_2S but not D_2L receptor-GIRK currents exhibit calcium-dependent desensitization.

(A) Representative traces of whole-cell voltage clamp recordings of the outward current in D_2S and D_2L neurons induced by bath application of quinpirole (30 μM) which was reversed by sulpiride (600 nM), using EGTA internal, compared with the BAPTA trace shown in Figure 6.1A (scaled and peak-aligned). (B, D) Using EGTA internal, the decline in quinpirole-induced current was greater in D_2S than D_2L neurons (B: two-way ANOVA followed by Bonferroni, D: n = 16 each, one-way ANOVA followed by Fisher's LSD). (C) The amplitude of quinpirole-induced currents in D_2S and D_2L neurons using EGTA internal did not differ (n = 16-17, unpaired t test). (D) In D_2S neurons, the decline in quinpirole-induced current was greater using EGTA internal compared to BAPTA, but not in D_2L neurons (n = 12-16, one-way ANOVA followed by Fisher's LSD). The time course of the decline can be found in Figure 6.6. (E) There was no difference in the decline in baclofen-induced current recorded with EGTA or BAPTA internal in either splice variant (n = 11-19, one-way ANOVA). (F) In neurons from transgenic D_2-Short mice, the amplitude of the quinpirole-induced current was larger using BAPTA than EGTA internal (n = 7-8, unpaired t test). (G-H) Representative scaled and peak-aligned traces of whole-cell voltage clamp recordings from neurons from transgenic D_2-Short mice, of the outward currents induced by bath application of quinpirole (10 μM), which were reversed by sulpiride. The decline in quinpirole-induced current was greater using EGTA internal compared to BAPTA (two-way ANOVA followed by Bonferroni). ns indicates not significant, *p<0.05, **p<0.01, ***p<0.001.

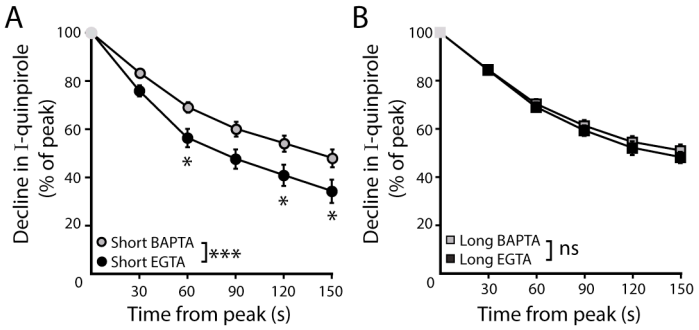

Figure 6.6. Time course of desensitization of D2 receptor splice variant-GIRK currents.

(A) In D2S neurons, the decline in quinpirole (30 μM) -induced current was greater using EGTA internal compared to BAPTA (*n*=10-16). (B) In D2L neurons, the decline in quinpirole-induced current using EGTA internal was no different from BAPTA internal (*n*=10-16). Two-way ANOVAs followed by Bonferroni). ns indicates not significant, *p<0.05, ***p<0.001.

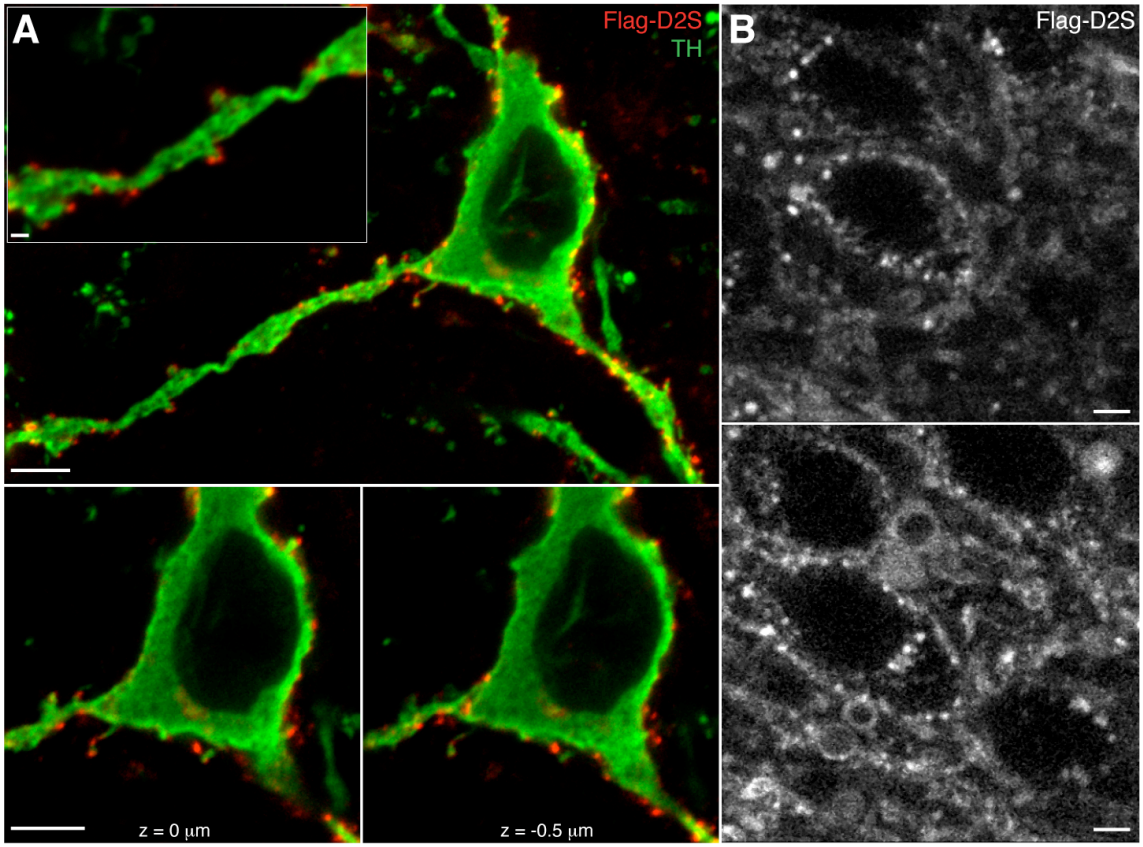

Figure 6.7. Expression and labeling of Flag-D_2S receptors in dopamine neurons.

(A) Representative confocal microscopy images of Flag-D_2S receptors clustered on the soma, dendrites, and spine-like structures of dopamine neurons, labeled by incubation of live slices in Alexa Fluor-594 conjugated anti-Flag M1 antibody (red, Flag-D_2S), then post-fixed and immunostained for tyrosine hydroxylase (green, TH), scale bars: 1 µm (upper left inset) and 5 µm. (B) Representative two-photon microscopy images of live dopamine neurons, where Flag-D_2S receptors were labeled by incubation of live slices in Alexa Fluor-594 conjugated anti-Flag M1 antibody (Flag-D_2S), scale bars: 5 µm.

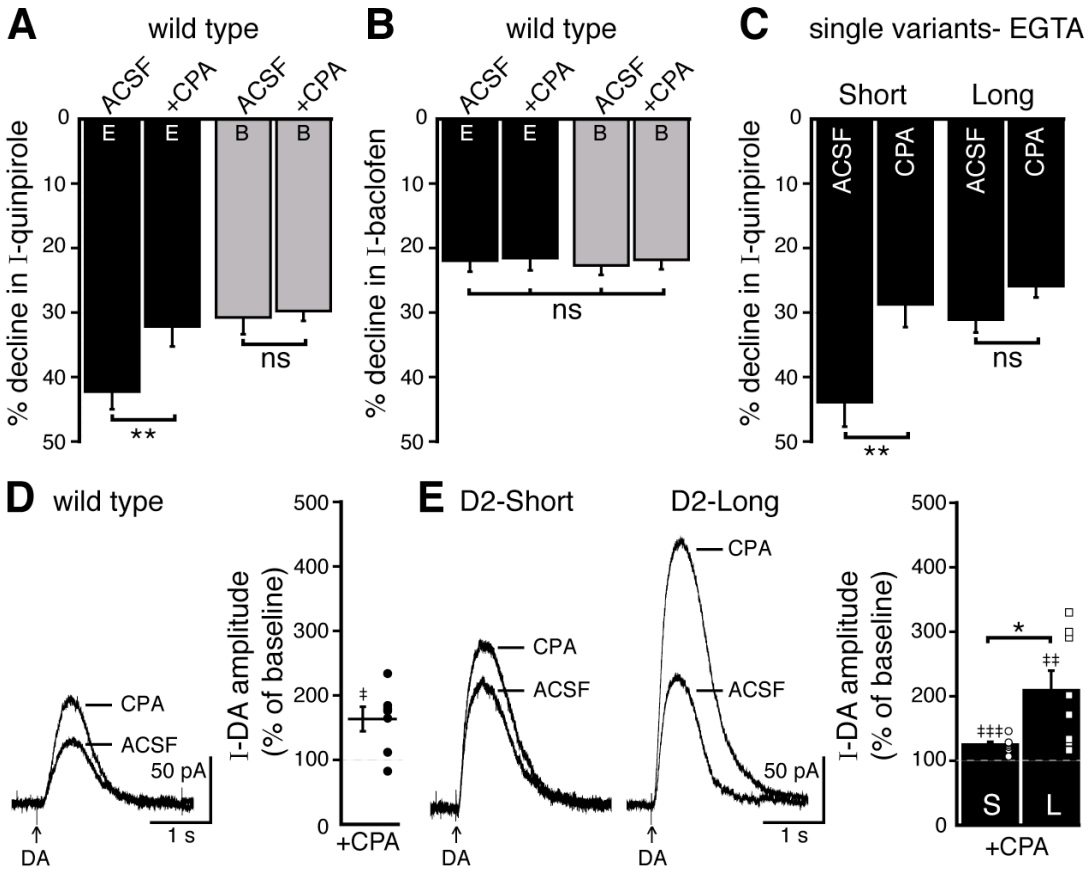

Figure 6.8. Depleting intracellular calcium stores differentially modified D_2S and D_2L receptor-dependent GIRK conductance.

(A) In wild type neurons, CPA (10 μM, > 20 min) reduced the decline in the quinpirole-induced current using EGTA internal and the effect was prevented with the use of BAPTA internal (*n* = 11-15, one-way ANOVA followed by Fisher's LSD). (B) CPA had no effect on the decline in baclofen-induced current recorded with EGTA or BAPTA internal in wild type neurons (*n* = 14-16, one-way ANOVA). (C) In D_2S, but not D_2L neurons, CPA reduced the decline in quinpirole-induced current using EGTA internal (*n* = 6-16, one-way ANOVA followed by Fisher's LSD). (D-E) D_2 receptor-dependent outward currents were produced by iontophoretic application of dopamine once every 50s while recording with EGTA internal (I-DA, arrows). (D) CPA (10 μM, 25-30 min) augmented I-DA in wild type neurons, shown in representative averaged traces (left) and grouped data (right, *n* = 7). (E) CPA augmented I-DA in D_2S and D_2L neurons, shown in representative averaged traces (left) and grouped data (right). The augmentation by CPA was greater in D_2L than D_2S neurons (*n* = 7-8, unpaired *t* test). The time course of the CPA-induced augmentation of I-DA can be found in Figure 6.9. Baseline: mean amplitude of six I-DAs preceding CPA application, ns indicates not significant, *p<0.05, **p<0.01, ***p<0.001, and ‡ indicates significance over baseline (within-group comparison, paired *t* tests).

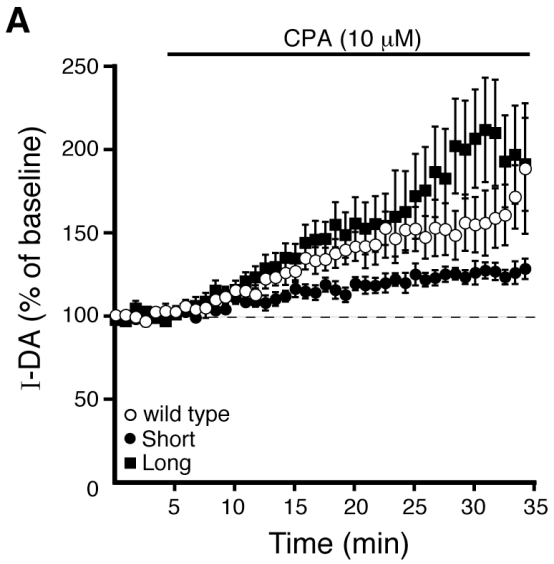

Figure 6.9. Prolonged CPA application enhances D_2 receptor-mediated currents produced by exogenous dopamine.

(A) D_2 receptor-dependent outward currents (I-DA) were produced once every 50 s by iontophoretic application of dopamine while recording with EGTA internal. Prolonged CPA (10 μM) application enhanced I-DA in wild type (open circles), D_2S (black circles), and D_2L (black squares) neurons. Baseline: mean amplitude of six I-DAs preceding CPA application.

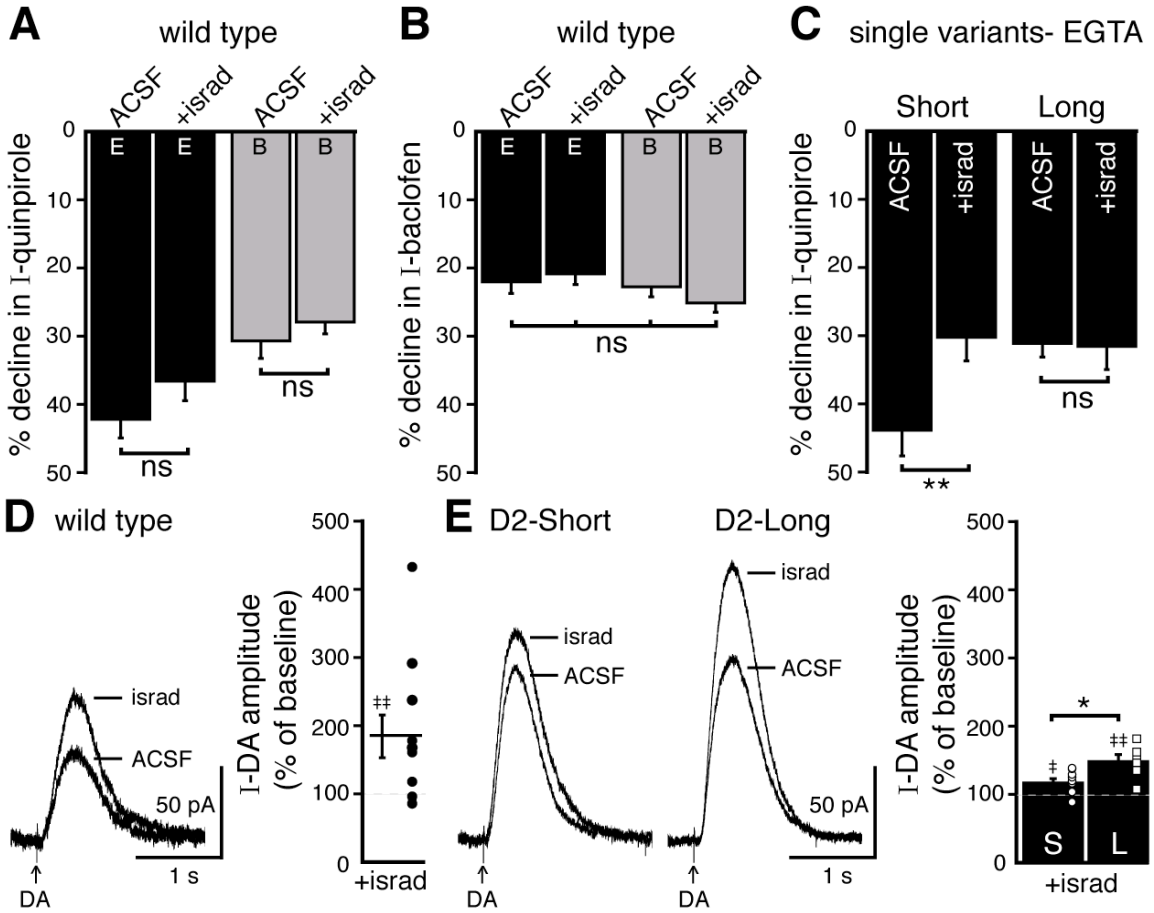

Figure 6.10. Blocking L-type calcium channels differentially modifies D_2S and D_2L receptor-dependent GIRK conductance.

(A-B) In wild type neurons, isradipine (300 nM, > 20 min) had no significant effect on the decline in quinpirole-induced (A) and baclofen-induced current (B) recorded with EGTA and BAPTA internal (quinpirole: n = 11-15, one-way ANOVA followed by Fisher's LSD; baclofen: n = 12-16, one-way ANOVA). (C) In D_2S, but not D_2L neurons, isradipine reduced the decline in quinpirole-induced current using EGTA internal (n = 6-16, one-way ANOVA followed by Fisher's LSD). (D-E) D_2 receptor-dependent outward currents were produced by iontophoretic application of dopamine once every 50s while recording with EGTA internal (I-DA, arrows). (D) Isradipine (300 nM, > 15 min) augmented I-DA in wild type neurons, shown in representative averaged traces (left) and grouped data (right, n = 11). (E) Isradipine augmented I-DA in D_2S and D_2L neurons, shown in representative averaged traces (left) and grouped data (right). The augmentation by isradipine was greater in D_2L than D_2S neurons (n = 6-11, unpaired t test). The time course of the isradipine-induced augmentation of I-DA can be found in Figure 6.11. Baseline: mean amplitude of six I-DAs preceding isradipine application, ns indicates not significant, *p<0.05, **p<0.01, and ‡ indicates significance over baseline (within-group comparison, paired t tests).

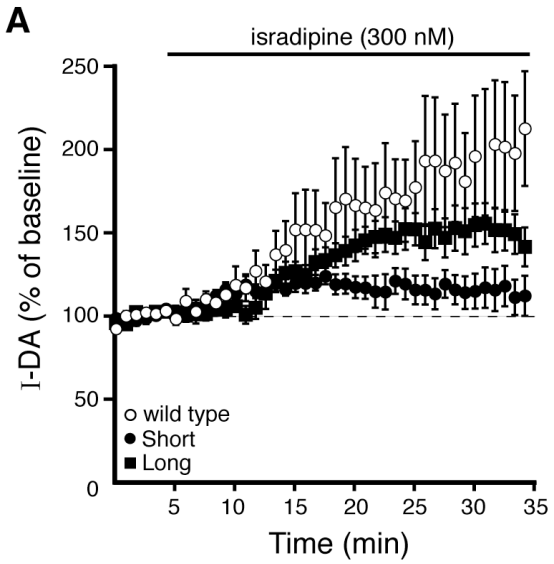

Figure 6.11. Prolonged isradipine application enhances D_2 receptor-dependent currents produced by exogenous dopamine.

(A) D_2 receptor-dependent outward currents (I-DA) were produced once every 50 s by iontophoretic application of dopamine while recording with EGTA internal. Prolonged isradipine (300 nM) application enhanced I-DA in wild type (open circles), D_2S (black circles), and D_2L (black squares) neurons. Baseline: mean amplitude of six I-DAs preceding isradipine application.

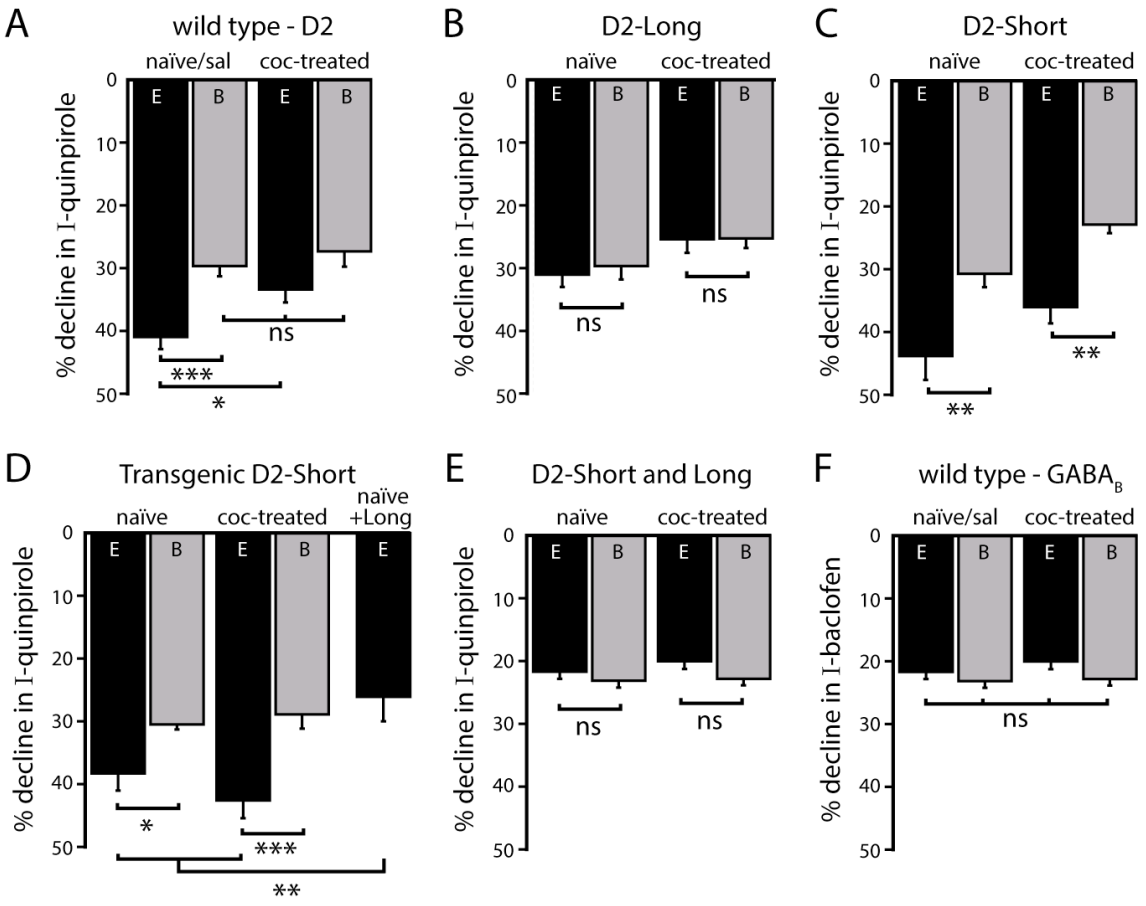

Figure 6.12. Effects of a single *in vivo* cocaine exposure on calcium-dependent D_2 autoreceptor desensitization.

(A) In neurons from cocaine-treated wild type mice using EGTA internal, the quinpirole-induced current declined less compared to naïve/saline-treated mice, to a level comparable to the decline recorded with BAPTA internal. Cocaine exposure did not alter the decline in the quinpirole-induced current when measured with BAPTA internal (*n*=11-26). (B) In D_2L neurons after *in vivo* cocaine exposure, there was no difference in the decline in quinpirole-induced current recorded with EGTA or BAPTA internal (*n*=6-7). (C-D) In neurons from (C) AAV-D_2S and (D) transgenic D_2-Short mice, the decline in quinpirole-induced current was still greater using EGTA internal compared to BAPTA after *in vivo* cocaine exposure (C: *n*=10 each, D: *n*=8-9). (D-E) Co-expression of both splice variants by (D) viral expression of D_2L in transgenic D_2-Short mice and (E) infection with a mixture of AAV-D_2S and AAV-D_2L removed the calcium-dependence of the decline in the quinpirole-induced current (D: *n*=5-8, E: *n*=6-9) and there was no change after *in vivo* cocaine (E: *n*=7-9). (F) Previous cocaine exposure had no effect on the decline in baclofen-induced current recorded with EGTA or BAPTA internal in wild type neurons (*n*=13-27). Comparisons were made with one-way ANOVAs followed when $p<0.05$ by Fisher's LSD. ns indicates not significant, *$p<0.05$, **$p<0.01$, ***$p<0.001$.

6.2 ADDITIONAL EXPERIMENTS

PKC activation enhances D_2 receptor-dependent currents

Activation of protein kinase C (PKC) has been implicated in phosphorylation, desensitization, and internalization of D_2S and D_2L receptors in biochemical assays (Ito *et al.*, 1999; Itokawa *et al.*, 1996; Liu *et al.*, 1992; Morris *et al.*, 2007; Namkung and Sibley, 2004; Thibault *et al.*, 2011; Van-Ham *et al.*, 2007). Previous studies have demonstrated that D_2S receptors are more sensitive to PKC activation than D_2L receptors, due to a PKC pseudosubstrate site specific to the third intracellular loop in D_2L receptors (Liu *et al.*, 1992; Morris *et al.*, 2007; Thibault *et al.*, 2011; Van-Ham *et al.*, 2007; but also see Namkung and Sibley, 2004). PKC-dependent phosphorylation may promote desensitization of D_2 receptors in a pathway specific manner. For instance, PKC activation reduces D_2 receptor-dependent stimulation of calcium mobilization, while having little effect on inhibition of adenylyl cyclase (Liu *et al.*, 1992). In previous studies, inhibition of PKC did not reduce acute D_2 autoreceptor-GIRK desensitization (Beckstead and Williams, 2007; Perra *et al.*, 2011). To further test the involvement of PKC in the regulation of D_2 autoreceptor-dependent GIRK signaling, slices were exposed to the direct PKC activator, phorbol 12, 13-dibutyrate (PDBu, 100 nM), >20 min prior to making recordings. In wild type dopamine neurons, PDBu decreased the decline in the quinpirole-induced current when using EGTA internal but not BAPTA internal (Figure 6.13A). The decline in baclofen-induced current was not changed by PDBu (Figure 6.13B). The decline in the quinpirole-induced current in D_2S neurons was also decreased by PDBu, but was unaffected in D_2L neurons (Figure 6.13C). Thus, in wild type and D_2S-

expressing dopamine neurons, activation of PKC reduced D_2 receptor-GIRK desensitization without affecting $GABA_B$ receptor desensitization.

Next, the effect of PDBu on I-DA was examined. In wild type dopamine neurons using EGTA internal, PDBu (100 nM) significantly augmented I-DA (Figure 6.13D). As was found with CPA and isradipine, the augmentation in I-DA by PDBu required prolonged application (Figure 6.14). The augmentation induced by PDBu on I-DA was also observed in D_2L-expressing neurons (Figure 6.13E). However, PDBu did not significantly change the amplitude of I-DA in D_2S-expressing neurons (Figure 6.13E). Thus, the activation of PKC selectively augmented D_2L receptor-dependent GIRK signaling. Taken together, these results suggest that activation of PKC differentially affects D_2S and D_2L receptor-dependent GIRK signaling. However, the mechanism remains to be determined. In cell lines, PKC activation eliminates D_2S and reduces D_2L receptor activation-dependent calcium mobilization (Liu *et al.*, 1992). Thus, the alteration in D_2 autoreceptor-GIRK signaling by PKC activation may be secondary to a change in another calcium-dependent pathway.

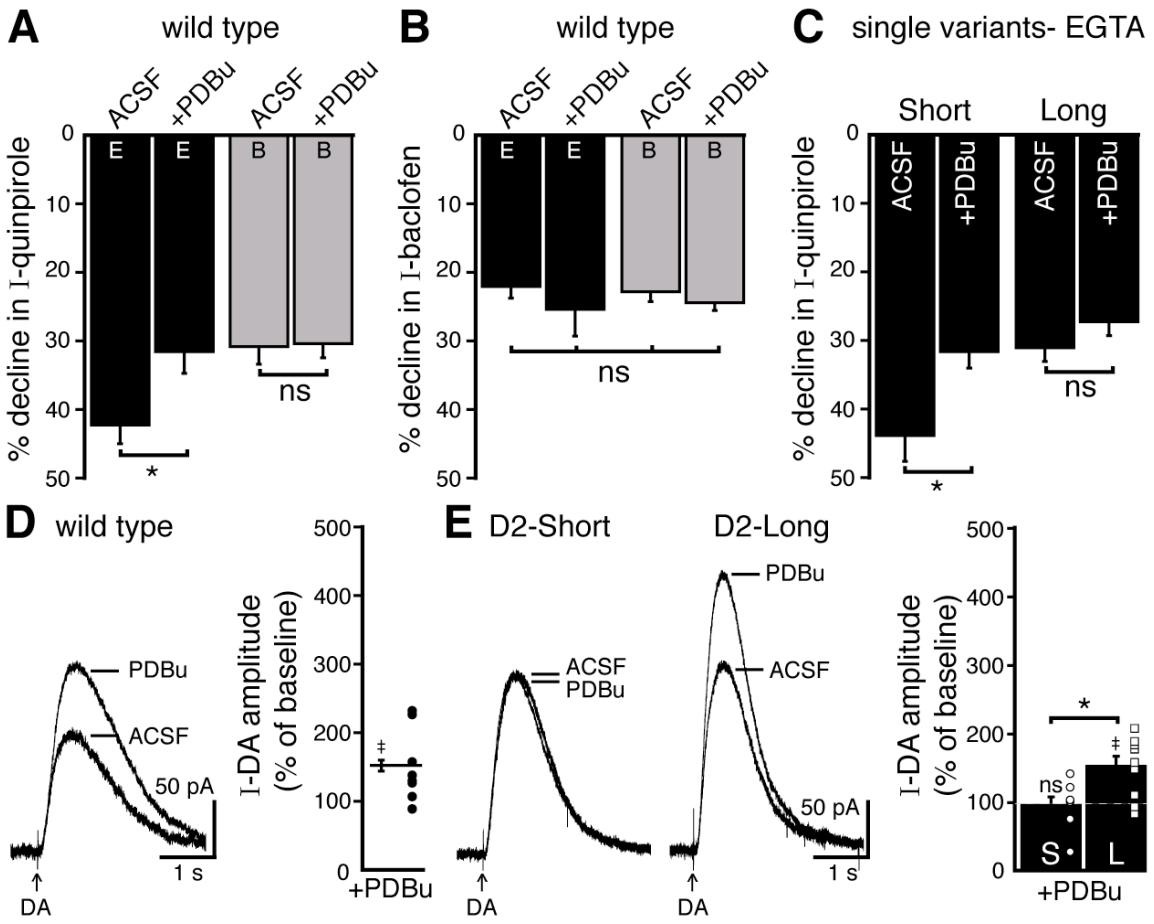

Figure 6.13. Activation of PKC with PDBu differentially modified D_2S and D_2L receptor-dependent GIRK conductance.

(A) In wild type neurons, PDBu (100 nM, > 20 min) reduced the decline in the quinpirole-induced current using EGTA internal solution and the effect was prevented with the use of BAPTA internal solution (n = 8-15, one-way ANOVA followed by Fisher's LSD). (B) PDBu had no effect on the decline in baclofen-induced current recorded with EGTA or BAPTA internal in wild type neurons (n = 7-14, one-way ANOVA). (C) In D_2S, but not D_2L neurons, PDBu reduced the decline in quinpirole-induced current using EGTA internal (n = 7-16, one-way ANOVA followed by Fisher's LSD). (D-E) D_2 receptor-dependent outward currents were produced by iontophoretic application of dopamine once every 50s while recording with EGTA internal (I-DA, arrows). (D) In wild type neurons, PDBu (100 nM, 25-30 min) augmented I-DA, shown in representative averaged traces (left) and grouped data (right, n = 8). (E) PDBu augmented I-DA in D_2L, but had no effect in D_2S neurons, shown in representative averaged traces (left) and grouped data (right, n = 8-9, unpaired t test). The time course of the PDBu-induced augmentation of I-DA can be found in Figure 6.14. Baseline: mean amplitude of six I-DAs preceding PDBu application, ns indicates not significant, *$p<0.05$, and ‡ indicates significance over baseline (within-group comparison, paired t tests).

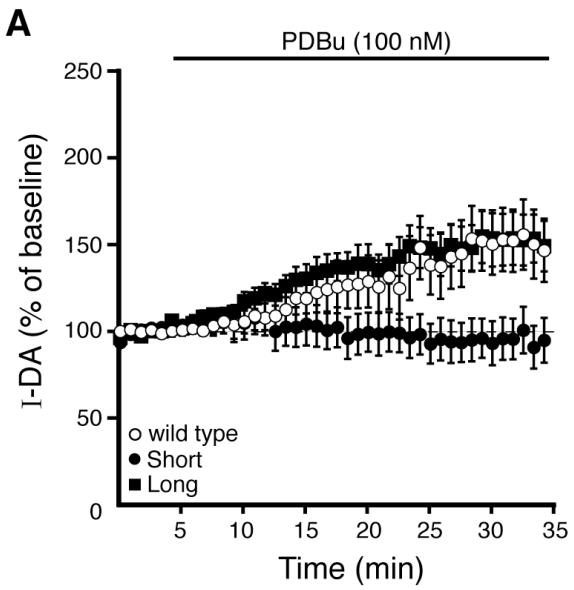

Figure 6.14. Prolonged PDBu enhances D_2 receptor-dependent currents produced by exogenous dopamine in wild type and D_2L-expressing neurons, but not D_2S-expressing neurons.

(A) D_2 receptor-dependent outward currents (I-DA) were produced once every 50 s by iontophoretic application of dopamine while recording with EGTA internal. Prolonged PDBu (100 nM) application enhanced I-DA in wild type (open circles), and D_2L (black squares), but not D_2S (black circles) neurons. Baseline: mean amplitude of six I-DAs preceding PDBu application.

Focal dopamine uncaging produces currents

While nearly all ultrastructure studies describe dendritic spines on midbrain dopamine neurons, they have not been well-characterized. To verify that the spine-like structures observed in dopamine neurons from TH-hD_2S mice was not an artifact of the overexpression of D_2 receptors, dopamine neurons from wild type mouse brain slices were filled with Alexa Fluor 594. Filled dopamine neurons were imaged with two-photon microscopy. It was clear that in wild type mice, there are dopamine neurons that have dendritic spines and filopodial structures (Figure 6.15).

Next, preliminary experiments were conducted to determine whether D_2 receptor-mediated currents could be elicited by focal uncaging of dopamine onto spine-like structures on dopamine neurons. Dopamine neurons were filled with an internal solution containing 10 mM BAPTA and Alexa Fluor 594 dye (10 μM). A spot near the dendrite or spine-like structure was chosen for focal dopamine uncaging. Rubi-Dopamine (5 mM) was puffed onto the slice (0.25 – 1 s) above the recorded neuron. Between 6 to 8 s after the puff, Rubi-Dopamine was uncaged (1-5 pulses, 5-50 ms, 810 nm). There were many technical challenges to these experiments that limited the investigation. Namely, in these preliminary experiments, application of Rubi-Dopamine produced an outward current prior to photolysis and recordings were rarely stable for multiple uncaging pulses. Nonetheless, these experiments provided the "proof-of-concept" that focal uncaging onto dopamine neurons was sufficient to elicit outward currents (Figure 6.17).

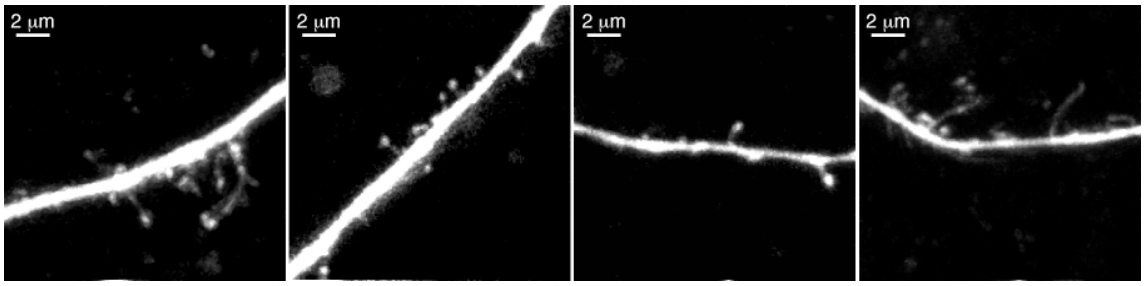

Figure 6.15. Spine-like structures are observed on wild type dopamine neurons dendrites in live brain slices.

Dopamine neuron dendrites in wild type mouse midbrain slices that have been filled with Alexa Fluor 594 dye and imaged with two-photon microscopy.

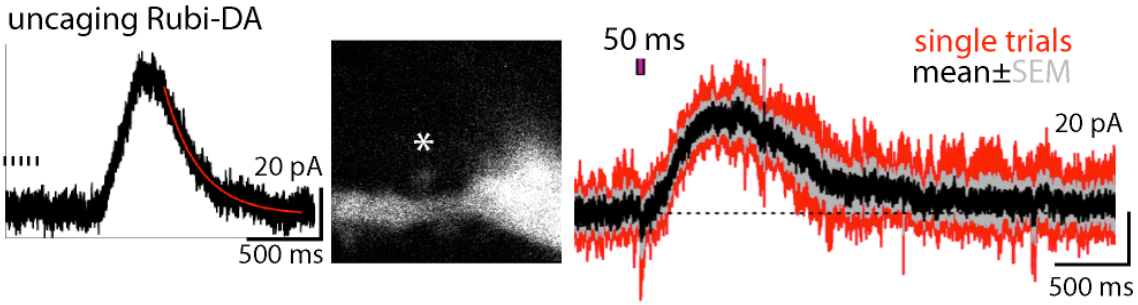

Figure 6.16. Dopamine uncaging on single dendritic spots is sufficient to produce outward currents.

(Left) Rubi-dopamine was uncaged (810 nm) on a dopamine dendrite (not shown) with a train of pulses (5, 5 ms). (Mid and right) Rubi-Dopamine was repeatedly focally uncaged (*) with a 50 ms pulse and produced very similar outward currents (n = 4 trials).

Chapter 7 PHYSIOLOGY TO PATHOLOGY

PREFACE

This chapter is a study that examined a mutant mouse line that expresses a rare DAT coding variant Val559 that has been identified in humans with attention-deficit hyperactivity, bipolar, and autism spectrum disorders. The functional impact of this mutation was determined by examining basal and amphetamine-evoked striatal dopamine levels, somatodendritic D_2 receptor function, and motor behaviors.

This study was done in collaboration with Dr. Randy D. Blakely at Vanderbilt University, led by Dr. Marc A. Mergy. My contribution was designing and performing all electrophysiological recordings in midbrain slices, analyzing and illustrating data, and assisting in the preparation of the manuscript.

The results show the DAT Val559 mutation leads to elevated basal striatal dopamine levels that reduced amphetamine-evoked striatal dopamine levels due to tonic D_2 autoreceptor-mediated inhibition. In the SNc, the kinetics of evoked and spontaneous D_2-IPSCs were slower in dopamine neurons from DAT Val559 mice. In addition, the amphetamine-induced augmentation of D_2-eIPSCs was reduced, without a change in methylphenidate-induced augmentation. Lastly, DAT Val559 mutants exhibited altered motor behaviors, particularly paradoxical responses to psychostimulants. The following results from this study are limited to my contribution, describing differences in electrical properties and basal and amphetamine-augmented D_2-IPSCs of dopamine neurons from DAT Val559 mice.

In the context of this dissertation, this study demonstrates that the occurrence of spontaneous D_2-IPSCs can be leveraged to gain a greater understanding of disturbances in dopamine transmission that may contribute to related pathologies.

INTRODUCTION

Dysfunction in the regulation of dopamine transmission is implicated in a number of disorders that present abnormal locomotor activity or impaired attention to salient cues, including attention-deficit hyperactivity disorder (ADHD). Proper regulation of dopamine transmission necessitates tight control of dopamine release and clearance of extracellular dopamine through reuptake by the dopamine transporter (DAT). The most effective pharmacotherapies for ADHD target the DAT, namely amphetamine (AMPH) and methylphenidate (MPH). Some features of ADHD are recapitulated in DAT knock-out mice (Giros *et al.*, 1996). However in humans, loss-of-function mutations in DAT results in profoundly different phenotypes than the DAT KO mouse (Ng *et al.*, 2014), questioning the validity of this mouse as a genetic model of ADHD. Therefore, these studies suggest ADHD may be due to more subtle changes in DAT function.

As a result, Randy Blakely's group identified rare DAT variants that were associated with bipolar disoder and ADHD, then examined their functionality in transfected cells. This *in vitro* screen led to the characterization of a rare coding variant, DAT Val559. When transfected in cells, DAT Val559 exhibited normal dopamine uptake rates. But when cells were preloaded with dopamine, dopamine "leaked" back out through the DAT. This DAT-mediated outward "leak" was termed anomalous dopamine efflux (ADE) (Mazei-Robison *et al.*, 2008). ADE was more pronounced when cells were depolarized due to an increased affinity for intracellular Na^+ driving efflux. Interestingly, AMPH triggered efflux in wild type DAT, but blocked DAT Val559-mediated ADE. These *in vitro* results were sufficient to prompt the genetic engineering of a mouse line that expresses DAT 559V from the native DAT-encoding *Slc6a3* locus.

7.1 THE RARE DAT CODING VARIANT VAL559 PERTURBS DA NEURON FUNCTION, CHANGES BEHAVIOR, AND ALTERS *IN VIVO* RESPONSES TO PSYCHOSTIMULANTS

Marc A. Mergy[a], Raajaram Gowrishankar[a], Paul J. Gresch[a,d], **Stephanie C. Gantz**[e], John T. Williams[e], Gwynne L. Davis[a], C. Austin Wheeler[a], Gregg D. Stanwood[a,d], Maureen K. Hahn[a,c], and Randy D. Blakely[a,b,d]

Departments of [a]Pharmacology, [b]Psychiatry and [c]Medicine , [d]Silvio O. Conte Center for Neuroscience Research, Vanderbilt University School of Medicine, Nashville, TN 37232-8548; [e]Vollum Institute, Oregon Health & Science University, Portland, OR 97239

[The following portion of this manuscript is presented as published in (Mergy *et al.*, 2014), *Proceedings of the National Academy of Sciences*, November 4, 2014; 111(44):E4779-88]

Results

DA Neurons from DAT Val559 Mice Display Alterations in Basal and AMPH-Augmented D_2R-Mediated IPSCs.

DAT is expressed somatodendritically on DA neurons where it can limit the ability of D_2Rs to reduce DA neuron firing, because D_2R activation in the midbrain is tightly controlled by reuptake (Ford *et al.*, 2010). Vesicular somatodendritic release of DA in the substantia nigra (SNc) and ventral tegmental area elicits an inhibitory postsynaptic current (IPSC) via D_2R activation of a G protein-coupled inwardly rectifying potassium (GIRK) channel, which can inhibit DA neuron firing (Beckstead *et al.*, 2004; Gantz *et al.*, 2013). To examine the impact of DAT Val559 on basic physiological properties of DA neurons, and D_2R-mediated currents, we performed whole-cell recordings of SNc DA neurons in acute brain slices. We found whole-cell capacitance to be reduced (WT: 35.8 ± 0.67 pF, n = 139; HOM: 32.7 ± 0.56 pF, n = 153; p = 0.001, Mann–Whitney test) and resistance to be increased (WT: 315.7 ± 14.1 MΩ, n = 138; HOM: 347.3 ± 12.6 MΩ, n = 149, p = 0.012, Mann–Whitney test). Resting membrane potential, percent of quiescent cells, and firing rates in response to current injection exhibited no genotype effects.

D_2R-mediated IPSCs were evoked by electrical stimulation with glutamatergic, GABAergic, and cholinergic inputs silenced with receptor blockers. A significant difference was observed in the time to peak of the D_2R-mediated IPSC evoked by a single stimulus (WT: 254.0 ± 7.3 ms, n = 32; HOM: 288.8 ± 8.8 ms, p = 0.001, ANOVA), and the duration of the IPSC evoked by a single or five stimuli (one stimulus, WT: 658.5 ± 24.5 ms, n = 32, HOM: 791.1 ± 40.5 ms, $p < 0.01$; five stimuli, WT: 702.0 ± 14.2 ms, n = 64; HOM: 775.2 ± 26.1, n = 67, $p < 0.05$, ANOVA with Fisher's LSD

post hoc test) (Figure 7.1A). In the midbrain, vesicular DA release occurs spontaneously, without electrical stimulation, eliciting spontaneous D_2R-mediated inhibitory postsynaptic currents (sIPSCs) (Gantz *et al.*, 2013). sIPSCs were also prolonged in DAT Val559 slices (WT: 380.7 ± 8.7 ms, n = 135 sIPSCs; HOM: 427.5 ± 10.9 ms, n = 150 sIPSCs, $p < 0.01$, Mann–Whitney) (Figure 7.1A), with no difference in amplitude. In contrast to D_2R-mediated currents, no differences were evident in the time to peak or duration of evoked $GABA_B$-mediated IPSCs (Figure 7.1B).

To assess AMPH effects on DA neurons, AMPH was bath applied to slices from which D_2R-mediated IPSCs were recorded. As expected from the actions of methamphetamine or [cocaine] COC (Beckstead *et al.*, 2004; Branch and Beckstead, 2012), the amplitude, time to peak, and duration of evoked D_2R-mediated IPSCs in WT slices treated with AMPH increased significantly relative to no-drug conditions and remained elevated throughout the AMPH application. However, the AMPH-induced increase in D_2R-mediated IPSC amplitude was blunted in DAT Val559 slices (Figure 7.1C), with some cells showing a brief enhancement followed by a decrease to baseline amplitude. However, there were no differences in the AMPH-induced increase in time to peak (WT: +89.9 ± 9.6 ms; HOM: +65.4 ± 11.7 ms, $p = 0.16$, Student's unpaired t test) and duration (WT: +330.6 ± 43.7 ms; HOM: +350.6 ± 122.0, $p = 0.90$, Student's unpaired t test) of D_2R IPSCs between genotype. To determine whether the changes seen in D_2R-mediated IPSC amplitude was a consequence of changes in DAT-mediated DA clearance versus a unique property of AMPH lost in the DAT Val559 mice, we repeated these studies by using MPH, finding no genotype differences in MPH augmentation of IPSC amplitude (Figure 7.1D). Finally, maximal D_2R-mediated currents were elicited by

iontophoretic application of DA onto DA neurons. Consistent with the midbrain D_2R binding studies, there was no difference in the maximal DA current between genotypes (WT: 10.0±0.4 pA/pF, n = 65; HOM: 9.4 ± 0.4 pA/pF, n = 76, p = 0.46, Mann–Whitney).

Discussion

Mergy *et al.* (2014) states:

> We also observed alterations in somatodendritic D_2R responses that may reflect ADE occurring at the cell body level, with a prolonged duration of D_2R- mediated IPSCs that may arise from a greater demand on DA clearance. Such an explanation seems reasonable in the context of a lack of genotype effects on midbrain DAT and D_2R levels, maximal D_2R-mediated current evoked by iontophoretic DA application, and in the time course of $GABA_B$-mediated IPSCs. Although compensations related to other aspects of cell structure and excitability cannot be ruled out, the fact that both D_2R and $GABA_B$ couple to the same GIRK channels to induce DA neuron inhibition suggests that the intrinsic machinery for these responses is intact…We also observed a blunted AMPH response at the cell body level with the loss of sustained effects of AMPH on D_2R IPSCs. We speculate that the appearance of this blunted response at late versus early time points may also derive from retention of the more rapid process of AMPH reuptake inhibition, which may predominate at earlier time points, versus loss of the slower, DAT-mediated DA release process (Jones *et al*., 1998), that may predominate at later times.

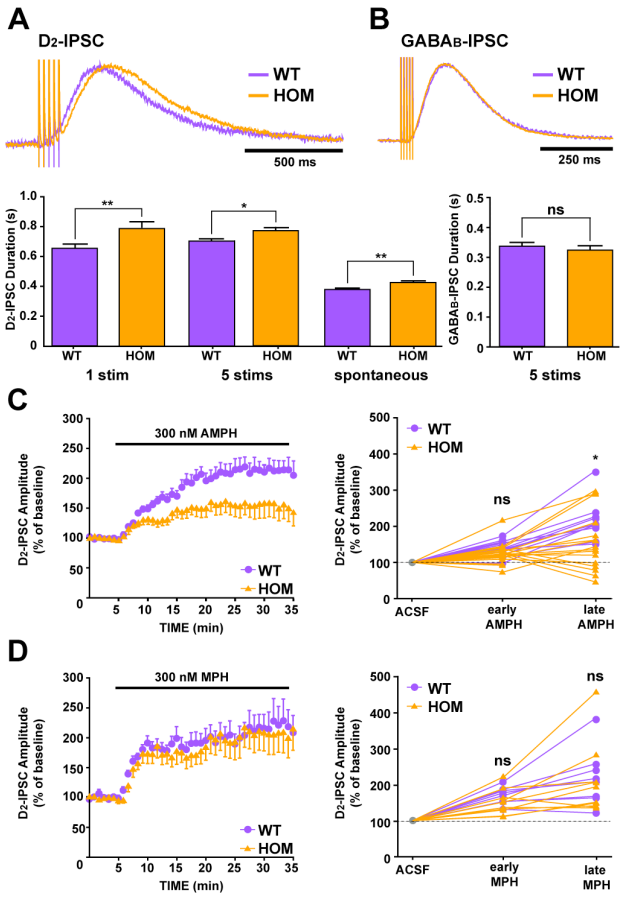

Figure 7.1. Dopamine D_2 receptor-mediated synaptic currents in midbrain slices from DAT559V mice have slower kinetics and blunted enhancement by AMPH, but not MPH.

Representative synaptic currents (IPSCs) mediated by dopamine D_2 receptors (A) or $GABA_B$ receptors (B) evoked by electrical stimulation in brain slices containing substantia nigra dopamine neurons. D_2-IPSCs in DAT559V slices are slower than in WT whether using a single or train of electrical stimuli to evoke dopamine release (1 stim: n = 32 cells WT, 35 cells HOM; p = 0.003; 5 stims: n = 64 cells WT, 67 cells HOM; p = 0.022, one-way ANOVA), or those occurring spontaneously (n = 135 sIPSCs WT, 150 sIPSCs HOM; p = 0.002, Mann-Whitney). There is no difference in the kinetics of $GABA_B$-IPSCs between genotypes (n = 18 cells WT, 17 cells HOM; p = 0.492, unpaired t test). Upon AMPH (C) or MPH (D) application, the amplitude of evoked D_2-IPSCs increases significantly. (C) The AMPH-induced increase in D_2-IPSC amplitude is blunted in DAT559V slices (*left*: time course of AMPH response; *right*: averaged increase in during first 2.5 - 5 mins (early) and averaged increase during 20 - 30 mins (late); normalized to pre-AMPH amplitude; n = 18 cells WT, 19 cells HOM, * = $p < 0.05$, two-way RMANOVA). (D) There is no difference in the MPH-induced increase in D_2-IPSC between genotypes (*left*: time course of MPH response; *right*: averaged increase in during first 2.5 - 5 mins (early) and averaged increase during 20 - 30 mins (late); normalized to pre-MPH amplitude; n = 10 cells WT, 11 cells HOM, $p > 0.05$, two-way RMANOVA).

7.2 ADDITIONAL EXPERIMENTS

Vesicular dopamine release underlies the evoked D_2-IPSCs in DAT Val559 slices

Previous studies found that depolarization enhances ADE in DAT Val559-expressing cells (Mazei-Robison *et al.*, 2008). Thus, electrical stimulation of slices from DAT Val559 mice could produce ADE. To determine if depolarization-induced ADE was occurring during stimulation, D_2-IPSCs were evoked with a train of 5 stimuli once every 50 s. Disrupting loading of dopamine into vesicles with reserpine (1 μM) abolished evoked D_2-IPSCs in WT and DAT Val559 slices with a similar time course (Figure 7.2). This result indicates that the evoked D_2-IPSC was due to vesicular release of dopamine, not ADE. In addition, AMPH, which blocks ADE in DAT Val559-expressing cells, did not alter the run-down of the evoked D_2-IPSCs in reserpine (Figure 7.2). This result suggests that vesicular packaging of dopamine was not compromised by DAT Val559. It is also unlikely that depolarization-induced ADE contributed to the slowed kinetics of the evoked D_2-IPSCs observed in DAT Val559 slices. Spontaneous D_2-IPSCs, which occur without action potentials or calcium entry via voltage-gated calcium channels (Gantz *et al.*, 2013), were also slower. The slowed kinetics more likely reflect impaired clearance of dopamine.

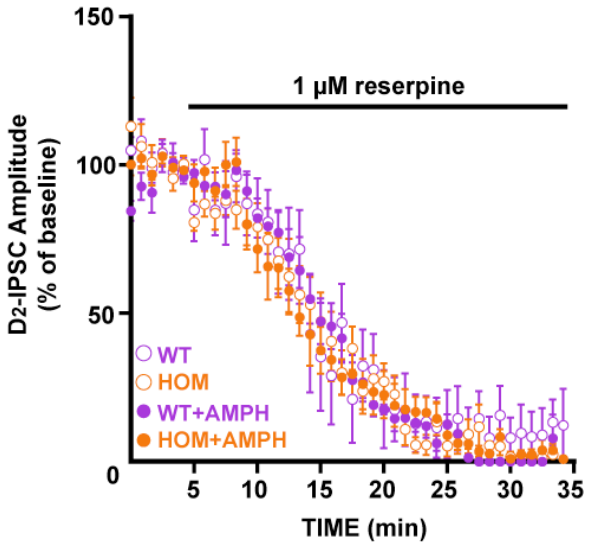

Figure 7.2. Vesicular dopamine release produces evoked D_2-IPSCs in dopamine neurons from DAT Val559 slices.

D_2-IPSCs were evoked by a train of 5 electrical stimuli once every 50 s. Application of reserpine (1 µM) abolished the evoked D_2-IPSC, in WT and HOM slices, with a similar time course. Amphetamine (300 nM) had no effect on the run-down of the evoked D_2-IPSC with reserpine in either genotype. *n* = 5 cells WT, 7 HOM, 6 WT in AMPH, and 8 HOM in AMPH.

Regulation of evoked dopamine release is altered in DAT Val559 slices

At many synapses, paired electrical stimuli with brief interstimulus intervals (paired-pulse) is used to assess presynaptic facilitation or depression of transmitter release. However, the inability to resolve individual evoked D_2-IPSCs, due to their slow intrinsic kinetics, complicates the use of a paired-pulse ratio. But, the amplitude of D_2-IPSCs produced by a train of 5 stimuli compared to 1 stimulus generates a ratio that is altered by increasing or decreasing probability of release, but not increasing transmitter content or impairing dopamine reuptake (Beckstead and Williams, 2007). Thus, the probability of dopamine release in WT and DAT Val559 slices were assessed by examining the amplitude of D_2-IPSCs produced with a train of 5 stimuli (5-D_2-IPSC) as a percent of the amplitude evoked by a single stimulus (1-D_2-IPSC) in the same neuron.

In dopamine neurons from WT slices, the amplitude of the 5-D_2-IPSC produced was 298 ± 28.5% of the 1-D_2-IPSC (n =16), consistent with a previous report (Beckstead and Williams, 2007). In dopamine neurons from DAT Val559 slices, the amplitude of the 5-D_2-IPSC was 223 ± 16% of the 1-D_2-IPSC (n = 17), which was significantly less than that observed in WT ($p = 0.03$, unpaired t test, data not illustrated). These results further suggest that dopamine release in DAT Val559 slices was altered due to a presynaptic mechanism.

Exogenous dopamine and AMPH produces a tonic D_2 receptor-dependent current only in DAT Val559 slices.

In dopamine neurons from DAT Val559 slices, AMPH did not increase the amplitude of the evoked D_2-IPSC to the extent observed in WT slices. However, the slowing of the evoked D_2-IPSC kinetics were similar between genotypes, suggesting dopamine and

AMPH were competing for DAT-mediated uptake. There were no differences between genotypes in D_2R binding or functional expression of D_2 receptors in the midbrain. The conclusion was the attenuated AMPH-induced increase in DAT Val559 slices was due to a presynaptic alteration.

To determine if there was a postsynaptic change in DAT Val559 slices, D_2 receptor-dependent currents were produced by brief, iontophoretic application of dopamine (I-DA) once every 50 s. In dopamine neurons from WT slices, application of AMPH (300 nM) significantly increased I-DA (150 ± 15% of baseline, $p = 0.02$, $n = 7$, paired *t* test). In contrast, in dopamine neurons from DAT Val559 slices, AMPH had no effect on I-DA (102 ± 17% of baseline, $p = 0.66$, $n = 7$, unpaired *t* test). But, only in DAT Val559 slices, only after dopamine exposure, there was a standing outward current in some cells (25 ± 18 pA, $n = 8$ cells). Then, AMPH produced an additional outward current (44 ± 19 pA, $n = 7$) that was not observed in experiments where slices were not exposed to exogenous dopamine. Application of the D_2 receptor antagonist, sulpiride (600 nM), reversed both the AMPH-induced and standing outward currents. Taken together, these results indicate that in DAT Val559 slices, exposure to dopamine produced a tonic D_2 receptor-dependent outward current. The tonic current was augmented by AMPH, which precluded I-DA. The mechanism by which AMPH augmented the tonic current was undetermined. The simplest explanation is that the D_2 receptor-dependent tonic current was either a result of impaired uptake following dopamine exposure or ADE. However, in cells expressing DAT Val559, AMPH blocked ADE. Thus, future studies should be aimed at determining the mechanism of the AMPH-induced D_2 receptor-dependent current after previous dopamine exposure.

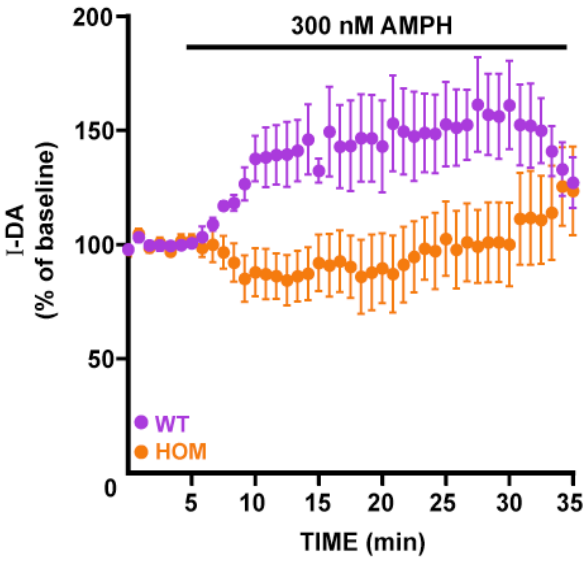

Figure 7.3. Amphetamine does not augment the D_2 receptor-dependent current produced by exogenous dopamine in dopamine neurons from DAT Val559V slices.

D_2 receptor-dependent currents were produced by brief, iontophoretic application of dopamine once every 50 s (I-DA). Amphetamine (300 nM) increased I-DA in dopamine neurons from WT but not HOM slices. *n* = 2-8 cells WT, 2-8 cells HOM.

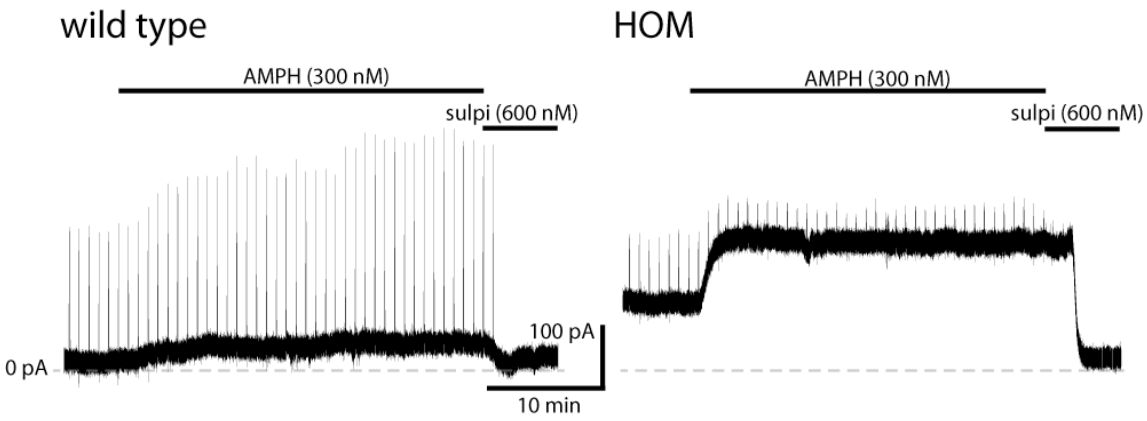

Figure 7.4. After exposure to dopamine, amphetamine augments a tonic D_2 receptor-dependent outward current.

Traces of whole-cell voltage clamp recordings of holding current and D_2 receptor-dependent currents produced by iontophoretic application of dopamine once every 50 s (upward deflections, I-DA). In WT slices after exogenous dopamine exposure, amphetamine (AMPH) augmented I-DA and produced a small outward D_2 receptor-dependent outward current that was reversed by the D_2 receptor antagonist, sulpiride. In HOM slices after exogenous dopamine exposure, there was a standing tonic current prior to AMPH application. AMPH augmented the tonic D_2 receptor-dependent current that was reversed by sulpiride. Both traces show the maximal outward current to AMPH observed in each genotype.

Chapter 8 DISCUSSION

Dopamine released through the activity of substantia nigra (SNc) dopamine neurons is important in multiple physiological processes ranging from movement to reinforcement learning. SNc dopamine neurons release dopamine at their extensive terminal projections and locally from somatodendritic sites. D_2 autoreceptor activation in somatodendritic sites regulates dopamine release throughout the brain through a negative-feedback system. Despite this critical regulatory role, many fundamental questions remain about the mechanisms that govern dopamine transmission. In this dissertation, data are presented that argue that the investigation of spontaneous D_2 receptor-mediated IPSCs will advance the understanding of dopamine transmission in the midbrain. The occurrence of spontaneous D_2 receptor-mediated IPSCs reveals insights into the structure of the dopamine synapse, the regulation and drug-induced plasticity of evoked and spontaneous dopamine transmission, and dopamine neuron excitability. More broadly, their occurrence also demonstrates that G protein-coupled receptor-dependent synaptic transmission is much more similar to ionotropic receptors than previously appreciated.

PREFACE

Many of the fundamental properties that governed evoked and spontaneous dopamine transmission were similar. Both forms of transmission required D_2 receptor activation of a GIRK conductance following exocytosis of dopamine-filled vesicles. The results of these studies support point-to-point dopamine transmission in the SNc as the primary mode of dopamine transmission. The following sections describes how the occurrence of spontaneous D_2 receptor-mediated IPSCs are indicative of dopamine release sites structurally close to D_2 receptors. In addition, advancements in the understanding of presynaptic and postsynaptic components and drug-induced plasticity of the dopamine synapse are described. Then, the influence spontaneous dopamine transmission may have to dopamine neuron excitability is discussed. Finally, the last section proposes future experiments to address unresolved questions.

PROXIMITY OF RELEASE SITES AND RECEPTORS

The strongest evidence for dopamine release sites and D_2 receptors being closely apposed is the presence of spontaneous D_2-IPSCs. Single vesicle fusion events produced spontaneous D_2 receptor-mediated IPSCs with rising kinetics that were previously found (Ford *et al.*, 2009) to be achieved only with high concentrations of dopamine ($\geq$ 10 μM). Thus, it is unlikely these currents are produced by extended diffusion of dopamine. In addition, when performing simultaneous whole-cell voltage clamp recordings from two dopamine neurons, spontaneous D_2-IPSCs were never found to co-occur in the two neurons. Thus, spontaneous D_2-IPSCs are physiological evidence of dopamine synapses and specificity of dopamine-mediated signaling between neurons.

At many synapses, neurotransmitter that is released or diffuses outside of the synaptic cleft can activate ‘extrasynaptic’ receptors. The existence of synaptic dopamine transmission does not preclude the activation of extrasynaptic D_2 receptors. Diffuse and

persistent dopamine release could create a standing "tonic" outward current through the activation of synaptic and extrasynaptic D_2 receptors. Indeed, impairing dopamine reuptake with cocaine or other psychostimulants results in a tonic dopamine-mediated current (Branch and Beckstead, 2012; Ford *et al.*, 2007). With reuptake intact, a tonic dopamine-mediated current was not observed, except in a few cases when the system was altered in other ways. For example, acute application of L-DOPA resulted in a D_2 receptor-mediated outward current that was due to non-vesicular dopamine release. While the density of dopaminergic neurons in the midbrain makes these neurons the likely source, it could have also arisen from 5-HT terminals (Chapter 5), noradrenergic terminals (Liprando *et al.*, 2004), or astrocytes (Juorio *et al.*, 1993). Another example was observed following viral-mediated expression of D_2 receptors in the SNc of *Drd2*$^{-/-}$ mice. Varigated viral infection produced some dopamine neurons that functionally over-expressed D_2 receptors by 1.5-2-fold, while others did not express D_2 receptors. In this case, a tonic dopamine-induced current was observed (Figure 8.1). The frequency and amplitude of spontaneous D_2-IPSCs was elevated relative to dopamine neurons from wild type mice. Thus, it is likely that the elevated spontaneous release of dopamine in conjunction with the over-expression of D_2 receptors contributed to the tonic current. Lastly, in dopamine neurons from DAT Val559 mice, a tonic D_2 receptor-dependent current was observed after a single saturating application of dopamine, or in response to amphetamine. Thus, it is not the case that tonic D_2 receptor-dependent outward currents cannot be observed. If a paracrine form of dopamine transmission were the predominant mode of signaling in brain slices, it would be detected.

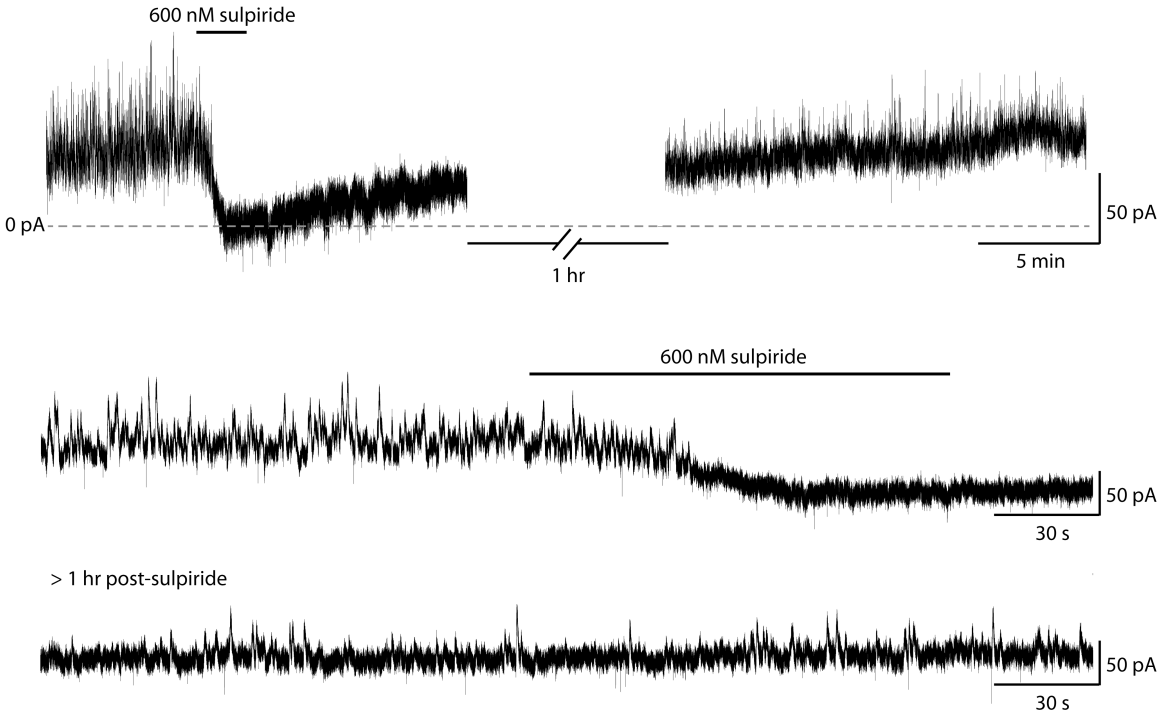

Figure 8.1. Viral overexpression of D_2 receptors in dopamine neurons reveals exceptional spontaneous D_2 receptor-mediated IPSCs and a standing D_2 receptor-dependent outward current.

Trace of a whole-cell voltage clamp recording using a 10 mM BAPTA-containing internal solution, of exceptional spontaneous D_2-IPSCs and a tonic D_2 receptor-dependent outward current. Application of the D_2 receptor antagonist, sulpiride (600 nM) blocked both the spontaneous D_2-IPSCs and the tonic current. After more than an hour of sulpiride wash out, both spontaneous D_2-IPSCs and the tonic outward current returned.

PRESYNAPTIC COMPONENTS

Sites of dopamine release

Dopamine neurons

In the SNc, the presence of extracellular dopamine (Björklund and Lindvall, 1975) despite a paucity of structural evidence for dopaminergic axon terminals led to the theory that dopamine is released from the somatodendritic compartment (Juraska *et al.*, 1977). The D_2-IPSC is dependent on dopamine production in dopamine neurons (Beckstead *et al.*, 2004), but the release sites are unknown. There is some structural evidence for

putative synapses between dopamine somas, dendrites, and spine-like structures; although relative to non-dopaminergic inputs to this area, the density is low (Bayer and Pickel, 1990; Groves and Linder, 1983; Nirenberg *et al.*, 1996a; 1996b; Wassef *et al.*, 1981). But, the presence of spontaneous D_2-IPSCs are indicative of closely apposed synaptic contacts. It is difficult to reconcile compelling electrophysiological data for somatodendritic synapses with the apparent lack of structural evidence.

Dopamine neurons in the ventral midbrain are a heterogeneous group, expressing different ion channels and receptors, and receiving or sending projections from different parts of the brain. In addition, dopamine neurons lack stereotyped positioning within the midbrain (e.g. lamination). The inability to frequently observe somatodendritic synapses could reflect the vastness of the region in conjunction with an apparent absence of structural organization. In addition, the majority of structural work has been done using rat midbrain slices. Electrical stimulation in rat midbrain slices, compared to mouse midbrain slices, produces less dopamine release and smaller amplitude D2-IPSCs (Courtney *et al.*, 2012). These results suggest there may by species differences in the density of somatodendritic dopamine synapses, and structural studies in mouse midbrain may be more fruitful. Another possibility is that somatodendritic dopamine synapses are transient structures, dynamically regulated by dopamine release – discussed in more detail in Future directions: Structure and function of dopamine neuron synapses (p. 152).

Another possibility is that dopamine neurons form synapses onto themselves (autapses). In single neuron microcultures, dopamine and 5-HT neurons form synapses onto themselves. In this culture system, depolarizing 5-HT neurons results in 5-HT-mediated inhibition, but dopamine-mediated inhibition does not occur after depolarizing

dopamine neurons (Johnson, 1994; Sulzer *et al.*, 1998). In brain slices, dopamine-dependent outward currents have not been observed following a single or train of action potentials, despite repeated attempts. But, all SNc dopamine neurons have the enzyme required for the production of dopamine, tyrosine hydroxylase, and produce D_2 receptor-dependent currents upon exposure to dopamine. Therefore, it is possible that the recording conditions required for observing dopamine autapses has simply not been determined. Alternatively, it is possible that there is cellular or subcellular division of pre- and postsynaptic elements, such that dopamine autapses do not exist. Serial section electron microscopy in the rat SNc found dendrodendritic synapses between dopamine neurons, with clear pre- and postsynaptic specializations. For the length that each dendrite could be followed (~ 4 μm), the postsynaptic dendrite was never observed to also have vesicles, indicative of becoming the presynaptic element at another synapse (Groves and Linder, 1983). Data presented in this dissertation demonstrate that spontaneous D_2-IPSCs are likely produced by spontaneous dopamine release from neighboring neurons, rather than from the recorded neuron itself. These results are consistent with the lack dopaminergic autapses, though the possibility is not formally excluded.

5-HT terminals

The data presented in this dissertation reveal an unexpected source of dopamine release from 5-HT terminals in the SNc, after exposure to the dopamine precursor L-DOPA. Dopamine neurons in the midbrain receive a prominent projection from 5-HT neurons in the raphe nuclei (Dray *et al.*, 1976; Moukhles *et al.*, 1997; Qi *et al.*, 2014; Van Bockstaele *et al.*, 1994). However, a fraction of the apposing 5-HT axons (20-50%) form

specializations indicative of synaptic contact. When synaptic contacts were present, the synapses had an asymmetric structure and contained mostly clear synaptic vesicles, though dense core vesicles have also been noted (Moukhles *et al.*, 1997; Van Bockstaele *et al.*, 1994). More recent studies have demonstrated that the asymmetric synapses immunolabel for the vesicular glutamate transporter (VGlut3) (Qi *et al.*, 2014), consistent with 5-HT terminals in the midbrain co-releasing glutamate and 5-HT (Liu *et al.*, 2014; McDevitt *et al.*, 2014). Thus, it has been suggested that 5-HT terminals form glutamatergic synapses onto dopamine neurons and 5-HT may be released at these sites or other sites that require diffusion to activate receptors on dopamine neurons.

5-HT neurons can convert L-DOPA to dopamine through the AADC (Arai *et al.*, 1994). The release of dopamine from 5-HT terminals in the SNc, after exposure to L-DOPA, is described in Chapter 5. When electrically stimulated, 5-HT terminals released dopamine, leading to augmentation of the evoked D_2-IPSC. When 5-HT terminals were selectively activated with ChR2, a D_2-IPSC was produced from 5-HT terminal-derived dopamine. The D_2-IPSC produced by ChR2 activation of 5-HT terminals was significantly slower than the D_2-IPSC produced by electrical stimulation. In addition, slowing diffusion with a dextran-containing solution reduced the L-DOPA-induced augmentation in the evoked D_2-IPSC. However, L-DOPA also increased the frequency of spontaneous D_2-IPSCs. Inhibiting transmitter release from 5-HT terminals through activation of 5-HT_{1B} receptors had no effect on the L-DOPA-induced increase in spontaneous D_2-IPSC frequency. The ability of 5-HT_{1B} receptors to inhibit Cd^{2+}-insensitive miniature glutamatergic and glycinergic synaptic currents has been observed (Muramatsu *et al.*, 1998; Umemiya and Berger, 1995). However, the sensitivity of

spontaneous 5-HT release to 5-HT_{1B} receptor-dependent inhibition needs to be confirmed, as the synaptic machinery involved in monoamine-filled vesicle release may be different. Nonetheless, slowing diffusion also had no effect on the increase in spontaneous D_2-IPSC frequency produced by L-DOPA application.

In summary, the results indicate that presynaptic VMAT2-dependent release sites on 5-HT terminals are positioned to influence dopamine neuron activity, but are not likely directly apposed to D_2 receptors. Following electrical stimulation the diffusion of 5-HT terminal-derived dopamine from many release sites activates D_2 receptors. However, 5-HT terminal-derived dopamine from a single release site may be insufficient (e.g. too diffuse) to elicit a spontaneous D_2-IPSC. Lastly, the results also imply that when electrically stimulated, dopamine release from somatodendritic release sites may activate more distant D_2 receptors, than those activated by spontaneous release – discussed in more detail in Postsynaptic components: Kinetics of D_2 receptor activation (p. 142).

Regulation of dopamine release

Mechanisms of release

Unstimulated somatodendritic dopamine release has been measured using high-performance liquid chromatography or amperometry from midbrain dopamine neurons in modified brain slices (Jaffe *et al.*, 1998) and cultures (Fortin *et al.*, 2006; Kim *et al.*, 2008; Mendez *et al.*, 2011). There is considerable agreement between these previous studies and the data presented in this dissertation. Previous studies reported that dopamine release occurs in the absence of action potentials, calcium entry into the cytosol through voltage-gated calcium channels or intracellular calcium stores, and in calcium-free external solution. Blockade of DAT elevates the detection of spontaneous

dopamine release aruging against release occuring through DAT-mediated reversal (Fortin *et al.*, 2006). Moreover, spontaneous somatodendritic dopamine release is due to vesicular dopamine release, as it requires SNARE proteins and synaptotagmin (Fortin *et al.*, 2006; Mendez *et al.*, 2011). Lastly, L-DOPA increased the frequency and amplitude of amperometric, presumed dopaminergic, spikes (Kim *et al.*, 2008). Even the frequency of spontaneous D_2-IPSCs was similar to the frequency of spontaneous release events reported to occur from the soma of midbrain dopamine neurons, 0.3 to 3 events/min (Jaffe *et al.*, 1998).

In contrast to the data presented in this dissertation, blocking action potentials or voltage-gated calcium channels decreases basal somatodendritic dopamine release in dopamine neuron cultures (Fortin *et al.*, 2006; Kim *et al.*, 2008; Mendez *et al.*, 2011). In brain slices, dopamine neurons are tonically active, firing regular "pacemaker" action potentials. It is difficult to understand why dopamine release does not occur to these action potentials even though evoked D_2-IPSCs require action potentials and voltage-gated calcium channels. It is clear that many questions regarding the mechanism and site of dopamine release remain unresolved. Nonetheless, the occurrence of spontaneous D_2-IPSCs demonstrates that spontaneous dopamine release in the SNc is functional and physiologically relevant and further indicates that the presynaptic regulation of evoked and spontaneous dopamine transmission is likely to be very different.

Vesicular content

Ultrastructural studies of the somatodendritic compartment of dopamine neurons have described a variety of vesicles types and sizes, including small clear synaptic, large dense core, and tubulovesicles or saccules (Bayer and Pickel, 1990; Groves and Linder, 1983;

Nirenberg *et al.*, 1996a; 1996b). Different classes of vesicles can package different amounts of dopamine (Anderson *et al.*, 1998; Chen and Ewing, 1995), but it is unlikely that all of these types contribute to the dopamine release underlying evoked or spontaneous D_2-IPSCs. A minimum stimulation protocol was used to compared the amplitude of the evoked D_2-IPSCs to spontaneous D_2-IPSCs. With the exception of some larger spontaneous events, the amplitudes were very similar. These results are suggestive of a quantal event. However, the low frequency of spontaneous D_2-IPSCs observed in brain slices from wild type mice necessitated the combining data from many cells, thereby limiting further quantitative analysis. Nonetheless, in individual recordings, it was not uncommon to observe discrete amplitudes (e.g. Figure 8.2, Figure 6.1E). At the very least, these data are indicative of some consistent packaging of dopamine in the presynaptic release site. Moreover, small changes in the vesicular dopamine content, by altering biosynthesis with L-DOPA or disrupting VMAT2 with reserpine, were detected as small changes in amplitude of the spontaneous D_2-IPSC. However, 97% of all spontaneous D_2-IPSCs amplitude were $\leq$ 30 pA. The remaining 3% recorded were as large as 500 pA. Therefore, it is possible another type of dopamine-filled vesicle is released infrequently, but the data are most consistent with uniform dopamine content in each release event.

Figure 8.2. Evoked and spontaneous dopamine release produces a very similar current.

Representative trace of a whole-cell voltage clamp recording. Minimum stimulation produced an evoked D_2-IPSC (arrow, stim) that was very similar to spontaneous D_2-IPSCs (red star).

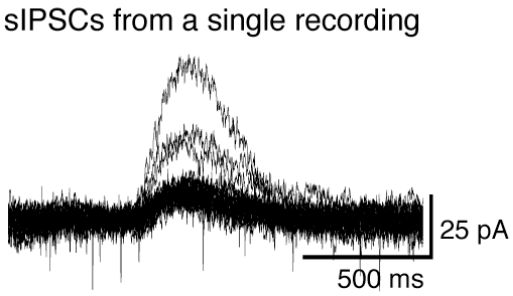

Figure 8.3. Discrete increments in the amplitude of spontaneous D_2-IPSCs suggest quantal release.

Sample traces of spontaneous D_2-IPSCs recorded from a single neuron.

Dependence on biosynthesis

The dependence of the evoked D_2-IPSC on biosynthesis of dopamine in dopamine neurons was described in the original report (Beckstead *et al.*, 2004). There is no evoked D_2-IPSC in midbrain slices from dopamine-deficient mice (Beckstead *et al.*, 2004). These mice are dopamine-deficient due to the specific loss of TH expression in dopamine neurons, but have normal levels of AADC (Zhou and Palmiter, 1995). As a consequence, bypassing the TH deficiency by application of L-DOPA restores evoked D_2-IPSCs in these mice (Beckstead *et al.*, 2004). Dopamine-deficient mice must be treated with L-DOPA to prevent profound hypoactivity, adispia, aphagia, and ultimately, death (Zhou and Palmiter, 1995). Similar to PD patients treated with L-DOPA, administration of L-DOPA to dopamine-deficient mice temporarily restores motor and feeding activity. These data, in conjunction with the inability to detect evoked D_2-IPSCs in these mice, despite daily L-DOPA treatment, highlights the transience of the evoked D_2-IPSC, in the absence

of ongoing dopamine biosynthesis. Other processes of dopamine recovery, such as DAT-mediated reuptake, is insufficient to maintain the vesicular pool.

The data presented in this dissertation demonstrate that biosynthesis of dopamine from L-DOPA augments dopamine release from dopamine neurons, consistent with previous reports concluding that dopamine content is labile (Beckstead *et al.*, 2004; Kim *et al.*, 2008; Pothos *et al.*, 1996). However, the data presented here shows that after L-DOPA exposure, the majority of electrically evoked dopamine release in the midbrain was from 5-HT terminals. By comparison, the boost in dopamine release from dopamine neurons produced by electrical stimulation was small and transient. However, L-DOPA also produced a D_2 receptor-dependent current. It is possible that the L-DOPA-induced augmentation in dopamine release was obscured by this outward current or D_2 receptor-mediated autoinhibition reduced dopamine release from dopamine neurons. Preventing dopamine synthesis by AADC inhibition also had little effect on the evoked D_2-IPSC over the course of an hour, stimulating once every 50 s. Therefore, electrically evoked dopamine release may not greatly dependent on dopamine biosynthesis in the short-term.

Spontaneous dopamine release may be more sensitive to dopamine biosynthesis. The production of dopamine from L-DOPA exposure increased the frequency of spontaneous D_2-IPSCs, with a modest increase in amplitude. Experiments in TH-hD_2S mice suggested that the increase in amplitude likely does not account for the increase in frequency. The L-DOPA-induced increase in frequency was also transient, waning 10 min following L-DOPA application. In dopamine axon terminals, newly synthesized dopamine is prefentially released from a compartment distinct from storage pools of dopamine (Besson *et al.*, 1969; Chiueh and Moore, 1975; Venton *et al.*, 2006; Yavich

and MacDonald, 2000). This work has yet to be extended to somatodendritic compartments. But it is possible that newly synthesized dopamine is preferentially released, producing an increase in spontaneous D_2-IPSC frequency.

POSTSYNAPTIC COMPONENTS

Kinetics of D_2 receptor activation

A high concentration of dopamine (> 10 μM) is required to produce currents with similar rise-time as the D_2-IPSC (Courtney and Ford, 2014; Ford *et al.*, 2009). Then, the concentration of dopamine must drop rapidly; otherwise the duration of the D_2-IPSC is prolonged, more closely resembling D_2-IPSCs when dopamine reuptake is impaired with cocaine (Ford *et al.*, 2009). The rise-time of evoked and spontaneous D_2-IPSCs were identical, suggesting both synaptic currents are produced by a brief high concentration of dopamine. However, the duration of the spontaneous D_2-IPSC was less than the evoked D_2-IPSC (~ 70%). This was observed in wild type C57BL/6J, DBA/2J, and hybrid 129S6/SvEvTAc and C57BL/6J mice. In addition, in dopamine neurons from DAT Val559 mice, where D_2-IPSCs were significantly slowed, the duration of spontaneous D_2-IPSCs was still less than evoked D_2-IPSCs.

The duration of the spontaneous D_2-IPSCs was most similar to the current produced by fast-flow application of a high concentration of dopamine onto somatic membrane patches (100 μM, 100 ms, Figure 8.4B). The late phase of the evoked D_2-IPSC required prolonged application of a low concentration of dopamine (100 nM, 500 ms, Ford *et al.*, 2009, Figure 8.4D). These results suggest that electrically evoked but not spontaneously released dopamine may diffuse to activate D_2 receptors, or lingers in the

extracellular space so that it continues to activate D_2 receptors. Thus, dopamine released by stimulation may travel farther than spontaneously released dopamine.

This is further supported by the observation that 5-HT terminal-derived dopamine (after L-DOPA exposure) can contribute to evoked D_2-IPSCs, but not spontaneous D_2-IPSCs. Dopamine from 5-HT terminals was likely arising from more distant sites, since dextran interfered with the L-DOPA-induced augmentation in the evoked D_2-IPSC. In addition, both the rise-time and the duration of the D_2-IPSC produced by selective stimulation of 5-HT terminals was significantly, but not dramatically slowed. The slow intrinsic signaling kinetics of the D_2-IPSC obscure some changes in D_2 receptor activation by dopamine. Upon stimulation in the midbrain, the peak concentration of extracellular dopamine precedes the peak of the D_2-IPSC by hundreds of milliseconds (Ford *et al*., 2009). This result indicates that much of the time course of the D_2-IPSC, especially the rising phase, is limited by the time required for metabotropic receptor signaling. (Ford *et al.*, 2009). Therefore, subtle changes in the rise time from 5-HT terminal-derived dopamine may signify larger changes in the onset of D_2 receptor activation following release.

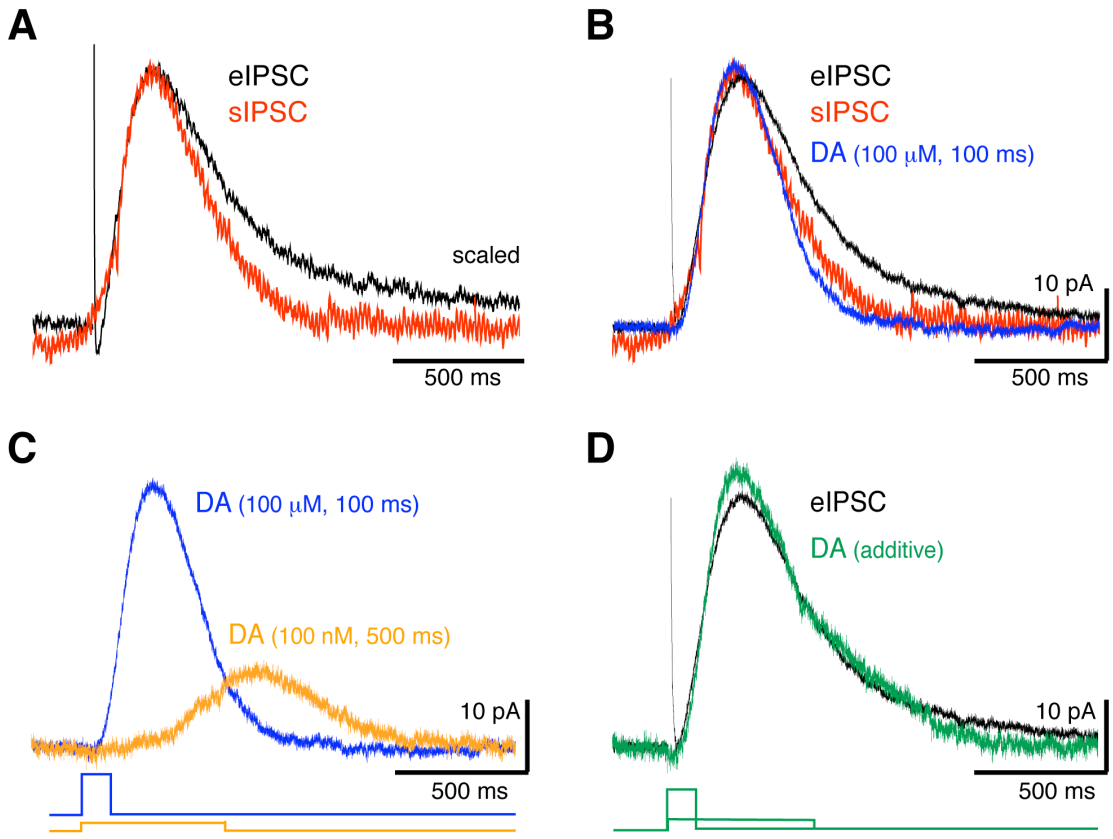

Figure 8.4. Currents produced by application of a high concentration of dopamine mimics spontaneous D_2-IPSCs

(A) Reproduction of Figure 4.1C, showing representative traces of averaged and scaled evoked (black) and spontaneous (red) D_2-IPSC. (B-D) Adapted from Figure 7 in Ford *et al.*, 2009. The kinetics of the spontaneous D_2-IPSC resembles the current produced by application of 100 μM dopamine for 100 ms onto dopamine neuron somatic membrane patches. In contrast, the kinetics of the evoked D_2-IPSC has a 'late-phase' that is mimicked by the application of 100 μM dopamine for 100 ms along with prolonged (500 ms) application of a 100 nM dopamine.

Since under basal conditions the evoked D_2-IPSC was unchanged by the dextran-containing solution, the diffusion of dopamine must be limited. Ultrastructural studies have described long stretches of very close dendrodendritic, somatosomatic, or somatodendritic appositions between dopamine neurons (Bayer and Pickel, 1990; Groves and Linder, 1983). This sort of structural arrangement could allow for lateral diffusion of dopamine that may not be disrupted by dextran. It is unclear if the difference in evoked

and spontaneous D_2-IPSC kinetics represents these kind of structural differences in the evoked and spontaneous release sites, or the location of D_2 receptors or DATs.

Another possible source of postsynaptic heterogeneity involves the expression of the two splice variants of the D_2 receptor, D_2S and D_2L. Midbrain dopamine neurons express D_2S and D_2L, with some expressing D_2L-only or D_2S-only (Dragicevic *et al.*, 2014; Jang *et al.*, 2011; Khan *et al.*, 1998). When expressed in dopamine neurons, activation of D2S or D2L receptors is equally capable of activating a GIRK conductance (Neve *et al*., 2013). The data presented in this dissertation extend these studies. Activation of D_2S or D_2L receptors produced spontaneous D_2-IPSCs with similar durations. Therefore, the difference in the durations of the evoked and spontaneous D_2-IPSCs is not explained by selective activation of D_2S or D_2L receptors.

Sites of D_2 receptors

Additional insights into postsynaptic components of the dopamine synapse were garnered from the generation and characterization of the TH-hD_2S mouse line. In this mouse line, the expression of Flag-tagged human D_2S receptors depends on the tyrosine hydroxylase promoter (TH-hD_2S Transgenic Mice, Figure 6.7). In brain slices from TH-hD_2S mice, immunolabeling Flag-D_2 receptors and confocal microscopy revealed that hD_2S receptors were on the soma, dendrites, and spine-like protrusions on dopamine neurons. The presence of D_2 receptors on the soma and dendrites are consistent with previous ultrastructural (Sesack *et al.*, 1994), immunocytochemical (Jomphe *et al.*, 2006), and electrophysiological (Ford *et al.*, 2009) studies.

There were two more striking observations. First, hD_2S receptors were clustered in distinct puncta. This structural arrangement is in contrast to diffuse labeling of Flag-

tagged μ-opioid receptors, which evenly surround the soma (Arttamangkul *et al.*, 2008). Second, the observation of spine-like structures on dopamine neurons may be considered unexpected. Nearly all structural studies on dopamine neurons mention the presence of dendritic spines (e.g. Bayer and Pickel, 1990; Groves and Linder, 1983; Khan *et al.*, 1998; Phillipson, 1979), but largely their presence has been overlooked in functional studies. In fact, only one study has investigated spine-related functional differences in dopamine neurons (Sarti *et al.*, 2007). While not rigorously characterized, it was not uncommon to observe D_2 receptors on spine- or filopodia-like structures emanating from the soma and dendrites. Dopamine neurons in the TH-hD_2S mice were not specially endowed with these structures. Similar structures were observed on the dendrites of dopamine neurons in wild type midbrain slices. Focal uncaging of dopamine onto similar spots was sufficient to produce D_2 receptor-dependent outward currents. Thus, these clusters of D_2 receptors may be the site(s) that mediate evoked and spontaneous D_2-IPSCs.

DRUG-INDUCED PLASTICITY IN DOPAMINE SIGNALING

Exposure to drugs of abuse are known to cause morphological and functional changes to dopamine neuron physiology. A number of studies have reported drug-induced plasticity in dopamine neurons that involves PKA, PKC, or are otherwise contingent on the method of recording or the calcium-buffering capabilities of the whole-cell internal solution, implicating calcium-dependence (Bonci and Williams, 1996; Borgland *et al.*, 2006; Dragicevic *et al.*, 2014; Luu and Malenka, 2008; Melis *et al.*, 2002; Perra *et al.*, 2011; Sharpe *et al.*, 2014). However, the mechanim(s) of drug-induced changes to D_2 receptor-dependent GIRK signaling have not been reported. The experiments presented in this

dissertation examined several drug-induced changes to dopamine transmisison in the midbrain. While not determining the precise mechanisms, the data provide insights that may increase the success of future experiments.

First, the frequency and amplitude of spontaneous D_2-IPSCs were elevated after a single *in vivo* exposure to cocaine. Drug exposure also potentiates spontaneous GABAergic and glutamatergic synaptic transmission to dopamine neurons, so these results show that spontaneous dopamine transmission is similarly plastic. The potentiation of spontaneous GABAergic transmission following drug exposure involves a protein kinase A (PKA)-dependent increase in GABA release (Bonci and Williams, 1997; Melis *et al.*, 2002). In one study, activation of PKA with forskolin increases the amplitude and frequency of spontaneous GABAergic synaptic currents in slices from control but not ethanol exposed mice (Melis *et al.*, 2002). Forskolin enhanced the amplitude and frequency of spontaneous D_2-IPSCs in slices from wild type mice, so these studies were extended to cocaine-exposed mice. After *in vivo* cocaine exposure, there was no increase in frequency or amplitude of spontaneous D_2-IPSCs by forskolin. These results suggest that enhanced spontaneous dopamine transmission following cocaine exposure may occur via PKA-dependent pathways. However, PKA activation, with forskolin (albeit at higher concentrations than used in this study) also augments the D_2 receptor-dependent current produced by exogenous dopamine (Beckstead *et al.*, 2009). It remains to be determined whether the cocaine-induced potentiation of spontaneous dopamine transmission is due to pre- or postsynaptic mechanism(s).

The increase in spontaneous D_2-IPSCs after *in vivo* cocaine exposure may be explained by morphological changes to dopamine neurons. A single *in vivo* cocaine

exposure also potentiates spontaneous glutamate transmission on dopamine neurons, which is accompanied by increase in the spine density on dopamine neuron dendrites (Sarti *et al.*, 2007; Ungless *et al.*, 2001). Since D_2 receptors were found on spine-like structures on dopamine neuron dendrites, cocaine exposure may be potentiating spontaneous dopamine transmission by increasing the density of spines. Alternatively, the increase in spontaneous D_2-IPSCs after *in vivo* cocaine exposure may also be explained by an increase in D_2 receptor availability. Overexpression of D_2 receptors in dopamine neurons from TH-hD_2S mice resulted in increased amplitude and frequency of spontaneous D_2-IPSCs. Indeed in the early studies (Chapter 4), the maximal D_2 receptor-dependent current (normalized to capacitance, dopamine current density) was greater in slices from cocaine-exposed mice than slices from naïve mice. But this result was not reproduced in later studies (Chapter 6) conducted under different recording conditions. It is possible that different recording conditions affected slices from wild type but not cocaine-exposed mice.

To better understand cocaine-induced postsynaptic changes, the pre- and postsynaptic elements had to be separated by producing D_2 receptor-dependent currents with exogenous D_2 agonist application. A few studies have reported drug-induced postsynaptic changes in D_2 receptor-dependent signaling, that are contingent on the calcium-buffering capabilities of the internal solution, including the removal of calcium-dependent D_2 receptor desensitization (Perra *et al.*, 2011; Sharpe *et al.*, 2014). However, whether this plasticity was due to a change in the calcium-dependent pathways or the D_2 receptors themselves was previously unresolved.

In data presented in this dissertation, after a single *in vivo* cocaine exposure, the calcium-dependent component of D_2 receptor desensitization was eliminated in wild type dopamine neurons. These studies were extended to examine desensitization of D_2S and D_2L receptors. D_2S but not D_2L receptors exhibited calcium-dependent desensitization. Pharmacologically depleting intracellular calcium stores, blocking L-type calcium channels, or directly activating PKC effectively reduced D_2S receptor desenstization, to a level comparable to D_2L desensitization. Since exposure to drugs can manipulate these calcium signaling pathways in a similar manner (Dragicevic *et al.*, 2014; Kramer and Williams, 2015; Luu and Malenka, 2008; Perra *et al.*, 2011; Steketee *et al.*, 1998; Steketee, 1997), it was surprising that *in vivo* cocaine exposure did not reduce calcium-dependent desensitization in dopamine neurons expressing D_2S-only. However, calcium-dependent desensitization in neurons expressing D_2S receptors was removed by the co-expression of D_2L receptors. These data suggest that cocaine-induced plasticity observed in wild type dopamine neurons may involve the upregulation of D_2L receptors, either by transcription, translation, or translocation of exisiting D_2L receptors from intracellular compartments (Filtz *et al.*, 1993; Giordano *et al.*, 2006; Ng *et al.*, 1997; Oomizu *et al.*, 2003; Starr *et al.*, 1995; Wernicke *et al.*, 2010; Zhang *et al.*, 1994). Furthermore, the data indicate that drug-induced changes may not involve changes in calcium signaling pathways, but rather the calcium sensitivity of receptors or effectors.

Taken together, these studies demonstrate several changes to dopamine transmission following drug exposure, including an increase in spontaneous dopamine transmission and a decrease in D_2 receptor desensitization. Whether these phenonmenon share a common mechanism remains to be determined. Moreover, the physiological

consequence of these cocaine-induced changes in unclear. D_2 autoreceptor deficient mice display enhanced cocaine-seeking behaviors (Holroyd *et al.*, 2015). Thus, enhancement of D_2 receptor-dependent autoinhibition, by changing to weakly desensitizing D_2 receptors and increasing spontaneous D_2-IPSCs, could be adaptive against compulsive drug-seeking. Alternatively, by decreasing dopamine release in projection areas, enhanced D_2 autoinhibition may contribute to a hypodopaminerigc state that drives drug seeking (Ranaldi *et al.*, 1999)

REGULATION OF DOPAMINE NEURON EXCITABILITY

Dopamine neurons fire regularly spaced action potentials in a tonic "pacemaker" mode. In response to rewards, or reward-predictive stimuli, dopamine neurons fire a short burst of action potentials. Single action potentials release a small amount of dopamine whereas phasic bursts of action potentials lead to a transient surge of dopamine release (Gonon, 1988). Through modulating the release of dopamine in the terminal projection areas, the rate and pattern of action potential firing is thought to mediate reinforcement learning (Schultz, 1986). Indeed, in behaving animals, selective photostimulation of midbrain dopamine neurons to drive phasic firing produces reward-seeking behaviors (Ilango *et al.*, 2014; Tsai *et al.*, 2009).

In the cell body region, D_2 receptor activation of GIRK channels leads to hyperpolarization and inhibition of firing in dopamine neurons. In brain slices, evoked dopamine release activates D_2 receptors and produces a transient inhibition of action potential firing (Beckstead *et al.*, 2004; Courtney *et al.*, 2012). The results presented in this dissertation demonstrate that spontaneous D_2-IPSCs are sufficient to inhibit action potential firing. Thus, spontaneous dopamine transmission contributes to the regulation of

dopamine neuron excitability. It is likely that sponantanous dopamine-mediated hyperpolarization and inhibition of firing has consequences in the cell body and terminals regions.

In dopamine neurons, the axon originates off a dendrite and may be several hundred microns from the soma (Häusser *et al.*, 1995). Action potentials are first recorded in the axon-bearing dendrite before backprogating to the soma and the rest of the dendritic arbor. Exogenous application of dopamine prevents the backpropagation of action potentials throughout the dendritic arbor, without changing action potentials in the axon-bearing dendrite, by increasing the availability of $I_{A\text{-like}}$ potassium channels preferentially located on the soma (Gentet and Williams, 2007). Thus, depending on the site(s) of D_2 receptor activation, spontaneous dopamine transmission may influence action potential backpropagation and somatodendritic action potential-dependent dopamine release.

Spontaneous dopamine transmission may also regulate dopamine release in the axon terminal projection regions. By inhibiting tonic action potential firing, spontaneous D_2-IPSCs may reduce tonic terminal release of dopamine. In addition, small changes to the soma membrane potential alters the synaptic strength of glutamatergic EPSCs generated in dopamine neurons dendrites (Hage and Khaliq, 2015). NMDA receptor activation is required for dopamine neurons to fire a burst of action potentals (reviewed in Paladini and Roeper, 2014). Therefore, small hyperpolarizations generated by spontaneous dopamine release may decrease the ability of dopamine neurons to burst fire, thereby reducing phasic dopamine signals.

FUTURE DIRECTIONS

Structure and function of dopamine neuron synapses

There are several possible follow-up studies pertaining to the structure and function of synapses in the midbrain. Under the context of L-DOPA treatment, understanding the regulation of dopamine release from 5-HT terminals is relevant. More broadly, it reveals putative synaptic connections between 5-HT terminals and midbrain dopamine neurons. Alternatively, it may suggest the capacity of somatodendritic dopamine synapses to form in response to extracellular dopamine. The results presented in this section may be extended in three ways.

First, the physiological role of 5-HT terminal-dopamine neuron synapses may be examined. In every dopamine neuron, the release of dopamine from 5-HT terminals, following L-DOPA application, was sufficient to produce D_2-IPSCs. A number of studies have demonstrated the expression and inhibitory role of 5-HT_{1A} and 5-$HT_{2A/C}$ receptors in a small subset dopamine neurons (Di Giovanni *et al.*, 2008). However, data presented in this disseration showed that only a small fraction of dopamine neurons had 5-HT_{1A} receptor-dependent IPSCs. Synaptic currents mediated by other 5-HT receptors were not observed. Although, a recent study in VTA dopamine neurons demonstrated that prolonged (3 s, 20 Hz) optical stimulation of 5-HT terminals produced slow inhibitory responses that were partially blocked by 5-$HT_{2A/C}$ receptors antagonists (Liu *et al.*, 2014). These results suggest a possible role for 5-$HT_{2A/C}$ receptors, but it is clear that many questions remain regarding the influence 5-HT normally exerts on dopamine neurons. It is expected that L-DOPA exposure would compromise native 5-HT transmission in the midbrain, as observed in the dorsal raphe. Therefore, these studies could be extended to

determine the impact of the loss of 5-HT transmission on midbrain dopamine neuron physiology.

Second, as described in "Sites of dopamine release – 5-HT terminals" (p.133), synaptic contacts between 5-HT terminals and dopamine neurons are generally asymmetric (Moukhles *et al.*, 1997; Van Bockstaele *et al.*, 1994). A portion of 5-HT neurons in the raphe nuclei and their terminals in the midbrain express the vesicular glutamate transporter (VGlut3) (Hioki *et al.*, 2010; Qi *et al.*, 2014). In agreement, selective activation of 5-HT terminals in the midbrain causes the release of serotonin and glutamate (Liu *et al.*, 2014; McDevitt *et al.*, 2014). These transmitters are likely packaged into vesicles by VMAT2 and vGlut3, respectively (Amilhon *et al.*, 2010), but many fundamental questions remain about vGlut3-expressing 5-HT terminals. Dopamine neurons, like 5-HT neurons, can co-release glutamate (Johnson, 1994; Sulzer *et al.*, 1998). A recent ultrastructure study found that in the same dopaminergic axon, there is distinct segregation of $VMAT2^+$ and $vGluT2^+$ vesicles and release sites (Zhang *et al.*, 2015). However, other work has demonstrated coimmunoprecipitation of VMAT2- and vGluT2-containing vesicles and that transport of glutamate enhances dopamine transport into the same vesicles (Hnasko *et al.*, 2010). The data in this dissertation indicate that L-DOPA may be used as an experimental tool to separate VMAT2- and VGluT3-dependent release to advance the understanding of co-release of 5-HT and glutamate from 5-HT terminals.

Lastly, data presented in Chapter 6 show D_2 receptors clustered on the soma dendrites and filopodia or spine-like strucutres. Somatodendritic D_2 receptors are often found retained in intracellular compartments (Sesack *et al.*, 1994), consistent with

intracellular retention in cell lines (Prou *et al.*, 2001; Takeuchi and Fukunaga, 2003). D_2 receptors translocate from intracellular compartments to the plasma membrane upon agonist exposure membrane (Filtz *et al.*, 1993; Ng *et al.*, 1997; Starr *et al.*, 1995; Tirotta *et al.*, 2008; Zhang *et al.*, 1994). Thus, it is possible dopamine-induced translocation of D_2 receptors is involved in the formation of D_2 receptor clusters, or synapses. Consistent with this, data presented in Chapter 4 demonstrates that the overexpression of D_2 receptors resulted in a greater frequency of spontaneous D_2-IPSCs. D_2 receptor activation is known to modulate synaptogenesis of dopamine terminals and spinogenesis in hippocampal neurons (Critchlow *et al.*, 2006; Fasano *et al.*, 2010; 2013). In other cell types, dendritic filopodia are transient structures and considered to be involved in the maturation of spines (reviewed in Nimchinsky *et al.*, 2002). Future studies with focal glutamate and dopamine uncaging could resolve the dynamism and functional significance of D2 receptors clusters and spine-like structures.

Drug-induced plasticity

There are several possible future studies pertaining to changes to dopamine neurons following drug exposure. First, data was presented in Chapter 6 that demonstrated that depleting intracellular calcium stores, directly activating PKC, or blocked L-type calcium channels effectively reduced D_2S receptor desenstization and augmented the magnitude of D_2L receptor-dependent GIRK currents. These pathways for calcium signaling are modulated by the activation of G_q-coupled receptors. Thus, future studies may address the possibility that G_q-coupled receptors act as endogenous regulators of D_2S and D_2L receptor signaling. Since a change in G_q-coupled metabotropic

glutamate receptor (mGluR) signaling is observed following a single *in vivo* cocaine exposure (Kramer and Williams, 2015), these studies may be extended to investigate cross-talk between mGluR and D_2 receptors following cocaine exposure.

Next, since dopamine was packaged readily in 5-HT terminals by VMAT2 following L-DOPA exposure, it may be that other chemical-induced states allow for a similar phenomenon. The dopamine (DAT) and serotonin transporters (SERT) are not perfectly selective for their cognate substrates. In striatal mouse brain slices, following chronic *in vivo* treatment with a SERT inhibitor antidepressant (SSRI), serotonin is released from dopaminergic terminals after uptake by DAT (Zhou *et al.*, 2005). Dopamine, at sufficiently high concentrations, is also transported by SERT (Larsen *et al.*, 2011). Since the ectopic release of dopamine from 5-HT neurons was costly to 5-HT-mediated synaptic transmission in the dorsal raphe. Therefore, it is plausible that exposure to dopamine or 5-HT reuptake inhibitors, whether pharmaceutical or illicit, will result in ectopic neurotransmitter release and subsequently decrease native neurotransmission.

Distinct regulation of evoked and spontaneous dopamine transmission

It is now widely recognized that stochastic vesicle exocytosis can produce spontaneous miniature synaptic currents. However, there is little consensus about the physiological role of spontaneous transmission. In fact, apart from the acknowledgement of this phenomenon, few interpretations regarding the regulation of spontaneous transmission aside from stochasticity are not met with some opposition. Regardless, comparisons between evoked and spontaneous transmission have become a powerful tool to understand the regulation of neurotransmitter release, presynaptic release sites, and

postsynaptic receptors. With the characterization of spontaneous D_2 receptor-mediated IPSCs, these studies may now be extended to advance the mechanistic understanding of the dopamine synapse and the physiological role of evoked and spontaneous dopamine transmission.

The regulation of evoked and spontaneous dopamine release is expected to be different. Primarily, the activation of receptors that inhibit calcium-dependent exocytosis will selectively affect evoked dopamine release. However, κ-opioid receptors inhibit evoked dopamine release through a mechanism distinct from hyperpolarization and inhibition of calcium channels (Ford *et al.*, 2007). Future studies can address the sensitivity of spontaneous dopamine release to κ-opioid activation.

At other synapses, differential sensitivity to inhibition of release may indicate different SNARE complexes or synaptotagmin isoforms. Axonal dopamine release is thought to be mediated by synaptotagmin 1 whereas somatodendritic release may be mediated by synaptotagmin 4 and 7 (Mendez *et al.*, 2011). The synaptotagmin isoforms have different selectivities for divalent cations to stimulate SNARE-mediated vesicle fusion (Bhalla *et al.*, 2005). This selectivity may be used to determine if one synaptotagmin isoform is preferentially involved in evoked or spontaneous dopamine release. Divalent selectivity and expression of specific synaptotagmin isoforms is also associated with different types and sizes of vesicles (Zhang *et al.*, 2011). These studies may be extended to conditions which have increased the frequency of spontaneous D2-IPSCs, namely forskolin, cocaine, L-DOPA. While this is a contentious topic at well-characterized ligand-gated ion channel synapses, data from these experiments could reveal that evoked and spontaneous D_2-IPSCs arise from separate vesicle pools.

SIGNALING BY G PROTEIN-COUPLED RECEPTORS

The main sites for transmission of information between neurons are synapses. A common feature at many synapses is the presence of spontaneous synaptic currents. For over sixty years, scientists have been electrically eavesdropping on the communication between neurons by recording spontaneous synaptic responses. These studies have lead to some of the most fundamental advancements in the understanding of synaptic transmission. To this day, the comparison between evoked and spontaneous synaptic transmission is used to garner insight into the origin and mechanism of transmitter release, but only where ionotropic receptors mediate the postsynaptic response.

Classically, electrical responses produced by the activation of G protein-coupled receptors are thought to be produced by extrasynaptic release of neurotransmitter that may travel some distance before activating receptors (Otis and Mody, 1992). As a result, the assumption is that these receptors exert slow, modulatory effects on a number of neurons without high specificity in signaling partners. But, at least at the somatodendritic dopamine synapse, the rate-limiting step is the intrinsic metabotropic signaling cascade, not the activation of receptors. To date, the research presented in this dissertation is the first record of spontaneous synaptic currents mediated by a G protein-coupled receptor. The occurrence of spontaneous D_2 receptor-mediated IPSCs demonstrates that dopamine release sites and D_2 receptors must be in close apposition; otherwise single vesicle release events would be too slow or diffuse to elicit a synaptic current. Therefore, synaptic communication through G protein-coupled receptors can be very different than originally believed and can be much more similar to communication mediated by ionotropic receptors. Recent development of new sensors for dopamine siganling in medium spiny

neurons, either the introduction of dopamine-gated chloride channels (Kress *et al*., 2014) or GIRK channels (Marcott *et al*., 2014) have also described phasic synaptic events consistent with fast and local dopamine signaling. In addition, the introduction of GIRK channels in medium spiny neurons has revealed spontaneous action potential-dependent muscarinic IPSCs (Mamaligas and Ford, 2015), demonstrating the phenomenon is not restricted to dopamine synapses. It is likely that spontaneously released neurotransmitters activate a G protein-coupled receptors throughout the brain, whether producing synaptic currents or modulating other signaling cascades. This is the beginning of an unrealized role for G protein-coupled receptor-dependent signaling in neuron regulation.

REFERENCES

Adler, E.M., Augustine, G.J., Duffy, S.N., and Charlton, M.P. (1991). Alien intracellular calcium chelators attenuate neurotransmitter release at the squid giant synapse. Journal of Neuroscience *11*, 1496–1507.

Amilhon, B., Lepicard, E., Renoir, T., Mongeau, R., Popa, D., Poirel, O., Miot, S., Gras, C., Gardier, A.M., Gallego, J., *et al.* (2010). VGLUT3 (vesicular glutamate transporter type 3) contribution to the regulation of serotonergic transmission and anxiety. Journal of Neuroscience *30*, 2198–2210.

Anderson, B.B., Chen, G., Gutman, D.A., and Ewing, A.G. (1998). Dopamine levels of two classes of vesicles are differentially depleted by amphetamine. Brain Research *788*, 294–301.

Anzalone, A., Lizardi-Ortiz, J.E., Ramos, M., De Mei, C., Hopf, F.W., Iaccarino, C., Halbout, B., Jacobsen, J., Kinoshita, C., Welter, M., *et al.* (2012). Dual control of dopamine synthesis and release by presynaptic and postsynaptic dopamine D2 receptors. Journal of Neuroscience *32*, 9023–9034.

Arai, R., Karasawa, N., Geffard, M., Nagatsu, T., and Nagatsu, I. (1994). Immunohistochemical evidence that central serotonin neurons produce dopamine from exogenous L-DOPA in the rat, with reference to the involvement of aromatic L-amino acid decarboxylase. Brain Research *667*, 295–299.

Arora, D., Hearing, M., Haluk, D.M., Mirkovic, K., Fajardo-Serrano, A., Wessendorf, M.W., Watanabe, M., Luján, R., and Wickman, K. (2011). Acute cocaine exposure weakens GABA(B) receptor-dependent G-protein-gated inwardly rectifying K+ signaling in dopamine neurons of the ventral tegmental area. Journal of Neuroscience *31*, 12251–12257.

Arttamangkul, S., Quillinan, N., Low, M.J., Zastrow, von, M., Pintar, J., and Williams, J.T. (2008). Differential activation and trafficking of μ-opioid receptors in brain slices. Molecular Pharmacology *74*, 972–979.

Bayer, V.E., and Pickel, V.M. (1990). Ultrastructural localization of tyrosine hydroxylase in the rat ventral tegmental area: relationship between immunolabeling density and neuronal associations. Journal of Neuroscience *10*, 2996–3013.

Beckstead, M.J., and Williams, J.T. (2007). Long-term depression of a dopamine IPSC. Journal of Neuroscience *27*, 2074–2080.

Beckstead, M.J., Ford, C.P., Phillips, P.E.M., and Williams, J.T. (2007). Presynaptic regulation of dendrodendritic dopamine transmission. European Journal of Neuroscience *26*, 1479–1488.

Beckstead, M.J., Gantz, S.C., Ford, C.P., Stenzel-Poore, M.P., Phillips, P.E., Mark, G.P.,

and Williams, J.T. (2009). CRF enhancement of GIRK channel-mediated transmission in dopamine neurons. Neuropsychopharmacology *34*, 1926–1935.

Beckstead, M.J., Grandy, D.K., Wickman, K., and Williams, J.T. (2004). Vesicular dopamine release elicits an inhibitory postsynaptic current in midbrain dopamine neurons. Neuron *42*, 939–946.

Belichenko, N.P., Belichenko, P.V., and Mobley, W.C. (2009). Evidence for both neuronal cell autonomous and nonautonomous effects of methyl-CpG-binding protein 2 in the cerebral cortex of female mice with Mecp2 mutation. Neurobiology of Disease *34*, 71–77.

Belin, D., Mar, A.C., Dalley, J.W., Robbins, T.W., and Everitt, B.J. (2008). High impulsivity predicts the switch to compulsive cocaine-taking. Science *320*, 1352–1355.

Bello, E.P., Mateo, Y., Gelman, D.M., Noaín, D., Shin, J.H., Low, M.J., Alvarez, V.A., Lovinger, D.M., and Rubinstein, M. (2011). Cocaine supersensitivity and enhanced motivation for reward in mice lacking dopamine D2 autoreceptors. Nature Neuroscience *14*, 1033–1038.

Besson, M.J., Chéramy, A., Feltz, P., and Glowinski, J. (1969). Release of newly synthesized dopamine from dopamine-containing terminals in the striatum of the rat. Proceedings of the National Academy of Sciences USA *62*, 741–748.

Bhalla, A., Tucker, W.C., and Chapman, E.R. (2005). Synaptotagmin isoforms couple distinct ranges of Ca^{2+}, Ba^{2+}, and Sr^{2+} concentration to SNARE-mediated membrane fusion. Molecular Biology of the Cell *16*, 4755–4764.

Björklund, A., and Lindvall, O. (1975). Dopamine in dendrites of substantia nigra neurons: suggestions for a role in dendritic terminals. Brain Research *83*, 531–537.

Bobker, D.H., and Williams, J.T. (1989). Serotonin agonists inhibit synaptic potentials in the rat locus ceruleus in vitro via 5-hydroxytryptamine1A and 5-hydroxytryptamine1B receptors. Journal of Pharmacology and Experimental Therapeutics *250*, 37–43.

Bonci, A., and Williams, J.T. (1996). A common mechanism mediates long-term changes in synaptic transmission after chronic cocaine and morphine. Neuron *16*, 631–639.

Bonci, A., and Williams, J.T. (1997). Increased probability of GABA release during withdrawal from morphine. Journal of Neuroscience *17*, 796–803.

Borah, A., and Mohanakumar, K.P. (2007). Long-term L-DOPA treatment causes indiscriminate increase in dopamine levels at the cost of serotonin synthesis in discrete brain regions of rats. Cell and Molecular Neurobiology *27*, 985–996.

Borgland, S.L., Taha, S.A., Sarti, F., Fields, H.L., and Bonci, A. (2006). Orexin A in the VTA is critical for the induction of synaptic plasticity and behavioral sensitization to cocaine. Neuron *49*, 589–601.

Branch, S.Y., and Beckstead, M.J. (2012). Methamphetamine produces bidirectional, concentration-dependent effects on dopamine neuron excitability and dopamine-mediated synaptic currents. Journal of Neurophysiology *108*, 802–809.

Bulwa, Z.B., Sharlin, J.A., Clark, P.J., Bhattacharya, T.K., Kilby, C.N., Wang, Y., and Rhodes, J.S. (2011). Increased consumption of ethanol and sugar water in mice lacking the dopamine D2 long receptor. Alcohol *45*, 631–639.

Cameron, D.L., and Williams, J.T. (1994). Cocaine inhibits GABA release in the VTA through endogenous 5-HT. Journal of Neuroscience *14*, 6763–6767.

Cameron, D.L., Wessendorf, M.W., and Williams, J.T. (1997). A subset of ventral tegmental area neurons is inhibited by dopamine, 5-hydroxytryptamine and opioids. Neuroscience *77*, 155–166.

Carta, M., Carlsson, T., Kirik, D., and Björklund, A. (2007). Dopamine released from 5-HT terminals is the cause of L-DOPA-induced dyskinesia in parkinsonian rats. Brain *130*, 1819–1833.

Chahrour, M., and Zoghbi, H.Y. (2007). The story of Rett syndrome: from clinic to neurobiology. Neuron *56*, 422–437.

Chan, C.S., Guzman, J.N., Ilijic, E., Mercer, J.N., Rick, C., Tkatch, T., Meredith, G.E., and Surmeier, D.J. (2007). “Rejuvenation” protects neurons in mouse models of Parkinson’s disease. Nature *447*, 1081–1086.

Chen, G., and Ewing, A.G. (1995). Multiple classes of catecholamine vesicles observed during exocytosis from the Planorbis cell body. Brain Research *701*, 167–174.

Chen, R.Z., Akbarian, S., Tudor, M., and Jaenisch, R. (2001). Deficiency of methyl-CpG binding protein-2 in CNA neurons results in a Rett-like phenotype in mice. Nature Genetics *27*, 327–331.

Chiueh, C.C., and Moore, K.E. (1975). D-amphetamine-induced release of "newly synthesized" and “stored” dopamine from the caudate nucleus in vivo. Journal of Pharmacology and Experimental Therapeutics *192*, 642–653.

Colebrooke, R.E., Humby, T., Lynch, P.J., McGowan, D.P., Xia, J., and Emson, P.C. (2006). Age-related decline in striatal dopamine content and motor performance occurs in the absence of nigral cell loss in a genetic mouse model of Parkinson's disease. European Journal of Neuroscience *24*, 2622–2630.

Cools, R., Barker, R.A., Sahakian, B.J., and Robbins, T.W. (2003). L-Dopa medication remediates cognitive inflexibility, but increases impulsivity in patients with Parkinson's disease. Neuropsychologia *41*, 1431–1441.

Courtney, N.A., and Ford, C.P. (2014). The timing of dopamine- and noradrenaline-mediated transmission reflects underlying differences in the extent of spillover and

pooling. Journal of Neuroscience *34*, 7645–7656.

Courtney, N.A., Mamaligas, A.A., and Ford, C.P. (2012). Species differences in somatodendritic dopamine transmission determine D2-autoreceptor-mediated inhibition of ventral tegmental area neuron firing. Journal of Neuroscience *32*, 13520–13528.

Critchlow, H.M., Maycox, P.R., Skepper, J.N., and Krylova, O. (2006). Clozapine and haloperidol differentially regulate dendritic spine formation and synaptogenesis in rat hippocampal neurons. Molecular and Cellular Neuroscience. *32*, 356–365.

Dahlstroem, A., and Fuxe, K. (1964). Evidence for the existence of monoamine-containing neurons in the central nervous system. I. Demonstration of monoamines in the cell bodies of brain stem neurons. Acta Physiologica Scandinavia Supplementum *232* 1–55.

Damãsio, A.R., Lobo-Antunes, J., and Macedo, C. (1971). Psychiatric aspects in Parkinsonism treated with L-dopa. Journal of Neurology, Neurosurgery, and Psychiatry. *34*, 502–507.

De Blasi, A., and Mennini, T. (1982). Selective reduction of one class of dopamine receptor binding sites in the corpus striatum of aged rats. Brain Research *242*, 361–364.

De Keyser, J., De Backer, J.P., Vauquelin, G., and Ebinger, G. (1991). D1 and D2 dopamine receptors in human substantia nigra: localization and the effect of aging. Journal of Neurochemistry *56*, 1130–1133.

Di Giovanni, G., Di Matteo, V., Pierucci, M., and Esposito, E. (2008). Serotonin-dopamine interaction: electrophysiological evidence. Progress in Brain Research. *172*, 45–71.

Dorocic, I.P., Fürth, D., Xuan, Y., Johansson, Y., Pozzi, L., Silberberg, G., Carlén, M., and Meletis, K. (2014). A whole-brain atlas of inputs to serotonergic neurons of the dorsal and median raphe nuclei. Neuron *83*, 663–678.

Dragicevic, E., Poetschke, C., Duda, J., Schlaudraff, F., Lammel, S., Schiemann, J., Fauler, M., Hetzel, A., Watanabe, M., Luján, R., *et al.* (2014). Cav1.3 channels control D2-autoreceptor responses via NCS-1 in substantia nigra dopamine neurons. Brain 137, 2287–2302

Dray, A., Gonye, T.J., Oakley, N.R., and Tanner, T. (1976). Evidence for the existence of a raphe projection to the substantia nigra in rat. Brain Research *113*, 45–57.

Dunn, H.G., and MacLeod, P.M. (2001). Rett syndrome: review of biological abnormalities. Canadian Journal of Neurological Sciences *28*, 16–29.

Edwards, F.A., Konnerth, A., and Sakmann, B. (1990). Quantal analysis of inhibitory synaptic transmission in the dentate gyrus of rat hippocampal slices: a patch-clamp study. Journal of Physiology *430*, 213–249.

Ersche, K.D., Turton, A.J., Pradhan, S., Bullmore, E.T., and Robbins, T.W. (2010). Drug addiction endophenotypes: impulsive versus sensation-seeking personality traits. Biological Psychiatry *68*, 770–773.

Eskow Jaunarajs, K.L., George, J.A., and Bishop, C. (2012). L-DOPA-induced dysregulation of extrastriatal dopamine and serotonin and affective symptoms in a bilateral rat model of Parkinson's disease. Neuroscience *218*, 243–256.

Eskow Jaunarajs, K.L., Angoa-Perez, M., Kuhn, D.M., and Bishop, C. (2011). Potential mechanisms underlying anxiety and depression in Parkinson's disease: consequences of l-DOPA treatment. Neuroscience & Biobehavioral Reviews *35*, 556–564.

Fasano, C., Kortleven, C., and Trudeau, L.E. (2010). Chronic activation of the D2 autoreceptor inhibits both glutamate and dopamine synapse formation and alters the intrinsic properties of mesencephalic dopamine neurons in vitro. European Journal of Neuroscience *32*, 1433–1441.

Fasano, C., Bourque, M.-J., Lapointe, G., Leo, D., Thibault, D., Haber, M., Kortleven, C., Desgroseillers, L., Murai, K.K., and Trudeau, L.-E. (2013). Dopamine facilitates dendritic spine formation by cultured striatal medium spiny neurons through both D1 and D2 dopamine receptors. Neuropharmacology *67*, 432–443.

Fatt, P., and Katz, B. (1952). Spontaneous subthreshold activity at motor nerve endings. Journal of Physiology *117*, 109–128.

Filtz, T.M., Artymyshyn, R.P., Guan, W., and Molinoff, P.B. (1993). Paradoxical regulation of dopamine receptors in transfected 293 cells. Molecular Pharmacology *44*, 371–379.

Fink, K.B., and Gothert, M. (2007). 5-HT Receptor Regulation of Neurotransmitter Release. Pharmacological Reviews *59*, 360–417.

Finn, J.P., and Edwards, R.H. (1997). Individual residues contribute to multiple differences in ligand recognition between vesicular monoamine transporters 1 and 2. Journal of Biological Chemistry *272*, 16301–16307.

Fishburn, C.S., Elazar, Z., and Fuchs, S. (1995). Differential glycosylation and intracellular trafficking for the long and short isoforms of the D2 dopamine receptor. Journal of Biological Chemistry *270*, 29819–29824.

FitzGerald, P.M., Jankovic, J., and Percy, A.K. (1990). Rett syndrome and associated movement disorders. Movement Disorders *5*, 195–202.

Foehring, R.C., Zhang, X.F., Lee, J.C.F., and Callaway, J.C. (2009). Endogenous calcium buffering capacity of substantia nigral dopamine neurons. Journal of Neurophysiology *102*, 2326–2333.

Fonseca, M.S., Murakami, M., and Mainen, Z.F. (2015). Activation of dorsal raphe

serotonergic neurons promotes waiting but is not reinforcing. Current Biology *25*, 306–315.

Ford, C.P. (2014). The role of D2-autoreceptors in regulating dopamine neuron activity and transmission. Neuroscience *282*, 13–22.

Ford, C.P., Beckstead, M.J., and Williams, J.T. (2007). Kappa opioid inhibition of somatodendritic dopamine inhibitory postsynaptic currents. Journal of Neurophysiology *97*, 883–891.

Ford, C.P., Mark, G.P., and Williams, J.T. (2006). Properties and opioid inhibition of mesolimbic dopamine neurons vary according to target location. Journal of Neuroscience *26*, 2788–2797.

Ford, C.P., Phillips, P.E.M., and Williams, J.T. (2009). The time course of dopamine transmission in the ventral tegmental area. Journal of Neuroscience *29*, 13344–13352.

Ford, C.P., Gantz, S.C., Phillips, P.E.M., and Williams, J.T. (2010). Control of extracellular dopamine at dendrite and axon terminals. Journal of Neuroscience *30*, 6975–6983.

Fortin, G.D., Desrosiers, C.C., Yamaguchi, N., and Trudeau, L.-E. (2006). Basal somatodendritic dopamine release requires snare proteins. Journal of Neurochemistry *96*, 1740–1749.

Frerking, M., Borges, S., and Wilson, M. (1995). Variation in GABA mini amplitude is the consequence of variation in transmitter concentration. Neuron *15*, 885–895.

Gantz, S.C., Bunzow, J.R., and Williams, J.T. (2013). Spontaneous inhibitory synaptic currents mediated by a G protein-coupled receptor. Neuron *78*, 807–812.

Gantz, S.C., Ford, C.P., Neve, K.A., and Williams, J.T. (2011). Loss of Mecp2 in substantia nigra dopamine neurons compromises the nigrostriatal pathway. Journal of Neuroscience *31*, 12629–12637.

Gantz, S.C., Levitt, E.S., Llamosas, N., Neve, K.A., and Williams, J.T. (2015a). Depression of serotonin synaptic transmission by the dopamine precursor L-DOPA. Cell Reports *12*, 944–954.

Gantz S.C., Robinson, B.G., Buck, D.C., Bunzow, J.R., Neve, R.L., Williams, J.T., and Neve, K.A. (2015b) Distinct regulation of dopamine D2S and D2L autoreceptor signaling by calcium. eLife *4*.

Gentet, L.J., and Williams, S.R. (2007). Dopamine gates action potential backpropagation in midbrain dopaminergic neurons. Journal of Neuroscience *27*, 1892–1901.

Giordano, T.P., Satpute, S.S., Striessnig, J., Kosofsky, B.E., and Rajadhyaksha, A.M. (2006). Up-regulation of dopamine D(2)L mRNA levels in the ventral tegmental area and

dorsal striatum of amphetamine-sensitized C57BL/6 mice: role of Ca(v)1.3 L-type Ca(2+) channels. Journal of Neurochemistry *99*, 1197–1206.

Giros, B., Jaber, M., Jones, S.R., Wightman, R.M., and Caron, M.G. (1996). Hyperlocomotion and indifference to cocaine and amphetamine in mice lacking the dopamine transporter. Nature *379*, 606–612.

Goldberg, M.S., Pisani, A., Haburcak, M., Vortherms, T.A., Kitada, T., Costa, C., Tong, Y., Martella, G., Tscherter, A., Martins, A., (2005). Nigrostriatal dopaminergic deficits and hypokinesia caused by inactivation of the familial Parkinsonism-linked gene DJ-1. Neuron *45*, 489–496.

Gonon, F.G. (1988). Nonlinear relationship between impulse flow and dopamine released by rat midbrain dopaminergic neurons as studied by in vivo electrochemistry. Neuroscience *24*, 19–28.

Groves, P.M., and Linder, J.C. (1983). Dendro-dendritic synapses in substantia nigra: descriptions based on analysis of serial sections. Experimental Brain Research *49*, 209–217.

Guy, J., Gan, J., Selfridge, J., Cobb, S., and Bird, A. (2007). Reversal of neurological defects in a mouse model of Rett syndrome. Science *315*, 1143–1147.

Guy, J., Hendrich, B., Holmes, M., Martin, J.E., and Bird, A. (2001). A mouse *Mecp2*-null mutation causes neurological symptoms that mimic Rett syndrome. Nature Genetics *27*, 322–326.

Guzman, J.N., Sánchez-Padilla, J., Wokosin, D., Kondapalli, J., Ilijic, E., Schumacker, P.T., and Surmeier, D.J. (2010). Oxidant stress evoked by pacemaking in dopaminergic neurons is attenuated by DJ-1. Nature *468*, 696–700.

Hagberg, B. (1985). Rett's syndrome: prevalence and impact on progressive severe mental retardation in girls. Acta Paediatrica Scandinavica *74*, 405–408.

Hage, T.A., and Khaliq, Z.M. (2015). Tonic firing rate controls dendritic Ca2+ signaling and synaptic gain in substantia nigra dopamine neurons. Journal of Neuroscience *35*, 5823–5836.

Häusser, M., Stuart, G., Racca, C., and Sakmann, B. (1995). Axonal initiation and active dendritic propagation of action potentials in substantia nigra neurons. Neuron *15*, 637–647.

Heeringa, M.J., and Abercrombie, E.D. (1995). Biochemistry of somatodendritic dopamine release in substantia nigra: an in vivo comparison with striatal dopamine release. Journal of Neurochemistry *65*, 192–200.

Heikkinen, A.E., Möykkynen, T.P., and Korpi, E.R. (2008). Long-lasting modulation of glutamatergic transmission in VTA dopamine neurons after a single dose of

benzodiazepine agonists. Neuropsychopharmacology *34*, 290–298.

Henry, D.J., Greene, M.A., and White, F.J. (1989). Electrophysiological effects of cocaine in the mesoaccumbens dopamine system: repeated administration. Journal of Pharmacology and Experimental Therapeutics *251*, 833–839.

Henry, J.M., Filburn, C.R., Joseph, J.A., and Roth, G.S. (1986). Effect of aging on striatal dopamine receptor subtypes in Wistar rats. Neurobiology of Aging *7*, 357–361.

Hioki, H., Nakamura, H., Ma, Y.-F., Konno, M., Hayakawa, T., Nakamura, K.C., Fujiyama, F., and Kaneko, T. (2010). Vesicular glutamate transporter 3-expressing nonserotonergic projection neurons constitute a subregion in the rat midbrain raphe nuclei. Journal of Computational Neurology *518*, 668–686.

Hnasko, T.S., Chuhma, N., Zhang, H., Goh, G.Y., Sulzer, D., Palmiter, R.D., Rayport, S., and Edwards, R.H. (2010). Vesicular glutamate transport promotes dopamine storage and glutamate corelease in vivo. Neuron *65*, 643–656.

Holroyd, K.B., Adrover, M.F., Fuino, R.L., Bock, R., Kaplan, A.R., Gremel, C.M., Rubinstein, M., and Alvarez, V.A. (2015). Loss of feedback inhibition via D2 autoreceptors enhances acquisition of cocaine taking and reactivity to drug-paired cues. Neuropsychopharmacology *40*, 1495–1509.

Hornykiewicz, O. (1975). Brain monoamines and parkinsonism. National Institute on Drug Abuse Research Monograph Series *3*, 13–21.

Hyttel, J. (1987). Age related decrease in the density of dopamine D1 and D2 receptors in corpus striatum of rats. Pharmacology & Toxicology *61*, 126–129.

Ilango, A., Kesner, A.J., Keller, K.L., Stuber, G.D., Bonci, A., and Ikemoto, S. (2014). Similar roles of substantia nigra and ventral tegmental dopamine neurons in reward and aversion. Journal of Neuroscience *34*, 817–822.

Isaacson, J.S., Solís, J.M., and Nicoll, R.A. (1993). Local and diffuse synaptic actions of GABA in the hippocampus. Neuron *10*, 165–175.

Ishibashi, K., Ishii, K., Oda, K., Kawasaki, K., Mizusawa, H., and Ishiwata, K. (2009). Regional analysis of age-related decline in dopamine transporters and dopamine D2-like receptors in human striatum. Synapse *63*, 282–290.

Ito, K., Haga, T., Lameh, J., and Sadée, W. (1999). Sequestration of dopamine D2 receptors depends on coexpression of G-protein-coupled receptor kinases 2 or 5. European Journal of Biochemistry *260*, 112–119.

Itokawa, M., Toru, M., Ito, K., Tsuga, H., Kameyama, K., Haga, T., Arinami, T., and Hamaguchi, H. (1996). Sequestration of the short and long isoforms of dopamine D2 receptors expressed in Chinese hamster ovary cells. Molecular Pharmacology *49*, 560–566.

Jaffe, E.H., Marty, A., Schulte, A., and Chow, R.H. (1998). Extrasynaptic vesicular transmitter release from the somata of substantia nigra neurons in rat midbrain slices. Journal of Neuroscience *18*, 3548–3553.

Jang, J.Y., Jang, M., Kim, S.H., Um, K.B., Kang, Y.K., Kim, H.J., Chung, S., and Park, M.K. (2011). Regulation of dopaminergic neuron firing by heterogeneous dopamine autoreceptors in the substantia nigra pars compacta. Journal of Neurochemistry *116*, 966–974.

Johnson, M.D. (1994). Synaptic glutamate release by postnatal rat serotonergic neurons in microculture. Neuron *12*, 433–442.

Jomphe, C., Tiberi, M., and Trudeau, L.-E. (2006). Expression of D2 receptor isoforms in cultured neurons reveals equipotent autoreceptor function. Neuropharmacology *50*, 595–605.

Jones, S.R., Gainetdinov R.R., Wightman R.M., Caron M.G. (1998) Mechanisms of amphetamine action revealed in mice lacking the dopamine transporter. Journal of Neuroscience *18*, 1979-1986.

Jones, S., Kornblum, J.L., and Kauer, J.A. (2000). Amphetamine blocks long-term synaptic depression in the ventral tegmental area. Journal of Neuroscience *20*, 5575–5580.

Juorio, A.V., Li, X.M., Walz, W., and Paterson, I.A. (1993). Decarboxylation of L-dopa by cultured mouse astrocytes. Brain Research *626*, 306–309.

Juraska, J.M., Wilson, C.J., and Groves, P.M. (1977). The substantia nigra of the rat: A golgi study. Journal of Computation Neurology *172*, 585–599.

Kannari, K., Tanaka, H., Maeda, T., Tomiyama, M., Suda, T., and Matsunaga, M. (2000). Reserpine pretreatment prevents increases in extracellular striatal dopamine following L-DOPA administration in rats with nigrostriatal denervation. Journal of Neurochemistry *74*, 263–269.

Khan, Z.U., Mrzljak, L., Gutierrez, A., la Calle, de, A., and Goldman-Rakic, P.S. (1998). Prominence of the dopamine D2 short isoform in dopaminergic pathways. Proceedings of the National Academy of Sciences USA 7731–7736.

Kim, Y., Park, M.K., and Chung, S. (2008). Voltage-operated Ca2+ channels regulate dopamine release from somata of dopamine neurons in the substantia nigra pars compacta. Biochemical and Biophysical Research Communications *373*, 665–669.

Kirby, L.G., Pernar, L., Valentino, R.J., and Beck, S.G. (2003). Distinguishing characteristics of serotonin and non-serotonin-containing cells in the dorsal raphe nucleus: electrophysiological and immunohistochemical studies. Neuroscience *116*, 669–683.

Kishi, N., and Macklis, J.D. (2010). MeCP2 functions largely cell-autonomously, but also non-cell-autonomously, in neuronal maturation and dendritic arborization of cortical pyramidal neurons. Experimental Neurology *222*, 51–58.

Kitahama, K., Nagatsu, I., Geffard, M., and Maeda, T. (2000). Distribution of dopamine-immunoreactive fibers in the rat brainstem. Journal of Chemical Neuroanatomy *18*, 1–9.

Koyrakh, L., Luján, R., Colón, J., Karschin, C., Kurachi, Y., Karschin, A., and Wickman, K. (2005). Molecular and cellular diversity of neuronal G-protein-gated potassium channels. Journal of Neuroscience *25*, 11468–11478.

Kramer, P.F., and Williams, J.T. (2015). Cocaine decreases metabotropic glutamate receptor mGluR1 currents in dopamine neurons by activating mGluR5. Neuropsychopharmacology *40*, 2418–2424.

Kress, G.J., Shu, H-J., Yu, A., Taylor, A., Benz, A., Harmon, S., and Mennerick, S. (2014). Fast phasic release properties of dopamine studied with a channel biosensor. Journal of Neuroscience *34*, 11792–11802.

Lacey, M.G., Mercuri, N.B., and North, R.A. (1987). Dopamine acts on D2 receptors to increase potassium conductance in neurones of the rat substantia nigra zona compacta. Journal of Physiology *392*, 397–416.

Larsen, M.B., Sonders, M.S., Mortensen, O.V., Larson, G.A., Zahniser, N.R., and Amara, S.G. (2011). Dopamine transport by the serotonin transporter: a mechanistically distinct mode of substrate translocation. Journal of Neuroscience *31*, 6605–6615.

Laurvick, C.L., de Klerk, N., Bower, C., Christodoulou, J., Ravine, D., Ellaway, C., Williamson, S., and Leonard, H. (2006). Rett syndrome in Australia: a review of the epidemiology. Journal of Pediatrics *148*, 347–352.

Li, Y.Q., Li, H., Kaneko, T., and Mizuno, N. (2001). Morphological features and electrophysiological properties of serotonergic and non-serotonergic projection neurons in the dorsal raphe nucleus. An intracellular recording and labeling study in rat brain slices. Brain Research *900*, 110–118.

Lindgren, N., Usiello, A., Goiny, M., Haycock, J., Erbs, E., Greengard, P., Hokfelt, T., Borrelli, E., and Fisone, G. (2003). Distinct roles of dopamine D2L and D2S receptor isoforms in the regulation of protein phosphorylation at presynaptic and postsynaptic sites. Proceedings of the National Academy of Sciences USA *100*, 4305–4309.

Liprando, L.A., Miner, L.H., Blakely, R.D., Lewis, D.A., and Sesack, S.R. (2004). Ultrastructural interactions between terminals expressing the norepinephrine transporter and dopamine neurons in the rat and monkey ventral tegmental area. Synapse *52*, 233–244.

Liu, G., Choi, S., and Tsien, R.W. (1999). Variability of neurotransmitter concentration and nonsaturation of postsynaptic AMPA receptors at synapses in hippocampal cultures

and slices. Neuron *22*, 395–409.

Liu, Y.F., Civelli, O., Grandy, D.K., and Albert, P.R. (1992). Differential sensitivity of the short and long human dopamine D2 receptor subtypes to protein kinase C. Journal of Neurochemistry *59*, 2311–2317.

Liu, Z., Zhou, J., Li, Y., Hu, F., Lu, Y., Ma, M., Feng, Q., Zhang, J.-E., Wang, D., Zeng, J., Bao, J., Kim, J.Y., Chen, Z.F., El Mestikawy, S., Luo, M. (2014). Dorsal raphe neurons signal reward through 5-HT and glutamate. Neuron *81*, 1360–1374.

Madhavan, A., Argilli, E., Bonci, A., and Whistler, J.L. (2013). Loss of D2 dopamine receptor function modulates cocaine-induced glutamatergic synaptic potentiation in the ventral tegmental area. Journal of Neuroscience *33*, 12329–12336.

Mamaligas, A.A., and Ford, C.P. (2015, October). *Acetylcholine evokes spontaneous muscarinic IPSCs in medium spiny neurons overexpressing GIRK channels*. Poster presented at the annual Society for Neuroscience meeting, Chicago, IL.

Marcott, P.F., Mamaligas, A.A., and Ford, C.P. (2014). Phasic dopamine release drives activation of striatal D2-receptors. Neuron *84*, 1–13.

Marinelli, M., and White, F.J. (2000). Enhanced vulnerability to cocaine self-administration is associated with elevated impulse activity of midbrain dopamine neurons. Journal of Neuroscience *20*, 8876–8885.

Marinelli, M., Cooper, D.C., Baker, L.K., and White, F.J. (2003). Impulse activity of midbrain dopamine neurons modulates drug-seeking behavior. Psychopharmacology *168*, 84–98.

Mazei-Robison, M.S., Bowton, E., Holy, M., Schmudermaier, M., Freissmuth, M., Sitte, H.H., Galli, A., and Blakely, R.D. (2008). Anomalous dopamine release associated with a human dopamine transporter coding variant. Journal of Neuroscience *28*, 7040–7046.

McDevitt, R.A., Tiran-Cappello, A., Shen, H., Balderas, I., Britt, J.P., Marino, R.A.M., Chung, S.L., Richie, C.T., Harvey, B.K., and Bonci, A. (2014). Serotonergic versus nonserotonergic dorsal raphe projection neurons: differential participation in reward circuitry. Cell Reports *8*, 1857–1869.

McGill, B.E., Bundle, S.F., Yaylaoglu, M.B., Carson, J.P., Thaller, C., and Zoghbi, H.Y. (2006). Enhanced anxiety and stress-induced corticosterone release are associated with increased Crh expression in a mouse model of Rett syndrome. Proceedings of the National Academy of Sciences USA *103*, 18267–18272.

Melis, M., Camarini, R., Ungless, M.A., and Bonci, A. (2002). Long-lasting potentiation of GABAergic synapses in dopamine neurons after a single in vivo ethanol exposure. Journal of Neuroscience *22*, 2074–2082.

Mendez, J.A., Bourque, M.J., Fasano, C., Kortleven, C., and Trudeau, L.E. (2011).

Somatodendritic dopamine release requires synaptotagmin 4 and 7 and the participation of voltage-gated calcium channels. Journal of Biological Chemistry *286*, 23928–23937.

Mercuri, N.B., Calabresi, P., and Bernardi, G. (1990). Responses of rat substantia nigra compacta neurones to L-DOPA. British Journal of Pharmacology *100*, 257–260.

Mergy, M.A., Gowrishankar, R., Gresch, P.J., Gantz, S.C., Williams, J., Davis, G.L., Wheeler, C.A., Stanwood, G.D., Hahn, M.K., and Blakely, R.D. (2014). The rare DAT coding variant Val559 perturbs DA neuron function, changes behavior, and alters in vivo responses to psychostimulants. Proceedings of the National Academy of Sciences USA, *111*, E4779–4788.

Milner, T.A., and Veznedaroglu, E. (1993). Serotonin-containing terminals synapse on septohippocampal neurons in the rat. Journal of Neuroscience Research *36*, 260–271.

Miralvès, J., Magdeleine, E., and Joly, E. (2007). Design of an improved set of oligonucleotide primers for genotyping MeCP2tm1.1Bird KO mice by PCR. Molecular Neurodegeneration *2*, 16.

Miyazaki, K.W., Miyazaki, K., Tanaka, K.F., Yamanaka, A., Takahashi, A., Tabuchi, S., and Doya, K. (2014). Optogenetic activation of dorsal raphe serotonin neurons enhances patience for future rewards. Current Biology *24*, 2033–2040.

Morelli, M., Mennini, T., Cagnotto, A., Toffano, G., and Di Chiara, G. (1990). Quantitative autoradiographical analysis of the age-related modulation of central dopamine D1 and D2 receptors. Neuroscience *36*, 403–410.

Morikawa, H., Manzoni, O.J., Crabbe, J.C., and Williams, J.T. (2000). Regulation of central synaptic transmission by 5-HT(1B) auto- and heteroreceptors. Molecular Pharmacology *58*, 1271–1278.

Morris, S.J., Itzhaki Van-Ham, I., Daigle, M., Robillard, L., Sajedi, N., and Albert, P.R. (2007). Differential desensitization of dopamine D2 receptor isoforms by protein kinase C: The importance of receptor phosphorylation and pseudosubstrate sites. European Journal of Pharmacology *577*, 44–53.

Moukhles, H., Bosler, O., Bolam, J.P., Vallée, A., Umbriaco, D., Geffard, M., and Doucet, G. (1997). Quantitative and morphometric data indicate precise cellular interactions between serotonin terminals and postsynaptic targets in rat substantia nigra. Neuroscience *76*, 1159–1171.

Moyer, R.A., Wang, D., Papp, A.C., Smith, R.M., Duque, L., Mash, D.C., and Sadee, W. (2011). Intronic polymorphisms affecting alternative splicing of human dopamine D2 receptor are associated with cocaine abuse. Neuropsychopharmacology *36*, 753–762.

Munoz, A., Li, Q., Gardoni, F., Marcello, E., Qin, C., Carlsson, T., Kirik, D., Di Luca, M., Björklund, A., Bezard, E., *et al.* (2008). Combined 5-HT1A and 5-HT1B receptor agonists for the treatment of L-DOPA-induced dyskinesia. Brain *131*, 3380–3394.

Muramatsu, M., Lapiz, M.D., Tanaka, E., and Grenhoff, J. (1998). Serotonin inhibits synaptic glutamate currents in rat nucleus accumbens neurons via presynaptic 5-HT1B receptors. European Journal of Neuroscience *10*, 2371–2379.

Namkung, Y., and Sibley, D.R. (2004). Protein kinase C mediates phosphorylation, desensitization, and trafficking of the D2 dopamine receptor. Journal of Biological Chemistry *279*, 49533–49541.

Navailles, S., Bioulac, B., Gross, C., and De Deurwaerdère, P. (2010). Serotonergic neurons mediate ectopic release of dopamine induced by L-DOPA in a rat model of Parkinson's disease. Neurobiology of Disease *38*, 136–143.

Navailles, S., Bioulac, B., Gross, C., and De Deurwaerdère, P. (2011). Chronic L-DOPA therapy alters central serotonergic function and L-DOPA-induced dopamine release in a region-dependent manner in a rat model of Parkinson's disease. Neurobiology of Disease *41*, 585–590.

Neul, J.L., Fang, P., Barrish, J., Lane, J., Caeg, E.B., Smith, E.O., Zoghbi, H., Percy, A., and Glaze, D.G. (2008). Specific mutations in methyl-CpG-binding protein 2 confer different severity in Rett syndrome. Neurology *70*, 1313–1321.

Neve, K.A., Ford, C.P., Buck, D.C., Grandy, D.K., Neve, R.L., and Phillips, T.J. (2013). Normalizing dopamine D2 receptor-mediated responses in D2 null mutant mice by virus-mediated receptor restoration: comparing D2L and D2S. Neuroscience *248*, 479–487.

Ng, G.Y., Ng, G.Y., Varghese, G., Varghese, G., Chung, H.T., Chung, H.T., Trogadis, J., Trogadis, J., Seeman, P., Seeman, P., *et al.* (1997). Resistance of the dopamine D2L receptor to desensitization accompanies the up-regulation of receptors on to the surface of Sf9 cells. Endocrinology *138*, 4199–4206.

Ng, J., Zhen, J., Meyer, E., Erreger, K., Li, Y., Kakar, N., Ahmad, J., Thiele, H., Kubisch, C., Rider, N.L., *et al.* (2014). Dopamine transporter deficiency syndrome: phenotypic spectrum from infancy to adulthood. Brain *137*, 1107–1119.

Ng, K.Y., Chase, T.N., Colburn, R.W., and Kopin, I.J. (1970). L-Dopa-induced release of cerebral monoamines. Science *170*, 76–77.

Nimchinsky, E.A., Sabatini, B.L., and Svoboda, K. (2002). Structure and function of dendritic spines. Annual Review of Physiology. *64*, 313–353.

Nirenberg, M.J., Chan, J., Liu, Y., Edwards, R.H., and Pickel, V.M. (1996a). Ultrastructural localization of the vesicular monoamine transporter-2 in midbrain dopaminergic neurons: potential sites for somatodendritic storage and release of dopamine. Journal of Neuroscience *16*, 4135–4145.

Nirenberg, M.J., Vaughan, R.A., Uhl, G.R., Kuhar, M.J., and Pickel, V.M. (1996b). The dopamine transporter is localized to dendritic and axonal plasma membranes of nigrostriatal dopaminergic neurons. Journal of Neuroscience *16*, 436–447.

Nyholm, D., Lennernäs, H., Gomes-Trolin, C., and Aquilonius, S.-M. (2002). Levodopa pharmacokinetics and motor performance during activities of daily living in patients with Parkinson's disease on individual drug combinations. Clinical Neuropharmacology *25*, 89–96.

O'Boyle, K.M., and Waddington, J.L. (1984). Loss of rat striatal dopamine receptors with ageing is selective for D-2 but not D-1 sites: association with increased non-specific binding of the D-1 ligand [3H]piflutixol. European Journal of Pharmacology *105*, 171–174.

Olanow, C.W., Gauger, L.L., and Cedarbaum, J.M. (1991). Temporal relationships between plasma and cerebrospinal fluid pharmacokinetics of levodopa and clinical effect in Parkinson's disease. Annals of Neurology *29*, 556–559.

Onali, P., Olianas, M.C., and Gessa, G.L. (1985). Characterization of dopamine receptors mediating inhibition of adenylate cyclase activity in rat striatum. Molecular Pharmacology *28*, 138–145.

Oomizu, S., Boyadjieva, N., and Sarkar, D.K. (2003). Ethanol and estradiol modulate alternative splicing of dopamine D2 receptor messenger RNA and abolish the inhibitory action of bromocriptine on prolactin release from the pituitary gland. Alcoholism: Clinical and Experimental Research *27*, 975–980.

Otis, T.S., and Mody, I. (1992). Differential activation of GABAA and GABAB receptors by spontaneously released transmitter. Journal of Neurophysiology *67*, 227–235.

Padgett, C.L., Lalive, A.L., Tan, K.R., Terunuma, M., Munoz, M.B., Pangalos, M.N., Martínez-Hernández, J., Watanabe, M., Moss, S.J., Luján, R., *et al.* (2012). Methamphetamine-evoked depression of GABA(B) receptor signaling in GABA neurons of the VTA. Neuron *73*, 978–989.

Paladini, C., and Roeper, J. (2014). Generating bursts (and pauses) in the dopamine midbrain neurons. Neuroscience *282*, 109–121.

Palumbo, D., and Kurlan, R. (2007). Complex obsessive compulsive and impulsive symptoms in Tourette's syndrome. Journal of Neuropsychiatric Disease and Treatment *3*, 687–693.

Pan, Z.Z., Colmers, W.F., and Williams, J.T. (1989). 5-HT-mediated synaptic potentials in the dorsal raphe nucleus: interactions with excitatory amino acid and GABA neurotransmission. Journal of Neurophysiology *62*, 481–486.

Panayotis, N., Ghata, A., Villard, L., and Roux, J.-C. (2011). Biogenic amines and their metabolites are differentially affected in the Mecp2-deficient mouse brain. BMC Neuroscience *12*, 47.

Patel, J.C., Witkovsky, P., Avshalumov, M.V., and Rice, M.E. (2009). Mobilization of

calcium from intracellular stores facilitates somatodendritic dopamine release. Journal of Neuroscience *29*, 6568–6579.

Pelc, K., Cheron, G., and Dan, B. (2008). Behavior and neuropsychiatric manifestations in Angelman syndrome. Journal of Neuropsychiatric Disease and Treatment *4*, 577–584.

Perra, S., Clements, M.A., Bernier, B.E., and Morikawa, H. (2011). In vivo ethanol experience increases D2 autoinhibition in the ventral tegmental area. Neuropsychopharmacology *36*, 993–1002.

Phillips, P.E.M., Hancock, P.J., and Stamford, J.A. (2002). Time window of autoreceptor-mediated inhibition of limbic and striatal dopamine release. Synapse *44*, 15–22.

Phillipson, O.T. (1979). A Golgi study of the ventral tegmental area of Tsai and interfascicular nucleus in the rat. Journal of Computation Neurology *187*, 99–115.

Pologruto, T.A., Sabatini, B.L., and Svoboda, K. (2003). ScanImage: flexible software for operating laser scanning microscopes. Biomedical Engineering Online *2*, 13.

Pothos, E.N., Davila, V., and Sulzer, D. (1998). Presynaptic recording of quanta from midbrain dopamine neurons and modulation of the quantal size. Journal of Neuroscience *18*, 4106–4118.

Pothos, E., Desmond, M., and Sulzer, D. (1996). L-3,4-dihydroxyphenylalanine increases the quantal size of exocytotic dopamine release in vitro. Journal of Neurochemistry *66*, 629–636.

Prou, D., Gu, W.J., Le Crom, S., Vincent, J.D., Salamero, J., and Vernier, P. (2001). Intracellular retention of the two isoforms of the D(2) dopamine receptor promotes endoplasmic reticulum disruption. Journal of Cell Science *114*, 3517–3527.

Puopolo, M., Raviola, E., and Bean, B.P. (2007). Roles of subthreshold calcium current and sodium current in spontaneous firing of mouse midbrain dopamine neurons. Journal of Neuroscience *27*, 645–656.

Qi, J., Zhang, S., Wang, H.-L., Wang, H., de Jesus Aceves Buendia, J., Hoffman, A.F., Lupica, C.R., Seal, R.P., and Morales, M. (2014). A glutamatergic reward input from the dorsal raphe to ventral tegmental area dopamine neurons. Nature Communications *5*, 5390.

Radl, D., De Mei, C., Chen, E., Lee, H., and Borrelli, E. (2013). Each individual isoform of the dopamine D2 receptor protects from lactotroph hyperplasia. Molecular Endocrinology. *27*, 953–965.

Ranaldi, R., Pocock, D., Zereik, R., and Wise, R.A. (1999). Dopamine fluctuations in the nucleus accumbens during maintenance, extinction, and reinstatement of intravenous D-amphetamine self-administration. Journal of Neuroscience *19*, 4102–4109.

Roeper, J. (2013). Dissecting the diversity of midbrain dopamine neurons. Trends in Neuroscience *36*, 336–342.

Saal, D., Dong, Y., Bonci, A., and Malenka, R.C. (2003). Drugs of abuse and stress trigger a common synaptic adaptation in dopamine neurons. Neuron *37*, 577–582.

Samaco, R.C., Mandel-Brehm, C., Chao, H.T., Ward, C.S., Fyffe-Maricich, S.L., Ren, J., Hyland, K., Thaller, C., Maricich, S.M., Humphreys, P., *et al.* (2009). Loss of MeCP2 in aminergic neurons causes cell-autonomous defects in neurotransmitter synthesis and specific behavioral abnormalities. Proceedings of the National Academy of Sciences USA *106*, 21966–21971.

Sarti, F., Borgland, S.L., Kharazia, V.N., and Bonci, A. (2007). Acute cocaine exposure alters spine density and long-term potentiation in the ventral tegmental area. European Journal of Neuroscience *26*, 749–756.

Sasabe, T., Furukawa, A., Matsusita, S., Higuchi, S., and Ishiura, S. (2007). Association analysis of the dopamine receptor D2 (DRD2) SNP rs1076560 in alcoholic patients. Neuroscience Letters *412*, 139–142.

Schanen, N.C. (1999). Molecular approaches to the Rett syndrome gene. Journal of Child Neurology. *14*, 806–814.

Schultz, W. (1986). Responses of midbrain dopamine neurons to behavioral trigger stimuli in the monkey. Journal of Neurophysiology *56*, 1439–1461.

Scott, M.M., Wylie, C.J., Lerch, J.K., Murphy, R., Lobur, K., Herlitze, S., Jiang, W., Conlon, R.A., Strowbridge, B.W., and Deneris, E.S. (2005). A genetic approach to access serotonin neurons for in vivo and in vitro studies. Proceedings of the National Academy of Sciences USA *102*, 16472–16477.

Sesack, S.R., Aoki, C., and Pickel, V.M. (1994). Ultrastructural localization of D2 receptor-like immunoreactivity in midbrain dopamine neurons and their striatal targets. Journal of Neuroscience *14*, 88–106.

Severson, J.A., and Finch, C.E. (1980). Reduced dopaminergic binding during aging in the rodent striatum. Brain Research *192*, 147–162.

Shahbazian, M., Young, J., Yuva-Paylor, L., Spencer, C., Antalffy, B., Noebels, J., Armstrong, D., Paylor, R., and Zoghbi, H. (2002). Mice with truncated MeCP2 recapitulate many Rett syndrome features and display hyperacetylation of histone H3. Neuron *35*, 243–254.

Sharpe, A.L., Varela, E., Bettinger, L., and Beckstead, M.J. (2014). Methamphetamine self-administration in mice decreases GIRK channel-mediated currents in midbrain dopamine neurons. International Journal of Neuropsychopharmacology *18*, 1–10.

Shimizu, S., and Ohno, Y. (2013). Improving the treatment of Parkinson's disease: a

novel approach by modulating 5-HT(1A) receptors. Aging and Disease *4*, 1–13.

Smith, J.W., Fetsko, L.A., Xu, R., and Wang, Y. (2002). Dopamine D2L receptor knockout mice display deficits in positive and negative reinforcing properties of morphine and in avoidance learning. Neuroscience *113*, 755–765.

Stansley, B.J., and Yamamoto, B.K. (2014). Chronic l-Dopa decreases serotonin neurons in a subregion of the dorsal raphe nucleus. Journal of Pharmacology and Experimental Therapeutics *351*, 440–447.

Starr, S., Kozell, L.B., and Neve, K.A. (1995). Drug-induced up-regulation of dopamine D2 receptors on cultured cells. Journal of Neurochemistry *65*, 569–577.

Stocchi, F., Vacca, L., Ruggieri, S., and Olanow, C.W. (2005). Intermittent vs continuous levodopa administration in patients with advanced Parkinson disease: a clinical and pharmacokinetic study. Archives of Neurology *62*, 905–910.

Sulzer, D., Joyce, M.P., Lin, L., Geldwert, D., Haber, S.N., Hattori, T., and Rayport, S. (1998). Dopamine neurons make glutamatergic synapses in vitro. Journal of Neuroscience *18*, 4588–4602.

Takeuchi, Y., and Fukunaga, K. (2003). Differential subcellular localization of two dopamine D2 receptor isoforms in transfected NG108-15 cells. Journal of Neurochemistry *85*, 1064–1074.

Tanaka, H., Kannari, K., Maeda, T., Tomiyama, M., Suda, T., and Matsunaga, M. (1999). Role of serotonergic neurons in L-DOPA-derived extracellular dopamine in the striatum of 6-OHDA-lesioned rats. NeuroReport *10*, 631–634.

Taneja, P., Ogier, M., Brooks-Harris, G., Schmid, D.A., Katz, D.M., and Nelson, S.B. (2009). Pathophysiology of locus ceruleus neurons in a mouse model of Rett syndrome. Journal of Neuroscience *29*, 12187–12195.

Terai, M., Hidaka, K., and Nakamura, Y. (1989). Comparison of [3H]YM-09151-2 with [3H]spiperone and [3H]raclopride for dopamine d-2 receptor binding to rat striatum. European Journal of Pharmacology *173*, 177–182.

Thibault, D., Albert, P.R., Pineyro, G., and Trudeau, L.-E. (2011). Neurotensin triggers dopamine D2 receptor desensitization through a protein kinase C and beta-arrestin1-dependent mechanism. Journal of Biological Chemistry *286*, 9174–9184.

Tirotta, E., Fontaine, V., Picetti, R., Lombardi, M., Samad, T.A., Oulad-Abdelghani, M., Edwards, R., and Borrelli, E. (2008). Signaling by dopamine regulates D2 receptors trafficking at the membrane. Cell Cycle *7*, 2241–2248.

Tohgi, H., Abe, T., Yamazaki, K., Saheki, M., Takahashi, S., and Tsukamoto, Y. (1995). Effects of the catechol-O-methyltransferase inhibitor tolcapone in Parkinson's disease: correlations between concentrations of dopaminergic substances in the plasma and

cerebrospinal fluid and clinical improvement. Neuroscience Letters *192*, 165–168.

Törk, I. (1990). Anatomy of the serotonergic system. Annals of the New York Academy of Science *600*, 9–34.

Tsai, H.-C., Zhang, F., Adamantidis, A., Stuber, G.D., Bonci, A., De Lecea, L., and Deisseroth, K. (2009). Phasic firing in dopaminergic neurons is sufficient for behavioral conditioning. Science *324*, 1080–1084.

Umemiya, M., and Berger, A.J. (1995). Presynaptic inhibition by serotonin of glycinergic inhibitory synaptic currents in the rat brain stem. Journal of Neurophysiology *73*, 1192–1201.

Ungless, M.A., Whistler, J.L., Malenka, R.C., and Bonci, A. (2001). Single cocaine exposure in vivo induces long-term potentiation in dopamine neurons. Nature *411*, 583–587.

Usiello, A., Baik, J.H., Rougé-Pont, F., Picetti, R., Dierich, A., LeMeur, M., Piazza, P.V., and Borrelli, E. (2000). Distinct functions of the two isoforms of dopamine D2 receptors. Nature *408*, 199–203.

Van Bockstaele, E.J., Biswas, A., and Pickel, V.M. (1993). Topography of serotonin neurons in the dorsal raphe nucleus that send axon collaterals to the rat prefrontal cortex and nucleus accumbens. Brain Research *624*, 188–198.

Van Bockstaele, E.J., Cestari, D.M., and Pickel, V.M. (1994). Synaptic structure and connectivity of serotonin terminals in the ventral tegmental area: potential sites for modulation of mesolimbic dopamine neurons. Brain Research *647*, 307–322.

Van-Ham, I.I., Banihashemi, B., Wilson, A.M., Jacobsen, K.X., Czesak, M., and Albert, P.R. (2007). Differential signaling of dopamine-D2S and -D2L receptors to inhibit ERK1/2 phosphorylation. Journal of Neurochemistry *102*, 1796–1804.

Venton, B.J., Seipel, A.T., Phillips, P.E.M., Westel, W.C., Gitler, D., Greengard, P., Augustine, G.J., and Wightman, R.M. (2006). Cocaine increases dopamine release by mobilization of a synapsin-dependent reserve pool. Journal of Neuroscience *26*, 3206–3209.

Vickery, R.G., and Zastrow, von, M. (1999). Distinct dynamin-dependent and -independent mechanisms target structurally homologous dopamine receptors to different endocytic membranes. Journal of Cell Biology *144*, 31–43.

Viemari, J.-C., Roux, J.-C., Tryba, A.K., Saywell, V., Burnet, H., Peña, F., Zanella, S., Bévengut, M., Barthelemy-Requin, M., Herzing, L.B.K., Moncla, A., Mancini, J., Ramirez, J.M., Villard, L., Hilaire, G. (2005). Mecp2 deficiency disrupts norepinephrine and respiratory systems in mice. Journal of Neuroscience *25*, 11521–11530.

Wang, Y., Xu, R., Sasaoka, T., Tonegawa, S., Kung, M.P., and Sankoorikal, E.B. (2000).

Dopamine D2 long receptor-deficient mice display alterations in striatum-dependent functions. Journal of Neuroscience *20*, 8305–8314.

Wassef, M., Berod, A., and Sotelo, C. (1981). Dopaminergic dendrites in the pars reticulata of the rat substantia nigra and their striatal input. Combined immunocytochemical localization of tyrosine hydroxylase and anterograde degeneration. Neuroscience *6*, 2125–2139.

Wenk, G.L., Naidu, S., Casanova, M.F., Kitt, C.A., and Moser, H. (1991). Altered neurochemical markers in Rett's syndrome. Neurology *41*, 1753–1756.

Wernicke, C., Hellmann, J., Finckh, U., and Rommelspacher, H. (2010). Chronic ethanol exposure changes dopamine D2 receptor splicing during retinoic acid-induced differentiation of human SH-SY5Y cells. Pharmacological Reports *62*, 649–663.

Williams, J.T., Colmers, W.F., and Pan, Z.Z. (1988). Voltage- and ligand-activated inwardly rectifying currents in dorsal raphe neurons in vitro. Journal of Neuroscience *8*, 3499–3506.

Williams, J.T., North, R.A., Shefner, S.A., Nishi, S., and Egan, T.M. (1984). Membrane properties of rat locus coeruleus neurones. Neuroscience *13*, 137–156.

Wolf, M.E., White, F.J., Nassar, R., Brooderson, R.J., and Khansa, M.R. (1993). Differential development of autoreceptor subsensitivity and enhanced dopamine release during amphetamine sensitization. Journal of Pharmacology and Experimental Therapeutics *264*, 249–255.

Yavich, L., and MacDonald, E. (2000). Dopamine release from pharmacologically distinct storage pools in rat striatum following stimulation at frequency of neuronal bursting. Brain Research *870*, 73–79.

Yoshimura, M., Higashi, H., and Nishi, S. (1985). Noradrenaline mediates slow excitatory synaptic potentials in rat dorsal raphe neurons in vitro. Neuroscience Letters *61*, 305–310.

Zhang, L.J., Zhang, L.J., Lachowicz, J.E., Lachowicz, J.E., and Sibley, D.R. (1994). The D2S and D2L dopamine receptor isoforms are differentially regulated in Chinese hamster ovary cells. Molecular Pharmacology *45*, 878–889.

Zhang, S., Qi, J., Li, X., Wang, H.-L., Britt, J.P., Hoffman, A.F., Bonci, A., Lupica, C.R., and Morales, M. (2015). Dopaminergic and glutamatergic microdomains in a subset of rodent mesoaccumbens axons. Nature Neuroscience *18*, 386–392.

Zhang, Z., Wu, Y., Wang, Z., Dunning, F.M., Rehfuss, J., Ramanan, D., Chapman, E.R., and Jackson, M.B. (2011). Release mode of large and small dense-core vesicles specified by different synaptotagmin isoforms in PC12 cells. Molecular Biology of the Cell *22*, 2324–2336.

Zhou, F.-M., Liang, Y., Salas, R., Zhang, L., De Biasi, M., and Dani, J.A. (2005). Corelease of dopamine and serotonin from striatal dopamine terminals. Neuron *46*, 65–74.

Zhou, Q.Y., and Palmiter, R.D. (1995). Dopamine-deficient mice are severely hypoactive, adipsic, and aphagic. Cell *83*, 1197–1209.

APPENDIX A AUXILLIARY WORK

PREFACE

This portion includes a characterization of age-dependent changes in a mouse model for Rett Syndrome that harbors a null mutation in the gene MeCP2. Girls with Rett Syndrome exhibit motor deficits similar to Parkinson's disease, suggesting defects in the nigrostriatal pathway. The functional impact of this mutation on the nigrostriatal pathways was determined by examining dopamine neuron membrane properties and morphology, somatodendritic D_2 receptor function, midbrain and striatal D_2 receptor density, and striatal dopamine release. Age-dependent changes in dopamine neurons of the substantia nigra were examined in wild type, pre-symptomatic, and symptomatic *Mecp2*$^{+/-}$ mice.

I conducted this study under the mentorship of Dr. John T. Williams. My contribution was performing all electrophysiology, immunohistochemistry, microscopy, morphology reconstruction, D_2 receptor binding assays under the mentorship and assistance of Dr. Kim A. Neve, analyzing and illustrating data, and writing the manuscript. The fast scan cyclic voltammetry was done by Dr. Christopher P. Ford. All authors assisted in the preparation of the manuscript.

In the context of this dissertation, this study is considered auxilliary work. Specifically, the age-dependent characterization of passive membrane properties of dopamine neurons has been helpful to identify dopamine neurons, particularly in Chapter 6, where D_2 receptors were ubiquitously expressed in the midbrain negating their expression as defining feature of a dopamine neuron. In addition, the direct relationship between cell capacitance and amplitude of the maximal dopamine-induced current (Figure A.3), dopamine current density, has been routinely used since it was identified in this study. Lastly, all the results from wild type mice will be useful for future studies into age-related changes in the dopamine system.

LOSS OF MECP2 IN SUBSTANTIA NIGRA DOPAMINE NEURONS COMPROMISES THE NIGROSTRIATAL PATHWAY

Stephanie C. Gantz[1], Christopher P. Ford[2], Kim A. Neve[3], and John T. Williams[1]

[1]Vollum Institute
Oregon Health and Science University
3181 SW Sam Jackson Park Road
Portland, OR 97239

[2]Department of Physiology and Biophysics
Case Western Reserve University
Cleveland, OH, 44106

[3]Research Service
Department of Veterans Affairs Medical Center
Portland, OR 97239

Acknowledgements: This work was supported by NIH grants, DA026417 (C.P.F.), NS007466 (S.C.G.) and DK007680 SCG, by the Department of Veterans Affairs, Veterans Health Administration, Office of Research and Development, Biomedical Laboratory Research and Development (K.A.N.) and by the International Rett Syndrome Foundation (J.T.W.). We thank Drs. Gail Mandel and Dan Lioy for guidance and discussions.

[This manuscript is presented as published in (Gantz *et al.*, 2011), *The Journal of Neuroscience*, August, 2011, 31(35):12629-12637]

Abstract

Mutations in the methyl-CpG-binding-protein 2 (MeCP2) result in Rett Syndrome (RTT), an X-linked disorder that disrupts neurodevelopment. Girls with RTT exhibit motor deficits similar to Parkinson's disease, suggesting defects in the nigrostriatal pathway. This study examined age-dependent changes in dopamine neurons of the substantia nigra (SNc) from wild type, pre-symptomatic, and symptomatic *Mecp2*$^{+/-}$ mice. Mecp2^{+} neurons in the SNc in *Mecp2*$^{+/-}$ mice were indistinguishable in morphology, resting conductance, and dopamine current density from neurons in wild type mice. However, the capacitance, total dendritic length, and resting conductance of Mecp2^{-} neurons were less than that of Mecp2^{+} neurons as early as four weeks after birth, prior to overt symptoms. These differences were maintained throughout life. In symptomatic *Mecp2*$^{+/-}$ mice, the current induced by activation of D2 dopamine autoreceptors was significantly less in Mecp2^{-} neurons than Mecp2^{+} neurons, although D_2 receptor density was unaltered in *Mecp2*$^{+/-}$ mice. Electrochemical measurements revealed that significantly less dopamine was released after stimulation of striatum in adult *Mecp2*$^{+/-}$ mice compared to wild type. The decrease in size and function of Mecp2^{-} neurons observed in adult *Mecp2*$^{+/-}$ mice was recapitulated in dopamine neurons from symptomatic *Mecp2*$^{-/y}$ males. These results show that mutation in *Mecp2* results in cell-autonomous defects in the SNc early in life and throughout adulthood. Ultimately, dysfunction in terminal dopamine release and D_2 autoreceptor dependent currents in dopamine neurons from symptomatic females support the idea that decreased dopamine transmission due to heterogeneous Mecp2 expression contributes to the parkinsonian features of RTT in *Mecp2*$^{+/-}$ mice.

Introduction

Rett syndrome (RTT) is an X-linked neurodevelopmental disorder occurring approximately once in 10,000 female births (Hagberg, 1985; Laurvick *et al.*, 2006). A large majority of the affected females have mutations in the gene encoding the DNA binding protein, methyl-CpG binding protein 2 (MeCP2) (Laurvick *et al.*, 2006; Neul *et al.*, 2008). The *MECP2* gene resides on the X-chromosome so that males with the mutation *(MECP2*$^{-/y}$), lack all functional *MECP2*, and usually die perinatally. Heterozygous females (*MECP2*$^{+/-}$) are mosaic for MeCP2 expression due to X-chromosome inactivation. Girls with RTT develop normally until 6 to 18 months of age, at which time they begin to regress, losing motor skills, particularly purposeful hand usage, ambulation, and postural control. In later stages, Parkinson-like symptoms including dystonia, festination, and inertia are often observed (Chahrour and Zoghbi, 2007; Schanen, 1999).

There are several *Mecp2* mutant mouse models for RTT (Chen *et al.*, 2001; Guy *et al.*, 2007; 2001; Shahbazian *et al.*, 2002). Both *Mecp2*$^{+/-}$ and *Mecp2*$^{-/y}$ mice develop a complex phenotype consistent with many features of the human disease, including compromised motor function. Similar to the human disease, *Mecp2*$^{+/-}$ mice exhibit a delayed onset of behavioral symptoms and live significantly longer than *Mecp2*$^{-/y}$ mice (Chen *et al.*, 2001; Guy *et al.*, 2001; McGill *et al.*, 2006; Viemari *et al.*, 2005). Most studies have focused on *Mecp2*$^{-/y}$ mice because the symptoms appear earlier and progress faster than in *Mecp2*$^{+/-}$ mice. However, RTT is almost exclusively a female disease so the *Mecp2*$^{+/-}$ mouse may be a more appropriate genetic model.

In this study, dopamine neurons of the substantia nigra (SNc) were examined because multiple lines of evidence suggest that they contribute to RTT pathology. In both RTT patients and *Mecp2* mutant mice, levels of biogenic amines are decreased and Parkinson-like motor deficits point to a disturbance of dopamine transmission (Dunn and MacLeod, 2001; Panayotis *et al.*, 2011; Wenk *et al.*, 1991). Conditional loss of *Mecp2* from tyrosine hydroxylase-expressing catecholamine neurons has been associated with a reduction in locomotion in mice (Samaco *et al.*, 2009). Furthermore, a recent report in *Mecp2*$^{-/y}$ mice found that SNc neurons exhibit gradual alterations in morphology and function with the progression of motor impairments (Panayotis *et al.*, 2011). However, the electrical properties and postsynaptic responses of dopamine neurons have not been studied. This study examined perturbations of dopamine neurons in the *Mecp2*$^{+/-}$ mouse brain at ages prior to and after the appearance of motor symptoms. Mecp2^{-} dopamine neurons are smaller with a reduced dendritic arbor, in both pre-symptomatic and symptomatic *Mecp2*$^{+/-}$ mice. In the SNc of symptomatic mice, there is a selective decrease in the outward current induced by exogenous dopamine only in Mecp2^{-} neurons, with no change in the density of dopamine D_2 receptors. Furthermore, in these animals, the amount of dopamine released in the dorsal striatum is reduced. The results support the idea that decreased dopamine transmission due to heterogeneous expression of Mecp2 contributes to the Parkinsonian features of RTT in *Mecp2*$^{+/-}$ mice.

Specific Materials and Methods

Most of the procedures for this manuscript can be found in Methods and Materials (p.8). The description provided here includes procedures specific to this manuscript.

Animals

Mice originally generated by the Bird laboratory (Guy *et al.*, 2001), were obtained from the Jackson Labs (strain no. 003890), maintained on a C57BL/6 background, and genotyped as previously described (Miralvès *et al.*, 2007). Mice originally generated by the Jaenisch laboratory (Chen *et al.*, 2001) were maintained on a BALB/c background, and genotyped by PCR. All experiments were performed on *Mecp2*B$^{-/y}$, *Mecp2*J$^{-/y}$, *Mecp2*$^{+/-}$ mice (Guy *et al.*, 2001), and age-, sex-, and strain-matched wild type controls. Females were divided into two age groups to separate pre-symptomatic and symptomatic *Mecp2*$^{+/-}$ mice, young (16-30 d) and adult (169-519 d). *Mecp2*B$^{-/y}$ males investigated were aged 30-57 d and *Mecp2*J$^{-/y}$ males were 101-105 d, ages where motor symptoms are observed (Chen *et al.*, 2001; Guy *et al.*, 2001). Motor symptoms in symptomatic animals, defined as hind limb clasping, tremor, hypoactivity, and inertia, were confirmed before being killed. Littermates were used as age-matched controls when possible. When appropriate, experiments were performed with the investigator blind to the sex, age, and genotype.

Brain tissue and slice preparation

Brain slices for electrophysiology and fast-scan cyclic voltammetry were prepared as described previously (Williams *et al.*, 1984). Briefly, horizontal midbrain slices (200-220 μm) or coronal slices containing dorsal striatum (250 μm) were obtained using a vibrating microtome (Leica) and incubated at 34 ºC in vials with 95/5% O_2/CO_2 saline with 10 μM MK-801 for at least 30 min. For binding assays, striata were dissected and thick (880 μm) midbrain sections were frozen on dry ice and stored at -80 ºC until use.

Immunohistochemistry and morphology measurements

To determine whether recorded neurons expressed Mecp2, 0.1% neurobiotin was included in the internal solution (Vector Laboratories, Inc.). Slices were fixed for 1 h in at room temperature in 4% paraformaldehyde in PBS. Free-floating slices were washed three times with PBS then incubated in PBS with 0.5% Triton-X and 10% fetal bovine serum for 5 h. Slices were incubated overnight at room temperature in rabbit anti-Mecp2 (Covance, 1:200). Slices were washed again in PBS and incubated in Alexa-488-conjugated goat anti-rabbit secondary antibody (1:1000, Invitrogen) for 2 h. Slices were then washed three times with PBS and incubated in Cy5-conjugated streptavidin (1:1000, Invitrogen) for 2 h. Following three PBS washes, slices were DAPI (300 nM) stained for 20 mins, rinsed and mounted. Images were collected on a Zeiss confocal laser scanning LSM 710 microscope with a 20x lens (0.8 NA). Morphology measurements were calculated with the help of the Simple Neurite Tracer plug-in for Fiji.

Radioligand Binding Assays

The striata and midbrain from one mouse provided enough membranes for independent [^{3}H]YM-09151-2 assays. The striata and midbrain section were homogenized with a PT 1200 E polytron (Kinematica, Inc.) for 10 s on ice in 4 ml Tris buffer (50 mM Tris-HCl, 0.9% NaCl, pH 7.4 at 4 ºC) and centrifuged at 30,000*g* for 20 min. The midbrain and striata membrane pellets were resuspended in 4 ml Tris buffer, incubated for 30 min at 25 ºC to release endogenous dopamine, centrifuged, and resuspended in 2.6 and 6.0 ml Tris buffer, respectively. Membranes (midbrain: 18-33 μg; striata: 2-7 μg) were incubated in duplicate in a total reaction volume of 1 ml with [^{3}H]YM-09151-2 (82.7 Ci/mmol;

PerkinElmer) at concentrations ranging from 0.009-0.15 nM and buffer (50 mM Tris containing 0.9% NaCl and 0.002% bovine serum albumin, pH 7.4 at 4 ºC). Nonspecific binding was measured in the presence of 1 μM (+)-butaclamol. Reactions were incubated at 25 ºC for 1 h and terminated by filtration through Wallac Filtermat A filters (PerkinElmer), presoaked with 0.05% polyethylenimine using a 96-well Tomtec cell harvestor and ice-cold wash-buffer (10 mM Tris-HCl, pH 7.4 at 4 ºC, and 0.9% NaCl). Filters were allowed to dry at least 1 h before adding scintillation fluid (50 μl) to each filtered spot. Radioactivity on the filters was determined using a Wallac 1450 microBeta scintillation counter. Proteins were measured using the BCA method (Pierce Biotechnology).

Fast-scan cyclic voltammetry

Glass encased carbon fibers (34-700, Goodfellow, PA; 7 μm diameter) were cut to a final exposed length of ~30 μm as previously described (Ford *et al.*, 2010) and placed in the dorsal striatum. Voltammetric recordings were performed with a custom built hardware (University of Washington, Electronics and Materials Engineering Shop, Seattle, WA) and software (Tarheel CV, Labview). To maximize the temporal resolution of the detection of dopamine, triangular waveforms from -0.4 V to 1.0 V to -0.4 V versus Ag/AgCl with a scan rate of 600 V/S at 60 Hz were used (Bath *et al.*, 2000). Between scans the electrode was maintained at -0.4 V (versus Ag/AgCl). Ten background cyclic voltammograms obtained before stimulation were used for subtraction. To determine the time course of voltammetrically-detected dopamine, the current at the peak oxidation (0.5 V-0.7 V) was plotted against time. Dopamine was evoked by a single pulse (0.35 μA, 0.5

ms) from a mono-polar stimulating electrode placed within the striatum near (30-50 μm) the exposed tip of the carbon fiber. After the experiment, the electrode was calibrated using dopamine solutions of known concentration.

Drugs

Dopamine hydrochloride, MK-801, DNQX, picrotoxin, and (+)-butaclamol were obtained from Sigma-Aldrich. Hexamethonium, sulpiride, baclofen were from Research Biochemicals International. CGP-35348 and quinpirole were obtained from Tocris. [^{3}H]YM-09151-2 (82.7 Ci/mmol) was from PerkinElmer.

Data analysis

All values are given as means ± SEM, with the exception of K_d values, which are given as geometric means followed by the limits defined by the SEM in parentheses. Linear correlations in distributions were tested with Spearman correlation tests. Data for saturation binding were analyzed by nonlinear regression (Prism 4.0) using a one-site hyperbola model to determine K_d and B_{max} values. The free concentration of radioligand was calculated as the concentration added minus the concentration specifically bound. A difference of $p < 0.05$ was considered significant (InStat 3.06 and Prism 4.0; GraphPad Software, Inc.).

Results

The effect of *Mecp2* mutation on the electrophysiological properties of dopamine neurons was determined in pre-symptomatic and symptomatic female *Mecp2*$^{+/-}$ mice. To unambiguously separate pre-symptomatic and symptomatic *Mecp2*$^{+/-}$ mice, all young

females [postnatal day (PND) 26 ± 1, n = 13] used in these experiments were asymptomatic whereas adult females (PND 347 ± 19, n = 23) displayed motor symptoms, including hind limb clasping and overt hypoactivity.

Mecp2^{-} dopamine neurons have decreased capacitance and resting conductance

To identify Mecp2^{-} and Mecp2^{+} neurons, cells were filled with 0.1% neurobiotin and after recording stained for the presence of Mecp2. In wild type female mice, the Mecp2 antibody labeled 94% of filled neurons (WT). As illustrated in Figure A.1A, dopamine neurons in heterozygous *Mecp2*$^{+/-}$ mice were mosaic for *Mecp2* expression with Mecp2^{+} (Figure A.1B) and Mecp2^{-} neurons (Figure A.1C), referred to as "HET^{+}" and "HET^{-}" respectively. In both *Mecp2*$^{+/-}$ and wild type mice, there was a developmental decline in cell surface area, as evidenced by a decrease in capacitance of WT, HET^{+}, and HET^{-} dopamine neurons between young and adult ages (WT: $p < 0.0001$; HET^{+}: $p = 0.0002$; HET^{-}: $p < 0.0001$). The relative reduction in cell surface area that occurred between one and eight months of age was similar between WT, HET^{+}, and HET^{-} neurons (two-way ANOVA, $F_{2, 258} = 0.04$, $p = 0.96$). Despite this change, at both ages, the capacitance of HET^{+} neurons was indistinguishable from neurons in wild type mice (Table 1; $p > 0.05$). On the contrary, HET^{-} neurons were smaller than HET^{+} and WT neurons. In all animals, the capacitance of HET^{-} neurons was significantly less than age-matched HET^{+} and WT neurons (Table 1; young: $p < 0.05$; adult: $p < 0.001$) (Figure A.1D).

Given limitations posed by the somatic recording electrode, capacitance measurements may not include more distal or fine processes. Therefore, morphology was examined by tracing neuron processes (axon and dendrites) in x, y, and z dimensions, to

determine the number, length, and total length of processes. Representative maximum intensity projection images of neurons and their tracings are shown in Figure A.2A. In both *Mecp2*$^{+/-}$ and wild type mice, the number of processes decreased between young and adult ages (Figure A.2B). Despite this developmental change, in all animals, the morphology of age-matched HET^{+} or WT neurons was indistinguishable (Table A.1; $p > 0.05$) (Figure A.2B-D). However, HET^{-} neurons from young females had fewer dendrites (Table 1, $p < 0.01$) but no significant difference in the average dendrite length (Table 1, $p > 0.05$) (Figure A.2B and D). In adulthood, the total length of the dendritic arbor of HET^{-} neurons remained smaller (Table A.1; $p < 0.05$) and the average dendrite length was reduced (Table A.1; $p < 0.05$) (Figure A.2C and D).

Overall, these results indicate the expression of *Mecp2* in HET^{+} neurons is sufficient to develop and maintain WT morphology. However, loss of Mecp2 in HET^{-} dopamine neurons results in less membrane surface area, due in part to fewer dendrites, months prior to the onset of any motor deficit. In symptomatic mice, HET^{-} neurons continue to have significantly less membrane surface area and a smaller dendritic arbor than Mecp2^{+} neurons.

As might be expected from the decrease in capacitance with age, the input resistance also increased in neurons from wild type and *Mecp2*$^{+/-}$ animals. The increase in resistance in WT and HET^{-} neurons was not, however, in proportion to the decrease in capacitance, indicating that after P30 there was a developmental decrease in the expression of ion channels that contribute to the resting conductance (WT: $p = 0.0002$; HET^{-}: $p = 0.0036$) (Figure A.1E). In both young and adult animals, the resistance of HET^{+} and WT neurons was indistinguishable (Table A.1; $p > 0.05$) (Figure A.2E).

However, HET^{-} neurons had an increased resistance at both ages (Table A.1; Young: $p < 0.001$; Adult: $p < 0.001$) (Figure A.2E). Overall, these results indicate that a specific consequence of Mecp2 loss is a reduction in the density of open ion channels underlying the resting conductance.

D_2 autoreceptor-activated current density is attenuated in symptomatic $Mecp2^{+/-}$ mice from a specific decrease in $Mecp2^{-}$ neurons

A fundamental property of SNc dopamine neurons is the presence of D_2 autoreceptors, which activate a potassium conductance. Therefore, binding of D_2 receptors and their activation, measured as the current induced by dopamine, in neurons from *Mecp2*$^{+/-}$ mice was examined. Initially, maximal D_2 receptor-activated outward currents were evoked by iontophoretic application of dopamine onto dopamine neurons in female wild type mice (Figure A.3A). The maximal dopamine current evoked by iontophoresis did not differ in amplitude from bath perfusion of the D_2 agonist quinpirole (10 μM, quinpirole: 248 ± 16 pA, $n = 29$; DA: 234 ± 6 pA, $n = 296$; $p > 0.05$; (Beckstead *et al.*, 2009). The amplitude of the maximal dopamine current decreased with age, which may not be surprising given the reduction in membrane surface area (Young: 280 ± 11 pA, $n = 95$; Adult: 196 ± 9 pA, $n = 111$; $p < 0.0001$) (Figure A.3B). When normalized to capacitance, the dopamine current density did not change with age in wild type mice (Table 1; $p > 0.05$) (Figure A.3D and Figure A.4A).

The activation of $GABA_B$ receptors on SNc dopamine neurons activates the same G-protein coupled inwardly rectifying potassium (GIRK) conductance as D_2 receptors (Beckstead *et al.*, 2004; Koyrakh *et al.*, 2005). Consistent with a previous report that $GABA_B$ receptors activate the GIRK conductance with greater efficacy (Beckstead *et al.*,

2009), the maximal current induced by the $GABA_B$ agonist, baclofen (10 μM) was significantly greater than the maximal dopamine current in neurons from adult wild type mice ($p < 0.05$). Similar to dopamine, the maximal baclofen-induced current decreased with age (Young: 311 ± 14 pA, $n = 61$; Adult: 237 ± 13 pA, $n = 40$; $p = 0.01$) (Figure A.3B), but when normalized to cell capacitance, there was no change in the baclofen current density with age (Young: 8.7 ± 0.4 pA/pF, $n = 61$; Adult: 9.1 ± 0.4 pA/pF, $n = 40$; $p > 0.05$) (Figure A.3A). Thus, in wild type animals, the correlation between capacitance and agonist-induced GIRK current amplitude indicated that cell size predicts the amplitude of the current induced by activation of these two G protein-coupled receptors (Spearman correlation, DA: $R_{294} = 0.64$, $p < 0.0001$, Figure A.3C; Baclofen: $R_{169} = 0.46$, $p < 0.0001$; not shown).

To evaluate the effect of *Mecp2* mutation on the sensitivity to exogenously applied dopamine, the dopamine current density in pre-symptomatic (young), symptomatic (adult) *Mecp2*$^{+/-}$, and age-matched wild type mice was compared. In young females, the dopamine current density of the combined population of Mecp2^{+} and Mecp2^{-} neurons in *Mecp2*$^{+/-}$ mice, referred to as "HET$^{+/-}$", (7.5 ± 0.2 pA/pF, $n = 100$) and wild type mice was not different ($p > 0.05$) (Figure A.4A). Nor was there a difference, in young females, between the dopamine current density in WT, HET^{+}, or HET^{-} neurons ($p > 0.05$) (Figure A.4D). However, in adult *Mecp2*$^{+/-}$ mice, the average dopamine current density of the HET$^{+/-}$ neuron population (6.5 ± 0.2 pA/pF, $n = 150$) was reduced significantly compared to the wild type controls ($p = 0.0001$) (Figure A.4A). The decrease in dopamine current density was due to a cell autonomous decrease in HET^{-} neurons (Table A.1; $p < 0.05$) (Figure A.4D). In both young and adult mice, HET^{+}

neurons were indistinguishable from WT neurons Table A.1; $p > 0.05$) (Figure A.4D). The decrease in dopamine current was selective because the average $GABA_B$ receptor-mediated current density of $HET^{+/-}$ neurons was unaltered at both ages in *Mecp2*$^{+/-}$ mice (Young: 8.4 ± 0.3 pA/pF, $n = 39$; $p > 0.05$; Adult: 8.5 ± 0.4 pA/pF, $n = 38$; $p > 0.05$) (Figure A.4A). The attenuated dopamine current density was observed in the presence and absence of $GABA_A$, AMPA, and nACh synaptic blockers. There was no standing outward current indicating a lack of significant constitutive D2 autoreceptor activation in the brain slice. Overall, these results suggest that the loss of Mecp2 reduces the sensitivity of dopamine neurons to dopamine, by adulthood.

The decrease in sensitivity of dopamine neurons to dopamine could be due to an alteration in the number of D_2 autoreceptors in the nigrostriatal pathway. Therefore, saturation binding experiments were performed on midbrain and striatum homogenates from young and adult wild type and *Mecp2*$^{+/-}$ mice, using a highly selective and potent D_2 receptor antagonist, [^{3}H]YM-09151-2 (Terai *et al.*, 1989). Mean K_d values in these regions were approximately 20 pM (Table A.2), consistent with previously reported values (Terai *et al.*, 1989). In both *Mecp2*$^{+/-}$ and wild type mice, there was no significant age-related change in the density of D_2 receptors in midbrain, as evidenced by comparable B_{max} values of [^{3}H]YM-09151-2 binding, between young and adult ages ($p > 0.05$; Table A.2). However, there was a developmental decline in the density of D_2 receptors in striatum, in both *Mecp2*$^{+/-}$ and wild type mice (wild type: $p < 0.05$; *Mecp2*$^{+/-}$: $p < 0.05$; Table A.2). The relative reduction in D_2 receptors was similar between wild type and *Mecp2*$^{+/-}$ mice (two-way ANOVA, Midbrain: $F_{1,19} = 0.02$, $p = 0.90$; Striatum: $F_{1,16} = 0.007$, $p = 0.94$). Furthermore, at both ages, the density of D_2 receptors in

midbrain and striatum from *Mecp2*$^{+/-}$ mice was indistinguishable from the density of D_2 receptors in wild type mice ($p > 0.05$; Table A.2). Thus, loss of Mecp2 in SNc dopamine neurons results in a cell autonomous reduction in membrane surface area and resting conductance, as well as a progressive decline in dopamine D_2 autoreceptor signaling, without altering the density of D_2 receptors in midbrain or striatum.

Similar cellular defects in symptomatic Mecp2$^{-/y}$ mice

Similar Parkinson-like motor deficits occur in *Mecp2*$^{-/y}$ males as in *Mecp2*$^{+/-}$ female mice. *Mecp2*$^{+/-}$ female mice used in this study were originally generated by the Bird laboratory and maintained on a C57BL/6 background. To determine gender or strain specific effects, two different mouse models of RTT were used. The electrophysiological properties of dopamine neurons were determined in symptomatic males *Mecp2*$^{-/y}$ mice generated by the Bird and Jaenisch laboratories (Bird: *Mecp2*B$^{-/y}$, MUT^{B}, PND 44 ± 4, n = 14; Jaenisch: *Mecp2*J$^{-/y}$, MUT^{J}, PND 103 ± 1, n = 4). Reduced capacitance was observed in Mecp2^{-} SNc dopamine neurons in *Mecp2*B$^{-/y}$ and *Mecp2*J$^{-/y}$ male mice (WT^{B}: 30.1 ± 0.9 pF, n = 70; MUT^{B}: 20.0 ± 0.7 pF, n = 48; $p < 0.0001$; WT^{J}: 25.7 ± 1.0 pF, n = 28; MUT^{J}: 18.0 ± 0.7 pF, n = 31; $p < 0.0001$) (Figure A.5A). Additionally, increased resistance was observed in Mecp2^{-} neurons from *Mecp2*B$^{-/y}$ and *Mecp2*J$^{-/y}$ male mice (WT^{B}: 9.5 ± 0.5 MΩ/pF, n = 56; MUT^{B}: 20.6 ± 2.4 MΩ/pF, n = 33; $p <$ 0.0001; WT^{J}: 14.3 ± 1.1 MΩ/pF, n = 28; MUT^{J}: 32.1 ± 3.3 MΩ/pF, n = 31; $p < 0.0001$; not shown). Finally, as was observed in experiments in adult *Mecp2*$^{+/-}$ females, the dopamine current density in the symptomatic *Mecp2*B$^{-/y}$ and *Mecp2*J$^{-/y}$ mice was significantly decreased (WT^{B}: 10.0 ± 0.4 pA/pF, n = 49; MUT^{B}: 7.6 ± 0.4 pA/pF, n = 32;

$p = 0.0002$; WT^J: 9.7 ± 0.6 pA/pF, $n = 25$; MUT^J: 5.5 ± 0.5 pA/pF, $n = 28$; $p = 0.002$) (Figure A.5B) while baclofen current density did not change significantly (WT^B: 8.9 ± 0.4 pA/pF, $n = 48$; MUT^B: 7.6 ± 0.6 pA/pF, $n = 15$; $p = 0.07$; WT^J: 9.8 ± 0.6 pA/pF, $n = 21$; MUT^J: 8.5 ± 0.8 pA/pF, $n = 17$, $p > 0.05$; not shown). Therefore, the cellular defects observed in $Mecp2^-$ neurons from symptomatic *Mecp2*$^{+/-}$ females were recapitulated in $Mecp2^-$ neurons from symptomatic *Mecp2*$^{-/y}$ male mice.

The cellular defects observed in $Mecp2^-$ neurons from young *Mecp2*$^{+/-}$ (PND 26-30, HET^-) and *Mecp2*$B^{-/y}$ (PND 30-45, MUT^B) mice were compared by two-way ANOVA, where a significant interaction between sex and proteotype indicates a difference in the severity of defects. When the capacitance of young MUT^B (66 ± 2% of WT) and HET^- (83 ± 6% of WT) neurons were compared, there was a significant interaction between sex and proteotype (two-way ANOVA, $F_{1, 108} = 5.9$, $p = 0.02$). This result indicates an additional reduction in surface area in young MUT^B neurons that was not detected in young HET^- neurons. When the resistance of young MUT^B (176 ± 19% of WT) and HET^- (170 ± 16% of WT) neurons were compared, there was no interaction between sex and proteotype (two-way ANOVA, $F_{1, 100} = 1.9$, $p = 0.18$). There was also no interaction when the dopamine current density of young MUT^B (73 ± 4% of WT) and HET^- (86 ± 7% of WT) neurons were compared (two-way ANOVA, $F_{1, 89} = 2.3$, $p = 0.13$). These results indicate that the decrease in resting conductance and dopamine current density relative to wild type was similar in MUT^B and HET^- neurons in young mice. In symptomatic adult *Mecp2*$^{+/-}$ mice, the specific attenuation in dopamine current density in HET^- neurons, reduces the average dopamine current density of the SNc to a

level comparable to symptomatic *Mecp2*B$^{-/y}$ mice (HET$^{+/-}$: 84 ± 3% of WT; MUT^{B}: 76 ± 4% of WT; two-way ANOVA, $F_{1, 338} = 2.7$, $p = 0.10$).

Less dopamine is released in the striatum of symptomatic Mecp2$^{+/-}$ mice

The release of dopamine in the dorsal striatum of adult *Mecp2*$^{+/-}$ mice was measured by fast-scan cyclic voltammetry (FSCV) to examine the possibility that morphological and functional defects observed in Mecp2^{-} SNc dopamine neurons affect terminal release. A single stimulus evoked dopamine release from SNc dopamine neuron axonal terminals in the dorsal striatum (Figure A.4B). The amount of dopamine released in adult *Mecp2*$^{+/-}$ mice (291 ± 32 nM, $n = 41$) was less than half the amount released in adult female wild type mice (614 ± 74 nM, $n = 35$; $p = 0.0002$) (Figure A.4B). These results suggest that when stimulated, less dopamine is released in the terminal projection area of dorsal striatum in adult mice, as a consequence of heterogeneous loss of Mecp2 in SNc dopamine neurons.

Discussion

The present study suggests that the mosaic expression of *Mecp2* in the SNc results in a compromised nigrostriatal pathway, in part due to morphological and functional alterations specific to Mecp2^{-} neurons. Examination of dopamine neurons in aging animals addressed three issues related to the cellular basis of Rett-like symptoms in mice: 1) the timing of defects with respect to the presentation of behavioral symptoms, 2) the consequence of Mecp2 loss on SNc dopamine neuron morphology and function and, 3) the consequence of heterogeneous *Mecp2* expression on the function of the nigrostriatal pathway.

Age-dependent changes in wild type dopamine neurons.

Numerous rodent and human studies have addressed the consequence of age on the number of D_2 receptors in the nigrostriatal pathway. Previous reports describe a reduction in D_2 receptor density in the striatum with age (De Blasi and Mennini, 1982; Henry *et al.*, 1986; Hyttel, 1987; Ishibashi *et al.*, 2009; Morelli *et al.*, 1990; O'Boyle and Waddington, 1984; Severson and Finch, 1980) but no change in the substantia nigra (De Keyser *et al.*, 1991; Morelli *et al.*, 1990). In agreement with these reports, the results of the present study indicated that the density of D_2 receptors in the mouse striatum decreased with age. Yet, the D_2 receptor density in midbrain and D_2 receptor-activated current density in SNc dopamine neurons remained stable with age.

There was a significant decrease in capacitance and number of dendrites of dopamine neurons in wild type females after one month of age. These results indicate that the size of dopamine neurons decreases at a relatively young age likely due, in part, to pruning of dendrites. In addition, the disproportionate increase in resistance of dopamine neurons suggested that there is a decline in the density of open ion channels that contribute to the resting conductance. Taken together, these results are indicative of tight regulation of dopamine transmission in the midbrain, despite a developmental decline in cell size and resting conductance.

Cellular defects in Mecp2^{-} neurons detected with respect to presentation of motor symptoms

In both wild type and *Mecp2*$^{+/-}$ mice, there was a developmental decline in membrane surface area of dopamine cells. Despite this, the morphology of HET^{+} and WT neurons

was indistinguishable in young and adult mice. Moreover, there was no difference in the resting conductance or dopamine current density between HET^{+} and WT neurons at both ages. Thus, the expression of *Mecp2* in dopamine neurons is sufficient to develop and maintain wild type morphology and function, whereas the loss of Mecp2 results in altered development and maintenance of morphology and function.

Consistent with a previous report in locus coeruleus (LC) neurons from pre-symptomatic *Mecp2*$^{+/-}$ mice (Taneja *et al.*, 2009), the present study shows that as early as 4 weeks of age, the capacitance of HET^{-} dopamine neurons from *Mecp2*$^{+/-}$ mice was less than that of HET^{+} and WT neurons. The decrease in membrane surface area is consistent with the smaller soma area reported previously for $Mecp2^{-}$ SNc dopamine neurons from *Mecp2*$^{-/y}$ mice (Panayotis *et al.*, 2011). Additionally, HET^{-} neurons had fewer dendrites, contributing to the reduced capacitance measurements. As was found in HET^{-} LC neurons, the resting conductance of HET^{-} dopamine neurons was also less than that of wild type females. Thus, the cellular consequences of Mecp2 loss occur several months prior to the manifestation of any obvious motor symptoms.

After the development of motor symptoms, the reduced capacitance, dendritic arbor, and resting conductance observed in HET^{-} neurons persisted. Additional cellular defects were observed only in HET^{-} neurons from symptomatic *Mecp2*$^{+/-}$ mice, including a significant decrease in the D_2 receptor-activated current density. The attenuated response to dopamine in HET^{-} neurons could be due to a specific decrease in midbrain D_2 autoreceptors. However, saturation binding analyses indicated that the D_2 receptor density and affinity for [^{3}H]YM-09151-2 in midbrain of *Mecp2*$^{+/-}$ mice was indistinguishable from wild type mice. These experiments do not preclude dysfunction in

D_2 receptor trafficking to the plasma membrane. Alternatively, the attenuated response to dopamine could be due to a change in the coupling of D_2 receptors to the GIRK channel. It is possible the higher efficacy with which $GABA_B$ receptors activate GIRK conductance obscures observation of significant perturbation in $GABA_B$ receptor-mediated current density. These results suggest that a specific consequence of Mecp2 loss is a progressive decline in the normal regulation of dopamine neurons, coinciding with motor behavior disturbances.

No detrimental effect of Mecp2^{-} cells on Mecp2^{+} dopamine neurons

Studies aimed at addressing the interplay between Mecp2^{+} and Mecp2^{-} cells have produced mixed results, supporting cell-autonomous as well as non-cell autonomous consequences of *Mecp2* mutation on neuronal morphology and function, that may be region specific (Belichenko *et al.*, 2009; Kishi and Macklis, 2010). In this study, Mecp2^{+} dopamine neurons from *Mecp2*$^{+/-}$ mice were indistinguishable from wild type dopamine neurons in morphology, conductance, and current induced by dopamine. This finding is consistent with reports that HET^{+} LC neurons are no different in size and conductance than wild type neurons (Taneja *et al.*, 2009). Taken together, this study indicates that the loss of Mecp2 in surrounding cells, including neurons and glia, did not affect Mecp2^{+} dopamine neurons in a detrimental manner.

Can the presence of Mecp2^{+} cells affect Mecp2^{-} neurons in a beneficial manner? The resting conductance and dopamine current density in Mecp2^{-} dopamine neurons from young *Mecp2*$^{+/-}$ females and *Mecp2*$^{-/y}$ males were comparable. Thus, it is unlikely that Mecp2^{+} cells have influenced resting conductance and D_2 receptor signaling in

Mecp2^{-} neurons. However, the comparison between young *Mecp2*$^{+/-}$ females and *Mecp2*$^{-/y}$ males suggested that Mecp2^{-} neurons in the males were more affected in terms of capacitance. Consistent with this, Belichenko *et al.*, (2009) reported that the severity of some dendritic abnormalities in Mecp2^{-} cortical neurons were greater in *Mecp2*$^{-/y}$ males than *Mecp2*$^{+/-}$ females. It is possible the declining health of the *Mecp2*$^{-/y}$ males, symptomatic by three weeks of age (Belichenko *et al.*, 2009; Guy *et al.*, 2001), brought about the more severe morphological defects observed. Alternatively, it is possible that a cell-autonomous consequence of Mecp2 loss is rendering the development and maintenance of morphology more vulnerable to environmental influences. The maintained expression of *Mecp2* in some cells may offer partial support or protection to Mecp2^{-} neurons. These findings illustrate the importance of investigating the outcome of heterogeneous *Mecp2* expression, as the mosaic pattern of *Mecp2* expression is an important aspect in the genetic model of RTT.

Compromised nigrostriatal pathway in adult Mecp2$^{+/-}$ mice coincides with motor deficits

Dopamine transmission in the midbrain is thought to contribute to learning, movement, reward processing, as well as a variety of neurological diseases. The motor deficits in Rett syndrome have been compared to those in Parkinson's disease (FitzGerald *et al.*, 1990; Wenk *et al.*, 1991), which results from the progressive degeneration of dopamine neurons in the substantia nigra. However, motor deficits have been shown to occur through disruption of dopamine transmission without degeneration in a mouse model for Parkinson's disease, where striatal dopamine content is reduced without dopamine cell death in the substantia nigra (Colebrooke *et al.*, 2006). In the present study, less

dopamine was released in the dorsal striatum in symptomatic *Mecp2*$^{+/-}$ mice. This is consistent with a previous report of reduced striatal dopamine levels in *Mecp2*$^{-/y}$ males that exhibit motor deficits (Panayotis *et al.*, 2011).

Activation of D_2 autoreceptors inhibits terminal release of dopamine (Phillips *et al.*, 2002). The present study identified a decrease in D_2 autoreceptor-mediated currents in symptomatic *Mecp2*$^{+/-}$ and *Mecp2*$^{-/y}$ mice. These results are seemingly inconsistent with reduced release of dopamine in the dorsal striatum measured electrochemically in *Mecp2*$^{+/-}$ mice. However, given that a single stimulation was used to evoke release, D_2 autoreceptor activation did not contribute to these measurements. Thus, the reduced dopamine level in striatum may be a consequence of fewer axon terminals or reduced dopamine synthesis. Conditional loss of *Mecp2* in catecholamine neurons has been shown to reduce dopamine synthesis and results in motor impairments (Samaco *et al.*, 2009). Taken together, dysfunction in terminal dopamine release and D_2 autoreceptor-dependent currents in dopamine neurons indicated that heterogeneous loss of Mecp2 compromises healthy functioning of the nigrostriatal pathway.

In summary, the present study identified morphological and functional consequences of loss of Mecp2 in SNc dopamine neurons. Mutation in *Mecp2* in *Mecp2*$^{+/-}$ mice led to cell-autonomous cellular changes in the SNc, some occurring months before and others coinciding with the appearance of motor symptoms. It should be noted that, as previously described (Taneja *et al.*, 2009), this study defines cell-autonomous as mechanisms that are strictly dependent on whether a cell expresses Mecp2. In this study, alterations were observed exclusively in Mecp2^{-} neurons while Mecp2^{+} dopamine neurons were indistinguishable from neurons from wild type females.

The results support the idea that decreased dopamine transmission due to heterogeneous Mecp2 loss contributes to the Parkinsonian features of RTT in *Mecp2*$^{+/-}$ mice. Ultimately, mutation in *Mecp2* compromises healthy functioning of the nigrostriatal pathway and supports the manifestation of motor deficits.

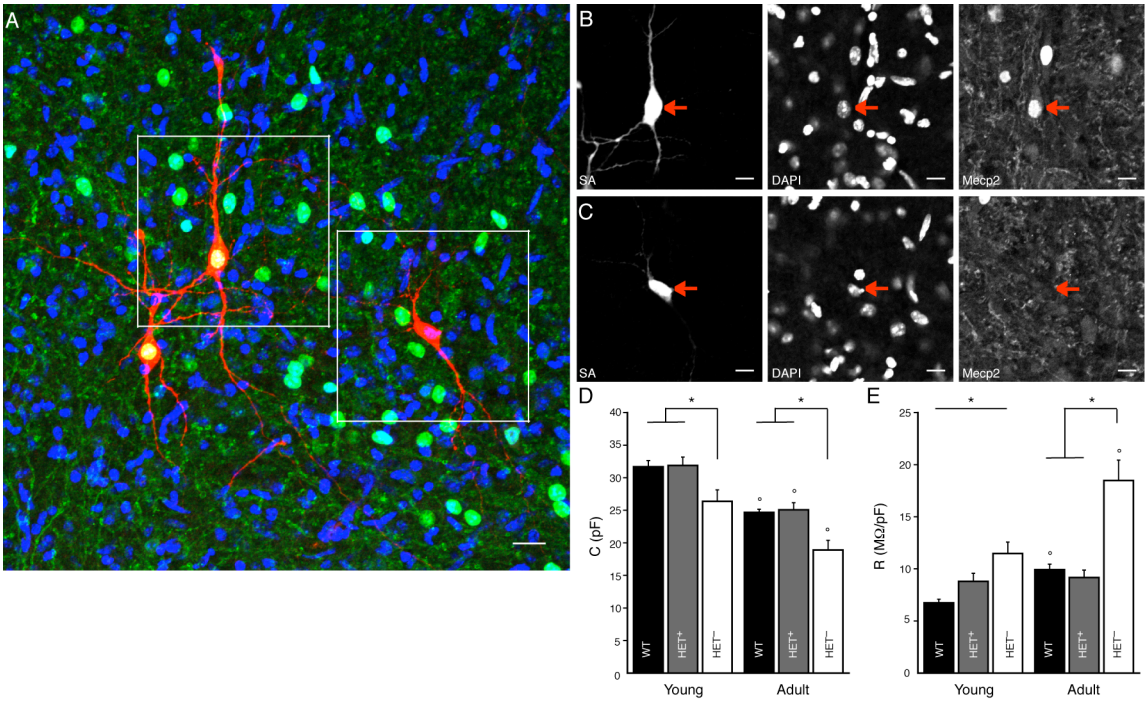

Figure A.1. Mecp2^{-} dopamine neurons in *Mecp2*$^{+/-}$ mice (HET^{-}) have decreased membrane capacitance and increased resistance compared to Mecp2^{+} neurons from wild type (WT) or *Mecp2*$^{+/-}$ (HET^{+}) female mice.

A-C, Representative maximum intensity projection confocal images of neurobiotin-filled HET^{+} and HET^{-} dopamine neurons from the SNc of a young *Mecp2*$^{+/-}$ female, immunostained with streptavidin (SA, red), antibody for Mecp2 (green), and DAPI (blue). Single plane confocal image of HET^{+} (**B**) and HET^{-} nuclei (**C**). Scale bar (**A**), 20 μm, (**B-C**), 10 μm. **D,** The capacitance (pF) of dopamine neurons decreased with age in wild type and *Mecp2*$^{+/-}$ mice, indicating a significant decrease in the surface area of dopamine neurons with age in both wild type and *Mecp2*$^{+/-}$ mice. Capacitance of HET^{-} dopamine neurons was significantly less than WT and HET^{+} in young and adult mice. **E**, Resistance (MΩ/pF) of dopamine neurons in wild type and *Mecp2*$^{+/-}$ mice increased with age. Resistance of HET^{-} neurons was greater than WT in young and adult mice. Mean ± SEM. * designates statistical significance within age group, ° designates statistical significance compared to young age.

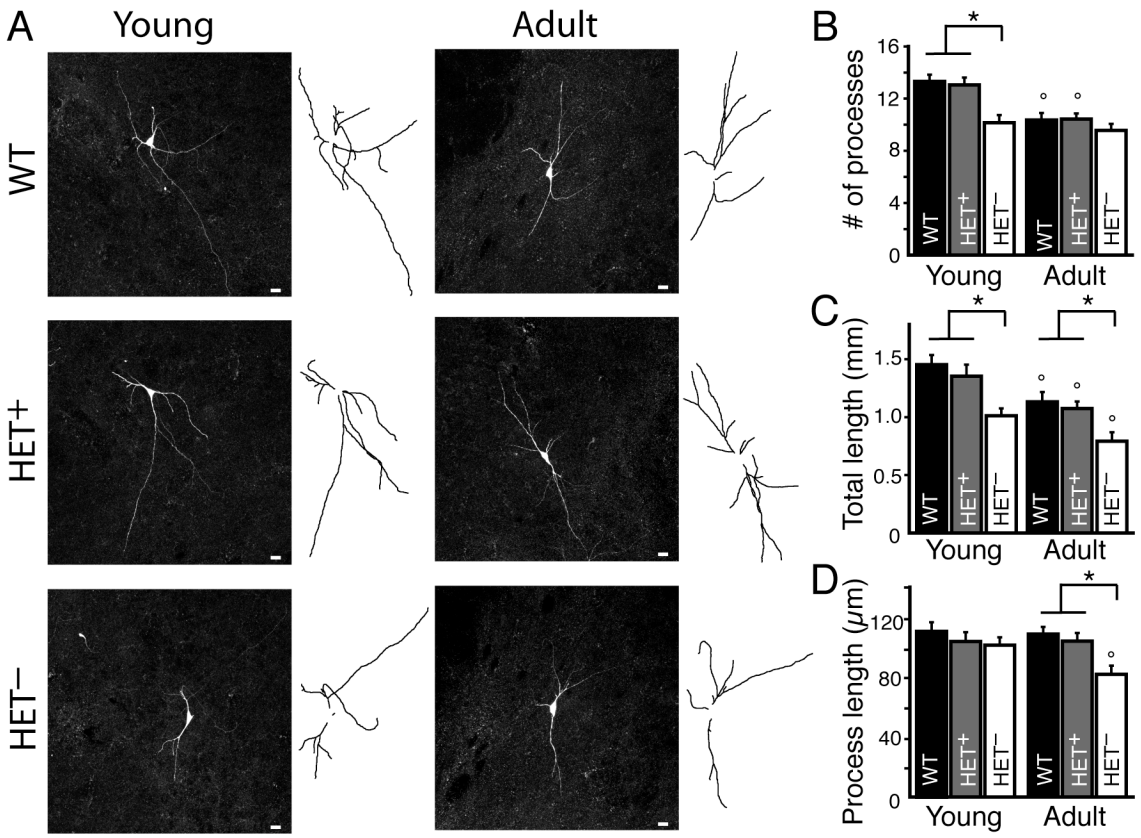

Figure A.2. Mecp2^{-} dopamine neurons in *Mecp2*$^{+/-}$ mice (HET^{-}) have a reduced dendritic arbor compared to Mecp2^{+} neurons from wild type (WT) or *Mecp2*$^{+/-}$ (HET^{+}) female mice.

A, Representative maximum intensity projection confocal images and tracings of neurobiotin-filled WT, HET^{+}, and HET^{-} dopamine neurons from the SNc of young and adult wild type and *Mecp2*$^{+/-}$ mice. **B**, The number of processes (dendrites and axon) on dopamine neurons decreased with age in wild type and *Mecp2*$^{+/-}$ mice, indicating a developmental pruning of dendrites. HET^{-} neurons had fewer dendrites than WT and HET^{+} neurons in young animals. There was no difference in the number of dendrites on WT and HET^{+} neurons. **C**, The total length of processes (mm) decreased with age in wild type and *Mecp2*$^{+/-}$ mice. The total length of processes in HET^{-} neurons was significantly less than WT or HET^{+} neurons in both young and adult animals. There was no difference in the total length of processes in WT and HET^{+} neurons. **D**, The average process length (μm) of WT and HET^{+} neurons was not different and did not change with age. Processes from HET^{-} neurons from adult *Mecp2*$^{+/-}$ mice were significantly shorter than age-matched WT and HET^{+} neurons. Mean ± SEM. * designates statistical significance within age group, ° designates statistical significance compared to young age.

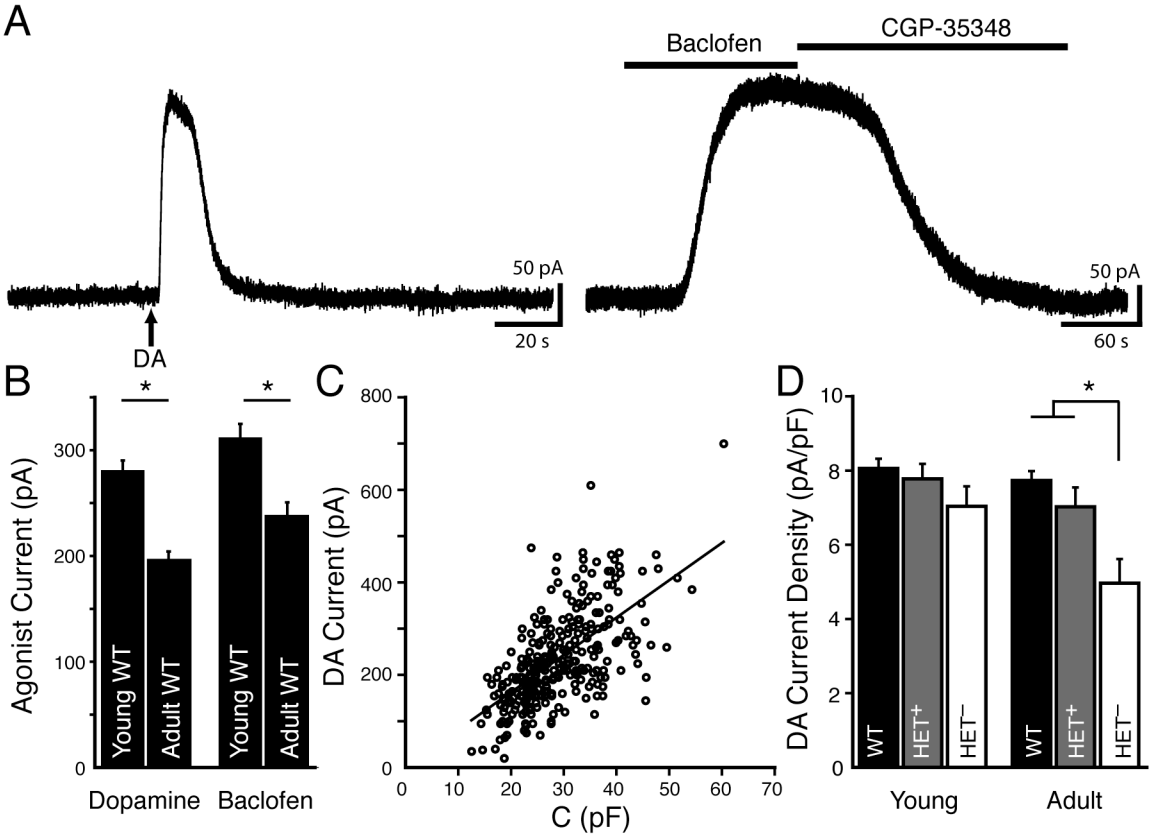

Figure A.3. Dopamine current density (pA/pF) was significantly reduced in HET^{-} neurons from the substantia nigra of symptomatic adult *Mecp2*$^{+/-}$ mice.

A, Representative trace of outward currents in wild type female mice induced by iontophoretic action of dopamine (arrow, 160 nA, 2 s) and bath application of baclofen (10 μM), which reversed with bath application of the $GABA_B$ antagonist CGP-35348 (30 μM). **B**, Raw current amplitudes (pA) showing a significant decrease in dopamine- and baclofen-induced currents in adult wild type mice. **C**, Linear correlation between capacitance (pF) and amplitude of dopamine-evoked outward current in wild type females (pA) ($R_{294} = 0.64$, $p < 0.0001$), indicating amplitude of dopamine-evoked outward current is directly proportional to membrane surface area. **D**, The dopamine current density (pA/pF) of WT and HET^{+} neurons was not different in young or adult mice. The dopamine current density of HET^{-} neurons was significantly less than WT and HET^{+} neurons in adult animals. Mean ± SEM. * designates statistical significance.

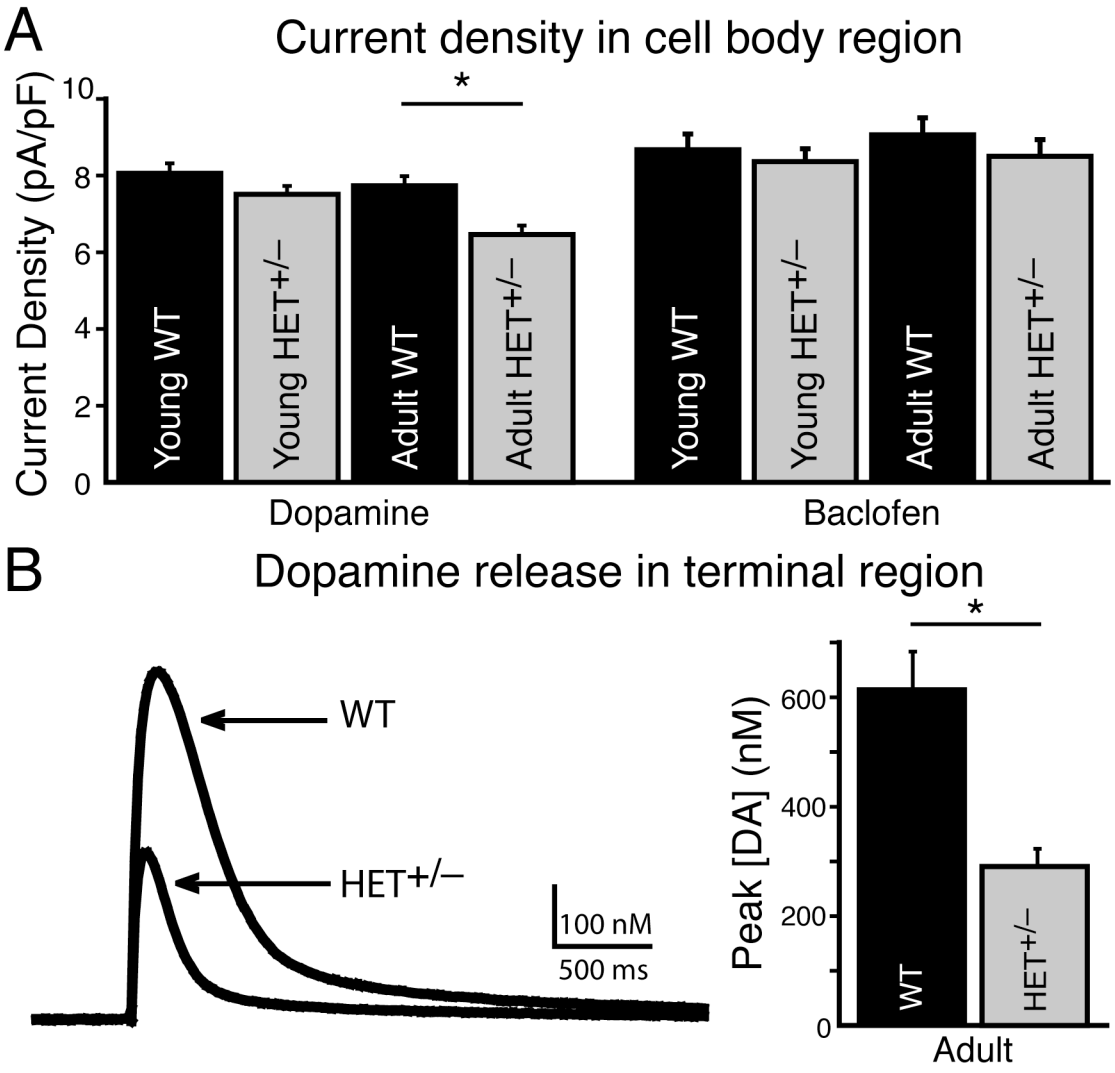

Figure A.4. Adult *Mecp2*$^{+/-}$ mice have decreased dopamine current density in the SNc and attenuated release of dopamine from axon terminals.

A, Dopamine and baclofen current densities (pA/pF) did not change with age in wild type females. The dopamine current density of the combined population of Mecp2^{+} and Mecp2^{-} dopamine neurons (HET$^{+/-}$) was significantly smaller in adult *Mecp2*$^{+/-}$ females compared to wild type. **B**, A single stimulation was used to evoke dopamine release from axon terminals in the dorsal striatum of adult wild type (WT) and *Mecp2*$^{+/-}$ (HET$^{+/-}$) mice. In adult *Mecp2*$^{+/-}$ mice, less than half the amount of dopamine was released than in wild type mice (left). Summarized data illustrating the peak concentration (nM) of the dopamine transient (right). Mean ± SEM. * designates statistical significance.

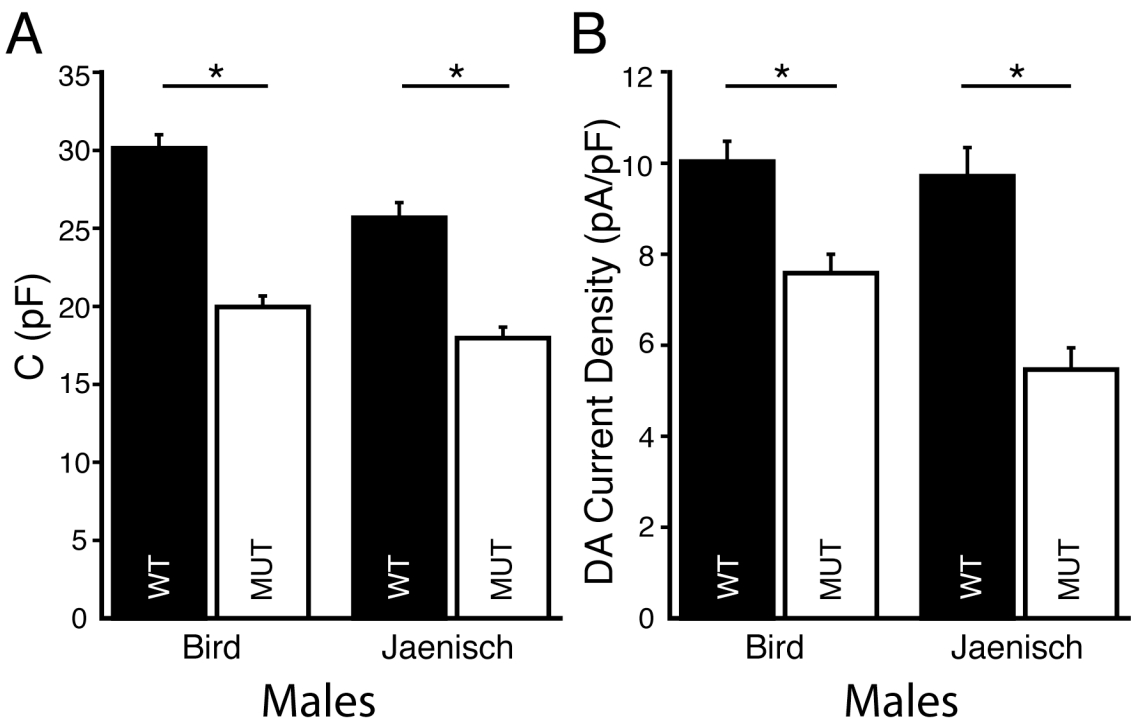

Figure A.5. Mecp2^{-} dopamine neurons from symptomatic *Mecp2*B$^{-/y}$ (Bird, PND 30-57) and *Mecp2*J$^{-/y}$ (Jaenisch, PND 101-105) mice have reduced capacitance (pF) and dopamine current density (pA/pF).

A, Capacitance of dopamine neurons in *Mecp2*$^{-/y}$ mice was significantly less than in wild type. **B**, The dopamine current density was significantly reduced in the *Mecp2*$^{-/y}$ mice. Mean ± SEM. * designates statistical significance.

Table A.1. Characteristics of dopamine neurons in wild type and *Mecp2*$^{+/-}$ females.

	Mecp2$^{+/+}$		*Mecp2*$^{+/-}$			
Age	Young (26 - 30 d)	Adult (250 - 812 d)	Young (27 - 30 d)		Adult (270 - 519 d)	
Mecp2	+	+	+	−	+	−
Capacitance (pF)	31.7 ± 1.0 (41)	**24.7 ± 0.5° (127)**	31.9 ± 1.3 (26)	**26.4 ± 1.8*‡ (20)**	**25.1 ± 1.1° (32)**	**18.9 ± 1.5*‡° (18)**
Resistance (MΩ/pF)	6.7 ± 0.3 (41)	**9.9 ± 0.5° (82)**	8.8 ± 0.8 (26)	**11.5 ± 1.1* (20)**	9.2 ± 0.7 (32)	**18.5 ± 2.0*‡° (18)**
Number of processes	13.3 ± 0.5 (25)	**10.4 ± 0.5° (25)**	13.0 ± 0.6 (23)	**10.2 ± 0.6*‡ (19)**	**10.4 ± 0.4° (30)**	9.6 ± 0.5 (16)
Length of processes (µm)	110.5 ± 6.0 (25)	108.7 ± 4.8 (25)	103.8 ± 6.2 (23)	101.3 ± 5.3 (19)	104.0 ± 5.5 (30)	**81.9 ± 5.8*‡° (16)**
Total length of processes (µm)	1453 ± 83 (25)	**1132 ± 84° (25)**	1353 ± 99 (23)	**1012 ± 64*‡ (19)**	**1074 ± 61° (30)**	**792 ± 78*‡° (16)**
Dopamine current density (pA/pF)	8.1 ± 0.3 (95)	7.7 ± 0.3 (111)	7.8 ± 0.4 (26)	7.0 ± 0.5 (19)	7.0 ± 0.5 (29)	**5.0 ± 0.7*‡° (17)**

Bold face designates statistical significance, * designates statistical significance compared to age-matched wild type, ‡ designates statistical significance compared to age-matched HET^{+}, ° designates statistical significance compared to young age within genotype, Number of cells in parentheses

Table A.2. Binding densities and affinities of [^{3}H]YM-09151-2 in midbrain and striatum do not differ between age-matched wild type and Mecp2$^{+/-}$ females.

The affinity (K_d) and density (B_{max}) of D2 receptors were determined by saturation analysis of binding of [^{3}H]YM-09151-2 in membranes prepared from 3 to 7 brains, described under "Materials and Methods". K_d values are the geometric means, followed by the limits defined by the SEM in parentheses. B_{max} values represent the mean ± SEM.

		K_d (pM)		B_{max} (fmol/mg protein)		*n*	
Region	Age	*Mecp2*$^{+/+}$	*Mecp2*$^{+/-}$	*Mecp2*$^{+/+}$	*Mecp2*$^{+/-}$	*Mecp2*$^{+/+}$	*Mecp2*$^{+/-}$
Midbrain	Young (26 – 37 d)	18 (16-20)	29 (19-44)	58.2 ± 6.9	58.8 ± 10.0	7	3
	Adult (169 - 446 d)	24 (23-26)	23 (19-27)	44.7 ± 2.0	43.8 ± 4.6	7	6
Striatum	Young (26 - 37 d)	16 (13-19)	18 (13-25)	709.7 ± 48.9	737.9 ± 12.8	4	3
	Adult (169 - 446 d)	17 (15-19)	17 (15-20)	**569.6 ± 17.9°**	**591.6 ± 45.2°**	7	6

Bold face designates statistical significance

° designates statistical significance compared to young age within genotype

APPENDIX B RECIPES

Internal solutions

KMS-based BAPTA and EGTA internal solutions

1. Add the following to 10 mL nanopure H_2O to obtain 100 mL of KMS 10 BAPTA intracellular solution
    - 1.54 g potassium methanesulfonate (115 mM)
    - 1 mL 2M NaCl (20 mM)
    - 150 μL 1M $MgCl_2$ (1.5 mM)
    - 0.26 g HEPES (K) (10 mM)
    - 0.628 g BAPTA (K4) (10 mM)
1. Add the following to 10 mL nanopure H_2O to obtain 100 mL of KMS 0.1 EGTA intracellular solution
    - 1.54 g potassium methanesulfonate (115 mM)
    - 1 mL 2M KCl (20 mM)
    - 100 μL 1M $MgCl_2$ (1 mM)
    - 0.26 g HEPES (K) (10 mM)
    - 0.0038 g EGTA (0.1 mM)
2. Constitute to a final volume of 100 mL
3. Filter with a 0.45 μm filter into 5 mL aliquots
4. Store aliquots at -20 C until needed
5. Before use, thaw a 5 mL aliquot and add the following:
    - 1 mg GTP (0.2 mM)
    - 5 mg ATP (2 mM)
    - 10 mg phosphocreatine (10 mM)
6. Add pH until between 7.3 and 7.4
7. Adjust osmolarity until between 270-280 mOsm
8. Aliquot into 1 mL fractions
9. Store unused aliquots at -20 C

Modifed Krebs buffer solution

1. Add the following to 1 L ddH2O to obtain 2 L modified Krebs buffer
    - 4.0 g D-glucose (11 mM)
    - 3.6 g $NaHCO_3$ (25 mM)
    - 200 mL 10x stock solution (1 L 10x stock recipe below)
        i. 7.363 g NaCl (126 mM)
        ii. 0.186 g KCl (2.5 mM)
        iii. 0.244 g $MgCl_2$ (1.2 mM)
        iv. 0.353 g $CaCl_2$ (2.4 mM)
        v. 0.166 NaH_2PO_4 (1.2 mM)
        vi. 1 L ddH2O

- Constitute to a final volume of 2 L with ddH_2O
- Incubate in a 35 C water bath, while oxygenating with 95%/5% O_2/CO_2 gas

Phosphate buffered saline

1. Add the following to 200 mL ddH_2O to obtain 1 L PBS:
    - 8.0 g NaCl
    - 0.2 g KHPO4
    - 1.1 g NaHPO4
    - 0.2 g KCl
2. Constitute to a final volume of 1 L with ddH_2O
3. Adjust pH, if necessary, to 7.4